FORMATION OF AROMATIC COMPOUNDS BY CYCLOPENTADIENE MOIETIES IN COMBUSTION PROCESSES

A Thesis
Presented to
The Academic Faculty

by

Do Hyong Kim

In Partial Fulfillment
of the Requirements for the Degree
Doctor of Philosophy in the
School of Civil and Environmental Engineering

Georgia Institute of Technology
August 2005

FORMATION OF AROMATIC COMPOUNDS BY CYCLOPENTADIENE MOIETIES IN COMBUSTION PROCESSES

Approved by:

Dr. James A. Mulholland, Advisor
School of Civil and Environmental Engineering
Georgia Institute of Technology

Dr. Armistead G. Russell
School of Civil and Environmental Engineering
Georgia Institute of Technology

Dr. Michael H. Bergin
School of Civil and Environmental Engineering
Georgia Institute of Technology

Dr. C. David Sherrill
School of Chemistry and Biochemistry
Georgia Institute of Technology

Dr. Kurt D. Pennell
School of Civil and Environmental Engineering
Georgia Institute of Technology

Date Approved: 06/29/2005

This dissertation is dedicated to my family

ACKNOWLEDGEMENTS

I would like to thank the following people for their help and support throughout my program at Georgia Tech. First of all, I would like to especially thank Dr. James. A. Mulholland, my advisor, for his endless and excellent guidance. Words cannot be good enough to express my gratitude toward him. It was always my pleasure to work and spend time with him during last seven years.

My gratitude also goes to Drs. Ted Russell, Kurt D. Pennell, Michael H. Bergin and David Sherrill for their guidance, helpful comments and time spent serving on my thesis committee. I like to thank Dr. Guangxuan Zhu, our lab manager, who has fixed many a problem and given excellent advice on analytical techniques in the lab. I also appreciate the professors, Andrea Be and Therese Rehkopf in Environmental Engineering, who have cultivated excellent working relationships with the students.

I am also grateful of my predecessors in our research group, Drs. Duane Nakahata, Mingming Lu and Jae-Yong Ryu who shared their wisdom and trained me. I must give special thank to Dr. Jae-Yong Ryu and his wife, Kyung-Hye Choi, for supporting and treating me as a family member, and meeting them was one of the greatest things in my graduate career at Georgia Tech. The National Science Foundation and the Environmental Protection Agency are also appreciated for financial support. Finally, I owe great debts of gratitude to my family for their love and support. It would be almost impossible for me to complete the Ph.D program without them. My mother, Sun Nam Yi, deserves special recognition for her encouragement and being a key to my success. I want to acknowledge my sisters, Young Hee and Young Shin Kim and my best friends, Minkyu Kim, Mark Yi, Jooho Rim, Jason Shin and Gongmin Kim.

TABLE OF CONTENTS

LIST OF TABLES

LIST OF FIGURES

SUMMARY

Polycyclic aromatic hydrocarbon (PAH) growth from cyclopentadiene (CPD) moieties has been investigated experimentally using a laminar flow reactor. Computational study using a semi-empirical molecular orbital method has also been performed as a screening tool to investigate alternative unimolecular reactions of the product of cyclopentadienyl (CPDyl) radical addition to CPD. Building on a published reaction pathways for CPD to naphthalene and indene to C-17 and C-18 compounds, routes are proposed for the formation of benzene, indene and naphthalene from CPD. Both experimental and computational results agree that indene formation via the intramolecular addition routes is favored at low temperatures (below 750^{o}C) and naphthalene formation via the β-scission routes is favored at high temperatures.

Reaction pathways from CPD with itself have been extended to PAH formation from the reaction of CPD and other compounds with different types of π bonds: acenaphthylene, styrene and phenanthrene. Low product yields and less variety of observed products from the pyrolysis of CPD-acenaphthylene, CPD-styrene and CPD-phenanthrene mixtures indicate that the reaction rates of CPDyl radical addition to other compounds without CPD moieties are much slower than the reaction of CPDyl radical addition to CPD. Nonetheless, increased yields of C_{16} species from CPD-acenaphthylene mixture and of biphenyl from CPD-styrene mixture relative to the yields of those compounds from CPD alone, though their yields are low, suggest that the pathway of CPDyl radical addition to different types of π bonds through a bridged intermediate has contributed to PAH growth from the mixtures. The reaction pathways from CPD may be important in PAH growth for conditions under which ring fragmentation is not significant.

Based on the previous work in this laboratory, an experimental investigation has been performed to test a hypothesis that polychlorinated naphthalenes (PCNs) can be formed from chlorinated phenols via CPDyl radicals. Formation of PCN and dioxin products from the slow

combustion of monochlorophenols in the laminar flow reactor has been studied over the range of 550 to 750^{o}C under oxidative conditions. Maximum PCN and polychlorinated dibenzofuran (PCDF) yields from monochlorophenols (MCPs) were observed between 625 and 725^{o}C. Different distributions of PCN congeners were produced from each MCP. Congener product distributions are consistent with proposed PCN and PCDF formation pathways both involving phenoxy radical coupling at unchlorinated ortho-carbon sites to form a dihydroxybiphenyl keto-tautomer intermediate. Tautomerization of this intermediate and subsequent fusion via H_2O loss results in PCDF formation whereas CO elimination and subsequent fusion with hydrogen and/or chlorine loss leads to PCN formation. The PCN isomer patterns observed are consistent with the major rearrangement path involving translation of the 9,10 carbons of dihydrofulvalene to the 9,10 carbon atoms in naphthalene.

The degree of chlorination of naphthalene and dibenzofuran products decreases as temperature increases, and, on average, the naphthalene congeners are less chlorinated than the dibenzofuran congeners. These results suggest that CO elimination that leads to naphthalene formation becomes increasingly favored relative to tautomerization that leads to dibenzofuran formation as temperature increases and as organic chlorine decreases. PCDF isomers via different ortho-ortho phenoxy radical couplings are found to be weakly dependent on temperature, suggesting that phenoxy radical coupling is a low activation energy process. PCN isomer distributions, on the other hand, are found to be more strongly dependent on temperature, with selectivity to particular isomers decreasing with increasing temperature.

A PCN formation scheme has been proposed and used to predict PCN product distributions from six dichlorophenols (DCPs) dissolved in benzene at 600^{o}C. These experimental results support the proposed pathways of PCN formation. The lack of detectable tetrachloronapthalene products from all DCPs except 3,4-DCP indicates that PCN formation is favored with one chlorine atom loss, particularly when chlorine is at an ortho position. The only

observed PCN peak that is not consistent with our prediction of major products is the formation of 1,8-DCN from 2,6-DCP.

Results of this research have contributed to understanding chemical mechanisms of PAH and soot formation from CPD moieties and PCN formation from chlorinated phenols in combustion systems.

CHAPTER 1

INTRODUCTION AND BACKGROUND

1.1 Formation of Polycyclic Aromatic Hydrocarbons and Soot in Combustion

Polycyclic aromatic hydrocarbons (PAHs) are of public health concern because of their toxicity and persistence in the environment. A number of epidemiologic studies have demonstrated a close relationship between an exposure to PAHs and an increased risk of cancer in humans (Kaden et al., 1979; Busby et al., 1988; Lafleur et al., 1990). In fact, the particle-bound PAHs can be transported long distances and can be deposited in water and on ground (Yang et al., 1991). The hazardous health effects of aerosols can be associated with PAHs (Miller et al., 1979). The Environmental Protection Agency (EPA) (1993) has classified several PAHs as carcinogens, and the 1990 Clean Air Act Amendments in the United States have regulated both PAHs and soot generated from transportation, manufacturing and power generation.

In the Unites States, it has been reported that smoking, wood burning, contaminated air and cooking are the greatest sources of PAH exposure to the general population, though people may also be exposed to PAHs in drinking water and through skin contact with soot and tars. The daily average intake of PAHs has been estimated to be 0.207 μg from air, 0.027μg from water, and 0.16-1.6μg from food. The total potential exposure to carcinogenic PAHs for adult males in the United States has been estimated to be 3 μg/day (ATSDR, 1995).

Most PAH emissions to environment are from both uncontrolled natural and anthropogenic sources as a result of incomplete combustion. Uncontrolled natural sources include forest fires and volcanoes (Back et al., 1991; NRC, 1983). Among the various anthropogenic PAH emission sources, fuel-burning from mobile sources has been known to be the greatest contributor in urban areas (Henderson et al., 1984; Pryysalo et al., 1987; Tuominen et al., 1988; Marinov et al., 1996; Schwela, 2000). Major stationary sources of PAHs are reported

to be residential heating (Ramdal, 1983; Harkov, 1985), power generation, and incineration (Shane et al., 1990; Wild et al., 1992). Other important sources are meat-cooking, open burning, the production of coal tar, coke, and asphalt (Back et al., 1991; Perwak et al., 1982). Additionally, cigarette smoke, gas cooking, and heating appliances are important sources of PAHs in indoor air (IARC, 1987; Chuang et al., 1991; Traynor et al., 1990). Ramdahl et al. (1982) have estimated that a total of 8,598 metric tons of PAHs are released to the atmosphere in the United States on an annual basis, with 75% of the total coming from the stationary sources while 25% comes from mobile source.

Formation of PAHs and soot in combustion has been observed from various fuels under a variety of conditions. Although the understanding of the formation and growth of PAHs and soot has improved substantially in recent years, many important details of PAH and soot formation remain poorly understood.

A pathway leading to the first aromatic ring (benzene) is the most important step in elucidating aromatic growth in combustion. Palmer and Cullis (1965) addressed the importance of cyclization reactions and the remarkable ease of carbon formation in benzene flames, suggesting that benzene forms either by polymerization of acetylene or in some other way under the certain conditions. Under fuel-rich conditions, aromatic ring formation is driven mainly by hydrogen abstraction and acetylene addition (HACA) (Homann and Wagner, 1967; Crittenden and Long, 1973; Bockhorn et al., 1983; Frenklach et al., 1984; Frenklach and Warnatz, 1987; Kazakov et al., 1995; Wang and Frenklach, 1997; Frenklach et al., 1998). The HACA mechanism has been most frequently cited to explain formation of PAHs and the kinetic information in many combustion systems. Cole et al. (1984) suggested the formation of benzene via acetylene addition to butadiene followed by a ring closure and a hydrogen loss. In addition, they suggested that the Diels-Alder addition appeared to be much slower than the experimental formation rate of aromatics. Westmoreland et al. (1989) identified the reactions of n-C_4H_5 and n-C_4H_3 with C_2H_2 as a major pathway for benzene formation; however, the contribution of n-C_4H_5

+ C_2H_2 was not sufficient to explain all the benzene formation. Comparing the model prediction with the experimental profiles of stable and radical species, Bastin et al. (1988) reported that benzene formation could not be fully explained by the reaction of C_4H_5 and C_2H_2.

The kinetic model of PAH growth from acetylene flame by Miller and Melius (1992) has shown that the recombination of two C_3H_3 molecules is a more attractive source of benzene; they have emphasized the potential importance of resonance-stabilized free radicals in forming aromatics and PAH in flames. Marinov and co-workers (1996) have concluded that the HACA mechanism is too slow to kinetically explain the formation of large PAHs and is not thermodynamically favorable. In addition, a recent study shows that nano organic carbon (NOC) which is comprised of soot from gasoline and diesel consists of elemental carbon and PAHs formed from aryl-aryl addition (D'Anna et al., 2005).

1.2 Roles of Resonance-Stabilized Radicals in PAH and Soot Formation

PAH growth from long chain aliphatic hydrocarbons in fuels and waste streams has demonstrated the importance of resonance-stabilized radicals. Domine (1989) reported the low product conversion and low yield of aromatic product from pyrolytic experiments of hexane and n-decane. Moreover, yields of benzene and toluene from pyrolysis of n-decane were much less than those of small alkenes, suggesting the aromatic compounds are secondary products (Bruinsma and Moulijin, 1988). High consumption rate of iso-octane and iso-butane compared to their straight-chained isomers under pyrolytic condition was attributed to the formation of more stable tertiary radicals (Billaud and Baronnet, 1987). Therefore, the quantities of pyrolytic products are largely dependent on the stabilities of intermediates (Lu, 2000).

Due to the resonance-stability, aromatic hydrocarbons are more resistant to fragmentation than aliphatic hydrocarbons. Thus, aryl-aryl addition becomes the major PAH growth mechanism in the regime where fragmentation of the aromatic ring is less important. In addition, the condensation of PAHs from aromatic compounds is much faster than from aliphatic compounds,

resulting in higher sooting tendencies. More recent studies have emphasized the potential importance of resonance-stabilized free radicals, such as propargyl and cyclopentadienyl radicals, in the formation of benzene and PAHs containing two to four rings (Wang and Frenklach, 1992; Lafleur et al., 1998; Frenklach et al., 1998). Recent experimental results obtained by Violi et al. (1999) suggest that high molecular mass structures, soot inception and particulate mass growth occur in oxidative environments predominantly through fast reactions of small PAH rather than acetylene.

The study of cyclopentadiene (CPD) pyrolysis by Spielmann and Cramers (1972) indicates that major products from CPD pyrolysis were aromatic hydrocarbons with higher carbon numbers (e.g. naphthalene, indene, and benzene) whose formation could not be adequately explained by the HACA mechanism alone. In a kinetic modeling study, Dente et al. (1979) show that benzene was formed via ethylene addition to CPD, forming a CH_2-bridged cyclohexane followed by hydrogen and methyl loss. Marinov et al. (1997) have proposed that in aliphatic hydrocarbon flames, the larger aromatics originate from resonance-stabilized cyclopentadienyl radicals. In a recent study, diesel fuel doped with ferrocene ($FeC_{10}H_{10}$), a fuel additive containing two cyclopentadiene rings in its molecular structure, produces more ultrafine soot, more oxidized hydrocarbons, and much less graphite carbons than diesel fuel alone (Chen et al, 2005).

The cyclopentadienyl (CPDyl) radical has been described as a neutral because it can achieve high concentration in thermal systems and as an ambident because they are reactive at multiple sites. In addition, PAHs containing CPD moiety such as indene can form resonance-stabilized radicals through hydrogen abstraction from the saturated carbon. These resonance-stabilized radicals are less likely to undergo unimolecular decomposition or to abstract hydrogen than to add to PAH to produce larger resonance-stabilized radicals. Due to delocalization of the radical site, these radicals can also form larger PAHs via several reaction channels of addition and subsequent condensation. Among various reaction channels from the CPDyl radical, the conversion between five- and six-member rings has been recognized as an important process not

only in combustion-generated PAH and soot emissions but also in combustion-generated fullerene production.

1.2.1 Source of Cyclopentadiene

CPD in combustion is generally formed via cyclization of aliphatic compounds (Westmoreland et al., 1989; Marinov et al., 1996) or decomposition of aromatic compounds such as phenol, benzene, toluene and xylenes (Spielmann and Cramers, 1972; Manion and Louw, 1989; Marinov et al., 1998; Ritcher et al., 2000). The premixed propane study by Marinov et al. (1996) showed that CPD was primarily formed by $C_3H_5 + C_2H_2$ and its formation was promoted by formation of allyl radicals.

Another pathway leading to the formation of CPD is the oxidation of benzene followed by loss of CO (Spielmann and Cramers, 1972; Manion and Louw, 1989; Marinov et al., 1998; Ritcher et al., 2000). The oxidation of benzene yields a phenoxy radical and the subsequent phenoxy radical decomposition produces CPD. Thermal decomposition of phenol, an oxidation product of benzene and one of most abundant specie in the combustion processes, has been confirmed to be a pathway to CPD formation (Jay, K. and Stieglitz, L, 1995; Wikstrom, E. and Marklund, S., 2000). Zhu and Bozzelli (2003) investigated CO elimination from the keto tautomer (2,4-cyclohexadienone) to form CPD via an acyclic intermediate. High temperature shock-tube pyrolysis of phenol has shown that decomposition of phenol to CPD and CO is the dominating initiation step. (Olivella et al., 1995; Liu et al., 1996) The formation pathway of CPD from phenol is depicted in Figure 1.1.

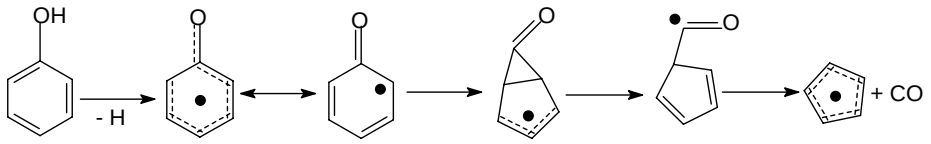

Figure 1.1 Phenol degradation reaction pathway to cyclopentadienyl radical (Olivella et al., 1995)

1.2.2 PAH Growth involving Cyclopentadiene

In recent years, a pathway leading to PAH growth from CPD has been the object of a substantial research effort. The formation of naphthalene via the reaction of two cyclopentadienyl radicals was included by Dean (1990) in a kinetic model of methane pyrolysis. The self-recombination route of CPDyl radicals has been suggested as a dominant route for naphthalene formation (Colvin, 1995; Melius et al., 1996; Friderichsen, 2001). Furthermore, Melius et al. (1996) conducted a detailed quantum chemical analysis of the elementary reaction steps for conversion of two CPDyl radicals to naphthalene. The formation mechanism of naphthalene via the recombination of CPDyl radicals is shown in Figure 1.2.

Dimerization of CPDyl radicals forms dihydrofulvalene followed by conversion of five-member rings to six-member rings via radical rearrangements involving three-member ring closing and opening of resonance-stabilized radicals. Building on the CPD-to-naphthalene mechanism in Figure 1.2, a phenanthrene formation pathway from the reaction of CPDyl and indenyl radicals has been proposed (Marinov et al., 1998). McEnally and Pfefferle (1998) have proposed the formation pathway of naphthalene from indene via methyl addition to indene followed by isomerization of benzofulvene; however, they did not report on higher molecular weight products.

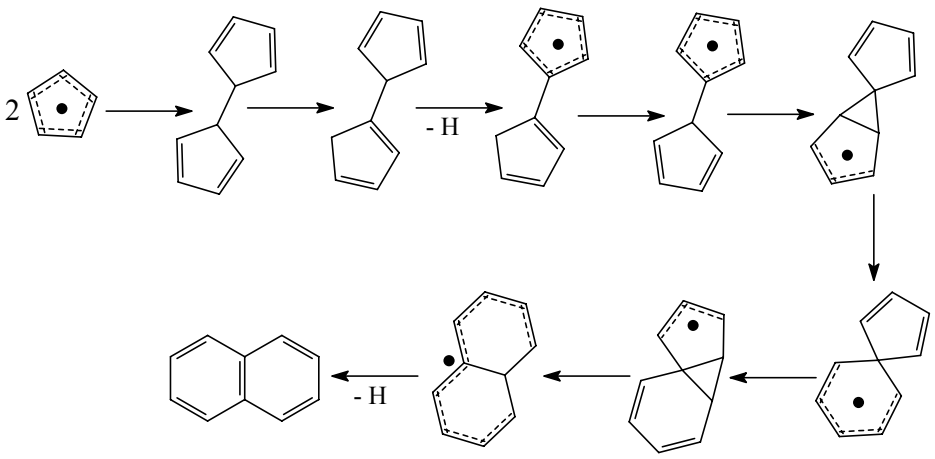

Figure 1.2 Reaction mechanism proposed by Melius et al. (1996) for the conversion of two cyclopentadienyl radicals to naphthalene

PAH growth from indene and a mixture of CPD and indene was investigated experimentally and computationally (Lu and Mulholland, 2001; Muholland et al., 2001). The observation of three $C_{18}H_{12}$ isomers from indene pyrolysis: chrysene, benz[a]anthracene, and benzo[b]phenanthrene, was explained by the pathway analogous to the CPD-to-naphthalene mechanism. In addition, an alternative route was proposed to address the formation of $C_{17}H_{12}$ products: benzo[a]fluorene and benzo[b]fluorene. This pathway occurs by indenyl radical addition to indene, followed by intramolecular addition to form a bridged intermediate containing the 7-norbornenyl moiety. Figure 1.3 depicts PAH formation pathways from indene.

The ratio of C_{17} and C_{18} product yields from indene pyrolysis showed that the intramolecular addition pathway, path (A) in Figure 1.3, was favored at low temperatures (below 700^{o}C) and the β-scission pathway, path (B), was favored at high temperatures. The temperature dependence of partitioning between two pathways is because the intramolecular addition pathway is less endothermic and is unfavorable in entropy due to the ring strain. The pathway involving a

bridged intermediate is important because the products from this route retain CPD moiety that poses greater facility for further growth.

1.2.3 Preliminary Experimental Results on CPD-indene Mixture, Indene and Indene-acenaphthylene Mixture Pyrolysis

PAH formation and growth from the pyrolysis of CPD-indene mixture were further investigated with an improved experimental setup. Experimental observations in CPD-indene mixture pyrolysis were consistent with hypothesized PAH products based on the pathways shown

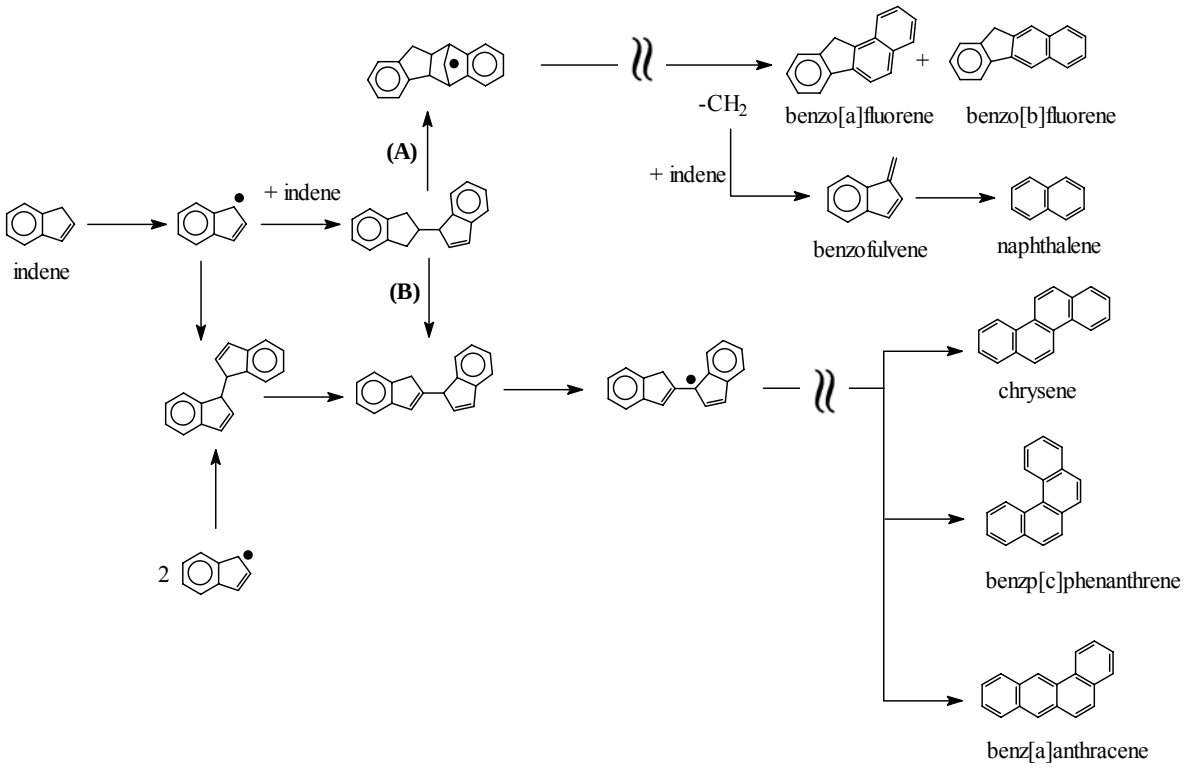

Figure 1.3 PAH growth pathway from indene (Lu, 2000)

in Figure 1.3. The intramolecular addition pathways resulted in formation of fluorene ($C_{13}H_{10}$), one carbon number less than the sum of reactants (CPD and indene), whereas the β-scission pathway produced the major $C_{14}H_{10}$ products: phenanthrene and anthracene. Product distributions from CPD-indene mixture pyrolysis are shown in Table A.1 in Appendix A.

Preliminary experiments with indene and indene-acenaphthylene mixture pyrolysis were also performed to study indenyl radical reactivity with aromatic species containing different types of π bonds. The pyrolysis of the mixture produced low product yields and less variety of products compared to the pyrolysis of indene alone. The major products (benzo[a]fluorene and benzo[b]fluorene, chrysene, benz[a]anthracene, and benzo[b]phenanthrene) and their yields from the pyrolysis of the mixture were similar to those from the pyrolysis of indene alone, indicating that the reactivity of indene to different π bonds is much less compared that of indene to itself. Observed products and their yields from indene and indene-acenaphthylene mixture pyrolysis are shown in Table A2 and A3, respectively, in Appendix A.

1.3 Computational Studies on PAH Growth involving Cyclopentadiene

Computer modeling in the study of PAH growth can complement the experimental search for yet unidentified species. Intermediates and transition states in the hypothesized reaction pathways that are not observed from experiments can be modeled using computational method. The capability of computational modeling to predict molecular properties of radical species leads to more detailed investigation on the contribution of resonance-stabilized radicals to PAH growth.

Melius and co-workers (1996) using the bond additivity corrected Moller-Plesset fourth-order perturbation (BAC-MP4) method have investigated the potential energy surface of the reaction pathway for the CPDyl radical reacting with the methyl radical to form benzene; they have suggested that the hydrogen migration on the CPD ring is important to gain resonance-stabilization for elimination and for the ring expansion of a five-member ring to a six-member ring. The computational study on the thermal isomerization of fulvene to benzene by Madden et

al. (1996) reached the same conclusion as Melius et al. (1996). Motivated by the role of resonance-stabilized radicals in PAH growth, Melius et al. (1996) has proposed computational study on the naphthalene formation by recombination of two CPDyl radicals.

Because of the expensive computing time of ab initio method for the large PAH of interest, an alternative computational method was needed. Wang and Frenklach (1993) supported the reliability of semi-empirical methods by providing the relatively consistent results on calculating heats of formations of benzenoid aromatic molecules and radicals compared to the experimental results. Then, Lu (2000) generated a similar energetic profile of the CPD-to-naphthalene mechanism with the semi-empirical PM3 (Parametric Method Number 3) method as that by BAC-MP4 method (Melius et al., 1996). Therefore, it was concluded that semi-empirical modeling could be used as a qualitative screening tool for assessing favored reaction channels in the reaction mechanisms involving large PAHs.

Furthermore, PAH growth pathways from the reaction of CPD and indene were studied computationally using PM3 method (Lu and Mulholland, 2001; Mulholland et al., 2001). Results of PM3 molecular modeling were consistent with the observed partitioning between $C_{18}H_{12}$ isomer product channels in indene pyrolysis (Lu and Mulholland, 2001) and the observed partitioning between intramolecular addition and β-scission pathways in DCPD and indene pyrolysis (Mulholland et al., 2001).

The use of kinetic modeling has allowed for the quantitative advances in the understanding of PAH and soot growth processes. The continuing investigation of elementary reactions using both experimental and computational techniques has helped to increase the reliability of the kinetic data included in reaction networks. An essential task for further work will be the construction of consistent thermodynamic databases using computational and experimental methods.

1.4 Formation of Polychlorinated Naphthalenes

During the past decades, the formation of halogenated aromatic compounds such as polychlorinated biphenyls (PCBs), polychlorinated dibenzo-p-dioxins (PCDDs) and polychlorinated dibenzofurans (PCDFs) in combustion processes has been getting much attention due to their persistence in the environment, bioaccumulation, and hazardous biological effects (Olie et al., 1977). Despite substantial improvements in the understanding of thermal formation processes of PCBs, PCDDs, PCDFs and other halogenated compounds, polychlorinated naphthalenes (PCNs) that are formed from combustion processes along with PCDDs and PCDFs (Olie et al., 1977; Eiceman et al., 1979) have been investigated far less than other halogenated compounds (Jänberg et al., 1999).

PCNs are a group of 75 possible congeners containing one to eight chlorine atoms bounded to two fused aromatic rings (IPCS, 2001). The molecular structures and numbering of PCNs are shown in Figure 1.4.

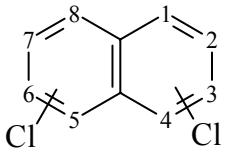

Figure 1.4 Structure and numbering for the polychlorinated naphthalenes

PCNs are recognized as man-made pollutants. Due to their high chemical and thermal stability, good weather resistance, low flammability and good electrical properties, PCNs had been produced industrially as mixtures of PCN congeners for the usage in capacitor dielectrics, cutting oils, engine oil additives, electroplating stop-off, die casting, wood and paper preservatives, and wire insulation (Crookes and Howe, 1993; Falandysz, 1998; Hayward, 1998;

Yamashita et al., 2000). The PCNs had been produced commercially world wide under various names including Halowaxes (Koppers, United States), Seekay Waxes (ICI, United Kingdom) and Nibren Waxes (Bayer, German). Volume of PCN production, however, decreased in the 1970s because of the growing evidence that PCNs were becoming pollutants on a global scale (Van de Plassche, 2002).

Although the production and the usage of PCNs have declined in the past, the presence of PCNs in the environment is still reported (Jansson et al., 1984; Falandysz et al., 1996; Falandysz, 1998; Asplund et al., 1994; Harner and Bidleman, 1997). Some reported PCN sources are commercial PCB formulation (Haglund et al., 1993; Jänberg et al., 1997; Kannan, 2000), the chloroalkali process (Schlabach et al., 1995), reclamation and smelting of aluminum and copper ore (Falandysz, 1998), and municipal waste incineration (Oehme et al., 1987; Benefenati et al., 1991; Imagawa et al., 1994; Takasuga et al., 1994; Schneider et al., 1998; Abad et al., 1999; Imagawa and Lee, 2001). The major current sources of PCNs are municipal and special incinerators and disposal of items containing PCNs to landfill (IPCS, 2001)

Information regarding the toxicity of individual PCNs is very limited. Several PCNs have been reported as strongly bioaccumulation and exhibiting dioxin-like toxicity (Hanberg et al., 1990; Engwall et al., 1994; Imagawa and Yamashita, 1994). Recent studies have indicated that liver damage and dermal alternations appear to be associated with the highly-chlorinated naphthalenes (Popp et al., 1997; Ward et al., 1996).

The formation mechanism of PCNs in combustion is not well known. Eiceman and co-workers (1974) first found PCNs in municipal waste incinerator (MWI) fly ash. In 1975, Cypres and Bettens (1975) reported on naphthalene formation from phenol. Since, chlorinated phenols have been reported as PCDD and PCDF precursors in the late 1980s (Born et al., 1989), many researchers have noted the simultaneous formation of PCNs and PCDDs/PCDFs. Sakai et al. (1996) reported that the amount of PCNs formed during incineration of solid wastes in laboratory was of the same order of magnitude as PCDDs/Fs. Schenider et al. (1998) reported that the

distribution of PCNs on fly ash from municipal waste incinerator was different than that in Halowax mixtures indicating PCN formation from different mechanisms than manufacturing commercial PCN mixtures. Moreover, different isomer patterns of PCNs between different types of incinerators were found (Imagawa and Takeuchi, 1995).

Formation of PCNs with PCDDs/PCDFs from chlorinated phenols was observed in both gas-phase pyrolysis (Akki, 1997) and oxidation (Nakahata, 2001). Imagawa and Lee (2001) observed the strong correlation between several PCN and PCDF congeners in MWI fly ash and suggested that the reaction pathways for the formation of PCN and PCDF might be very similar; however, the detailed mechanisms of PCN formation were not elucidated yet. .

Recently, Iino and co-workers (2001) have proposed the PCN formation mechanism via de novo synthesis; PCNs are formed from the macromolecular organic carbon and inorganic chlorine under the catalytic influence of transition metals such as $CuCl_2$. Cieplik et al. (2002), on the other hand, have proposed reaction pathways for the formation of naphthalene in the thermal hydrogenolysis of dibenzo-p-dioxin and dibenzofuran. These reaction schemes involve radical intermediates similar in structure to the dihydroxybiphenyls and phenoxyphenols, which are known to be intermediates in dibeznofuran and dibenzo-p-dioxin formation, respectively, from phenols.

1.5 References

Abad, E., Caixach, J. and Rivera, J., Dioxin like compounds from municipal waste incinerator emissions: assessment of the presence of polychlorinated naphthalenes. *Chemosphere* 38:109-120 (1999).

Akki, U., Gas phase formation pathways and mechanisms of polychlorinated dibenzo-p-dioxins and dibenzofurans. Ph.D. Thesis, Georgia Institute of Technology, Atlanta, USA (1998).

Asplund, L., Jakobsson, E., Haglund, P. and Bergman, Å., 1,2,3,5,6,7-Hexachloronaphthalene and 1,2,3,4,6,7-hexachloronaphthalene - selective retention in rat liver and appearance in wildlife. *Chemosphere* 28:2075-2086 (1994).

ATSDR (Agent for Toxic Substance and Disease Registry), Public health statement for polycyclic aromatic hydrocarbons (PAHs) http://www.atsdr.cdc.gov/toxfaq.html (1995).

Back, S.O., Field, R.A. and Goldstone, M.E., A review of atmospheric polycyclic aromatic hydrocarbons: Sources fast and behavior. *Water Air Soil Pollut.* 60(3-4):279-300 (1991).

Bastin, E., Delfau, J.-L., Reuilon, M., Vovelle, C. and Warnatz, J., Experimental and computational investigation of the structure of a sooting C_2H_2-O_2-Ar flame. *Proc. Combust. Inst.* 26:312-22 (1988).

Benfenati, E., Mariani, G., Faneli, R. and Zuccotti, S., "De novo" synthesis of PCDD, PCDF, PCB, PCN and PAH in a pilot incinerator. *Chemosphere* 22:1045-1052 (1991).

Billaud, F. and Baronnet, F., Order and self-inhibition of the pyrolysis of isobutene. J. *Analytical and applied pyrolysis* 10:181-197 (1987).

Bockhorn, H., Fetting, F. and Wenz, H.W., Investigation of the formation of high molecular hydrocarbons and soot in premixed hydrocarbon-oxygen flames. *Ber Bunsenges Phys. Chem.* 87:1067-1073 (1983).

Born, J.G.P., Louw, R. and Mulder, P., Formation of dibenzodioxins and dibenzofurans in homogeneous gas-phase reactions of phenols. *Chemosphere* 19:401-406 (1989).

Bruinsma, O.S.L. and Moulijin, J.A., The pyrolytic formation of polycyclic aromatic hydrocarbons from benzene, toluene, ethylbenze,e, styrene, phenylacetylene and n-decane in relation to fossil fuels utilization. *Fuel Processing Technology* 18:213-236 (1988).

Busby, W.F., Stevens, E.K., Kellenbach, E.R., Cornelisse, J. and Lugtenburg, J., Dose-response relationships of the tumorigenicity of cyclopenta[c,d]pyrene, benzo[a]pyrene and 6 nitrochrysene in a newborn mouse lung and adenoma bioassay. *Carcinogenesis* 9:741-746 (1988).

Chen, Y., Shah, N., Braun, A., Huggins, F.E., Linak, W.P., Miller, C.A., Kelley, K., Lighty, J. and Sarofim, A.F., Investigation of carbonaceous PM produced by fossil fuel combustion. *Abstract for 9th International Congress on Combustion By-Products and their Health Effects* (2005).

Chuang, J.C., Mack, G.A. and Kuhlman, M.R., Polycyclic aromatic hydrocarbons and their derivatives in indoor and outdoor air in an eight-home study. *Atmos.Environ. Part B Urban Atmos* 25(3):369-380 (1991).

Cieplik, M.K., Epena, O.J. and Louw, R., Thermal Hydrogenolysis of Dibenzo-p-dioxin and Dibenzofuran. *Eur. J. Org. Chem.* 2002:2792-2799 (2002).

Cole, J.A., Bittner, J.D., Longwell, J.P. and Howard, J.B., Formation mechanisms of aromatic compounds in aliphatic flames. *Combust. Flame* 56:51-70 (1984).

Colket, M.B., The pyrolysis of acetylene and vinylacetylene in a single-pulse shock tube. *Proc. Combust. Inst.* 21:851-864 (1986).

Crookes, M.J. and Howe, P.D., Environmental hazard assessment : halogenated naphthalenes. Toxic Substances Division, Directorate for Air, Climate and Toxic Substances, Department of the Environment. TSD/13 (1993).

Crittenden, B.D. and Long, R., Formation of polycyclic aromatics in rich premixed acetylene and ethylene flames. *Combust. Flame* 20 :359-368 (1973).

Cypres, R. and Bettens, B., La formation de la plupart des composes aromatiques produits lors de la pyrolyse du phenol, ne fait pas intervenir le carbone porteur de la fonction hydroxyle. *Tetrahedron* 39:359-365 (1975).

Dean A.M., Detailed kinetic modeling of autocatalysis in methane pyrolysis. *J. Phys. Chem.* 94:1432-1439 (1990).

Dente, M., Ranzi, E. and Goossens, A.G., Detailed prediction of olefin yields from hydrocarbon pyrolysis through a fundamental simulation model (SPYRO). *Computer Chem. Eng.* 3:61-75 (1979).

Domine, F., Kinetics of hexane pyrolysis at very high pressures. 1. Experimental study. *Energy & Fuels* 3:89-96 (1989).

Eiceman, G.A., Clement, R.E., and Karasek, F.W., Analysis of fly ash from municipal incinerators for trace organic compounds. *Anal. Chem.* 51:2343-2350 (1979).

Engwall, M., Brundstrom, B. and Jakobsson, E., Ethoxyresorufin O-deethylase (EROD) and aryl hydrocarbon hydroxylase (AHH)-inducing potency and lethality of chlorinated naphthalenes in chicken (Gallus domesticus) and eider duck (Somateria mollissima) embryos. *Archives of Toxicology* 68:37-42 (1994).

EPA, Provisional guidance for quantitative risk assessment of polycyclic aromatic hydrocarbons. Environmental Criteria and Assessment Office. Cincinnati, OH. ECAO-CIN-842 (1993).

Falandysz, J., Polychlorinated naphthalenes: an environmental update. *Environ. Pollut.* 101:77-90 (1998).

Falandysz, J., Standberg, L., Berggvist, P.-A., Kulp, S.E., Standberg, B. and Rappe, C., Polychlorinated naphthalenes in sediment and biota from the Gdansk basin, Baltic Sea. *Environ. Sci. Technol.* 30:3266-3274 (1996).

Frenklach, M., Clary, D.W., Cardiner, W.C. and Stein, S.E., Detailed kinetic modeling of soot formation in shock-tube pyrolysis of acetylene. *Proc. Combust. Inst.* 20:887-901 (1984).

Frenklach M., Moriarty N.W. and Brown N.J., Hydrogen migration in polyaromatic growth. *Proc. Combust. Inst.* 27:1655-1661 (1998).

Frenkalch, M. and Warnatz, J., Detailed modeling of PAH profiles in a sooting low-pressure acetylene flame. *Combust. Sci. Technol.* 51:265-283 (1987).

Friderichsen, A.V., Shin, E.-J., Evans, R.J., Nimlos, M.R., Dayton, D.C. and Ellison, G.B., The pyrolysis of anisole ($C_6H_5OCH_3$) using a hyperthermal nozzle. *Fuel* 80:1747-1555 (2001).

Haglund, P., Jakobsson, E., Aspuld, L., Athanasiadou, M. and Bergman, Å., Determination of polychlorinated naphthalenes in polychlorinated biphenyl products via capillary gas chromatography-mass spectrometry after separation by gel permeation chromatography. *J. Chromat.* 634:79-86 (1993).

Hanberg, A., Wærn, F., Asplund, L., Haglund, E., and Safe, S., Swedish dioxin survey: determination of 2,3,7,8-TCDD toxic equivalent factors for some polychlorinated biphenyls and naphthalenes using biological tests. *Chemosphere* 20:1161-1164 (1999).

Harkov, R., and Greenberg, A., Benzo(a)pyrene in New Jersey-Results from a Twenty-Seven-Site Study. *J. Air Pollut. Control Assoc.* 35:238-243 (1985).

Harner, T. and Bidleman, T.F., Polychlorinated naphthalenes in urban air. *Atmos. Environ.* 31:4009-4016 (1997).

Hayward, D., Identification of bioaccumulating polychlorinated naphthalens and their toxicological significance. *Environ. Res. section A* 76:1-8 (1998).

Henderson, T.R., Sun, J.D., Li, A.P., Bechtold, W.E., Harvey, T.M., Shabanowitz, J., and Hunt, D.F., GC/MS and MS/NS studies of diesel exhaust mutagenicity and emissions from chemically defined fuels. *Environ. Sci. Technol.* 18:428-434 (1984).

Homann, K.H. and Wagner, H.G., Some new aspects of the mechanism of carbon formation in premixed flames. *Proc. Combust. Inst.* 11:371-376 (1967).

IARC, Monographs on the evaluation of the carcinogenic risks of chemicals to humans: Vol. 1-42. Supplement 7. Lyon, France: World Health Organization, International Agency for Research on Cancer (1987).

Imagawa, T. and Takeuchi, M., Relation between isomer compositions of polychlorinated naphthalens and congener compositions of PCDDs/PCDFs from incinerators. *Organohalogen Compounds* 23:487-490 (1995).

Imagawa T., and Lee, C.W., Correlation of polychlorinated naphthalenes with polychlorinated dibenzofurans formed from waste incineration. *Chemosphere* 44:1511-1520 (2001).

Imagawa, T. and Yamashita, N., Isomer specific analysis of polychlorinated naphthalenes in halowax and fly ash. *Organohalogen Compounds* 19:215-218 (1994).

Iino, F., Imagawa, T., Takeuchi, M., and Sadakata, M., De novo synthesis mechanism of polychlorinated dibenzofurans from polycyclic aromatic hydrocarbons and the characteristic isomer of polychlorinated naphthalenes. *Environ. Sci. Technol.* 33:1038-1043 (1999).

IPCS, Concise International Chemical Assessment Document (CICAD) Chlorinated naphthalenes No. 34. Geneva, World Health Organization, International Program on Chemical Safety (2001).

Järnberg, U.G., Asplund, L.T., Egeäck, A.L., Jasson, B., Unger, M., and Wideqvist, U., Polychlorinated Naphthalene Congener Profiles in Background Sediments Compared to a Degraded Halowax 1014 Technical Mixture. *Environ. Sci. Technol.* 33:1-6 (1999).

Jansson, B., Asplund, L. and Olsson, M., Analysis of polychlorinated naphthalenes in environmental samples. *Chemosphere* 13:33-41 (1984).

Jay, K and Stieglitz, L., Identification and quantification of volatile organic components in emissions of waste incineration plants. *Chemosphere* 30:1249-1260 (1995).

Kaden, D.A., Hites, R.A. and Thiliy, W.G., Mutagenicity of soot and associated polycyclic aromatic hydrocarbons to Salmonella typhimurium. *Cancer. Res.* 39:4152-4159 (1979).

Kannan, K., Imagawa, T., Decoen, W., Blankenship, A.L. and Giesy, J.P., Isomer-specific analysis and toxic evaluation of polychlorinated naphthalenes in soil, sediment, and biota collected near the site of a former chloro-alkali plant. *Environ. Sci. Technol.* 34:566-572 (1998).

Kazakov, A., Wang, H. and Frenklach, M., Detailed modeling of soot formation in laminar premixed ethylene flames at a pressure of 10 bar. *Combust. Flame* 100:111-120 (1995).

Lafleur, A.L., Howard, J.B., Plummer, E., Taghizadeh, K., Necula, A., Scott, L.T. and Swallow, K.C., Identification of some novel cyclopenta-fused polycyclic aromatic hydrocarbons in ethylene flames. *Polycycl. Aromatic Compds.* 12(4):223-237 (1998).

Lafleur, A.L., Longwell, J.P., Shirnamé-Moré, L., Monchamp, P.A., Peters,W.A. and Plummer, E.F., Chemical characterization and bacterial mutagenecity testing of ethylene combustion products from a jet-stirred/plug-flow reactor. *Energy and Fuels* 4:307-319 (1990).

Liu, R., Morokuma, K., Mebel, A.M. and Lin, M.C., *Ab inito* study of the mechanism for the thernal decomposition of the phenoxy radicals. *J. Phys. Chem.*100:9314-9322 (1996).

Lu, M., Formation of growth of polycyclic aromatic hydrocarbons by cyclopentadienyl moieties in combustion. Ph. D. thesis, Georgia Institute of Technology, Atlanta, USA (2000).

Lu, M. and Mulholland, J.A., Aromatic hydrocarbon growth from indene. *Chemosphere* 42:189-197 (2001)

Madden, L.K., Mebel, A.M., Lin, M.C. and Melius, C.F., Theoretical study of the thermal isomerization of fulvene to benzene. *J. Phys. Org. Chem*. 9(12):801-810 (1996).

Manion, J. and Louw, R., Rates, products, and mechanisms in the gas-phase hydrogenolysis of phenol between 922 and 1175 K. *J. Phys. Chem*. 93:3563-3574 (1989).

Marinov, N.M., Pitz, W.J., Westbrook, C.K., Castaldi, M.J., and Senken, S.M., Modeling of aromatic and polycyclic aromatic hydrocarbon formation in premixed methane and ethane flames. *Combust. Sci. Technol.* 116:117-211 (1996).

Marinov, N.M., Pitz, W.J., Westbrrok, C.K., Vincitore, A.M., Castaldi, M.J., Senkan, S.M. and Melius, C.F., Aromatic and polycyclic aromatic hydrocarbon formation in a laminar premixed n-butane flame. *Combust. Flame* 114:192-213 (1998).

Marinov, N.M. Castaldi, M.J., Melius, C.F., and Tsang, W., Aromatic and Polycyclic Aromatic Hydrocarbon Formation in a Premixed Propane Flame. *Combust. Sci. Technol.* 128:295-342 (1997).

McEnally, C.S. and Pfefferle, L.D., An experimental study in non-premixed flames of hydrocarbon growth processes that involve five-membered carbon rings. *Combust. Sci. Technol.* 131(1-6):323-344 (1998).

Melius, C.F., Miller, J.A. and Evleth, E.M., Unimolecular reaction mechanisms involving C_3H_4, C_4H_4, and C_6H_6 hydrocarbon species. *Proc. Combust. Inst.* 24:621-628 (1992).

Melius, C.F., Colvin, M.E., Marinov, N.M., Pitz, W.J. and Senkan, S.M., Reaction mechanisms in aromatic hydrocarbon formation involving the C_5H_5 cyclopentadienyl moiety. *Proc. Combust. Inst.* 26:685-692 (1996).

Miller, F.J., Gardner, D.E., Graham, J.A., Lee Jr., R.E., Wilson, W.E. and Bachmann, J.D., Size considerations for establishing a standard for inhalable particles. *J. Air Pollut. Control Assoc.* 29:610-615 (1979).

Miller, J.A. and Melius, C.F., Kinetic and thermodynamic issues in the formation of aromatic compounds in flames of aliphatic fuels. *Combust. Flame* 91:21-39 (1992).

Miller, J.A., Theory and modeling in combustion chemistry. *Proc. Combust. Inst.* 26:461-480 (1996).

Mulholland, J.A., Lu, M. and Kim D.H., Pyrolytic growth of polycyclic aromatic hydrocarbons by cyclopentadienyl moieties. *Proc. Combust. Inst.* 28:2593-2599 (2000).

Nakahata, D.-T., Determination of relative formation rates of dibenzofurans via gas-phase condensation of phenols. Ph. D. Thesis, Georgia Institute of Technology, Atlanta (2001).

NRC, Polycyclic aromatic hydrocarbons: Evaluation of sources and effects. Washington D.C. National Academic Press (1983).

Oehme, M., Mano, S. and Mikalsen, A., Formation and presence of polychlorinated and polycyclic compounds in the emission of small and large scale municipal waste incinerators. *Chemosphere* 16:143-153 (1987).

Olie, K., Vermeulen, P.L. and Hutzinger, O., Chlorodibenzo-p-dioxins and chlorodibenzofurans are trace components of fly ash and flue gas of some incinerators in the Netherlands. *Chemosphere* 6:455-459 (1977).

Olivella, S., Sole, A. and García-Raso, A., *Ab intio* calculations for the potential surface for the thermal decomposition of the phenoxy radicals. *J. Phys. Chem.* 99:10549-10556 (1995).

Palmer, H.B., and Cullis, C.F., The formation of carbon from gases. In: Walker, P.L., editor. Chemistry and physics of carbon, vol 1. New York: Marcel Dekker (1965).

Perwak, J., Byrne, M. and Coons, S., An exposure and risk assessment for benzo[u]pyrene and other polycyclic aromatic hydrocarbons. Vol. 4, Washington, D.C. US Environmental Protection Agency, Office of Water Regulations and Standards, EPA 440/4-85-020-v4 (1982).

Popp, W., Norporth, K., Vahrenholz, C., Hamm, S., Balfanz, E., and Theisen, J., Polychlorinated Naphthalene Exposures and Liver Function Changes. *Am. J. Ind. Med.* 32:413-416 (1997).

Pryysalo, H., Tuominen, J., Wickström, K., Skytta, E., Tikkanen, L., Salomaa, S., Morsa, M., Nurmela, T., Mattla, T., and Pohjola, V., Polycyclic organic material (POM) in urban air: fractionation, chemical analysis and genotoxicity of particulate and vapor phases in an industrial town in Finland. *Atmos. Environ.* 21:1167-1180 (1987).

Ramdahl, K.J., Alfheim, I. and Bjorseth, A., Nitrated polycyclic aromatic-hydrocarbons in urban air particles. *Environ. Sci. Technol.* 16:861-865 (1982).

Ramdal T., Retene, a molecular marker of wood combustion in ambient air. *Nature* 306:580-582 (1983).

Richter, H., Benish, T.G., Mazyar, O.A., Green, W.H. and Howard, J.B., Formation of polycyclic aromatic hydrocarbons and their radicals in a nearly sooting premixed benzene flame. *Proc. Combust. Inst*. 28:2609-2618 (2000).

Schalbach, M., Biseth, A., Gundersen, H. and Knutzen, J., Congener specific determination and levels of polychlorinated naphthalenes in cod liver samples from Norway. *Organohalogen Compounds* 24:489-492 (1995).

Schwela, D., Air Pollution and health in urban area. *Reviews on Environmental Health* 15:13-42 (2000).

Sakai, S., Hiraoka, M., Takeda, N., and Shiozaki, K., Behavior of coplanar PCNs and PCNs in oxidative conditions of municipal waste incineration. *Chemosphere* 32:79-88 (1996).

Schneider, M., Stieglitz, L., Will, R. and Zwick, G., Formation of polychlorinated naphthalenes on fly ash. *Chemosphere* 37:2055-2070 (1998).

Shane, B.S., Henry, C.B. and Hotchkiss, J.H., Organic toxicants and mutagens in ashes from eighteen municipal refuse incinerators. *Arch. Environ. Contam. Toxicol.* 19(5):665-673 (1990).

Spielmann, R. and Cramers, C.A., Cyclopentadienic compounds as intermediates in the thermal degradation of phenols. Kinetics of thermal decomposition of cyclopentadiene. *Chromatographia* 5:295-300 (1972).

Tuominen, J.P., Pyysalo, H.S. and Sauri, M., Cereal products as a source of polycyclic aromatic hydrocarbons. *J. Agri. Food Chem.* 36(1):118-120 (1988).

Traynor, G.W., Apte, M.G. and Sokol, H.A., Selected organic pollutant emissions from unvented kerosene space heaters. *Environ. Sci. Technol.* 24(8):1265-1270 (1990).

Van de Plassche, E.J., Preliminary risk profile: polychlorinated naphthalenes. Ministry of Housing, Physical Planning and the Environment (VROM), Netherlands (2002).

Violi, A., D'anna, A. and D'Alessio, A., Modeling of particulate formation in combustion and pyrolysis. *Chem. Eng. Sci.* 54:3433-3442 (1999).

Wang, H. and Frencklach, M., Enthalpies of formation of benzenoid aromatic molecules and radicals. *J. Phys. Chem.* 97:3867-3874 (1992).

Wang, H. and Frenklach, M., A detailed kinetic modeling study of aromatics formation in laminar premixed acetylene and ethylene flames. *Combust. Flame* 110:173-221 (1997).

Ward, E.M., Ruder, A.M., Suruda, A., Smith, A.B., Fessler-Flesch, C.A. and Zahm, S.H., Acute and chronic liver toxicity resulting from exposure to chlorinated naphthalenes at a cable manufacturing plant during World War II. *Am. J. Ind. Med.* 30:225-233 (1996).

Westmoreland, P.R., Dean, A.M., Howard, J.B., and Longwell, J.P., Forming Benzene in Flames by Chemically Activated Isomerizations. *J. Phys. Chem.* 93:8171-8180 (1989).

Wikstrom, E. and Marklund, S., Secondary formation of chlorinated dibenzo-*p*-dioxins, dibenzofurans, biphenyls, benzenes and phenols during MSW combustion. *Environ. Sci. Technol.* 34:604-610 (2000).

Wild, S.R., Mitchell, D.J. and Yelland, C.M., Wasted municipal solid waste incinerator fly ash as a source of polynuclear aromatic hydrocarbons (PAHs) to the environment. *Waste. Manag. Res.* 10(1):99-111 (1992).

Yang, S.Y.N, Connell, D.W. and Hawker, D.W., Polycyclic aromatic hydrocarbons in air soil and vegetation in the vicinity of an urban roadway. *Sci. Total Enciron*. 102:229-240 (1991).

Yamashita, N., Kann, K., Imagawa, T., Miyazaki, A., and Giesy, J.P., Concentrations and Profiles of Polychlorinated Naphthalene Congeners in Eighteen Technical Polychlorinated Biphenyl Preparations. *Environ. Sci. Technol.* 34:4236-4241 (2000).

Zhu, L. and Bozzelli, J.B., Kinetics and thermochemistry for the gas-phase keto-enol tautomerization of phenol ⟷ 2,4-cyclohexadiene. *J. Phys. Chem. A* 107:3696-3703 (2003).

CHAPTER 2

RESEARCH OBJECTIVES

The overall goal of this research is to investigate polycyclic aromatic hydrocarbon (PAH) formation from reactions involving cyclopentadiene (CPD) in combustion systems. Two regions of the combustion process are studied: the pyrolysis zone where resonance-stabilized radicals are expected to contribute to the process of soot inception, and the post-flame zone where resonance-stabilized radicals can combine to form toxic combustion byproducts. In the post-flame zone, it has been reported that polychlorinated naphthalene (PCN) products are formed along with dioxin products.

High-temperature chemistry of PAH and PCN formation involving CPD were studied in a laminar flow reactor along with the preliminary computational study using a semi-empirical molecular modeling method. Specific objectives are addressed as follows:

1. *Formation of Naphthalene, Indene and Benzene from Cyclopentadiene*

   CPD pyrolysis is performed to examine formation of aromatic compounds over a temperature range of 600-950^{o}C, which simulates the slightly sooting region in flames in which CPD self-combination may form aromatic compounds. Preliminary computational study using a semi-empirical molecular orbital method has also been performed to investigate alternative unimolecular reactions of the product of cyclopentadienyl (CPDyl) radical addition to CPD.

2. *PAH Formation and Growth from the Pyrolysis of CPD, Acenaphthylene, Styrene and Phenanthrene Mixtures*

The pyrolysis of CPD–acenaphthylene, CPD-styrene and CPD-phenanthrene mixtures is conducted to investigate PAH formation and growth from the reaction of CPD with aromatic compounds containing different types of π bonds over a temperature range of 600-1000^{o}C. The underlying chemistry of PAH formation and growth from those mixtures is addressed.

3. Formation of Polychlorinated Naphthalenes from Monochlorophenols

Congener-specific analysis of PCNs from monochlorophenols over a temperature ranged from 550 to 750^{o}C under oxidative conditions, simulating the conditions in downstream gas of the combustion zone in an incinerator, is conducted to test *a priori* hypothesis that PCNs can be formed from chlorinated CPDyl radicals. PCN formation pathway from monochlorophenols is proposed. The temperature-dependence and governing factors of PCN formation pathway are also addressed.

4. Formation of Polychlorinated Naphthalenes from Dichlorophenols

PCN and dioxin products from dichlorophenols at 600^{o}C under oxidative condition are studied to examine if the proposed PCN formation scheme from monochlorophenols is able to predict the distributions of PCN and dioxin products from dichlorophenols.

CHAPTER 3

COMPUTATIONAL AND EXPERIMENTAL PROCEDURES

This chapter reviews and summarizes computational and experimental methods used in the various parts of the research in this thesis. Detailed descriptions are referred to related chapters.

3.1 Computational Methods

An essential requirement for reliable modeling of PAH growth is the availability of accurate thermodynamic and kinetic parameters. With help of the evolution of computational power, computational chemistry has, in recent years, improved in the accurate calculation of thermodynamic properties, such as the enthalpy, entropy, and heat capacity, that can complement experimental studies. Moreover, reaction intermediates and transition states that are often not measured in experiments can be modeled.

From quantum mechanics, the energy and many properties of molecules can be determined by solving the Schrödinger equation, $H\Psi_i = E_i\Psi_i$, in which H is the Hamiltonian operator and E_i is the sum of kinetic and potential energies. The solutions of electronic wavefunctions Ψ_i contain a full description of the system. However, it is recognized that solution of the Schrödinger equation is formidable because of its complexity (Hehre *et al.* 1985). In practice, approximated mathematical models based on Schrödinger equation are being used. While *ab initio* methods that use a variety of mathematical functions and approximations to solve the fundamental equation are able to produce reasonable results on thermodynamic properties of compounds of interest as compared to experimental data, computing time of *ab initio* methods for large PAHs is expensive and can be prohibitive.

Semi-empirical methods reduce the computational cost by using parameters obtained from experimental data to simplify calculations (Sadley, 1985). The major assumption of semi-

empirical methods is to neglect or to parameterize the two-electron, multi-center integrals, and only valence shell electrons are considered whereas in *ab inito* such as the Hartree-Fock method these integrals are solved explicitly (Jensen, 1999). Because of the use of empirical parameters for calculations, semi-empirical methods perform well for systems where experimental information is available; however, the reliability of semi-empirical results for other compound types is questionable. Nonetheless, semi-empirical methods are useful in the study of large molecules that require massive computing time. For example, Wang and Frenklach (1993) showed the reliability of semi-empirical methods for calculating heats of formation of benzenoid aromatic molecules and radicals in comparison with the experimental results.

MOPAC (version 6.0), a semi-empirical molecular orbital package, on an IBM RISC system/6000 at Georgia Institute of Technology, was used for the computational study. There are three different the semi-empirical Hamiltonians in MOPAC (Stewart, 1994): MNDO (Modified Neglect of Diatomic-differential Overlap), AM1 (Austin Model), and PM3 (Parametric Method 3). These MNDO, AM1 and PM3 methods are parameterizations of the same level of approximation, NDDO (Neglect of Diatomic Differential Overlap) (Stewart, 1990). MNDO is the earliest method and it has been succeed by the AM1 and PM3 methods (Dewar and Thiel, 1977). No aromatic specie data were used in the development of MNDO. Since AM1 contains more adjustable parameters than MNDO (Dewar et al., 1985), and since PM3 can be considered as a version of AM1 with all parameters fully optimized (Stewart, 1989), the performance of the PM3 methods is expected to be better than that of the MNDO and AM1 methods. Average errors in heat of formation for the MNDO, AM1 and PM3 methods are: 46 kcal/mol, 27.6 kcal/mol and 11.6 kcal/mol (Stewart, 1990). All calculations in this study were conducted using the PM3 method. Additional programs, CHEMDRAW, CHEM-3D (PC version), and RasMol (version 2.5) were used to help visualizing and interpreting MOPAC output data.

3.1.1. Molecular Modeling with MOPAC

Input data files for MOPAC are generated using the internal coordinate definition system. In this system, each molecule is created by defining one atom in space, and then sequentially adding atoms and defining their positions with respect to the previously defined atoms. The input geometry should be approximated as close to the optimized geometry as possible; otherwise, MOPAC aborts the optimization process due to its failure to reach the convergence criteria.

This problem becomes more significant when large molecules are being optimized. To reduce this problem, the initial geometry was refined with CHEMDRAW and CHEM3D programs. The drawing of a molecular structure of interest with CHEMDRAW was visualized in 3-dimension using CHEM3D that gives bond lengths, bond angles, and dihedral angles. These values were used as input data for MOPAC. Because MOPAC output data that are written in a tabular form are not intuitively obvious, the optimized structures were confirmed visually with RasMol (version 2.5), a graphical interface for viewing molecular structures.

In addition to the geometry of the optimized structure, the MOPAC output file provides heat of formation, zero-potential energy, ionization energy, electron-density matrix and the coordinates of the optimized structure. All other thermodynamic data such as entropy, enthalpy, and heat capacity are not shown in this output file; however, these data can be obtained from thermodynamic calculation using a keyword, THERMO.

Once an optimized geometry was identified, a force calculation was performed to characterize the nature of the stationary point and to obtain normal vibrational modes and frequencies. The vibrational frequencies are used to compute the zero-point correction to the energy, which accounts for the effects of molecular vibrations that exist even at 0 K. The transition and stationary states are verified using FORCE calculation results by the number of imaginary frequencies (NIMF), with NIMF=0 for stable species and NIMF=1 for transition states.

3.1.2 Transition State Modeling

The objective of transition state calculation is to find the highest energy point on the path of lowest energy connecting reactant and product. In order to calculate transition state structures, geometries of reactants and products should first be fully optimized. Because the transition state calculation is achieved by a continuous deformation between reactants and products, the two geometries must be arranged in the same orientation, and the numbering of atoms must be matched. Then, the transition state is calculated using a keyword, SADDLE. More details about the saddle calculation method are presented in MOPAC manual (version 6.0).

After a saddle calculation was done, the geometry of transition state was refined by keyword NLLSQ or TS. A refining process of the transition state was repeated until one negative force constant was found. Even if the refined transition-state structure has only one negative force constant, it may not be ready for the thermodynamic calculation because the thermodynamic calculation can be done on the geometry with a gnorm less than 10. If the gnorm for the transition-state structure is over 10, then it has to go through NLLSQ or TS calculation until its gnorm is less than 10. If the transition state from SADDLE and path calculation methods do not seem to have one negative force constant through the refining process with NLLSQ or TS, then the recommendation is to abandon the work and to go back to SADDLE and path calculation process again to get another possible transition state point.

The technique discussed above is not the only way to get the transition state with MOPAC. There are other techniques for transition state calculation in MOPAC. The keyword sequences used for this study are summarized:

1. To locate the stationary point such as reactant and product:

   PM3 GNORM=*n,nn* CHARGE=*n* T=*n*

2. To locate the transition state using SADDLE method:

   PM3 SADDLE GNORM=*n,nn* BAR=0.15 XYZ CHARGE=*n* T=*n*

3. To locate the transition state using a path calculation method:

PM3 GNORM=*n,nn* CHARGE=*n* T=*n*

4. To calculate force constants:

   PM3 FORCE TRANS GNORM=*n,nn* CHARGE=*n* T=*n*

5. To refine the transition state given from SADDLE and a path calculation methods:

   PM3 NLLSQ GNORM=*n,nn* CHARGE=*n* T=*n*

6. To perform the thermodynamic calculation:

   PM3 NOINTER NOXYZ ROT=1 THERMO(*n, m, l*) TRANS CHARGE=*n*

   T=*n*

3.2 Experimental Methods

The reactor system, experimental conditions, procedures, and sample collection methods used for all of experiments are described in this section.

3.2.1 Reactor System and Operating Conditions

The laminar flow reactor system used for experiments is depicted in Figure 3.2. The reactor consists of a furnace (Thermolyne Model 21100- Dubuque, IA), a digital temperature controller and a quartz tube of 48 cm long and 1.7 cm in diameter.

A vaporizer located upstream of reactor inlet is a three-way glass vessel for fuel input and evaporation. A single reactant or multiple reactants were delivered into the system with a syringe pump (Sage Instruments Model 341B- Boston, MA) to maintain a constant feeding rate. If necessary, benzene was added to get all reactants into solution since it is less reactive than the other organics and contains only aromatic carbon.

The carrier gas inlet line and the vaporizer were wrapped with heating tape to vaporize a single reactant or multiple reactants. The inlet temperature was monitored by a thermocouple at the vaporizer. Two types of carrier gases were used: nitrogen (high purity) for CPD and mixture experiments under pyrolytic condition, and 8% oxygen in nitrogen for experiments of chlorinated

phenols under oxidative conditions. The flow rate or gas velocity of the carrier gas was controlled using a flow meter (Matheson Model FM-1050, Montgomeryville, PA). The flow rate of carrier gas was set at 402 standard ml/min to yield a nominal residence time of 4 seconds for pyrolysis experiments (range: 3-5 s) whereas the flow rate was set at 218 standard ml/min to yield a nominal residence time of 10 seconds for oxidation experiments (range: 8-12 s).

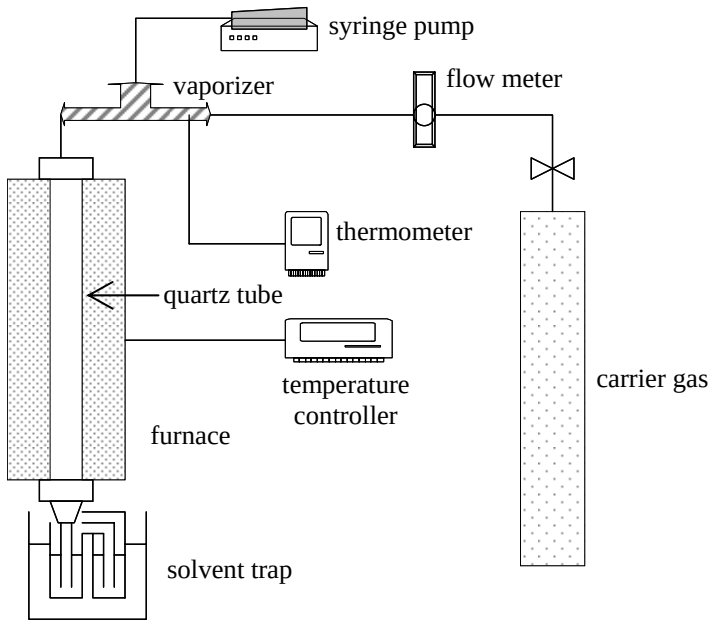

Figure 3.1 A schematic diagram of experimental apparatus

Temperature profiles inside the quartz tube reactor were measured using a thermocouple for different temperature settings and a gas flow rate of 200 standard ml/min (Yang, 1999); these are shown in Figure 3.2. Measurements of the reactor temperature profiles indicate that temperatures at the top 8 cm and bottom 9 cm of the quartz tube are lower than the set value. The gas temperatures in the remaining 31 cm of the reactor, defined as a reaction zone, are

approximately constant within $\pm$ 10°C of the set value. Radial variation of temperature was assumed to be negligible due to small tube diameter.

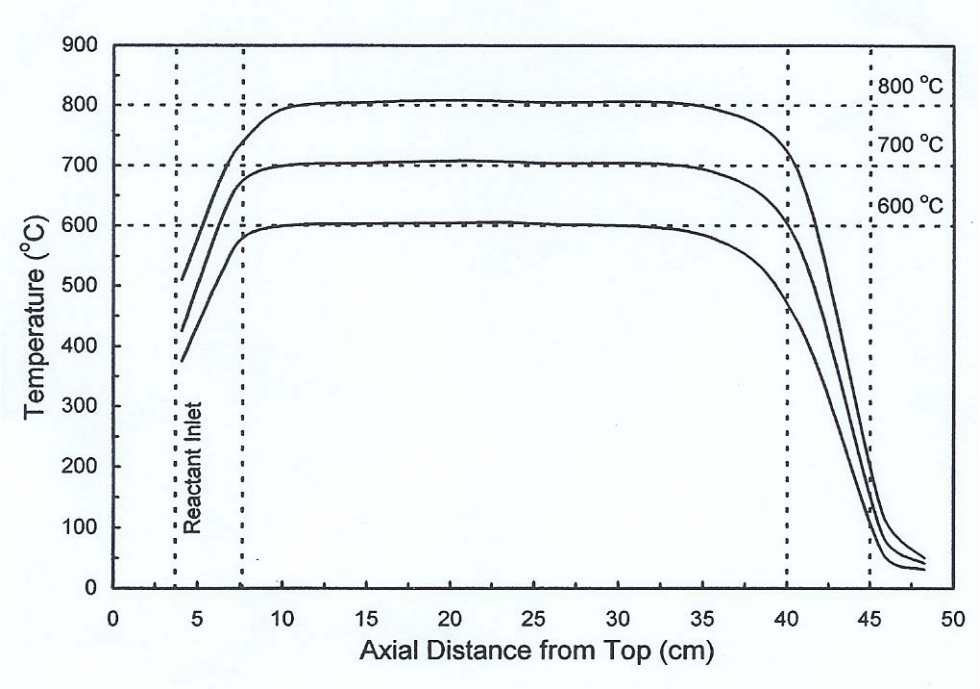

Figure 3.2 The axial temperature profile of the quartz tube reactor (Yang, 1999)

3.2.2 Sample Collection and Analysis

The entire product gas stream was rapidly quenched at the bottom of the reactor by blowing room temperature air to facilitate product collection. Aromatic samples were collected in a dual ice-cooled dichloromethane (DCM) trap. After each experiment, the quartz tube, all fittings, and collection trap were also rinsed with DCM to remove any products deposited on the surface. Rinsed DCM was combined with the DCM in the collection trap. Sample and rinsed solutions were filtered with polytetrafluorothylene (PTFE) membrane filter of 0.25μl pore diameter by vacuum filtration to remove soot, defined as the DCM-insoluble fraction. Soot yields were determined gravimetrically. For calculation of total carbon recovery, soot was assumed to be pure carbon.

Filtered samples were analyzed by gas chromatography coupled with mass spectroscopy (GC/MS) - HP 6890 series GC with model 5973 MSD). The GC column employed was a HP-5MS capillary column with 30m x 0.25mm with a 0.25ul film of cross-linked 5% PH ME siloxane (HP Part No. 19091S-433). Occasionally samples underwent the evaporative concentration process with nitrogen for better identification and detection of products with low concentrations.

3.2.3 PAH Products Analysis

GC methods were developed with reference to EPA standard methods for effective identification of PAH products, and corresponding MS methods were also developed with proper mass to charge ranges, scanning rates and a solvent delay time. GC temperature programming used for product analysis from CPD, indene, and mixture experiments is shown in Table 3.1. A lower starting temperature of 32^{o}C in CPD and its mixture experiments was selected for benzene identification.

Products were identified mainly by comparing the MS-spectra and retention times with commercially available chemical standards. Response factors were obtained through four dilutions of chemical standards (listed in Table 3.2). Standard analysis was performed for each batch of experiments run within a week. When standards were not available, product structures were hypothesized by their MS-spectrum and reference books. Yields of the observed products were calculated with the response factors and peak areas expressed in a percent carbon input. For the products without standards, their yields were estimated using response factors of compounds having similar structures.

Table 3.1 GC temperature programming for PAH product analysis

Start (^{o}C)	End (^{o}C)	Rate (^{o}C/min)	Time (min)
32	32	0	2
32	250	5	43.60
250	280	8	3.75
280	280	0	3

Table 3.2 Chemical standards used for PAH product analysis

Name	Manufacturer	CAS
2-methyl indene	Aldrich	2177-47-1
4H-cyclopentaphenanthrene	Aldrich	206-64-5
acenaphthene	Chem Service	83-32-9
acenaphthylene	Ultra Scientific	208-96-8
acetaldehyde	Alfa Aesar	75-07-0
anthracene	Acros	120-12-7
azulene	Aldrich	275-51-4
benzene	Fisher Scientific	71-43-2
benzo[*a*]fluorene	Ultra Scientific	238-84-6
benzo[*a*]pyrene	Acros	50-32-8
benzo[*c*]phenanthrene	Sigma	195-19-7
benzo[*k*]fluoranthene	Acros	207-08-9
benzo[*b*]fluoranthene	CHEM SERVICE	205-99-2
benzo[*j*]fluoranthene	CHEM SERVICE	205-82-3
biphenyl, 99%	Aldrich	92-52-4
chrysene	Acros	218-01-9
dicyclopentadiene	CHEM SERVICE	77-73-6
fluoranthene	Acros	206-44-0
fluorene	Aldrich	86-73-7
fluorene, 98%	Acros	86-73-7
formaldehyde	AVOCADO	50-00-0
indene	Alfa Aesar	95-13-6
naphthalene	Aldrich	91-20-3
perylene	Acros	198-55-0
phenanthrene	Ultra Scientific	85-01-8
phenanthrene, 93%	AVOCADO	85-01-8
Pyrene	Aldrich	129-00-0

3.2.4 PCN Analysis

Due to the lack of standards of individual PCN congeners, Halowax 1001, 1014, and 1051, commercially manufactured PCN mixtures were used as PCN standards. Halowaxes used for this study are analyzed and the results are summarized in Table 3.3. Unchlorinated naphthalene was used as a universal response factor for PCN products.

Table 3.3 Composition of Halowax Standards

Halowax	Cl-content	Chlorinated degree Cl_xN	Concentration
1000	26%	x=1,2	100µg/ml in MeOH
1001	50%	x=(1,2)3,4,(5)	100µg/ml in MeOH
1014	62%	x=(3) 4,5,6,(7)	100µg/ml in MeOH
1051	70%	x=7,8	100µg/ml in MeOH

Preliminary identification of PCN products was done according to published reports (Abad et al, 1999; Schneider et al., 1998; Jänberg et al., 1994). The HP-5MS column provided the following separation of PCN isomer peaks: 2 peaks/2 monochloronaphthalene (MCN) isomers, 7 peaks/10 dichloronaphthalene (DCN) isomers, 8 peaks/14 trichloronaphthalene (T_3CN) isomers, 13 peaks/ 22 tetrachlronaphthalene (T_4CN) isomers, 12 peaks/14 pentachloronaphthalene (P_5CN) isomers, 6 peaks/ 10 hexachloronaphthalene (H_6CN) isomers, 2 peaks/2 heptachloronaphthalene (H_7CN) isomers. The GC temperature program for PCN product identification is shown in Table 3.4. For quantification, the mass spectrometer was operated in selective ion mode at the two most intensive and characteristic ion masses. Mass spectral information on PCN is provided in Table 3.5.

Seventy-four of 76 PCN congeners including unchlorinated naphthalene have been identified, and the elution order of identified PCNs is shown in Table 3.6. Elution orders of congeners not identified in our analytic system are also listed in accordance with the published reports. Co-eluted congeners are shown in bold boxes.

Table 3.4 GC temperature program for PCN analysis

Start (^{o}C)	End (^{o}C)	Rate (^{o}C/min)	Time (min)
38	38	0	2
38	180	3	47.33
180	180	0	2
180	250	5	14
250	250	0	5
250	280	6	5
280	280	0	3
280	300	2	10

Table 3.5 Selected Ion for PCN analysis

Compounds	M+	M+2	Ion ratio
MCNs	162.02	164.02	3.07
DCNs	195.98	197.98	1.55
T_3CNs	229.95	231.94	1.04
T_4CNs	263.61	265.90	0.78
P_5CNs	299.86	301.86	1.55
H_6CNs	333.83	335.82	1.24
H_7CNs	367.79	369.78	1.04
OCN	401.75	403.75	0.89

Table 3.6 Elution order of PCNs on HP-5ms column

N	MCN	DCN	T_3CN	T_4CN	P_5CN	H_6CN	H_7CN	OCN
naphthalene (20.93)	2-(29.37) 1-(29.63)	13-(36.06) 14-(36.57) 15-(36.73) 16-(36.73) 17-(36.73) 26-(37.07) 27-(37.07) 12-(37.42) 23-(37.66) 18-(39.68)	136-(42.49) 135-(42.49) 137-(42.94) 146-(42.94) 124-( ) 125-(43.62) 126-(43.90) 127-(44.23) 167-(44.55) 236-(44.55) 123-( ) 138-( ) 145-(45.45) 128-(46.87)	1357-(47.47) 1257-(48.62) 1246-(48.62) 1247-(48.62) 1367-( ) 1467-(49.39) 1368-(49.92) 1256-(49.92) 1235-(50.23) 1358-(50.23) 1237-(50.62) 1234-(50.70) 1267-(50.86) 1245-(51.14) 2367-( ) 1248-(51.43) 1258-( ) 1268-(51.94) 1458-(53.12) 1238-( ) 1278-(53.88) 1289-( )	12357-(54.84) 12467-(54.84) 12457-(55.44) 12468-(55.69) 12346-(55.86) 12356-(55.97) 12367-(56.70) 12456-(56.84) 12478-(57.07) 12358-(57.25) 12368-(57.25) 12458-(57.69) 12345-(57.93) 12378-(58.77)	123467-(60.19) 123567-(60.19) 123457-(60.73) 123568-(60.73) 123578-(60.94) 124568-(61.16) 124578-(61.16) 123456-(61.89) 123458-(62.31) 123789-( )	1234567-(64.98) 1234568-(65.08)	12345678- (73.50)

* note: elution time of each congener is written in parenthesis, and congeners shown in boxes co-elute; the order of congeners without elution times is based on literature elution order using similar columns.

3.2.5 PCDD/F Analysis

Identification of PCDD/F products was based on the previous studies (Nakahata, 2001; Ryu, 2002). Elution times and available standards for isomers were crosschecked against each other. The temperature program for GC-MS was same as that for PCN analysis shown in Table 4.3. 74 of 75 PCDD congeners and 121 of 135 PCDF congeners have been identified. Details on identification and the elution orders of PCDD/F congeners in our analytic system are presented elsewhere (Nakahata, 2000; Ryu, 2001). Universal response factors were used for PCDD/Fs based on dibenzo-*p*-dioxin (DD) and dibenzofuran (DF), respectively.

3.3 Raw Data

Product yields from the pyrolysis of CPD, indene and the mixtures of CPD, indene and other compounds are summarized in Table A.1-A.7 in Appendix A. Phenol product yields from monochlorophenols and dichlorophenols are shown in Table A.8 and A.9. Ion chromatogram and a mass spectrum of cyclopentadiene in the gas sample from dicyclopentadiene pyrolysis are shown in B.1 in Appendix B. Total ion chromatograms and mass spectra of selected aromatic products from CPD and CPD-acenaphthylene mixture pyrolysis are shown in B.2 and B.3. In addition, total ion chromatograms and mass spectra of PCN congeners in Halowax mixtures (1000, 1001, 1014 and 1051) are shown in B.4-B.7.

3.4 References

Abad, E., Caixach, J. and Rivera, J., Dioxin like compounds from municipal waste incinerator emissions: assessment of the presence of polychlorinated naphthalenes. *Chemosphere* 38:109-120 (1999).

Akki, U., Gas phase formation pathways and mechanisms of polychlorinated dibenzo-p-dioxins and dibenzofurans. Ph.D. Thesis, Georgia Institute of Technology, Atlanta, USA (1998).

Dewar, M.J.S., Zoebisch, E.G., Healy, E.F. and Stewart, J.J.P., AM1: a new general purpose quantum mechanical molecular model. *J. Am. Chem. Soc.* 107:3902-3909 (1985).

Dewar, M.J.S. and Thiel, W., Ground states of molecules. 38. The MNDO method. Approximations and parameters. *J. Am. Chem. Soc*., 99:4899-4907 (1977).

Hehre, W.J., Radom, L., Schleyer, P.v.R. and Pople, J.A., Ab intio molecular orbital theory. John Wiley and Sons, New York (1985).

Imagawa, T. and Yamashita, N., Isomer specific analysis of polychlorinated naphthalenes in halowax and fly ash. *Organohalogen Compounds* 19:215-218 (1994).

Järnberg, U., Asplund, C. and Jakobsson, E., Gas chromatographic retention of polychlorinated naphthalenes on non-polar, polarizable, polar and semectic capillary columns. *J. Chromat*. 683A:385-396 (1994).

Jensen, F., Introduction to computational chemistry. John Wiley and Sons, Chichester, England (1999)

Lu, M., Formation of growth of polycyclic aromatic hydrocarbons by cyclopentadienyl moieties in combustion. Ph. D. thesis, Georgia Institute of Technology, Atlanta, USA (2000).

Nakahata, D.-T. and Mulholland, J.A., Effects of dichlorophenol substitution pattern on furan and dioxin formation. *Proc. Combust. Inst.* 28:2701-2707 (2000).

Nakahata, D.-T., Determination of relative formation rates of dibenzofurans via gas-phase condensation of phenols. Ph. D. Thesis, Georgia Institute of Technology, Atlanta (2001).

Ryu, J.-Y., Dioxin formation on copper (II) chloride from chlorinated phenol, dibenzo-p-dioxin and dibenzofuran precursors. Ph.D. Thesis, Georgia Institute of Technology, Atlanta, USA (2002).

Sadley, J., Semi-empirical methods of quantum chemistry, John Wiley and Sons, New York (1985).

Schneider, M., Stieglitz, L., Will, R. and Zwick, G., Formation of polychlorinated naphthalenes on fly ash. *Chemosphere* 37:2055-2070 (1998).

Stewart, J.J.P., Optimization of parameters for semiempirical methods I. Method. *J. Comput. Chem.* 10: 209-220 (1989).

Stewart, J.J.P., MOPAC: A semiempirical molecular orbital program. *J. Com. Mol. Design* 4:1-105 (1990).

Stewart, J.J.P., MOPAC 93 Manual. 2nd rev. Fujitdu Limited (1994).

Wang, H. and Frenklach, M., Enthalpies of formation of benzenoid aromatic molecules and radicals. *J. Phys. Chem*. 97:3867–3874 (1993).

CHAPTER 4

FORMATION OF NAPHTHALENE, INDENE AND BENZENE FROM CYCLOPENTADIENE PYROLYSIS

[Material presented in this chapter was submitted to *Combustion and Flame* entitled, "Formation of naphthalene, indene and benzene from cyclopentadiene pyrolysis: experimental and preliminary computational results."]

Abstract

Polycyclic aromatic hydrocarbon (PAH) growth from cyclopentadiene (CPD) pyrolysis was investigated using a laminar flow reactor operated at temperatures ranging from 600 to 950^{o}C. Major products from CPD pyrolysis are benzene, indene and naphthalene. Formation of observed products from CPD is explained as follows. Addition of the cyclopentadienyl radical to a CPD π-bond produces a resonance-stabilized radical, which further reacts by one of three unimolecular channels: intramolecular addition, C-H bond β-scission, or C-C bond β-scission. The intramolecular addition pathway produces a 7-norbornenyl radical, which then decomposes to indene. Decomposition by C-H bond β-scission produces a biaryl intermediate which then undergoes a ring fusion sequence that has been proposed for dihydrofulvalene-to-naphthalene conversion. In this study, we propose C-C bond β-scission pathway as an alternative reaction channel to naphthalene from CPD. As preliminary computational analysis, Parametric Method 3 (PM3) molecular calculation suggests that intramolecular addition to form indene is favored at low temperatures and C-C bond β-scission leading to naphthalene is predominant at high temperatures.

4.1 Introduction

Improved chemical mechanisms for the formation and growth of polycyclic aromatic hydrocarbons (PAHs) in combustion are needed to predict and control emissions of toxic air pollutants and soot. Several PAHs formed from incomplete combustion are known to be mutagenic or carcinogenic. Under fuel-rich conditions, aromatic ring formation is driven mainly by hydrogen abstraction and acetylene addition (HACA), which suggested the sequential formation of PAH products (Homann and Wagner, 1967; Crittenden and Long, 1973; Bockhorn et al., 1983; Frenklach et al., 1984; Cole et al., 1984). It has been suggested, however, that the HACA mechanism is too slow to kinetically explain the formation of large PAHs and the HACA mechanisms were not thermodynamically favorable (Westmoreland et al., 1989). To account for that, the potential importance of resonantly stable free radicals in forming aromatics and PAH in flames was emphasized (Marinov et al., 1996).

The importance of resonantly stable free radicals such as propargyl and cyclopentadienyl (CPDyl) radicals in forming aromatics and PAH in flames has been addressed because they can achieve high concentrations in thermal systems (Westmoreland et al., 1989; Miller and Melius, 1992; Marinov et al., 1996). Recent studies show that key reactions in the formation of high molecular mass aromatics in flames are the combinations of resonantly stabilized radicals, including cyclopentadienyl self-combination, propargyl addition to benzyl radicals, and the sequential addition of propargyl radicals to aromatic rings (D'Anna and Violi, 1998; Violi et al., 1999; Violi et al., 2001). The authors also showed that the total organic material collected in the flame is the result of a fast reactive coagulation of these small aromatics, forming structures of high molecular mass. Soot formation occurs through a slow process of dehydrogenation and aromatization of the high molecular mass compounds. This process seems to be the controlling step in slightly sooting conditions, which are of practical interest in diffusion flames (D'Anna, 2000). Due to the delocalization of the radical, these resonance-stabilized radicals can undergo several reaction channels at multiple sites of addition and subsequent condensation to form larger,

fused PAH (Spielmann and Cramers, 1972; Gomez et al., 1984; Manion and Louw, 1989; Lamprecht et al, 2000).

Recent experimental results obtained by Violi et al. (1999) suggest that fast reactions of small PAHs rather than acetylene predominantly contribute to formation of high molecular mass structures, soot inception and particulate mass growth in oxidative environments. Due to delocalization of the radical site, these resonance-stabilized radicals can undergo several reaction channels at multiple sites of addition and subsequent condensation to form larger, fused PAHs (Spielmann and Cramers, 1972; Gomez et al., 1984; Manion and Louw, 1989; Lamprecht et al., 2000).

The CPDyl radical is considered to be an important intermediate in PAH formation due to its ability to undergo self-recombination (Westmoreland et al., 1989; Manion and Louw, 1989) and form aromatic products (Friderichsen et al., 2001). Recombination and rearrangement of CPDyl radicals has been recognized as an important route to naphthalene formation in flames (Dean, 1985; Melius et al., 1996; Ritcher et al., 2000; Lu, 2000; Mulholland et al., 2000), and the pathways have been included in several kinetic models describing PAH growth (Dean, 1985; Marinov et al., 1996; Ritcher et al., 2000). Based on a theoretical approach, Melius and co-workers (1996) proposed the formation of naphthalene from the self-recombination of CPDyl radicals to form 9,10-dihydrofulvalene, followed by conversion of five-member rings to six-member rings. Ritcher et al. (2000) confirmed that CPDyl radical self-recombination was the major pathway to naphthalene in a benzene premixed flame. Furthermore, the recent observation of 9,10-dihydrofulvalene formation from anisole (Friderichsen et al., 2001) gives more support for the recombination route of CPDyl radicals to naphthalene.

Researchers in our laboratory experimentally investigated PAH growth from cyclopentadiene and indene, a benzoderivative of cyclopentadiene, in the postflame conditions (Lu, 2000; Mulholland et al., 2000; Lu and Mulholland, 2001). Reaction pathways for the formation of chrysene, benz[a]anthracene and benzo[c]phenanthrene from indene were proposed

in analogy to the dihydrofulvalene-to-naphthalene mechanism proposed by Melius et al. (1996). We also highlighted a possible reaction pathway for the formation of benzofluorenes ([a] and [b] isomers) from indene and a pathway for the formation of indene from cyclopentadiene involving a bridged intermediate.

In this chapter, a detailed study for the formation of PAH from cyclopentadiene in pyrolytic conditions using a laminar flow reactor is presented. Preliminary computational results using semi-empirical molecular orbital methods are presented to describe the reaction pathways for the addition of cyclopentadienyl addition to cyclopentadiene.

4.2 Experimental Section

A laminar flow, isothermal quartz tube reactor (40 cm in length and 1.7 cm in diameter) was used to study PAH formation from cyclopentadiene. Due to the instability of cyclopentadiene (CPD) at room temperature, commercially available dicyclopentadiene ($C_{10}H_{12}$), dimer of CPD, was used as a reactant. Dicyclopentadiene (DCPD) is converted into CPD when heated beyond its boiling point of 175^{o}C (Lu, 2000). DCPD was heated to liquid form (34^{o}C) and fed by a syringe pump into a heated glass vessel where the reactant was vaporized and mixed with a nitrogen gas stream. The gas stream entering the reactor consisted of 0.7 % molar CPD vapor in nitrogen. Experiments were conducted at temperatures ranging from 600 to 950^{o}C. A reactor residence time of 2 to 3 seconds was maintained. The product stream was immediately quenched at the outlet of the reactor and collected in a dual ice-cooled dichloromethane trap. Soot, defined as the dichloromethane insoluble fraction, was separated by vacuum filtration and measured gravimetrically.

Filtered samples were analyzed using by Hewlett Packard GC/MS with HP5-ms column. Due to high volatility of CPD and its co-elution with the solvent, CPD concentrations were separately measured from gas samples with direct injection of the gas samples into the GC-MS column. Aromatic products were identified and quantified using chemical standards, which

included benzene, indene, naphthalene, toluene, styrene, fluorene, phenanthrene, anthracene, 2-methyl indene, and 1,2-dihydrofulvalene.

The heat of formation, ΔH_f, for intermediate and transition state species for the dihydrofulvalene-to-naphthalene mechanism of Melius et al. (1996) and for alternative CPDyl-CPD product rearrangements were calculated using the Parametric Method 3 (PM3) empirical quantum method in the MOPAC version 6.0, suite of codes. Transition state species were determined using the SADDLE and TRANS options in the MOPAC program and following standard procedures for optimizing and checking results (Stewart, 1990; Stewart, 1994). Then, thermodynamic properties of reactant and transition states for alternative CPDyl-CPD product rearrangements were calculated and used to obtain the kinetic constants. The transition state theory expression used to determine the rate constant is

$$k(T) = \frac{k_B T}{h} \exp(\Delta S^t / R) \exp(-\Delta H^t / RT)$$

where k_B is Boltzmann's constant, h is Planck's constant, ΔH^t and ΔS^t are the differences in enthalpy and entropy, respectively, between the transition state and the reactant, R is the universal gas constant and T is the absolute temperature.

4.3 Results and Discussion

4.3.1 Pyrolytic Product Yields

Yields of total carbon recovery, aromatic compounds, CPD and soot over the temperature ranged from 600 to 950°C are shown in Figure 4.1, expressed as a percent of carbon input. Soot was assumed to be pure carbon. Carbon recoveries of 80% and above were achieved until 850°C. Low carbon recoveries at temperatures of 875°C and above are attributed primarily to unrecovered soot that could not be rinsed from the quartz tube wall. PAH product yields ranged from 2.7% of carbon input at 600°C to 82% at 850°C. Observed CPD yields were greater than

90% of carbon input until 700°C. DCPD was below detection. Above 700°C, CPD begins to react in significant amounts with more than 99% of the CPD reacted at 825°C. Soot formation was observed at 850°C and above, with soot yield increasing with temperature.

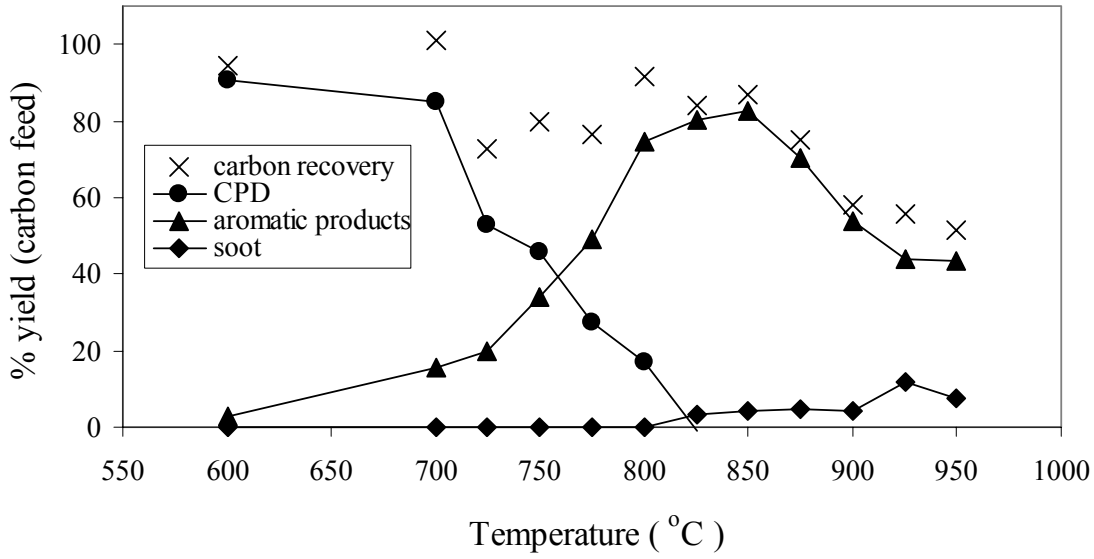

Figure 4.1 Yields of total carbon recovery, CPD, aromatic compounds and soot from CPD pyrolysis

The major products from CPD pyrolysis were benzene, indene and naphthalene, and their yields are shown in Figure 4.2. The amount of indene produced exceeded that of naphthalene and benzene for temperatures lower than 775°C. Between 775°C and 900°C, naphthalene yield was greatest, and above 900°C, benzene formation becomes predominant. The high carbon recovery and the absence of other products indicate that CPD ring fragmentation and subsequent growth through the HACA mechanism is not dominant until temperatures exceed 850°C. Naphthalene yield started decreasing at temperatures above 850°C whereas benzene yield increased with

temperature. This trend may indicate that the reaction between CPD and acyclic fragment becomes the dominant reaction in this temperature range.

The formation of benzene and indene supports the existence of the CPDyl-CPD addition pathway (Lu, 2000; Mulholland et al., 2000; Lu and Muholland, 2001; Lu and Muholland, 2004). Naphthalene can be formed by the CPDyl-CPD addition pathway or the CPDyl-CPDyl recombination pathway (Melius et al., 1996). Intermediates with molecular formula $C_{10}H_{10}$ in the formation of these products were detected. Yields of two methyl indenes, a dihydronaphthalene, and one unidentified $C_{10}H_{10}$ intermediate are shown in Figure 4.3.

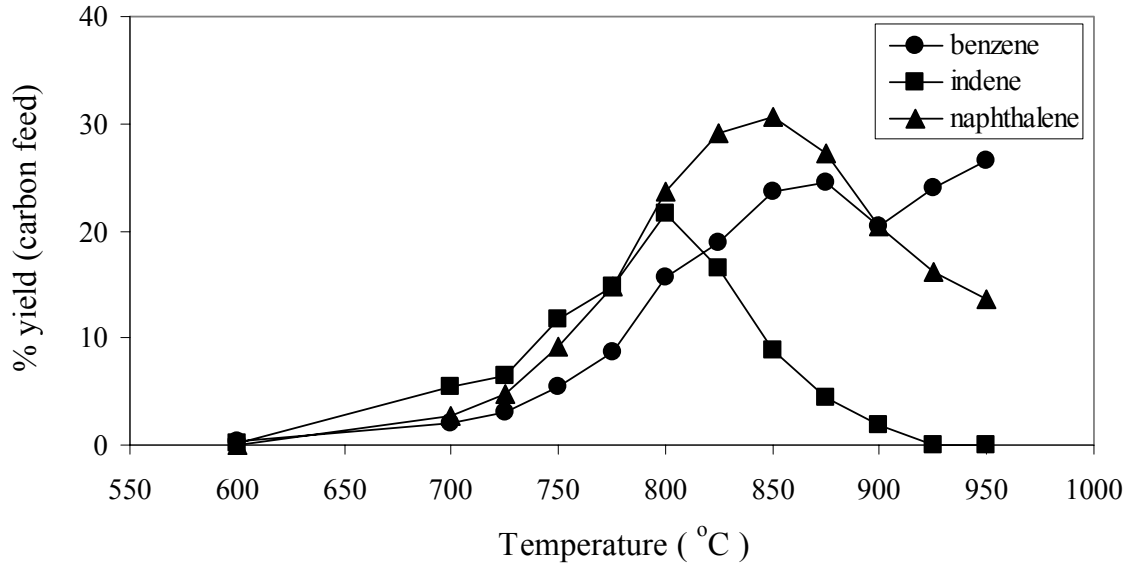

Figure 4.2 Major product yields from CPD pyrolysis

Based on the mass spectrum of the unidentified $C_{10}H_{10}$ compound, we believe that this hydrocarbon is either methyl indene or dihydronaphthalene, not dihydrofulvalene. The order of principal m/z peaks associated with this hydrocarbon (130, 129, and 115) is not consistent with the published order of principal m/z peaks in a dihydrofulvalene (129 and 130) (Beach, 1990).

Moreover, this hydrocarbon does not have a big half-ion peak at 65 m/z whereas both 1,1- and 1,2-biinenyl containing a dihydrofulvalene moiety have a distinguished feature of a big half-ion peak at 115 m/z (Lu, 2000). Formation pathways involving these intermediates will be discussed later.

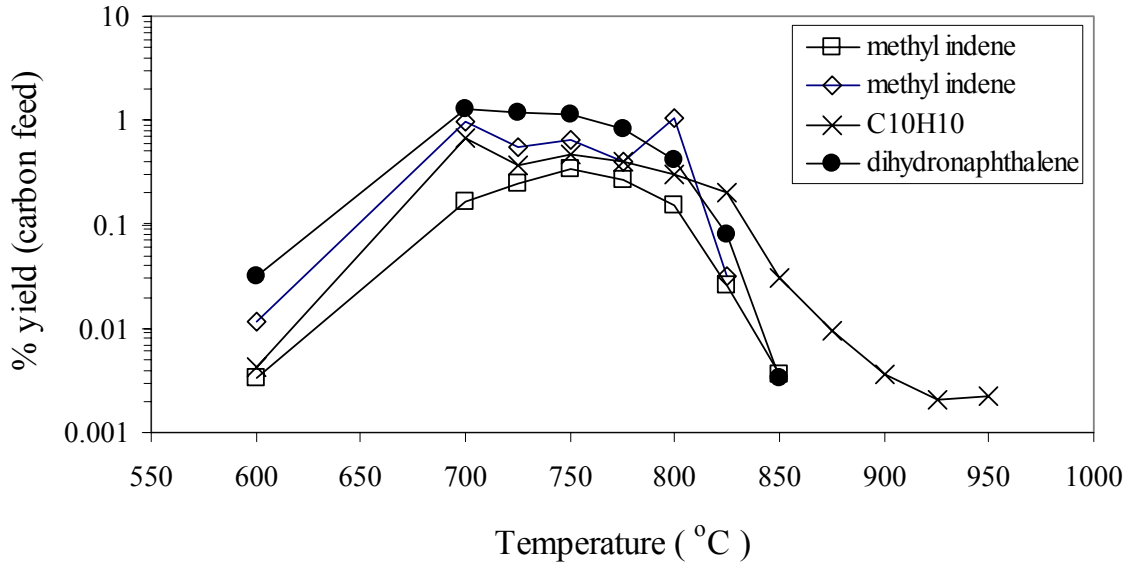

Figure 4.3 $C_{10}H_{10}$ product yields from CPD pyrolysis

Other aromatic compounds experimentally observed were toluene, styrene, fluorene, phenanthrene and anthracene, and their yields are shown in Figure 4.4. Fluorene, phenanthrene and anthracene can be formed from the reaction between CPD and indene, consistent with previous studies (Lu, 2000; Mulholland et al., 2000; Lu and Muholland, 2001; Lu and Muholland, 2004). Toluene and styrene are likely formed from the reactions involving CPD, benzene and acyclic fragments.

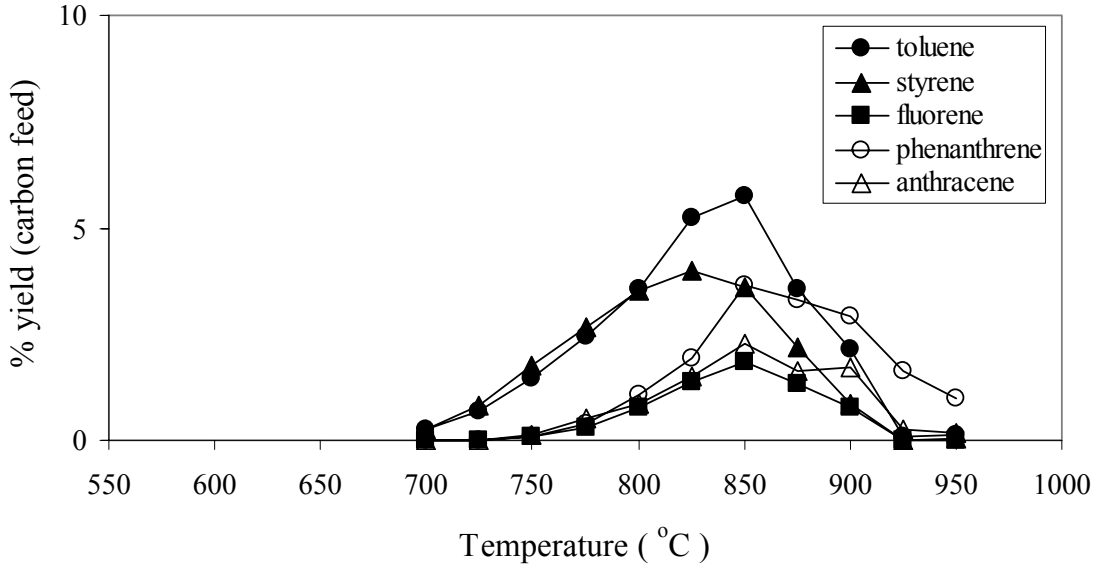

Figure 4.4 Other aromatic product yields from CPD pyrolysis

4.3.2 Pathways of Naphthalene, Indene and Benzene Formation from CPD

Based on previous experimental work on indene (Lu, 2000) and a mixture of CPD and indene (Mulholland et al., 2000), and on the computational study of CPD (Melius et al., 1996), possible reaction pathways from CPD are proposed to explain the major products of CPD pyrolysis: benzene, indene, and naphthalene (Figure 4.5).

All of the routes begin with the addition of CPDyl to CPD to form intermediate I1. Alternative intramolecular rearrangements lead to the major products via this intermediate. In Figure 4.5, the intramolecular addition reactions (R1 and R2) lead to the formation of bridged intermediates. Bridge opening and loss of H atom produce 4-methyl indene or 7-methyl indene; subsequent loss of methyl radical produces indene. Methyl radical produced by this pathway can react with CPD to form fulvene, which can isomerize to benzene (Madden et al., 1996). Our experimental observation of two methyl-indenes and indene is consistent with the intramolecular addition pathways R1 and R2.

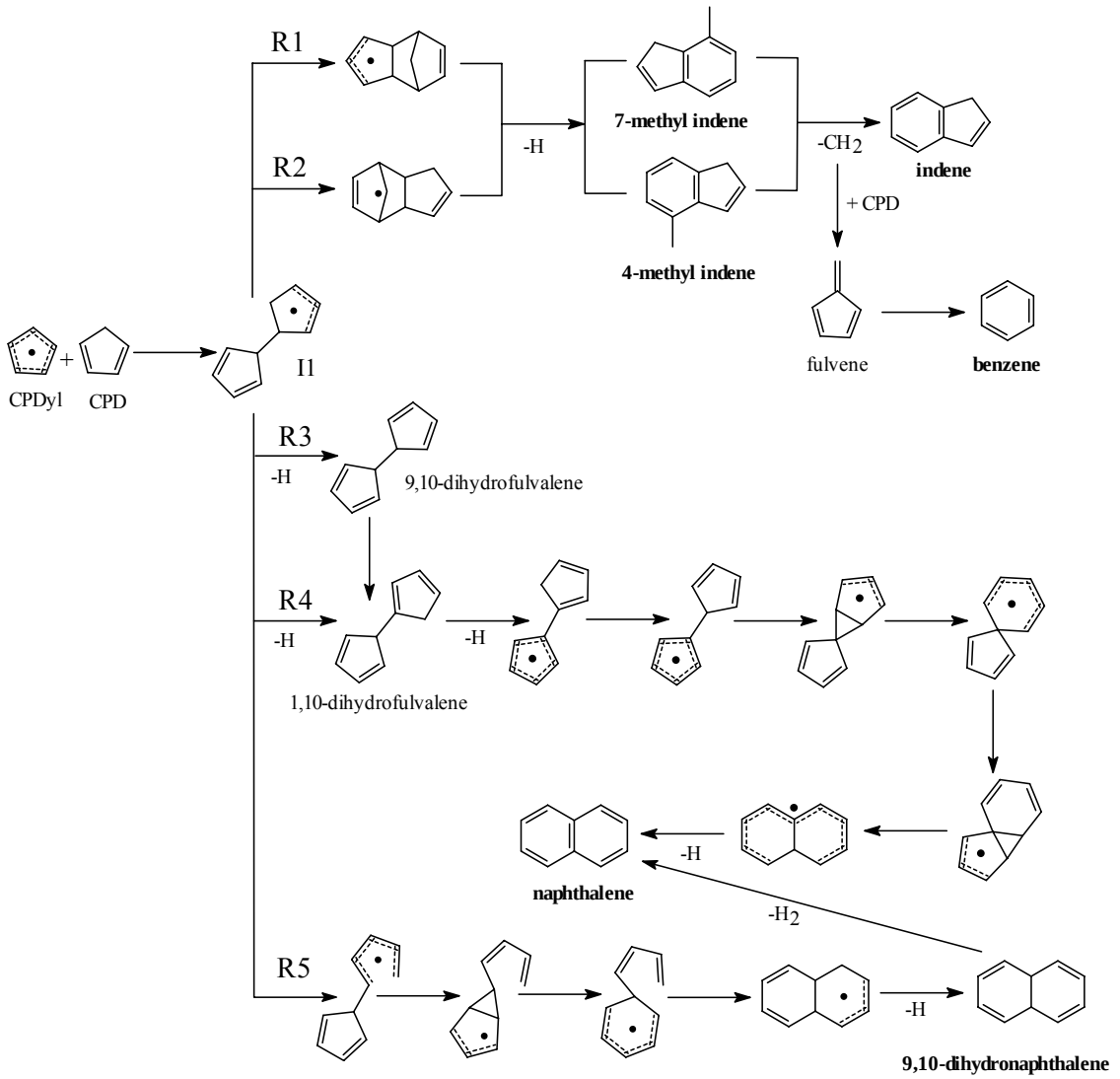

Figure 4.5 Reaction pathways to indene, benzene and naphthalene from CPDyl-CPD (I1); products observed in experiments are written in bold

Competing with the formation of the bridged compounds via intramolecular addition is the formation of dihydrofulvalenes via beta-scission of H atom (R3 and R4, Figure 4.5). The reaction mechanism of the dihydrofulvalene-to-naphthalene has been studied using the BAC-MP4

and BAC-MP2 methods (Melius et al., 1996). The CPDyl-CPD intermediate (I1) undergoes C-H bond cleavage to form either 9,10-dihydrofulvalene (R3) or 1,10-dihydrofulvalene (R4). 9,10-dihydrofulvalene can form 1,10-dihydrofulvalene via H-atom shift (Melius et al., 1996). As described elsewhere (Melius et al., 1996; Friderichsen et al., 2001), the fusion of the bicyclic dihydrofulvalene occurs by three-member ring closure and ring opening, resulting in naphthalene.

Another competing reaction channel is C-C β-scission, shown as R5 in Figure 4.5. Ring expansion of cyclopentadiene to a six-member ring via the formation of a three-member ring, analogous to the conversion of methylcyclopentadienyl radical to benzene (Madden et al., 1996; Dubnikova and Lifshitz, 2002), leads to the formation of butyl-cyclohexadienyl radical. Cyclodehydrogenation leads to naphthalene. The experimental identification of dihydronaphthalene, which is not expected from the C-H β-scission routes (Figure 4.5), supports the proposed C-C β-scission route.

4.3.3 Preliminary Computational Analysis of Alternative CPDyl-CPD (I1) Reactions

The PM3 method was selected for preliminary analysis because it is efficient and more accurate for aromatic systems than the other semi-empirical methods (Lu, 2000; Stewart, 1990, 1994). In order to verify the accuracy of the PM3 method for our system, we compare PM3 results with BAC-MP2 method results (Melius et al., 1996) on the heats of formation for the intermediates and the transition states in the dihydrofulvalene-to-naphthalene mechanism (R4, Figure 4.5). The comparison is shown in Figure 4.6. The main discrepancy between the two methods is in the computed values for the heat of formation of the two three-member ring closing transition states. However, the qualitative agreement between the two methods indicates that the PM3 method can be used as a screening tool for preliminary computational study of this system.

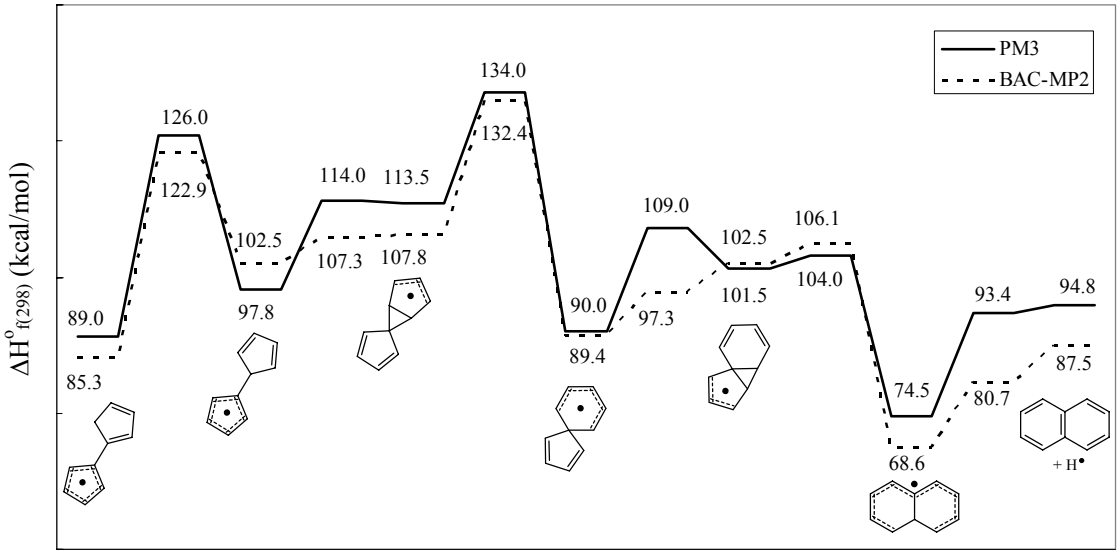

Figure 4.6 Comparison between PM3 and BAC-MP2 methods for the dihydrofulvalene-to-naphthalene reaction pathway (R4)

The relative energies of the reactant (I1), transition states and products of the alternative reaction steps in R1 through R5 are shown in Figure 4.7. The two intramolecular addition channels that form norborenyl structures are the lowest energy paths, The C-C bond β-scission reaction (R5) is lower in energy than the C-H bond β-scission reactions (R3 and R4). On the other hand, formation of the nonborenyl structures by intracmolecular addition (R1 and R2) is expected to be less favored over β-scission reactions (R3 and R5) based on entropy consideration.

Using transition state theory, rate constants for the second-steps in the radical-molecule pathways were calculated. The calculated rate constants are plotted in Figure 4.8 as a function of temperature. The results show that the rate constants for the five unimolecular reactions are of comparable magnitudes at a temperature of about 1000 K (725^{o}C).

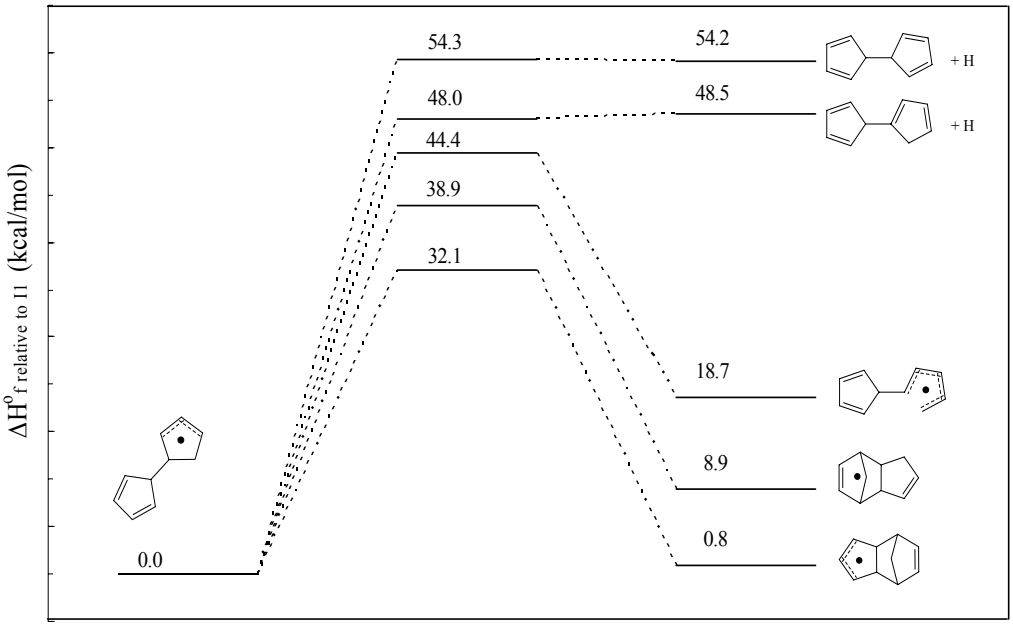

Figure 4.7 PM3 energy diagrams for alternative unimolecular reactions of CPDyl-CPD (I1)

At lower temperatures, the intramolecular addition pathways (R1 and R2) are favored over the β-scission pathways due to lower transition state enthalpies. At high temperatures, the β-scission pathways (R3, R4 and R5) are favored due to higher transition state entropies. These results are qualitatively consistent with the experimental observation that the intramolecular addition product, indene, is favored at temperatures below 750^{o}C whereas the β-scission product, naphthalene, is favored at temperatures above 800^{o}C.

It should be noted that these reaction pathways consist of a series of reaction steps. In order to determine overall reaction kinetics, complete energy profiles for each reaction channel need to be calculated. In addition, bimolecular reactions, such as H-atom abstraction by H atom, were not considered. Thus, the computational results are appropriate for H-atom poor conditions. In Part II of this submission, a more detailed computational analysis is performed on this system using higher level molecular modeling methods.

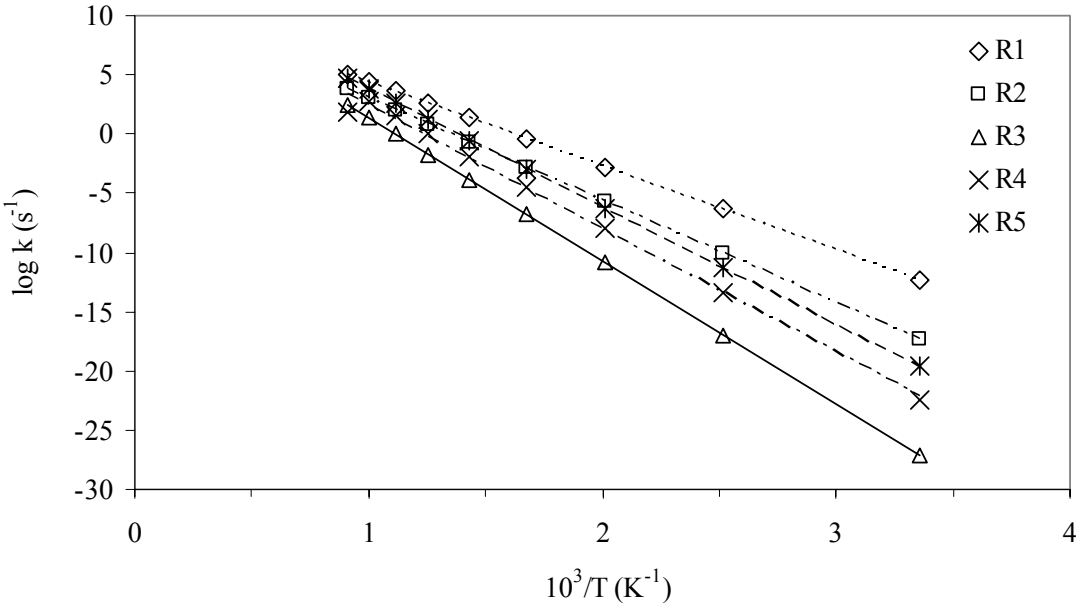

Figure 4.8 Arrhenius plots for the alternative unimolecular reactions of CPDyl-CPD (I1)

4.4 Conclusions

Experimental study of PAH formation from CPD pyrolysis was carried out in a laminar flow tube reactor between 600 and 950°C. The main products identified were indene and benzene through the intramolecular addition routes (R1 and R2) and naphthalene via β-scission routes (R3, R4 and R5). Identification of stable intermediates supports the proposed formation routes. The intramolecular addition products were favored at low temperatures whereas β-scission product was favored at high temperatures. At temperatures above 850°C, the reaction between CPD and acyclic fragments appears to be dominant. Observation of fluorene, phenanthrene and anthracene indicates that the reaction of CPD with indene leads to the formation of other PAHs via similar reaction routes.

Preliminary computational study using PM3 was performed on the proposed radical-molecule pathways. Comparison of PM3 results with BAC-MP2 method on the heats of formation for the intermediates and the transition states in the dihydrofulvalene-to-naphthalene mechanism (R4) show that PM3 can be used as a screening tool for higher level theory. The

preliminary computational results are in qualitative agreement with the experimental findings. Further computational study is needed to provide more detailed kinetic information for the proposed pathways.

4.5 References

Beach, D.B., Design of low-temperature thermal chemical vapor deposition processes. *IBM J. Res. Develop.* 34(6):795-805 (1990).

Bockhorn, H., Fetting, F. and Wenz, H.W., Investigation of the formation of high molecular hydrocarbons and soot in premixed hydrocarbon-oxygen flames. *Ber Bunsenges Phys. Chem.* 87:1067-1073 (1983).

Crittenden, B.D. and Long, R., Formation of polycyclic aromatics in rich premixed acetylene and ethylene flames. *Combust. Flame.* 20:359-368 (1973).

Cole, J.A., Bittner, J.D., Longwell, J.P. and Howard, J.B., Formation mechanisms of aromatic compounds in aliphatic flames. *Combust. Flame* 56:51-70 (1984).

D'Anna, A., Violi, A., A kinetic model for the formation of aromatic hydrocarbons in premixed laminar flames. *Proc. Combust. Inst.* 27 :425-433 (1998).

D'Anna, A., Violi, A., D'Alessio, A., Modeling the rich combustion of aliphatic hydrocarbons. *Combust. Flame* 121:418-429 (2000).

Dean, A.M., Predictions of pressure and temperature effects upon radical addition and recombination reactions. *J. Phys. Chem.* 89:4600-4608 (1985).

Dubnikova, F. and Lifshitz, A., Ring expansion in methylcyclopentadiene radicals: Quantum chemical kinetic calculations. *J. Phys. Chem. A* 106:8173-8183 (2002).

Frenklach, M., Clary, D.W., Cardiner, W.C. and Stein, S.E., Detailed kinetic modeling of soot formation in shock-tube pyrolysis of acetylene. *Proc. Combust. Inst.* 20:887-901 (1984).

Friderichsen, A.V., Shin, E.-J., Evans, R.J., Nimlos, M.R., Dayton, D.C. and Ellison, G.B., The pyrolysis of anisole ($C_6H_5OCH_3$) using a hyperthermal nozzle. *Fuel* 80:1747-1755 (2001).

Gomez, A., Sidebotham, G. and Glassman, I., Sooting behavior in temperature controlled laminar diffusion flames. *Combust. Flame* 58:5845-5857 (1984).

Homann, K.H. and Wagner, H.G., Some new aspects of the mechanism of carbon formation in premixed flames. *Proc. Combust. Inst.* 11:371-376 (1967).

Lamprecht, A., Atakan, B. and Kohse-Höinghaus, K., Fuel-rich flame chemistry in low-pressure cyclopentadiene flames. *Proc. Combust.* Inst. 28:1817-1824 (2000).

Lu, M., Formation of growth of polycyclic aromatic hydrocarbons by cyclopentadienyl moieties in combustion. Ph. D. thesis, Georgia Institute of Technology, Atlanta, USA (2000).

Lu, M. and Mulholland, J.A., Aromatic Hydrocarbon Growth from Indene. *Chemosphere* 42:189-197 (2001).

Lu, M. and Mulholland, J.A., PAH growth from the pyrolysis of CPD, indene and naphthalene mixture Chemosphere 55:605-610 (2004).

Madden, L.K., Mebel, A.M., Lin, M.C. and Melius, C.F., Theoretical study of the thermal isomerization of fulvene to benzene. *J. Phys. Org. Chem.* 9(12):801-810 (1996).

Manion, J. and Louw, R., Rates, products, and mechanisms in the gas-phase hydrogenolysis of phenol between 922 and 1175 K. *J. Phys. Chem.* 93:3563-3574 (1989).

Marinov, N.M., Pitz, W.J., Westbrook, C.K., Castaldi, M.J. and Senken, S.M., Modeling of aromatic and polycyclic aromatic hydrocarbon formation in premixed methane and ethane flames. *Combust Sci. Technol.* 116:117-211 (1996).

Melius, C.F., Colvin, M.E., Marinov, N.M., Pitz, W.J. and Senkan, S.M., Reaction mechanisms in aromatic hydrocarbon formation involving the C_5H_5 cyclopentadienyl moiety. *Proc. Combust. Inst.* 26:685-692 (1996).

Miller, J.A. and Melius, C.F., Kinetic and thermodynamic issues in the formation of aromatic compounds in flames of aliphatic fuels. *Combust. Flame* 91:21-39 (1992).

Mulholland, J.A., Lu, M. and Kim D.-H., Pyrolytic growth of polycyclic aromatic hydrocarbons by cyclopentadienyl moieties. *Proc. Combust. Inst.* 28:2593-2599 (2001).

Richter, H., Benish, T.G., Mazyar, O.A., Green, W.H. and Howard, J.B., Formation of polycyclic aromatic hydrocarbons and their radicals in a nearly sooting premixed benzene flame. *Proc. Combust. Inst.* 28:2609-2618 (2000).

Spielmann, R. and Cramers, C.A., Cyclopentadienic compounds as intermediates in the thermal degradation of phenols: Kinetics of thermal decomposition of cyclopentadiene. *Chromatographia* 5:295-300 (1972).

Stewart, J.J.P., MOPAC: A semiempirical molecular orbital program. *J. Com. Mol. Design* 4:1-105 (1990).

Stewart, J.J.P., MOPAC 93 Manual. 2nd rev. Fujitdu Limited (1994).

Violi, A, D'anna, A. and D'Alessio, A., Modeling of particulate formation in combustion and pyrolysis. *Chem. Eng. Sci.* 54:3433-3442 (1999).

Violi, A., Sarofim, A.F., Truong, T.N., Quantum mechanical study of molecular weight growth process by combination of aromatic molecules. *Combust. Flame* 126(1/2):1506-1515 (2001).

Westmoreland, P.R., Dean, A.M., Howard, J.B. and Longwell, J.P., Forming Benzene in Flames by Chemically Activated Isomerizations. *J. Phys. Chem.* 93:8171-8180 (1989).

CHAPTER 5

PAH GROWTH FROM PYROLYSIS OF CYCLOPENTADIENE, ACENAPHTHYLENE, STYRENE AND PHENANTHRENE MIXTURES

Abstract

Polycyclic aromatic hydrocarbon (PAH) growths from cyclopentadiene (CPD)-acenaphthylene, CPD-styrene and CPD-phenanthrene mixtures were investigated in a laminar flow reactor over a temperature range of 600^{o}C to 1000^{o}C under pure pyrolysis conditions. The pyrolysis of all three mixtures produced low product yields and less variety of products compared to the pyrolysis of CPD alone. The major products (naphthalene, indene and benzene) and their yields from the pyrolysis of the mixtures were similar to those from the pyrolysis of CPD alone, indicating that the reactivity of CPD to different π bonds is much less comparative than that of CPD to itself. The main difference between CPD and CPD-acenaphthylene mixture pyrolysis is the yields of fluoranthene, acephenanthrylene and aceanthrylene. A comparison of the product distributions from both pyrolysis indicates that fluoranthene, acephenanthrylene and aceanthrylene are formed from the reaction between CPD and acenaphthylene. The higher yield of fluoranthene compared to yields of acephenanthrylene and aceanthrylene suggests that CPDyl radicals likely add to the external π-bond of acenaphthylene. In CPD-styrene mixture pyrolysis, both CPD-CPD reaction and styrene decomposition are dominant reaction channels to major products: benzene, toluene, naphthalene and indene. Yields of biphenyl and benzene from CPD-styrene mixture were a couple of orders greater than those from CPD alone. In case of CPD-phenanthrene mixture pyrolysis, low consumption rates of phenanthrene indicate that PAH growth from the addition of CPDyl radical to a π-bond on fused aromatic rings is much less favorable. To explain the observed products, the formation pathways involving a bridged intermediate were proposed.

5.1 Introduction

A better understanding of the formation and growth of PAH in combustion is needed to predict and control emissions of toxic air pollutants and soot. Several PAHs formed from incomplete combustion are known to be mutagenic or carcinogenic. Under fuel-rich conditions, aromatic ring formation is driven mainly by hydrogen abstraction and acetylene addition (HACA) (Franklach et al., 1984; Westmoreland et al., 1989). Marinov and co-workers (1996), however, concluded that acetylene addition processes could not account for the PAH levels observed in experimental flames; their results suggest that the large aromatics originate from resonance-stabilized CPDyl radicals, produced in the flames by cyclization of aliphatic compounds and by decomposition of aromatic compounds such as phenol, benzene, toluene and xylenes. The importance of cyclopentadienyl (CPDyl) radical in PAH growth and soot formation has been addressed recently because this radical is resonantly stabilized over all of its five carbon atoms and have high sooting tendencies (McEnally and Pfefferle, 1998).

Using a quantum molecular modeling method, Melius and co-workers (1996) proposed the formation of naphthalene from the self-recombination of CPDyl radicals to form 9,10-dihydrofulvalene, followed by conversion of five-member rings to six-member rings. The recent observation of 9,10-dihydrofulvalene formation from anisole (Friderichsen et. al, 2001) provides additional support for the recombination route of CPDyl radicals to naphthalene. Marinov et al. (1996) suggested that phenanthrene could have been formed by indenyl and CPDyl combination in propane pyrolysis experiment.

In addition to the recombination route of CPDyl radical, researchers in our laboratory proposed a pathway of CPDyl radical addition to CPD molecule involving a bridged intermediate (containing the 7-norborenyl moiety) to account the observed aromatic products from CPD and indene individually and as a mixture (Lu and Mulholland, 2001; Mulholland et al., 2001). This alternative route leads to the products retaining CPD moiety that have a great facility to undergo more reactions for further growth. Moreover, the formation of five-member rings in combustion

system is more concerned because of the genotoxic activity of the compounds with five-member rings (Gooijer et al., 1998). Other fused PAHs in a combustion system are also susceptible to the CPDyl radical addition and subsequent condensation to form larger PAHs; however, PAH formation and growth from the reaction of CPD to compounds without CPD moieties were not reported.

In this chapter, the reaction pathways of CPDyl radical are extended to aromatic species containing different types of π bonds; acenaphthylene, styrene and phenanthrene. Acenaphthylene was selected for this study because it is one of the most prevalent PAH and is representative of fully conjugated PAHs containing both an external five-member ring and an aromatic ring. Styrene is a simple aromatic molecule containing a vinyl substituent that is most susceptible to radical addition. Phenanthrene has a reactive π-bond that is part of a six-member ring.

In all three cases, rearrangement of the addition product to form a structure containing a dihydrofulvalene moiety, which is a prerequisite for PAH fusion by the CPD-to-naphthalene mechanism, is not possible without disrupting an aromatic ring. Moreover, the carbon-carbon bond *beta*-scission (other than the addition reverse reaction) would yield a vinyl-type radical rather than a resonance-stabilized allyl-type radical. Therefore, the major PAH products from CPD reaction with acenaphthylene, styrene and phenanthrene will be those listed below, produced via norbornenyl-type bridged intermediates.

$$2\ \text{CPD} + \text{acenaphthylene} \rightarrow \text{fluoranthene} + \text{benzene}$$

$$2\ \text{CPD} + \text{styrene} \rightarrow \text{biphenyl} + \text{benzene}$$

$$2\ \text{CPD} + \text{phenanthrene} \rightarrow \text{triphenylene} + \text{benzene}$$

5.2 Experimental Method

Thermal reactivity of CPD with acenaphthylene, styrene and phenanthrene was studied in a laminar flow, isothermal quartz tube reactor with 1.7 cm internal diameter and 40 cm length over a temperature range of 600^{o}C to 1000^{o}C. Dicyclopentadiene (DCPD), acenaphthylene, styrene and phenanthrene are commercially available. DCPD is converted to CPD when heated above its boiling point (170^{o}C).

Both acenaphthylene and DCPD are solids at room temperature. Since single or multiple reactants should be in a liquid form to use a syringe pump to maintain a constant feeding rate and to avoid an additional organic solvent, DCPD was preheated above its melting point of 34^{o}C, and then, acenaphthylene was added. The molar ratio of acenaphthylene to DCPD in the mixture was maintained to be 1 to 2 due to the limited solubility of acenaphthylene in DCPD; the mixture remained in liquid state at room temperature. CPD-styrene mixture was prepared by dissolving DCPD in styrene and comprised equal molar of CPD and styrene. CPD-phenanthrene mixture was prepared by dissolving phenanthrene in liquidized DCPD after DCPD was heated above melting point. Molar ratio of DCPD to phenanthrene in the mixture was 4 to 1 due to the low solubility of phenanthrene in DCPD.

The reactants were introduced by the syringe pump into a glass vessel heated above 200^{o}C, and then were vaporized to nitrogen carrier gas. A nominal reactor residence time of 1-5 s was maintained. Input organic vapor concentrations were 0.56% molar CPD and 0.14% molar acenaphthylene in CPD-acenaphthylene pyrolysis, 0.3% molar CPD and 0.3% molar styrene in CPD-styrene pyrolysis, and 0.6% molar CPD and 0.1% phenanthrene in CPD-phenanthrene pyrolysis. The entire gas stream was immediately quenched at the outlet of the reactor.

Aromatic products and soot were collected in a dichloromethane (DCM) dual trap system. Soot, defined as the DCM insoluble fraction, was separated by vacuum filtration and measured gravimetrically. Filtered samples were analyzed by using a Hewlett-Packard 6890 series gas chromatography instrument with HP-5MS column (30m, 0.25 mm i.d., 0.25 μm film

thickness) coupled to a Hewlett-Packard 5973 mass spectrometer. Due to high volatility of CPD and its co-elution with solvent, CPD concentrations were separately measured from the gas sample with direct injection of gas sample into the GC column. Most of the aromatic products were identified and quantified using chemical standards. In the case that there were no standards available, aromatic products were identified on the basis of elution order and quantified by using response factors for compounds of similar size and structure.

5.3 Results and Discussion

5.3.1 CPD-acenaphthylene Mixture Pyrolysis

Total carbon recoveries, reactant recoveries and yields of aromatic compounds and soot are shown as a percent carbon input in Figure 5.1. Total carbon recoveries were higher than 80% until 825^{o}C. Low carbon recoveries at the temperature of 850^{o}C and above are likely due in large part to unextractable soot that cannot be rinsed from the wall of the reactor. Soot was assumed to be pure carbon. Observed CPD yields 700^{o}C were greater than 70% of carbon input until 700^{o}C; DCPD was below detection over the temperatures studied. Above 700^{o}C, CPD consumption rate significantly increased, and yields of CPD were less than 0.4% at temperatures of 900^{o}C and above. Acenaphthylene consumption rate ranged from 8% at 700^{o}C to 99% at 1000^{o}C. Yields of aromatic products reached highest values at 850^{o}C with the conversion of 60%. Soot was formed at 800^{o}C and above with its yield increasing with temperature. For temperature above 850^{o}C, low carbon recovery and a broad range of aromatic products were observed, indicative of CPD and acenaphthylene ring fragmentation.

Major products from the mixture of CPD and acenaphthylene pyrolysis were naphthalene, indene and benzene (Figure 5.2). Naphthalene yield reached a maximum at 850^{o}C with yield of 22%. Yield of benzene ranged from 1% to 17%. Indene yield peaked at 800^{o}C and then decreased with temperature. High yields of benzene, indene and naphthalene suggest the CPD-CPD reaction is a dominant reaction in the pyrolysis of CPD-acenaphthylene mixture.

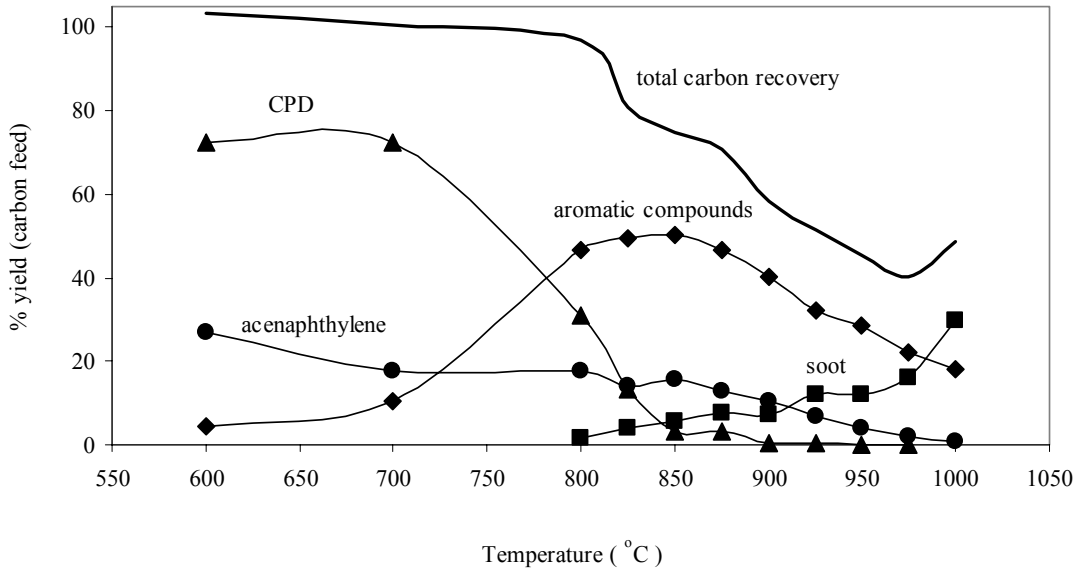

Figure 5.1 Total carbon recoveries, yields of total aromatic products, soot and unreacted reactant from CPD-acenaphthylene mixture pyrolysis

Yields of other aromatic compounds produced are shown in Figure 5.3. Formation of toluene and styrene, that are likely formed from the reaction involving CPD, benzene and acyclic fragments, reached a maximum near 850ºC with yield of 1.5% and 1.7%, respectively. Peak yields of fluorene, phenanthrene and anthracene, which can be formed from the CPD-indene reaction, occurred at 850°C. Formation of C-16 and C-17 species that are expected to be formed from the reaction of CPD and acenaphthylene were not observed at temperatures below 800°C. Observed C-16 compounds were fluoranthene and acephenanthrylene, and their yields are also shown in Figure 5.3. Fluoranthene and acephenanthrylene yields peaked at 900°C (0.6%) and at 875ºC (0.03%), in that order.

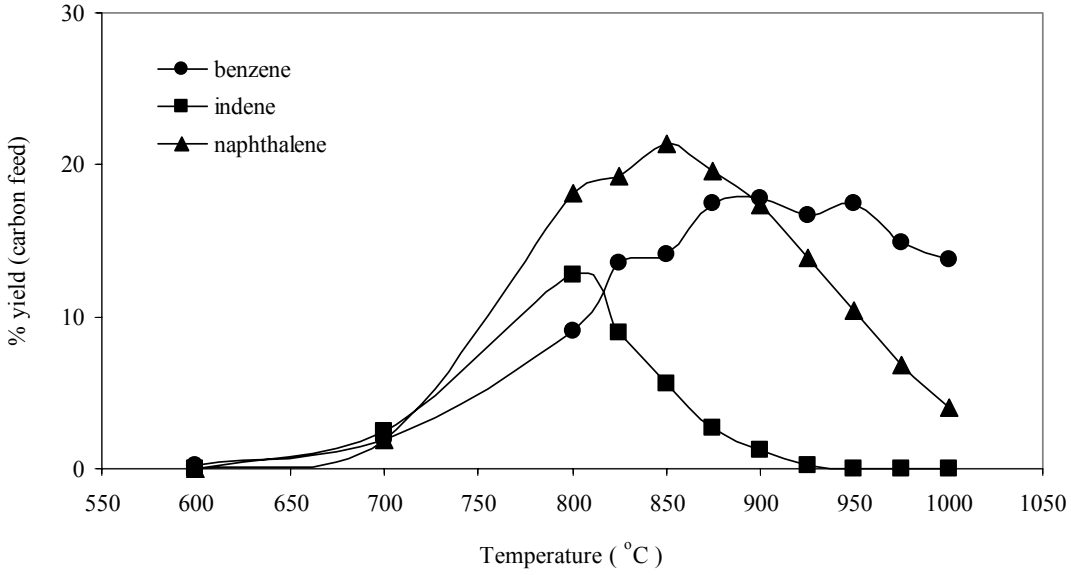

Figure 5.2 Major product yields from CPD-acenaphthylene mixture pyrolysis

Acenaphthylene is both a reactant and a product in the pyrolysis of CPD-acenaphthylene mixture because formation of acenaphthylene was observed even from the pyrolysis of CPD alone (Table A.2 in Appendix A). In order to have a better assessment on PAH growth from the reaction of CPD and acenaphthylene, yields of aromatic products from the pyrolysis of CPD-acenaphthylene mixture are compared with those from the pyrolysis of CPD alone. Product yields from both pure CPD and CPD-acenaphthylene mixture pyrolysis are normalized by CPD input. Data are expressed as a molar ratio of product and CPD input in Figure 5.4 and 5.5.

In Figure 5.4, molar ratios of naphthalene, indene and benzene to CPD input from both pyrolysis are almost same over the temperatures studied; the results support that the CPD-CPD reaction is the dominant reaction in the pyrolysis of CPD-acenaphthylene mixture. The biggest difference between CPD and CPD-acenaphthylene mixture pyrolysis is yields of fluoranthene and acephenanthrylene (Figure 5.5). Both fluoranthene and acephenanthrylene are likely formed from the reaction of CPD and acenaphthylene. The yield of fluoranthene from CPD-acenaphthylene

mixture is greater by a factor of 4 than that from CPD alone. In addition, the ratio of yield of acephenanthrylene from CPD-acenaphthylene mixture relative to that from CPD alone is 3 to 1 and 5 to 1, respectively.

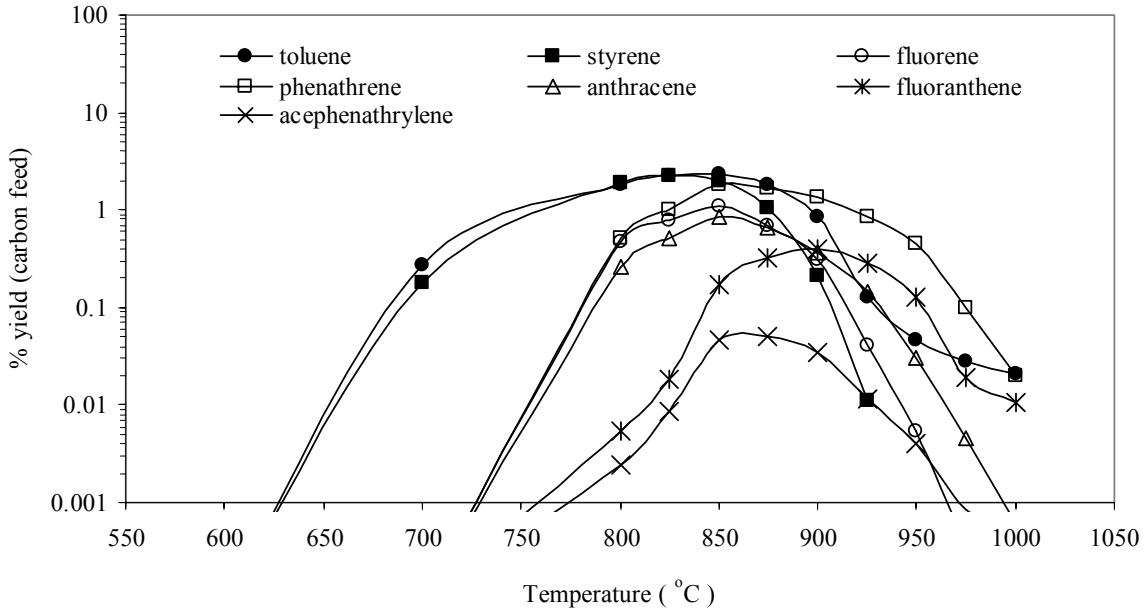

Figure 5.3 Other aromatic product yields from CPD-acenaphthylene mixture pyrolysis

Reaction pathways for naphthalene, indene and benzene formation from CPD have been shown in Chapter 4. Detection of $C_{10}H_{10}$ compounds including methyl indenes and dihydronaphthalene supports the existence of both the pathway of CPDyl addition to CPD molecule involving a bridged intermediate (Mulholland et al., 2000; Lu and Mulholland, 2001) and the CPD-to-naphthalene mechanism (Melius et al., 1996) in CPD-acenaphthylene mixture pyrolysis.

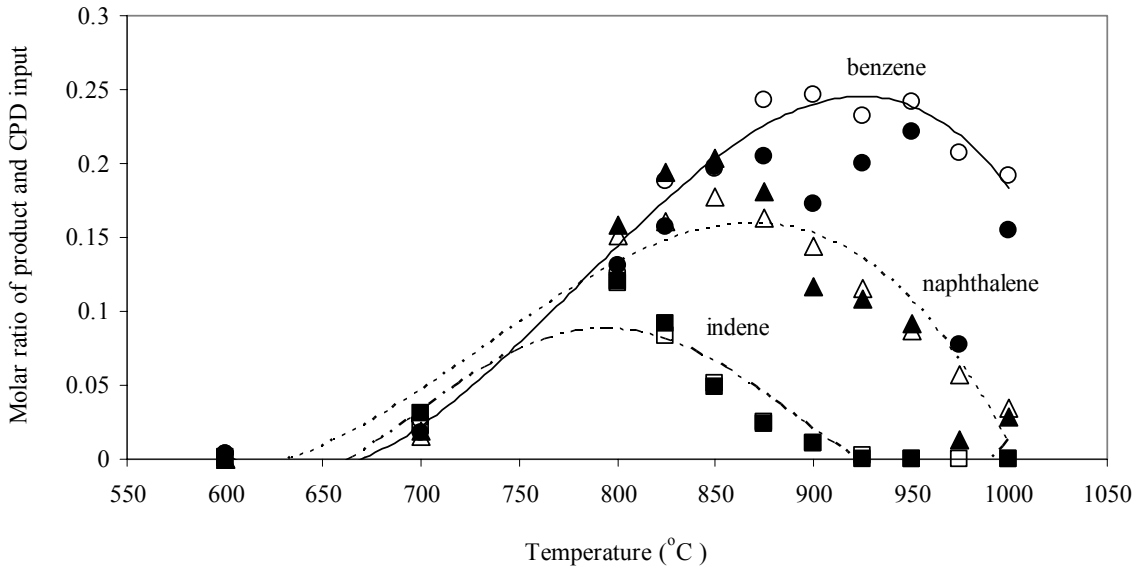

Figure 5.4 Comparison of major aromatic products yields from pure CPD and CPD-acenaphthylene mixture pyrolysis; filled symbols are used for CPD-acenaphthylene mixture pyrolysis products and hollow symbols are used for CPD pyrolysis products

In the case of the CPD-acenaphthylene reaction, rearrangement of the addition product to form a structure containing a dihydrofulvalene moiety, which is a prerequisite for PAH fusion by the CPD-to-naphthalene mechanism, is not possible without disrupting an aromatic ring. None of the $C_{17}H_{14}$ products were detected over the entire temperature studied, suggesting that the contribution of the pathway via three-member ring closures and openings was not important. Thus, it is concluded that the PAH products from CPD reaction with acenaphthylene were produced via norbornenyl-type bridged intermediates.

Here, the reaction pathways for $C_{16}H_{12}$ products from the mixture of CPD and acenaphthylene are proposed (Figure 5.6). Trace amounts of intermediates with molecular formula $C_{17}H_{12}$ in the formation of these products were also detected, but those intermediates were not identified due to the lack of standards.

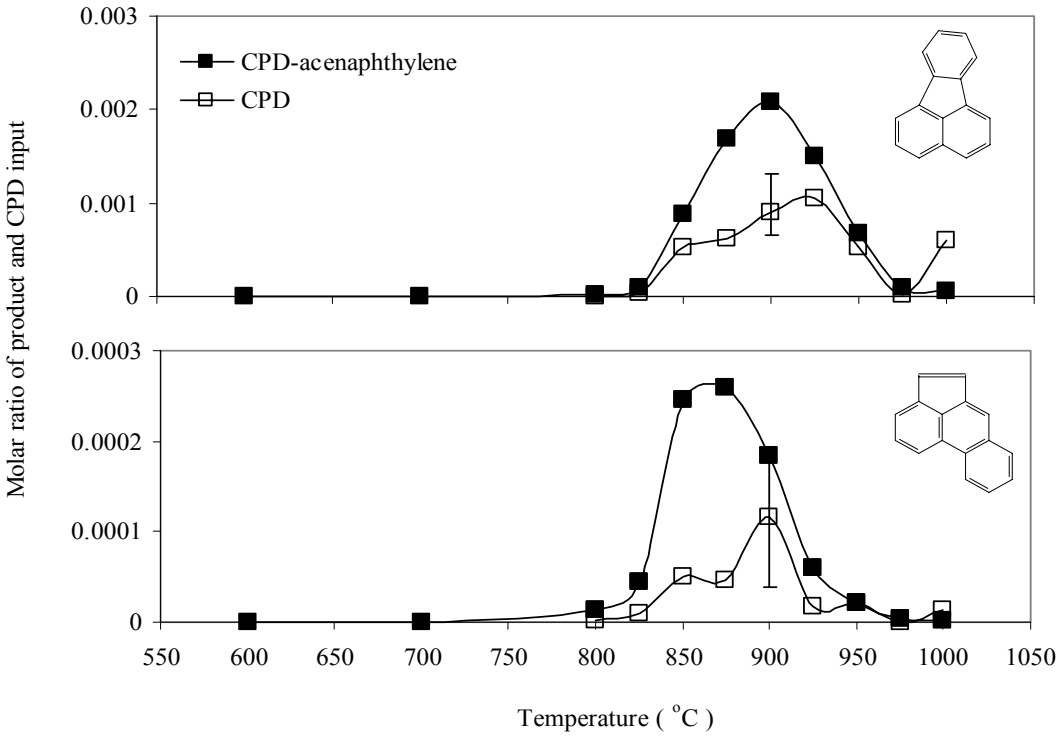

Figure 5.5 Comparison of the $C_{16}H_{12}$ products from CPD and acenaphthylene-CPD mixture pyrolysis; fluornanthene (top) and acephenanthrylene (bottom). Filled symbols are used for CPD-acenaphthylene mixture pyrolysis products and hollow symbols are used for CPD pyrolysis products

CPDyl radical is able to add to two different π-bond of acenaphthylene. The first one is addition of CPDyl radical to the external π-bond of acenaphthylene, which yields a radical intermediate containing the 7-norborneyl moiety followed by a decomposition of methyl fluoranthene to fluoranthene with loss of CH_2. The single carbon species released then combines with CPD to form benzene.

The other three reaction channels initiate with an addition of CPDyl radical to π-bonds in fused six-member rings followed by the same reaction route involving a norborneyl intermediate. Among four channels, the pathway of CPDyl radical addition to the external π-bond in acenaphthylene appears be favored because the yield of fluoranthene was an order of magnitude higher than the yield of acephenanthrylene (Figure 5.3) and only trace amount of aceanthrylene (not shown) was observed.

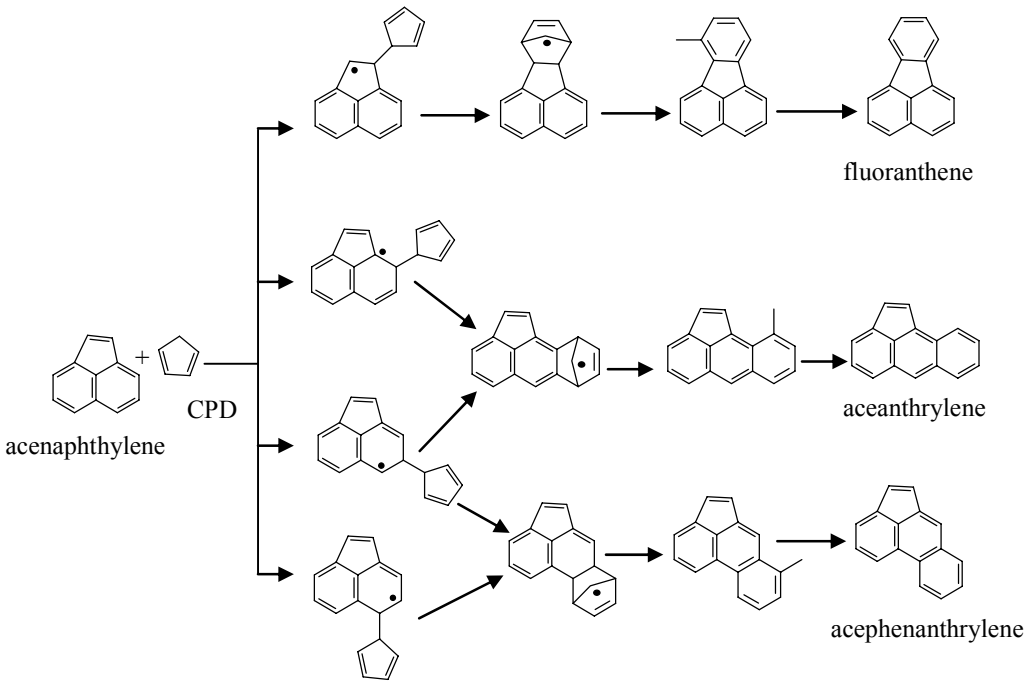

Figure 5.6 Hypothesized pathways of aromatic growth from CPD-acenaphthylene reaction

On the other hand, addition of acenaphthylenyl radical to a π-bond of CPD molecule would also lead to the same $C_{16}H_{12}$ products observed. That is, however, much less favorable

channel since radical formation from fully conjugated PAH is not as easy as that from CPD. Any products from the aryl-aryl reaction of acenaphthylene were not observed.

Although the yields of the products from CPD-acenaphthylene reaction is relatively low, the increased soot formation compared to CPD pyrolysis was observed at the temperatures studied, indicating carbon growth. Low product yields and less variety of products compared to the pyrolysis of CPD alone suggest that the carbon growth products from addition of carbon fragments (e.g. methyl) are also small. Alternatively, the soot growth may be resulted from deposition of reactant vapor on the reactor tube, then growth while on the surface. At high temperatures, this is a common problem. On the other hand, the analytical methods may not be sufficient to collect and analyze the high molecular compounds of interest. In order to better assess PAH formation and growth from CPD-acenaphthylene reaction, it is suggested to use carbon labeled CPD or acenaphthylene and to modify the experimental setup.

5.3.2 CPD-styrene Mixture Pyrolysis

Total carbon recovery, reactant recovery and aromatic compound and soot yields from the pyrolysis of CPD-styrene mixture are shown in Figure 5.7, expressed in a percent yield of carbon feed. Low carbon recoveries at temperatures of 600^{o}C and 700^{o}C are attributed to that CPD yields could not be measured due to the co-elution of CPD with DCM solvent in GC column. However, CPD yields in the exhaust-gas samples from CPD and CPD-acenaphthylene mixture pyrolysis (Figure 4.2 and Figure 5.2) show that more than 90% of DCPD is converted to CPD at a temperature ranging from 600 to 700^{o}C. Carbon recovery rate of 80% to 99% was achieved in the temperature range of 750 to 850^{o}C. Low carbon recoveries at temperatures above 850^{o}C are primarily due to unrecovered soot that could not be rinsed from the quartz tube wall.

More than 90% of styrene (66% of carbon input) was recovered at low temperatures. Decomposition of styrene began around 750^{o}C, and styrene was reacted mostly at 900^{o}C. Yield of total aromatic products (excluding the reactants CPD and styrene) increased with temperature

and peaked at 850°C with a yield of 66%. Soot formation was observed at temperatures of 850°C and above, with soot yield increasing with temperature. Soot was assumed to be pure carbon.

Major products were benzene, toluene, naphthalene and indene, which yields are shown as a percent carbon input in Figure 5.8. Yields of benzene and naphthalene increased with temperature and leveled off. Yields of toluene and indene peaked at 800°C with 6.7% and 4.1%, in that order and then decreased. Unlike CPD and CPD-acenaphthylene mixture pyrolysis, benzene and toluene yields were greater than indene and naphthalene yields at low temperatures, indicating that benzene and toluene are likely formed from the decomposition of styrene. High yields of indene and naphthalene suggest that the reactivity of CPD to itself is much higher than to styrene.

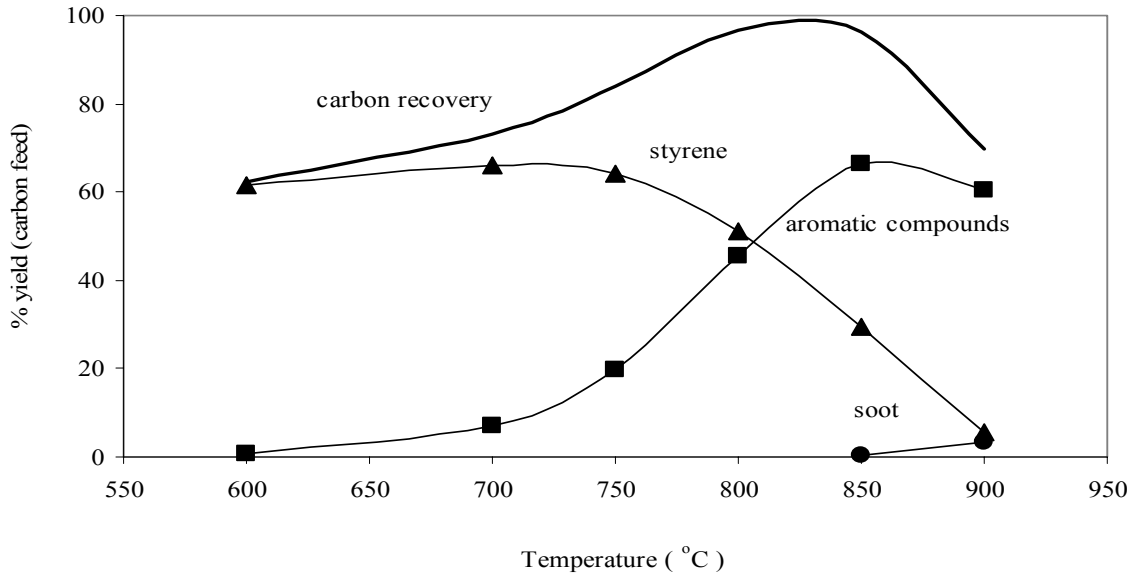

Figure 5.7 Overall reaction profile of CPD-styrene mixture pyrolysis

Formation of biphenyl, fluorene and phenanthrene was observed at temperatures of 750°C and above. We believe that both fluorene and phenanthrene are formed from the reaction

between CPD and indene based the previous results from CPD-indene mixture pyrolysis (Lu, 2000; Mulholland et al., 2000). Formation of indene, naphthalene, fluorene and phenanthrene suggests the existence of both a radical-radical pathway analogous to the CPD-to-naphthalene mechanism and a radical-molecule pathway involving a bridged intermediate in CPD-styrene mixture pyrolysis.

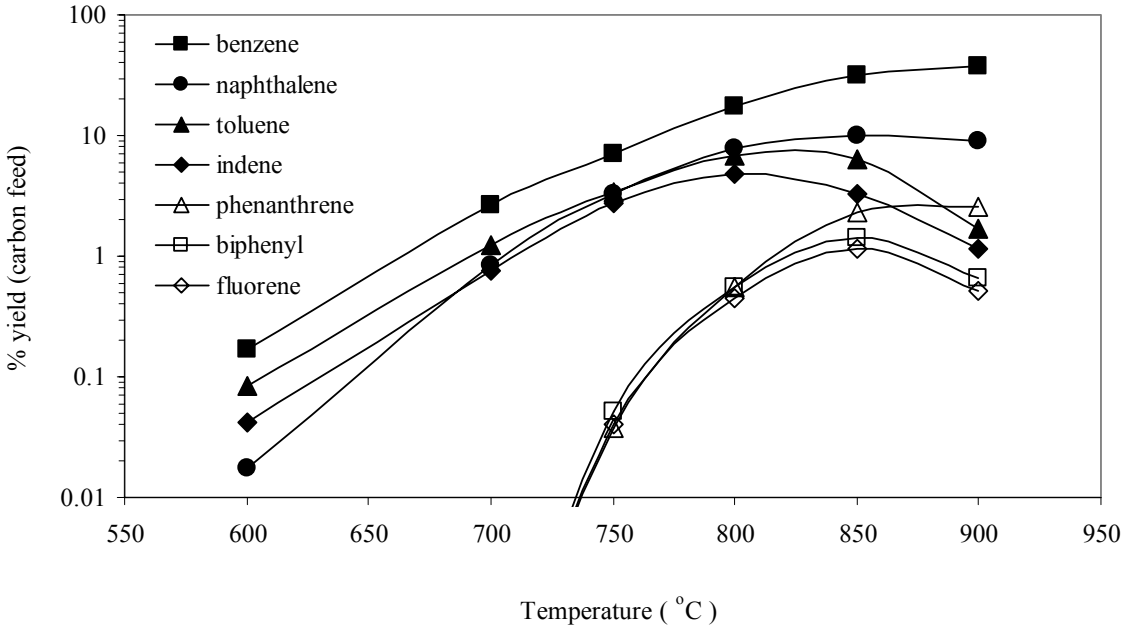

Figure 5.8 Yields of products from CPD-styrene mixture pyrolysis

In order to assess PAH formation and growth from the reaction of CPD and styrene, the product yields from CPD pyrolysis are compared with those from CPD-styrene mixture. Data are presented in Figure 5.9, expressed in the molar ratio of product yield and CPD input. In Figure 5.9, the yield of benzene from CPD-styrene mixture is greater than that from CPD with a factor of 2. Also, the ratio of biphenyl yield to CPD input from CPD-styrene mixture is a couple of order greater than that from CPD alone. Theses results are consistent with our hypothesis.

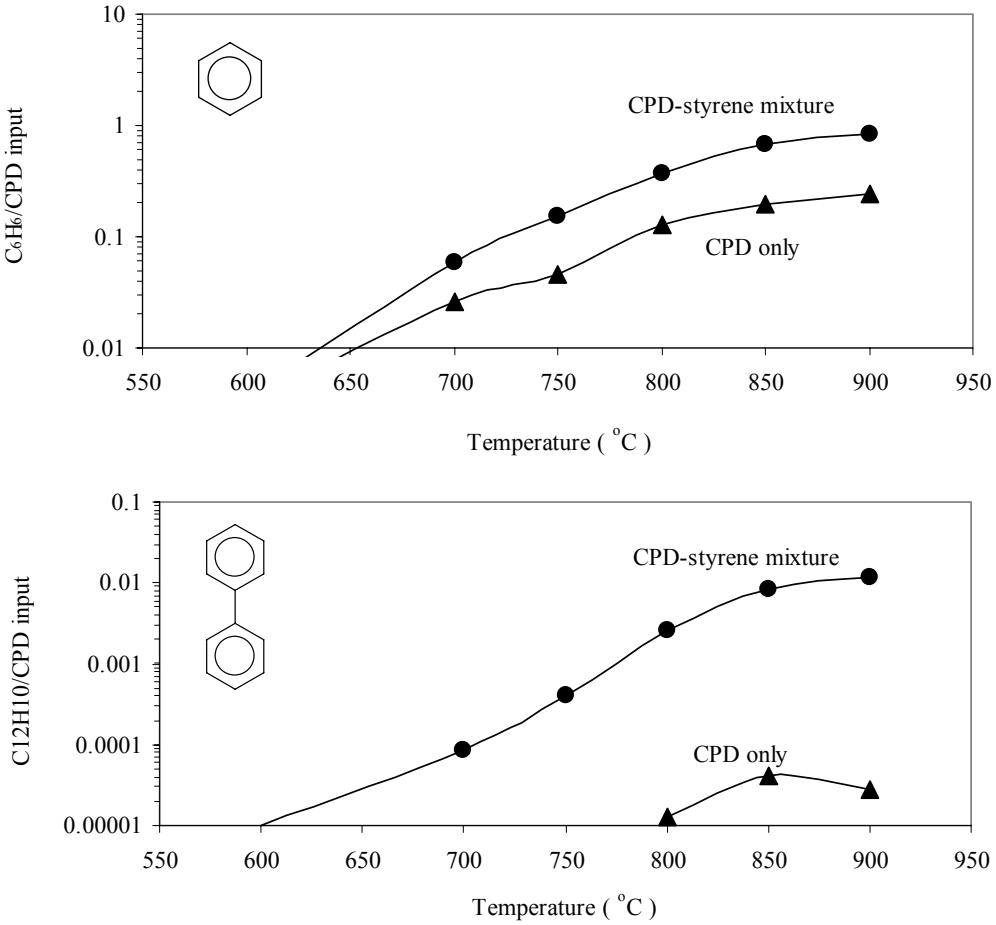

Figure 5.9 Comparison of products from CPD-styrene mixture and CPD pyrolysis; benzene (top) and biphenyl (bottom)

PAH formation pathways from the mixture of CPD and styrene are depicted in Figure 5.10. A radical-radical pathway of CPDyl radicals produces naphthalene whereas a radical-molecule pathway of CPD leads to indene and benzene. Details of these pathways are shown in Chapter 4. The addition of CPDyl radical to the external π-bond of styrene produces a resonance-stabilized radical adduct, which forms a radical intermediate containing the 7-norborneyl moiety via intramolecular addition. Subsequent loss of $CH_3^{\bullet}$ yields to biphenyl. Then, the released $CH_3^{\bullet}$

can combine with CPD to form benzene and with styrene to form indene. Indene from both CPD-CPD and CPD-styrene reactions can further react with CPD to produce fluorene via the pathway involving a bridged intermediate and phenanthrene and anthracene via the pathway involving three-member ring closures and openings.

In case of benzene formation from CPD-styrene mixture, a dominant route might, however, be the decomposition of styrene. Also, CPD-CPD reaction might be a dominant reaction channel for indene formation.

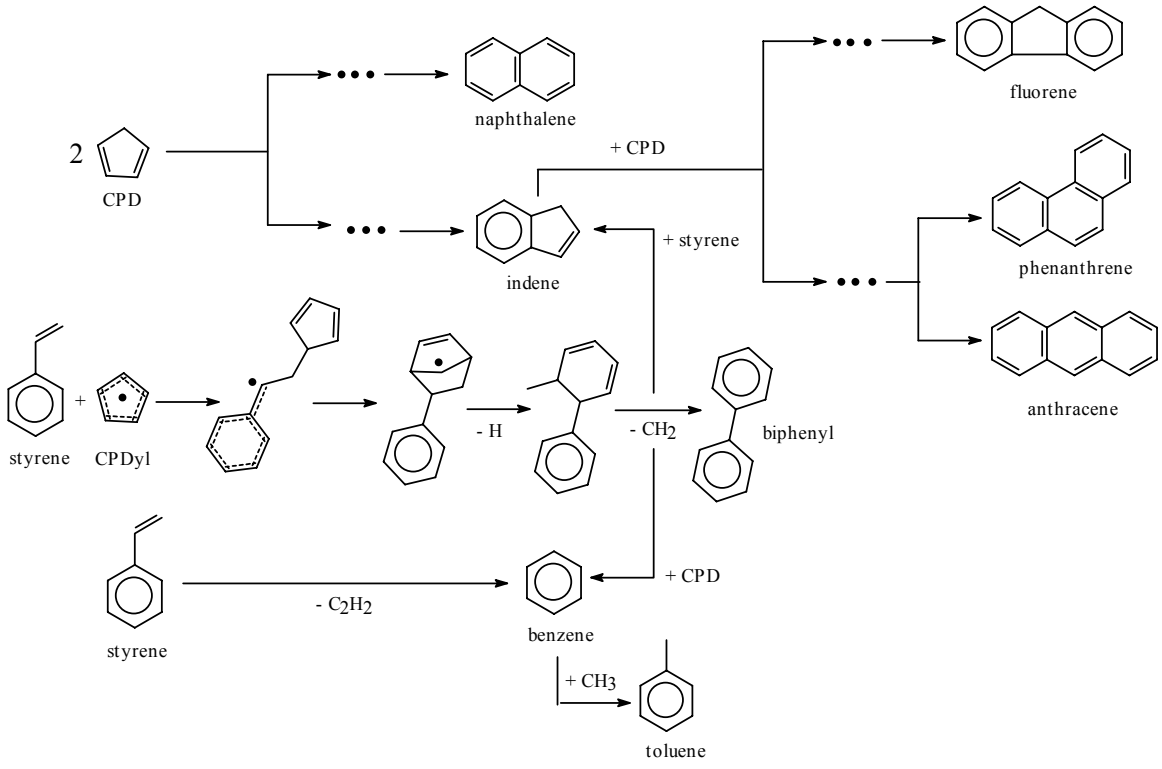

Figure 5.10 PAH growth pathways from CPD-styrene mixture pyrolysis

5.3.3 CPD-Phenanthrene Mixture Pyrolysis

The overall reaction profile of CPD-phenanthrene mixture pyrolysis is shown in Figure 5.11. Carbon recovery, reactant recovery and yields of aromatic compounds and soot are expressed in a percent yield of carbon input. Due to the co-elution of CPD with DCM, CPD yields could not be measured in the DCM sample, resulting in low carbon recoveries at low temperatures. Carbon recovery ranged from 20 to 80%; yield of aromatic compounds excluding the reactants was 10% at 700°C and peaked at 850°C with a yield of 55%.

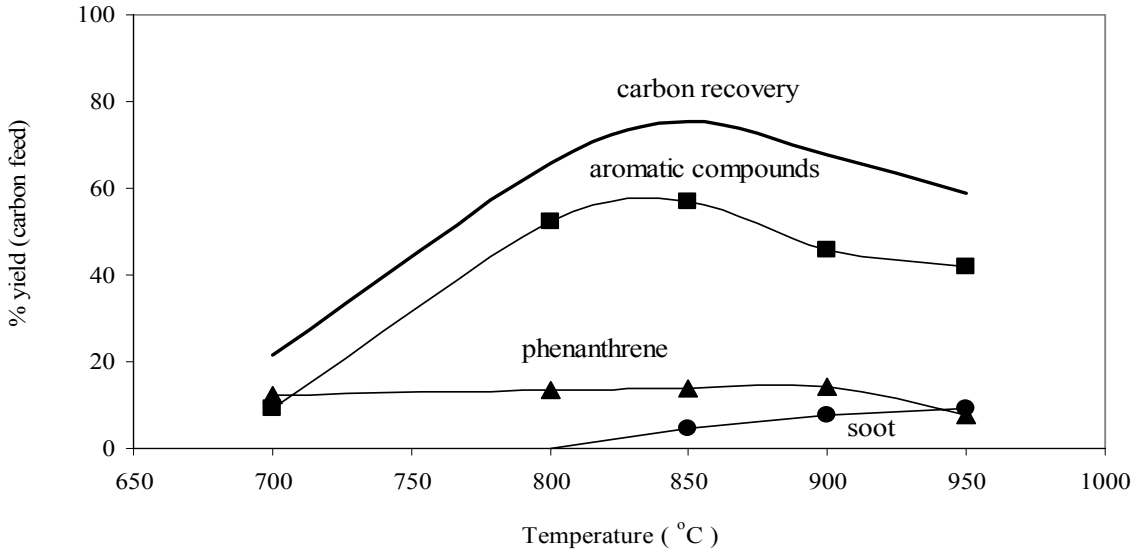

Figure 5.11 Recovery and yields of aromatic compounds, phenanthrene and soot from CPD-phenanthrene mixture pyrolysis

Phenanthrene, 20% of total carbon input, is both a reactant and a product that can be formed from CPD-indene reaction (Lu, 2000; Mulholland et al., 2000). Recovery of phenanthrene with more than 90% of input phenanthrene was observed until 900°C. More than a

half of input phenanthrene was reacted at 950°C though its yield increases slightly as a result of CPD-indene reaction. Soot formation was observed at 850°C and above.

Benzene, naphthalene and indene were major products. Also, toluene, anthracene, fluorene and acenaphthylene were observed. Yields of the observed products are shown as a percent carbon input in Figure 5.12. Yields of benzene, naphthalene and indene ranged from 2 to 20%, 2 to 22% and 0.2 to 10% in that order. Lack of high molecular weight products and high recovery rate of phenanthrene indicates that phenanthrene is much less reactive than CPD. Given the high yields of naphthalene, indene and benzene, the major reaction channel appears to be the reaction of CPD to itself, consistent with the results from CPD-styrene and CPD-acenaphthylene mixture pyrolysis.

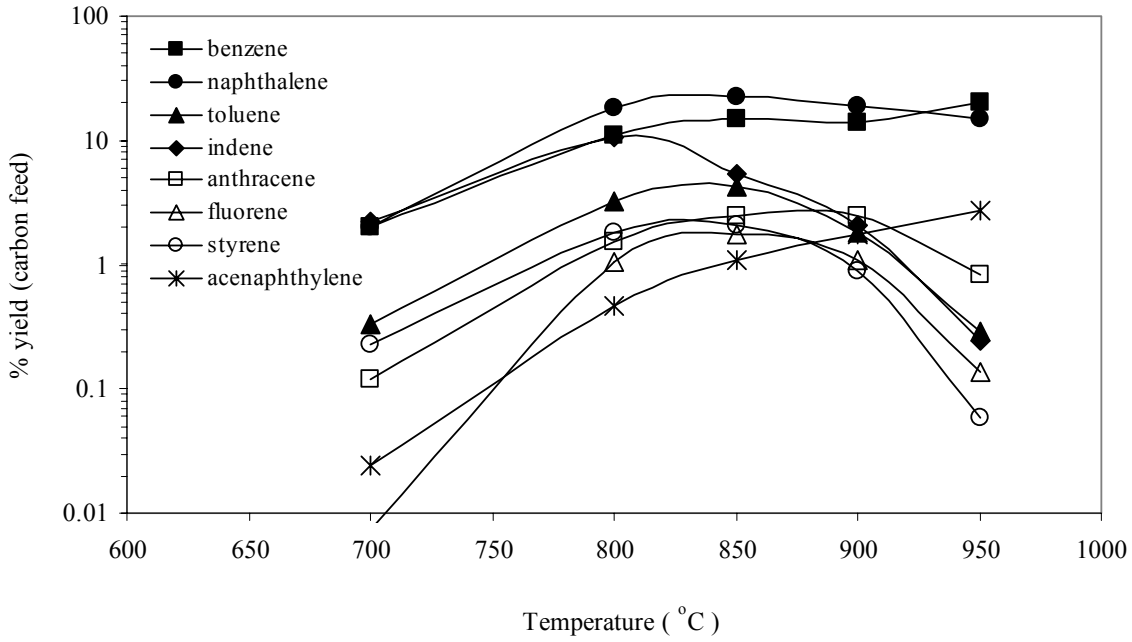

Figure 5.12 Yields of products from CPD-phenanthrene mixture pyrolysis

Contrary to the hypothesis, formation of triphenylene was not observed. Our rationale is that the reactivity of CPDyl radical to phenanthrene is much less than that to CPD itself and/or

amount of phenanthrene in CPD-phenanthrene mixture may not be adequate to yield observable quantity of products from CPD-phenanthrene reaction.

5.4 Conclusions

PAH growth from the pyrolysis of CPD, acenaphthylene, styrene and phenanthrene mixtures was investigated using a laminar flow reactor over a temperature range of 600-1000^{o}C. In all three pyrolysis, the major products were naphthalene, indene and benzene, which suggest that CPD-CPD reaction is a dominant reaction channel.

In CPD-acenaphthylene mixture pyrolysis, experimental results show that the reaction of CPD and acenaphthylene contributes to increasing yields of fluoranthene and acephenanthrylene, though absolute yields of those C_{16} species from CPD-acenaphthylene mixture pyrolysis were low. Based on the observed product distribution, CPDyl radicals likely add preferentially to the external π-bond of acenaphthylene.

Although both CPD-styrene and CPD-phenanthrene reactions are much less comparative to CPD-CPD reaction, CPD-styrene mixture pyrolysis, consistent with the hypothesis, produced more biphenyl and benzene compared to CPD pyrolysis; the formation of biphenyl and benzene can be explained by a radical-molecule pathway of CPDyl and styrene. Contrary to the hypothesis, triphenylene was not observed from CPD-phenanthrene mixture pyrolysis; the distributions of products are similar to those from CPD alone.

All experiments were performed in the absence of non-cyclic hydrocarbons, which are known to contribute to aromatic growth and soot formation in flames, and at temperatures below which ring fragmentation becomes significant. The relative contribution of these pathways was not addressed.

5.5 References

Castaldi, M.J., Marinov, N.M., Melius, C.F., Huang, J., Senkan, S.M., Pitz, W.J. and Westbrrok, C.K., Experimental and modeling investigation of aromatic and polycyclic aromatic hydrocarbon formation in a premixed ethylene flame. *Proc. Combust. Inst.* 26:693-702 (1996).

Ciajolo, A., D'Anna, A., Barbella, R., Tregrossi, A. and Violi, A., The effect of temperature on soot inception in premixed ethylene flames. *Proc. Combust. Inst.* 26:2327-2333 (1996).

D'anna, A. and Violi, A., A kinetic model for the formation of aromatic hydrocarbons in premixed laminar flames. *Proc. Combust. Inst.* 27:425-433 (1998).

Frenklach, M., Clary, D.W., Cardiner, W.C. and Stein, S.E., Detailed kinetic modeling of soot formation in shock-tube pyrolysis of acetylene. *Proc. Combust. Inst.* 20:887-901 (1984).

Frenklach, M., Moriarty, N.W. and Brown, N.J., Hydrogen migration in polyaromatic growth. *Proc. Combust. Inst.* 27:1655-1661 (1998).

Friderichsen, A.V., Shin, E.-J., Evans, R.J., Nimlos, M.R., Dayton, D.C. and Ellison, G.B., The pyrolysis of anisole ($C_6H_5OCH_3$) using a hyperthermal nozzle. *Fuel* 80:1747-1555 (2001).

Gooijer, C., Kozin, I., Velthorst, N.H., Sarobe, M., Jenneskens, L.M. and Viletstra, E.J., The Sphol'skii fluorescence spectrum of cyclopenta[c,d]pyrerme. Novel evidence for anomalous S-2-emission. *Spectrochim. Acta Part A* 54:1443-1449 (1998).

Lafleur, A.L., Howard, J.B., Plummer, E., Taghizadeh, K., Necula, A., Scott, L.T. and Swallow, K.C., Identification of some novel cyclopenta-fused polycyclic aromatic hydrocarbons in ethylene flames. *Polycycl. Aromatic Compounds* 12(4):223-237 (1998).

Laskin, A. and Lifshitz, A., Thermal decomposition of indene, experimental results and kinetic modeling. *Proc. Combust. Inst.* 27:323-344 (1998).

Ledesma, E.B., Kalish, M.A. and Wornat, M.J., Observation of cyclopenta-fused and ethynyl-substituted PAH during the fuel-rich combustion of primary tar from a bituminous coal. *Energy and Fuels* 13:1167-1172 (1999).

Lu, M. and Mulholland, J.A., Aromatic Hydrocarbon Growth from Indene. *Chemosphere* 42:189-197 (2001).

Marinov, N.M., Pitz, W.J., Westbrook, C.K., Castaldi, M.J., and Senken, S.M., Modeling of aromatic and polycyclic aromatic hydrocarbon formation in premixed methane and ethane flames. *Combust. Sci. Technol.* 116:117-211 (1996).

Marinov, N.M., Pitz, W.J., Westbrrok, C.K., Vincitore, A.M., Castaldi, M.J., Senkan, S.M. and Melius, C.F., Aromatic and polycyclic aromatic hydrocarbon formation in a laminar premixed n-butane flame. *Combust. Flame* 114:192-213 (1996).

Marsh, N.D. and Wornat, M.J., Formation of pathways of ethynyl-substituted and cyclopenta-fused polycyclic aromatic hydrocarbons. *Proc. Combust. Inst.* 28:2585-2592 (2000).

McEnally, C.S. and Pfefferle, L.D., An experimental study in non-premixed flames of hydrocarbon growth processes that involve five-membered carbon rings. *Combust. Sci. Technol.* 131(1-6):323-344 (1998).

Melius, C.F., Colvin, M.E., Marinov, N.M., Pitz, W.J. and Senkan, S.M., Reaction mechanisms in aromatic hydrocarbon formation involving the C_5H_5 cyclopentadienyl moiety. *Proc. Combust. Inst.* 26:685-692 (1996).

Moriarty, N.W. and Frenklach, M., *Ab intio* study of naphthalene formation by addition of vinylacetylene to phenyl. *Proc. Combust. Inst.* 28:2563-2568 (2000).

Mulholland, J.A., Lu, M. and Kim D.H., Pyrolytic growth of polycyclic aromatic hydrocarbons by cyclopentadienyl moieties. *Proc. Combust. Inst.* 28:2593-2599 (2000).

Violi, A., D'anna, A. and D'Alessio, A., Modeling of particulate formation in combustion and pyrolysis. *Chem. Eng. Sci.* 54:3433-3442 (1999).

Violi, A., Truong, T.N. and Sarofim, A.F., Kinetics of Hydrogen Abstraction Reactions from Polycyclic Aromatic Hydrocarbons by H Atoms. *J. Phys. Chem. A* 108:4846–4852 (2004).

Westmoreland, P.R., Dean, A.M., Howard, J.B., and Longwell, J.P., Forming Benzene in Flames by Chemically Activated Isomerizations. *J. Phys. Chem.* 93:8171-8180 (1989).

Westmoreland, P.R., Howard, J.B. and Longwell, J.P., Tests of published mechanisms by comparison with measured laminar flame structure in fuel-rich acetylene combustion. *Proc. Combust. Inst.* 21:773-782 (1988).

CHAPTER 6

FORMATION OF POLYCHLORINATED NAPHTHALENES FROM MONOCHLOROPHENOLS

[Material in this chapter is adapted from the manuscript published in *Proc. Combust. Inst.* 30:1249-1257 entitled, "Formation of polychlorinated naphthalenes from chlorophenols" (2004) and from the manuscript accepted to *ES&T* entitled, "Temperature-dependent formation of polychlorinated naphthalenes (PCNs) and dibenzofurans (PCDFs) from chlorophenols."]

Abstract

The gas-phase formation of polychlorinated naphthalenes (PCNs) and dibenzofurans (PCDFs) was experimentally investigated by slow combustion of the three chlorophenols (CPs): 2-chlorophenol (2-CP), 3-chlorophenol (3-CP) and 4-chlorophenol (4-CP), in a laminar flow reactor over the range of 550 to 750^{o}C under oxidative condition. Contrary to the a priori hypothesis, different distributions of PCN isomers were produced from each CP. To explain the distributions of polychlorinated dibenzofuran (PCDF) and PCN congeners, a pathway is proposed that builds on published mechanisms of PCDF formation from chlorinated phenols and naphthalene formation from dihydrofulvalene. This pathway involves phenoxy radical coupling at unsubstituted ortho-carbon sites followed by CO elimination to produce dichloro-9,10-dihydrofulvalene intermediates. Naphthalene products are formed by loss of H and/or Cl atoms and rearrangement. The degree of chlorination of naphthalene and dibenzofuran products decreased as temperature increased, and, on average, the naphthalene congeners were less chlorinated than the dibenzofuran congeners. PCDF isomers were found to be weakly dependent to temperature, suggesting that phenoxy radical coupling is a low activation energy process. Different PCN isomers, on the other hand, are formed by alternative fusion routes from the same phenoxy radical coupling intermediate. PCN isomer distributions were found to be more temperature sensitive, with selectivity to particular isomers decreasing with increasing temperature.

6.1 Introduction

It has been known for some time that polychlorinated naphthalenes (PCNs) are formed from combustion processes along with polychlorinated dibenzo-*p*-dioxins (PCDDs) and polychlorinated dibenzofurans (PCDFs) (Olie et al, 1977; Eiceman et al., 1979). There are 75 PCN congeners containing one to eight chlorine atoms. Although data on the toxicity of individual PCNs are very limited, some PCNs are known to strongly bioaccumulate and to exhibit dioxin-like toxicity (Hanberg et al., 1990; Engwall et al., 1994; Imagawa et al., 1994; Falandysz, 1998). While substantial improvements in the understanding of thermal PCDD/PCDF formation processes have resulted from extensive laboratory study, much less fundamental study of PCN formation has been conducted.

In 1975, Cypres and Bettens (1975) first reported on naphthalene formation from phenol. Chlorinated phenols are known PCDD and PCDF precursors, as first reported in the late 1980s (Born and Louw, 1989). Since that time, many researchers have noted the simultaneous formation PCNs and PCDDs/PCDFs. In previous studies in this laboratory, formation of PCNs with PCDDs/PCDFs from chlorinated phenols was observed in gas-phase pyrolysis (Yang et al., 1998) and oxidation (Nakahata and Mulholland, 2001); however, no attempt was made to elucidate the detailed mechanism of PCN formation.

One possible mechanism of PCN formation from chlorinated phenols is based on reactions known to occur in the counterpart system without chlorine. Phenoxy radical decomposes via CO loss to produce the cyclopentadienyl (CPDyl) radical, and CPDyl radicals combine and rearrange to form naphthalene (Spielmann and Cramers, 1972; Lovell et al., 1988; Manion and Louw, 1989; Frank et al., 1994; Castaldi et al., 1996; Marinov et al., 1997; Friderichsen et al., 2001). The CPDyl radical is resonance-stabilized over all of its five carbon atoms. It has been shown to contribute to polycyclic aromatic hydrocarbon growth in flames. A detailed mechanism of naphthalene formation from CPDyl radicals was proposed by Melius *et al.* (1996) using quantum chemical modeling methods. This mechanism has been extended to indene

and other aromatic species containing external five-member rings (Mulholland et al., 2000). Melius et al. (1996) proposed dimerization of CPDyl radicals to form 9,10-dihydrofulvalene followed by conversion of five-member rings to six-member rings via radical rearrangements involving three-member ring closing and opening (Figure 1.2). Due to resonance, there are several alternative routes for the radical rearrangements shown. In the unchlorinated system, all of these routes lead to the same product – naphthalene. When chlorine is present, however, the alternative routes give rise to the formation of several PCN products from a single 9,10-dihydrofulvalene. This will be discussed later.

In a methane/air diffusion flame containing benzene, toluene, and styrene, McEnally and Pfefferle (2000) concluded that naphthalene formed from CPDyl self-reaction was not significant compared to naphthalene formed from propargyl addition to benzyl radical and from the H-abstraction/carbon-addition mechanism. In post-combustion gas, however, under conditions in which PCDDs and PCDFs are formed from chlorinated phenols, PCNs may be formed from chlorinated CPDyl radicals produced by chlorinated phenoxy radical decomposition.

Recently, Cieplik *et al.* (2002) proposed reaction pathways for the formation of naphthalene in the thermal hydrogenolysis of dibenzo-*p*-dioxin and dibenzofuran. These reaction schemes involve radical intermediates similar in structure to the dihydroxybiphenyls and phenoxyphenols which are known to be intermediates in dibenzofuran and dibenzo-*p*-dioxin formation, respectively, from phenols. Therefore, an alternative hypothesis for the mechanism of PCN formation from phenols would be that phenoxy radical combination leads to intermediates of PCNs as well as PCDDs/Fs. Unlike the CPDyl radical in which all five carbon atoms are reactive, resonance in the phenoxy radical results in only three of its six carbon atoms (the ortho and para sites) as reactive sites. Thus, this alternative mechanism results in more isomer selectivity in the product distribution.

To test the first hypothesis that PCNs can be formed from chlorinated phenols via cyclopentadienyl radicals in post-combustion gas, the slow combustion of three chlorophenols

(CPs) was studied in a flow reactor. This chapter describes the experimental methods and approach, presents a priori predictions of PCN formation from CPs, shows the experimental results of congener-specific PCN and dioxin (PCDD and PCDF) measurements, and proposes a modified mechanism of PCN formation from phenols to account for differences between the a priori hypotheses and the experimental results. In addition, the effect of temperature on gas-phase PCN and PCDF formation from CPs was also investigated to gain further mechanistic insight on these processes.

6.2 Experimental Methods

A laminar flow, isothermal quartz tube reactor (40 cm in length and 1.7 cm in diameter) was used to study PCN formation from three chlorophenols (CPs). Two of the chlorophenols, 2-CP and 3-CP, were heated to liquid form and fed by syringe pump into a heated glass vessel where the reactant was vaporized and mixed with a nitrogen/oxygen gas stream. The third chlorophenol, 4-CP, formed a melt that was too viscous to be fed by syringe. This reactant was heated directly in the glass vessel and vaporized at the same rate as the syringe-fed liquid reactants were fed. The gas stream entering the reactor consisted of nitrogen with 8% oxygen and 0.3% CP vapor. The three CP reactants were obtained from Aldrich, Inc. (Milwaukee, WI) with specified chemical purities of greater than 98%. From chemical analysis, the major impurities were found to be phenol (0.2-0.3% by weight) and other chlorophenols and dichlorophenols (0.03-0.08% by weight). Experiments were conducted in triplicate at 600°C, the temperature at which total PCN yield was greatest; duplicate experiments for 2-CP were conducted at 700, 725 and 750^{o}C.. A reactor residence time of 10 seconds was maintained. The entire product stream was immediately quenched at the outlet of the reactor and collected in a dual ice-cooled dichloromethane trap. Samples were filtered to remove soot.

Identification and quantification of PCN, PCDD, and PCDF congeners was accomplished with a Hewlett-Packard 6890 series gas chromatography with HP-5MS column (30m, 0.25 mm

i.d., 0.25 μm film thickness) coupled to a Hewlett-Packard 5973 mass spectrometer. The column oven temperature was programmed from 38 to 80°C at a rate of 3°C/min, 180 to 250°C at a rate of 5°C/min, 250 to 280°C at a rate of 6°C/min, and a final hold time of 3 min. For quantification, the mass spectrometer was operated in selective ion mode at the two most intensive and characteristic ion masses. Elution time was used to identify isomers. Naphthalene, dibenzo-*p*-dioxin, and dibenzofuran products are formed from two phenol reactants. Therefore, expected products in these experiments were congeners containing up to two chlorine atoms.

PCN isomers were identified based on the elution order of PCNs in Halowax 1001, 1014, and 1051 standards (Abad et al., 1999; Schneider et al., 1988; Järnberg et al., 1994). Both monochloronaphthalene (MCN) isomers, 1- and 2-MCN, were separated, and seven peaks were separated for the ten dichloronaphthalene (DCN) isomers. DCN isomers co-eluting were as follows: 1,5-/1,6-/1,7-DCN and 2,6-/2,7-DCN. Naphthalene was used as a universal response factor to estimate PCN product yields.

PCDD and PCDF products were also measured. Procedures for identifying these products have been published previously (Yang et al., 1998; Nakahata and Mulholland, 2001). Both monochlorodibenzo-*p*-dioxin (MCDD) isomers and all four monochlorodibenzofuran (MCDF) isomers were separated. Seven peaks were obtained for the ten dichlorodibenzo-*p*-dioxin (DCDD) isomers; two of these peaks contain co-eluting isomers (1,6-/1,7-/1,8-DCDD and 2,7-/2,8-DCDD). It is interesting to note that the DCDD isomers that co-elute in our system are structurally analogous to the DCN isomers that co-elute. (Due to their identical symmetry, the number of DCN and DCDD isomers is the same. The numbering system is different, however, with the unfused portion of the PCN second ring composed of the 5, 6, 7, and 8 carbon atoms whereas these are 6, 7, 8, and 9 in the PCDD numbering system.) In the case of dichlorodibenzofuran (DCDF) isomers, 15 peaks were obtained for the 16 DCDF isomers; only the 2,7-/1,2-DCDF isomers co-elute. In addition, CO measurements in the exhaust gas were

performed with a Hewlett-Packard 5890 II series gas chromatography coupled to thermal conductivity detector (TCD) with HP-MOLSIV column (15m, 0.53 mm i.d., 0.25 μm film thickness).

6.3 A Priori Hypotheses

Before performing experiments, PCN isomer products from the three CPs were predicted based on the *a priori* hypothesis that phenoxy radicals decompose to CPDyl radicals, which combine and rearrange to form naphthalenes via the mechanism proposed by Melius and coworkers (1996). The three CPs form the same chloro-CPDyl radical (Figure 6.1). *Hypothesis 1: While the total yield of PCN products may vary from the three CP reactants due to differences in their rates of decomposition, the distribution of PCN products will be similar from each.*

To predict which PCN products will be formed, we consider all possible combinations of the chloro-CPDyl radical at unsubstituted carbon atoms. The presence of chlorine inhibits carbon-carbon coupling at substituted sites. Three dichlorodihydrofulvalenes can be formed (Figure 6.1). These dihydrofulvalenes are then converted to naphthalenes via the mechanism shown in Figure 1.2. In translating the dihydrofulvalene-to-naphthalene mechanism to a chlorinated system, we include an alternative radical formation step involving carbon-chlorine bonds, which are much weaker than carbon-hydrogen bonds. If hydrogen migrates to a chlorinated site in the conversion of 9,10-dihydrofulvalene to 1,10-dihydrofulvalene (first reaction in Figure 1.2), loss of that chlorine can occur (replacing the second and third reactions shown in Figure 1.2).

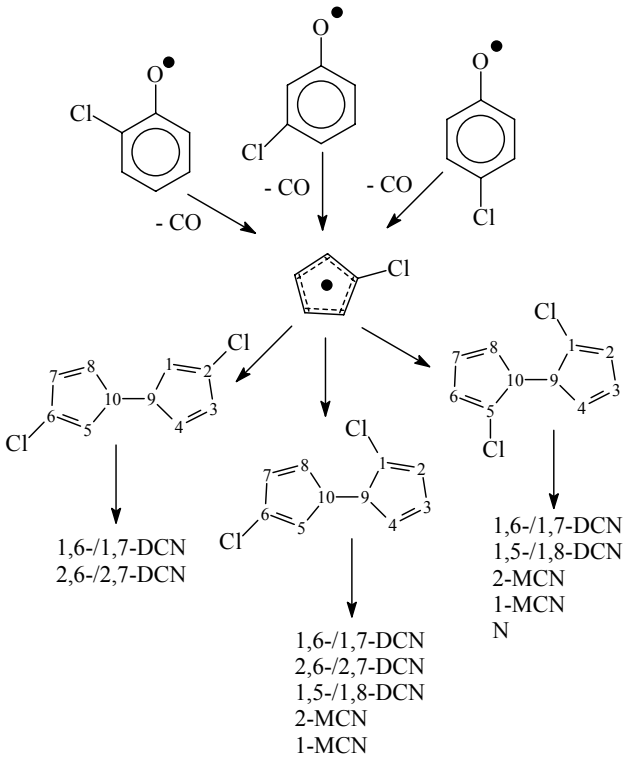

Figure 6.1 A priori hypothesis of PCN formation from chlorophenols

The fused bond in naphthalene, between the 9 and 10 carbon atoms, is formed by any of the following five carbon pairs in dihydrofulvalene: 9,10; 9,5; 9,8; 10,1; and 10,4. Via each of these routes, a pair of PCN products is formed. Thus, ten PCN products could be formed from each 9,10-dihydrofulvalene. Due to symmetry, not all of the products are unique. For example, from the 2,6-dichloro-9,10-dihydrofulvalene shown in the leftmost pathway of Figure 6.1, fusion across the 9,10 carbon atoms, 9,8 carbon atoms, and 10,4 carbon atoms yields the 2,6-/2,7-DCN pair. Fusion across the 9,5 carbon atoms and 10,1 carbon atoms yields the 1,6-/1,7-DCN pair. In the case of the 1,6-dichloro-9,10-dihydrofulvalene shown in the center pathway of Figure 6.1, eight different PCN products can be formed: 1,6-, 1,7-, 2,6-, 2,7-, 1,5- and 1,8-DCN and 2- and 1-MCN. The third CPDyl combination produces 1,5-dichloro-9,10-dihydrofulvalene (rightmost pathway in Figure 6.1), which leads to seven naphthalene products: 1,6-, 1,7-, 1,5- and 1,8-DCN,

1- and 2-MCN, and naphthalene. *Hypothesis 2: From each CP, we expect six dichloronaphthalene products (2,6-, 2,7-, 1,6-, 1,7-, 1,5-, and 1,8-DCN), both monochloronaphthalene products (1- and 2-MCN), and naphthalene.*

In addition to the PCN products, dioxin products are expected from gas-phase reactions of phenols. Oxygen-carbon coupling of phenoxy radicals occurs at ortho sites with chlorine substituents, and subsequent five-member ring closure and rearrangement leads to dibenzo-*p*-dioxin products (Born et al., 1989). Carbon-carbon coupling of phenoxy radicals occurs at ortho sites without chlorine substituents, and subsequent tautomerization followed by loss of H_2O yields dibenzofuran products (Weber and Hagenmaier, 1997). Based on previous studies (Yang et al., 1998), 2-CP is expected to produce DD, 1-MCDD, and 4,6-DCDF, 3-CP is expected to produce 1,7-, 3,7-, and 1,9-DCDF, and 4-CP is expected to produce 2,8-DCDF. We found the yields of these PCDD and PCDF products from CPs to vary significantly, with highest yields from 3-CP and lowest yields from 2-CP. These differences in PCDD/PCDF formation propensity are associated with electronic and steric factors in the coupling of chlorophenoxy radicals. *Hypothesis 3: Since phenoxy radical decomposition to form CPDyl radicals, that then combine to form PCN products, competes with phenoxy radical coupling leading to PCDD and PCDF products, we posit that PCDD/PCDF yield will be inversely related to PCN yield.*

6.4 Preliminary Results on PCN and PCDF Formation from CPs at 600°C

To test a priori hypotheses, PCN and PCDF products from CP reactants at 600°C were investigated, and CP reactant recovery and yields of phenol, total naphthalene, total dibenzofuran and total dibenzo-*p*-dioxin products from the individual CP reactant experiments are shown in Figure 6.2. The amount of unreacted CP recovered at 600°C and 10 seconds ranged from 21% for 3-CP to 33% for 2-CP, indicating that 3-CP is most easily destroyed thermally, whereas 2-CP is least easily destroyed. Phenol yield ranged from 0.16% to 0.29% of CP reactant. Phenol, an impurity in the CP reactant, may result from incomplete reaction or may be produced by CP

hydrodechlorination. Phenol yields increased with temperature over the range of 450 to 750°C (not shown). Thus, CP hydrodechlorination appears to be the major source of phenol in these experiments. Phenol yield was greatest from 2-CP. The formation of phenol can lead to other, less chlorinated naphthalene and dioxin products, as will be discussed.

As expected, naphthalene and dioxin products were observed. Total yields of naphthalenes ranged from 0.0073% from 4-CP to 0.013% from 3-CP; total yields of dibenzofurans ranged from 0.0075% from 2-CP to 3.4% from 3-CP. Dibenzo-*p*-dioxin was observed from 2-CP, with a yield of 0.0014%.

Much of the CP reactants undergo decomposition and oxidation to form low molecular weight products. Since the oxidation pathways were not the subject of this investigation, these products were not measured. Based on the low yield of benzene (not shown) and lack of toluene and styrene products, we conclude that naphthalene formation via addition of two- or three-carbon species was negligible.

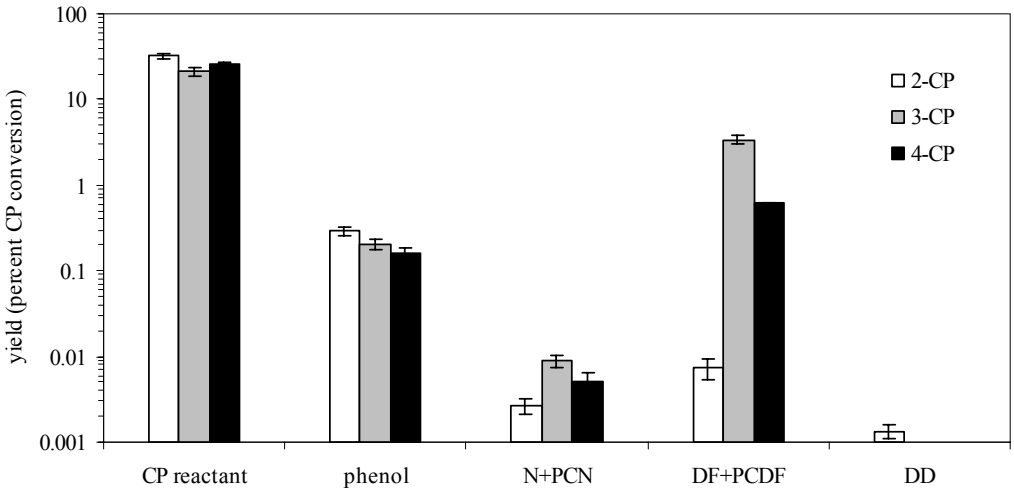

Figure 6.2 CP recovery and phenol product yield

Total yields of naphthalene (N) and chlorinated naphthalenes (MCN and DCN), and dibenzofuran (DF) and chlorinated dibenzofurans (MCDF and DCDF) are shown in Figure 6.3 on a percent CP molar conversion basis. The PCN homologue distribution produced by 2-CP is very different than those produced by 3- and 4-CP. Only a trace amount (less than 0.0001%) of DCN was detected from 2-CP. From 3-CP, 0.0017% DCN yield was observed. From 3- and 4-CP, MCN yields were highest; from 2-CP, naphthalene yield was greatest. These results suggest that the major route of PCN formation from chlorinated phenols is via loss of at least one chlorine atom. The high yields of DF and MCDF as well as N and MCN suggest that phenol contributed significantly to the formation of dibenzofuran and naphthalene products.

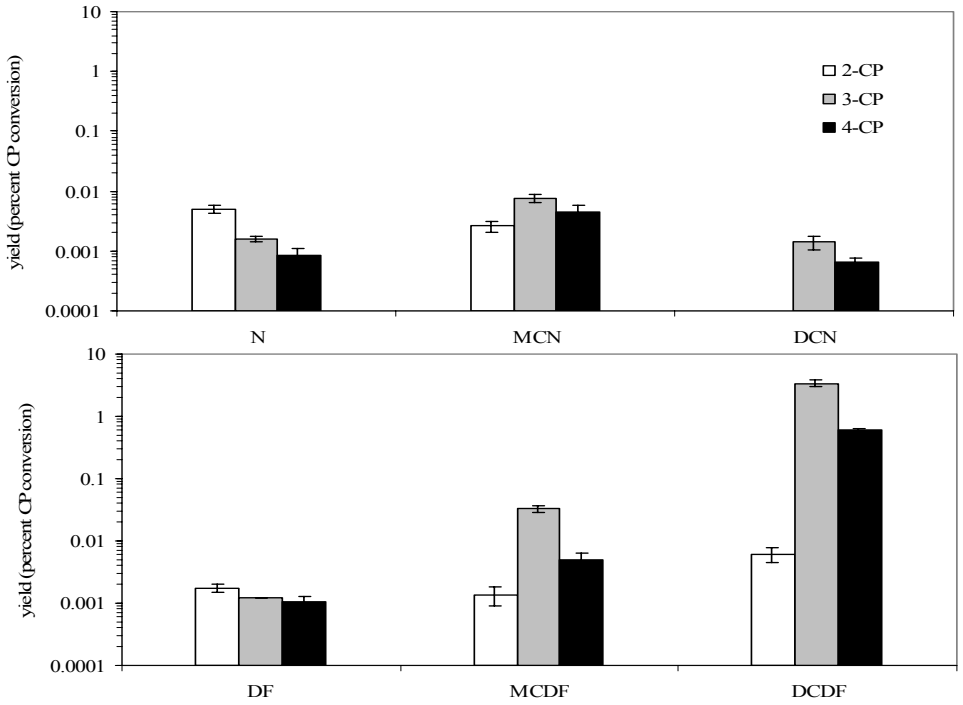

Figure 6.3 Naphthalene (top) and dibenzofuran (bottom) homologue distributions

Within each homologue, the total naphthalene and dibenzofuran yields from the different CP reactants have a similar pattern. That is, 2-CP produced the highest N and DF yields and 4-CP produced the lowest N and DF yields. In the case of the monochlorinated and dichlorinated products, 3-CP produced the highest yields. Thus, there appears to be a strong, positive correlation between naphthalene formation and dibenzofuran formation from CPs, rather than an inverse relationship. This leads us to reject *a priori* hypothesis 3. To address hypotheses 1 and 2, PCN isomer distributions need to be examined.

In Figure 6.4, MCN and DCN isomer distributions are shown. All but one of the expected PCN congeners were detected and quantified. That is, 1-MCN, 2-MCN and 1,5-/1,6-/1,7-DCN, and 2,6-/2,7-DCN were observed; we were not able to detect 1,8-DCN. None of the other DCN congers were detected. These results would appear to support hypothesis 2. It is noted, however, that 2-CP produced only a trace amount of DCN (1,5-/1,6-/1,7-DCN peak).

The MCN isomer patterns from the three CPs are completely different. 2-CP produced mostly 1-MCN, 3-CP produced nearly equal amounts of 1- and 2-MCN, and 4-CP produced mostly 2-MCN. The DCN isomer patterns from 3-CP and 4-CP are also different. 3-CP produced nearly equal amount of the 1,5-/1,6-/1,7-DCN and 2,6-/2,7-DCN peaks, whereas 4-CP produced 2,6-/2,7-DCN almost exclusively. Thus, we reject hypothesis 1 that the PCN isomer patterns would be the same from the three CP reactants due to a common radical precursor chloro-CPDyl.

PCDF isomer distributions are shown in Figure 7.5. All expected isomers were observed: 4,6-DCDF from 2-CP; 1,7-, 3,7-, and 1,9-DCDF from 3-CP; 4,6-DCDF from 2-CP. In addition, DF and MCDF isomers were detected. From 2-CP and phenol, 4-MCDF is formed. From 3-CP and phenol, 1- and 3-MCDF are formed. From 4-CP and phenol, 2-MCDF is formed. DF is produced from two phenols. The relative yields of phenol, DF, and N from the three CP reactants are consistent. That is, 2-CP produced the most phenol, N, and DF, and 4-CP produced the least phenol, N, and DF. Thus, the CP hydrodechlorination to form phenol leads to the formation of

less chlorinated naphthalene and dibenzofuran products than those produced from the parent CP alone.

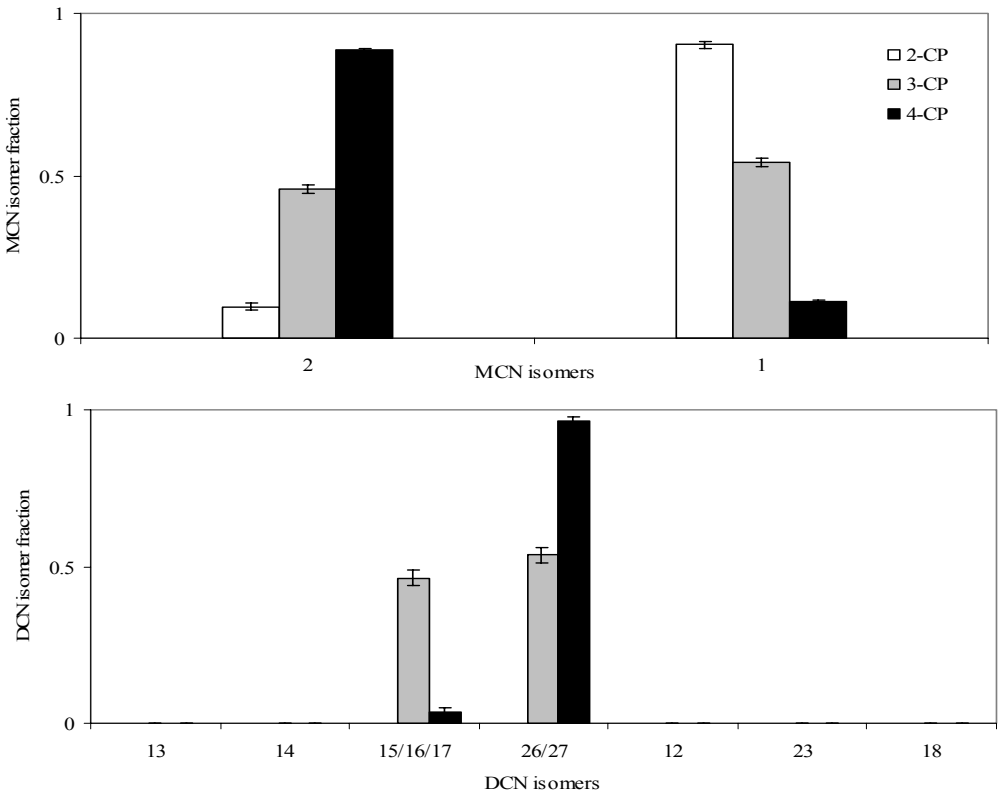

Figure 6.4 MCN (top) and DCN (bottom) isomer distributions. Isomers are listed in order of elution

To account for the differences in PCN isomer distributions, and to explain the apparent correlation of PCN and PCDF yields, an alternative formation mechanism is needed. The dependence of PCN isomer distributions on CP reactant chlorination pattern suggests that coupling must involve a reactant derivative other than the chloro-CPDyl radical. Moreover, the correlation of PCN and PCDF product formation suggests that they might be formed from a

common intermediate, the formation of which is rate limiting. These observations lead us to modify our proposed scheme for PCN formation from CPs.

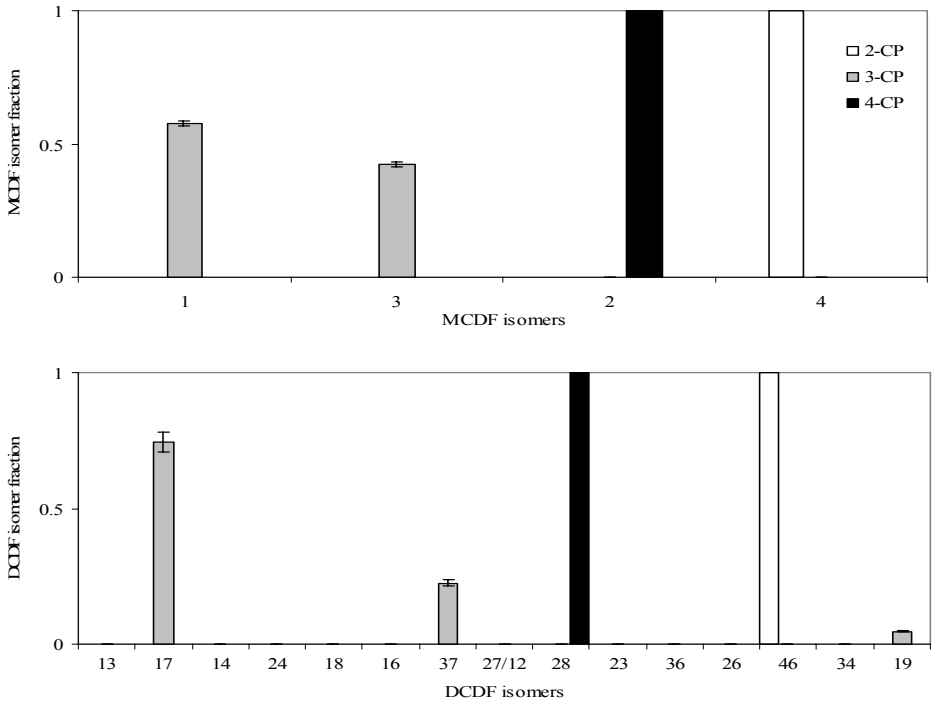

Figure 6.5 MCDF (top) and DCDF (bottom) isomer distributions. Isomers are listed in order of elution

6.5 Proposed Pathway of PCN Formation from CPs

Based on the observed simultaneous formation of PCNs and PCDFs from CPs, PCN formation pathways from CPs are proposed that build on the dihydrofulvalene-to-naphthalene mechanism of Melius et al. (1996). The proposed overall reaction pathway for PCDF and PCN formation from chlorophenols is depicted in Figure 6.6; the detailed reaction schemes from each CP are presented in Figure 6.7-6.9.

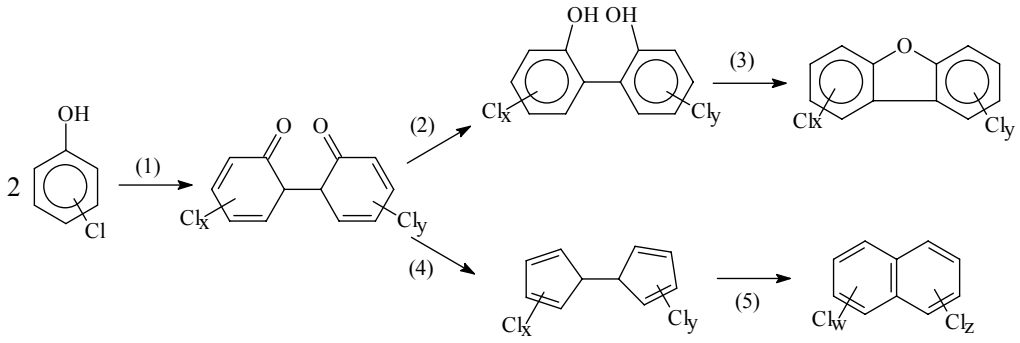

x = 1 or Ø; y = 1 or Ø; w = x or Ø; z = y or Ø

Figure 6.6 Overall PCDF and PCN formation pathways from chlorophenols

Chlorophenols can lose hydrogen or chlorine to produce chlorophenoxy or phenoxy (with hydrogen migration) radicals. These resonance-stabilized radicals can couple at unchlorinated ortho carbon sites to produce the diketo tautomer of DOHB (step 1 in Figure 6.6). In PCDF formation, this intermediate undergoes keto-enol tautomerization to form DOHB (step 2); subsequent elimination of H_2O yields the PCDF product (step 3). Alternatively, dihydrofulvalene is formed by CO elimination from the diketo-dimer intermediate (step 4). Elimination of CO from both stable and radical systems of phenol has been studied (Olivella et al., 1995; Liu et al., 1996; Zhu and Bozzelli, 2003). Subsequent fusion of dihydrofulvalene to form naphthalene products is depicted by step 5. Unlike PCDF formation, PCN formation from the diketo-dimer intermediate may involve chlorine loss.

Experimental evidence of the preferred translation of the 9,10 carbon atoms of 9,10-dihydrofulvalene to the 9,10 carbon atoms of naphthalene is that 4-CP produced a large 2,6-/2,7-DCN peak and a small 1,5-/1,6-/1,7-DCN peak (Figure 6.4). Translation of the 9,10 carbon atoms of 9,10-dihydrofulvalene to the 9,10 carbon atoms of naphthalene produces 2,6- and 2,7-DCNs whereas translation of the 9,5 or 10,4 carbon atoms of 9,10-dihydrofulvalene to the 9,10 carbon atoms of naphthalene produces 1,6- and 1,7-DCNs.

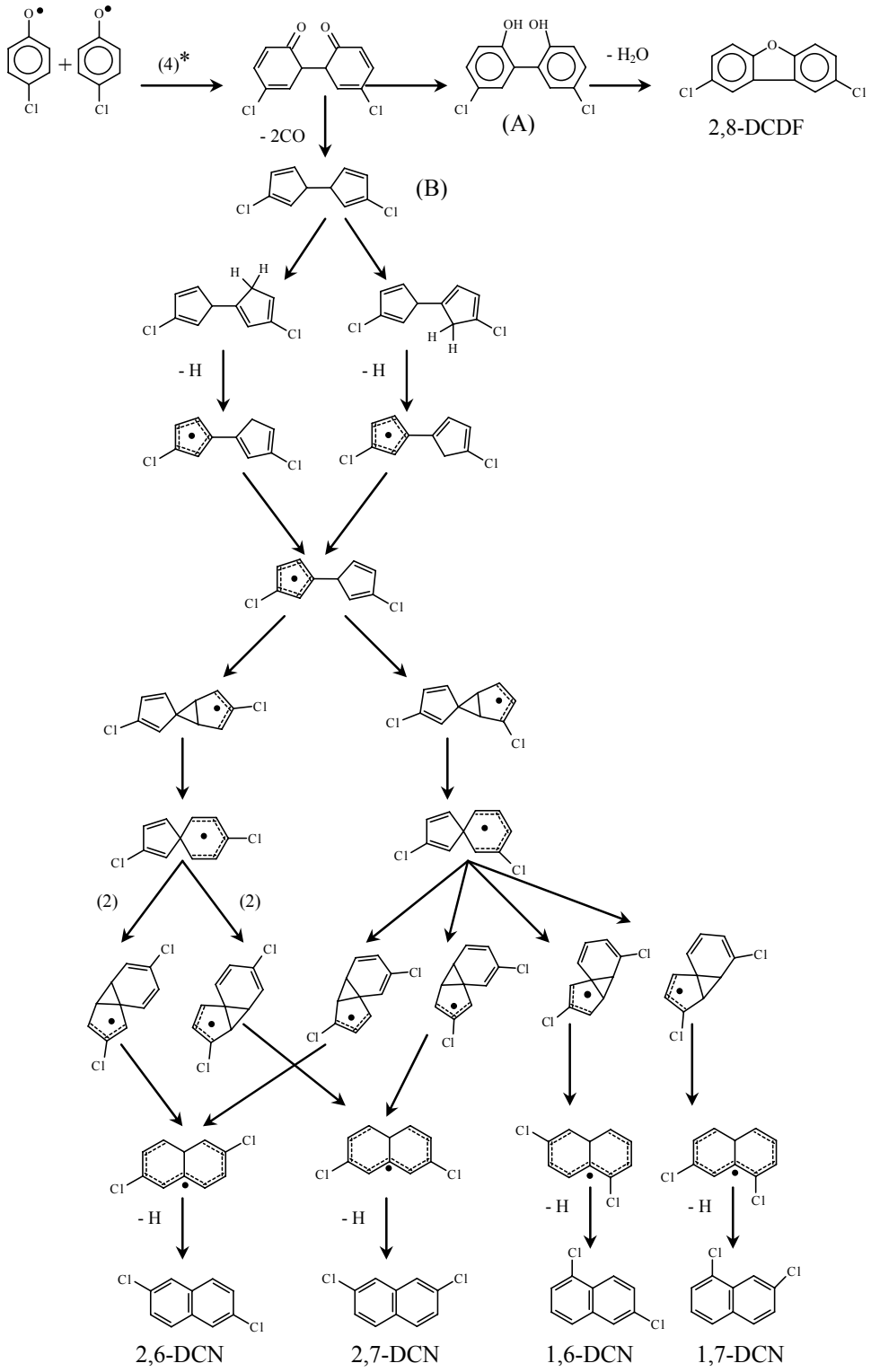

* numbers in parentheses represent reaction path degeneracy

Figure 6.7 PCDF and PCN formation pathways from 4-CP

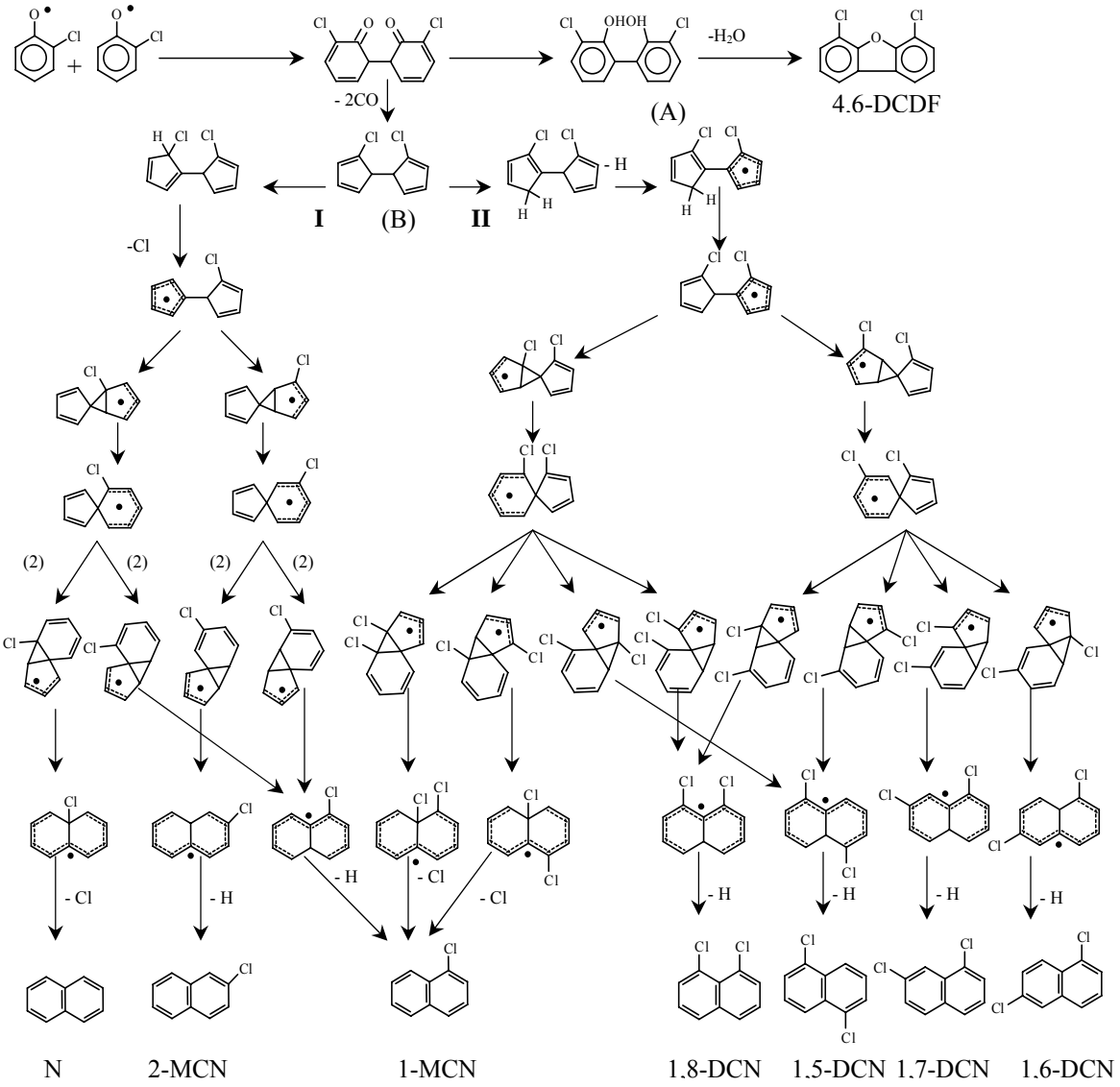

Figure 6.8 PCDF and PCN formation pathways from 2-CP

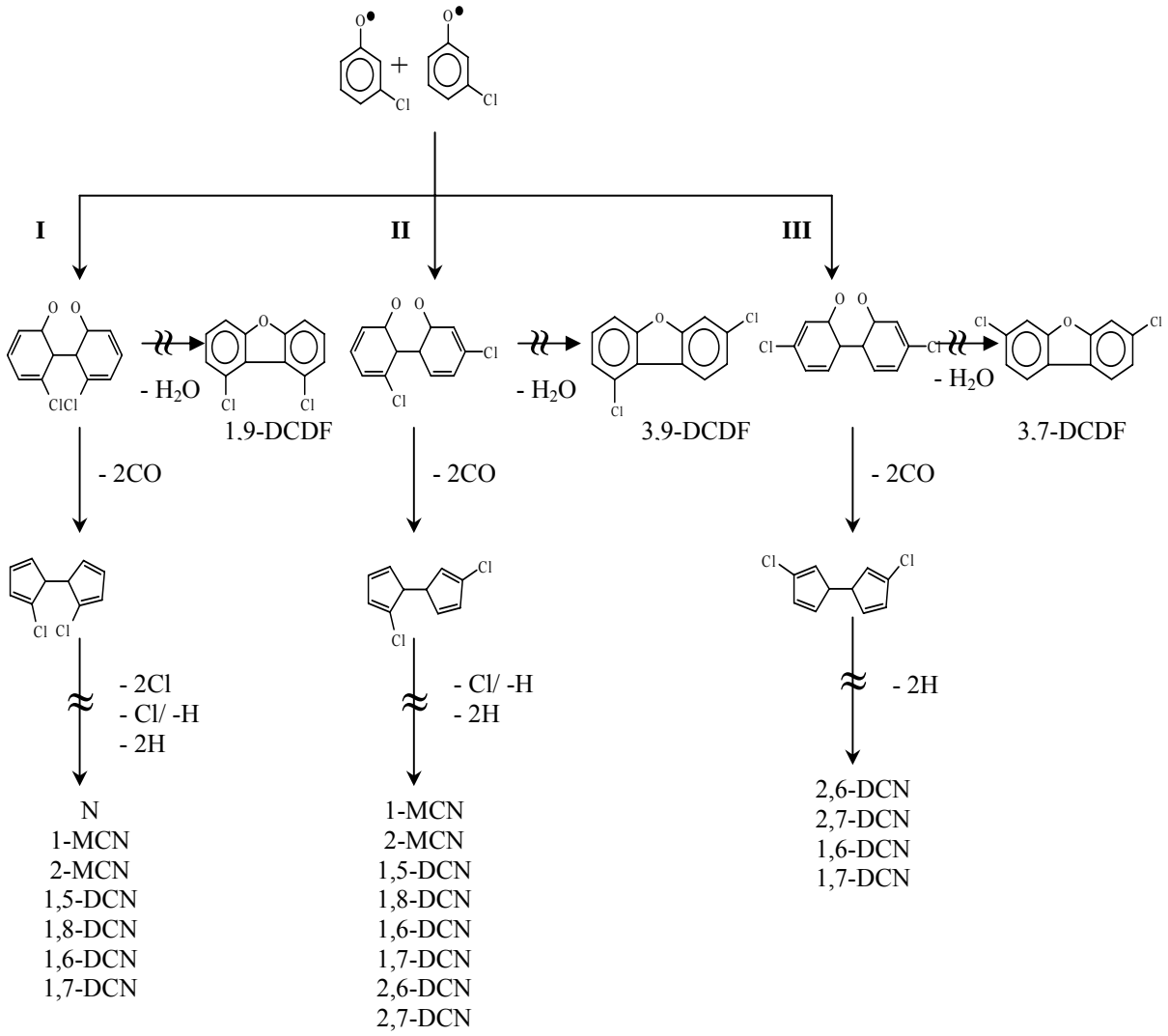

Figure 6.9 PCDF and PCN formation pathways from 3-CP

Experimental evidence of the preferred hydrogen migration to a chlorinated site in the conversion of 9,10-dihydrofulvalene to 1,10-dihydrofulvalene, followed by loss of that chlorine atom, is that 2-CP produced very little DCNs (Figure 6.3). Formation of much more 1-MCN than 2-MCN from 2-CP (Figure 6.4) is consistent with translation of the 9,10 carbon atoms of 9,10-dihydrofulvalene to the 9,10 carbon atoms of naphthalene.

In the case of 3-CP, three ortho-ortho couplings are possible, leading to the formation of three dichloro-o,o-dihydroxybiphenyls and three dichloro-9,10-dihydrofulvalenes. In Table 6.1, predicted PCDF and PCN products from 3-CP are listed, as well as those from 4-CP and 2-CP. In addition, predicted PCDF and PCN products formed via these pathways from combinations involving phenol are listed. Predictions based on the proposed reaction scheme are consistent with the observed PCN and PCDF isomer distributions, shown in Figures 6.4 and 6.5, respectively.

Overall, PCN products were less chlorinated than PCDF products (Figure 6.3). For example, DCDF yields were a factor of 100 greater than DCN yields, whereas naphthalene and dibenzofuran yields were similar. This may be due to loss of chlorine in PCN formation and not in PCDF formation. Although phenol concentrations were much lower than CP reactant concentrations in these experiments, phenol appears to have played an important role in both PCN and PCDF formation. In previous work (Nakahata and Mulholland, 2000), it was observed that PCDF formation from the less chlorinated phenol congeners was greater than that from more chlorinated phenol congeners. The experimental results presented here indicate that chlorine suppresses PCN formation as well. One explanation is that the withdrawal of electron density by chlorine substituents from the ring systems suppresses CO elimination and PCN formation.

Other reaction schemes might also be consistent with the experimental observations. For example, radical-molecule routes involving either CPDyl or phenoxy radical adding to CP reactant would result in isomer specificity in PCN products. The correlation of PCDF and PCN product distributions suggests to us that the rate-determining step is likely the same, however.

That is, if PCDF formation from phenols involves only phenoxy radical coupling, then PCN formation likely does as well since the rate of CO elimination to form CPDyl radical is likely to be different from the three CPs. We further investigated the effect of temperature on gas-phase PCN and PCDF formation from chlorophenols to gain more mechanistic insight on these processes, which the experimental results are shown in next section.

Table 6.1 Predicted PCN and PCDF products from chlorophenols

Chlorophenol reactant	Naphthalene products	Dibenzofuran and dibenzo-*p*-dioxin products
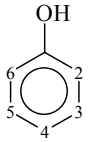	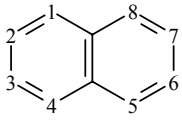	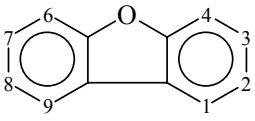
2-CP	1,5-, 1,6-, 1,7-, 1,8-, 2,6-, 2,7-DCNs 1-, 2-MCNs N	4,6-DCDF DD
3-CP	1,5-, 1,6-, 1,7-, 1,8-, 2,6-, 2,7-DCNs 1-, 2-MCNs N	1,7-, 3,7-, 1,9-DCDFs
4-CP	1,6-, 1,7-, 2,6-, 2,7-DCNs	2,8-DCDF

6.6 Temperature-dependent Formation of PCNs and PCDFs from CPs

6.6.1 CP Recovery and Overall Product Distribution

Chlorophenol reactant recovery and yields of CO, phenol (Ph), total naphthalene (labeled PCN, and includes unchlorinated naphthalene), total dibenzofuran (labeled PCDF, and includes unchlorinated dibenzofuran) and total dibenzo-p-dioxin (DD) products are shown in Figure 6.10

as percent yields of carbon feed. Unreacted CP was 51%, 36%, and 35.5% for 2-CP, 3-CP and 4-CP, respectively, at 550^{o}C and less than 1% at 750^{o}C. Unsubstituted phenol was one of major products from all three chlorophenols; its yield was a maximum at 675^{o}C, with yields of 1.7% from 2-CP, 0.5% from 3-CP and 2% from 4-CP. The results demonstrate that hydrodechlorination is greatest for ortho and para chlorine in the parent phenol. The formation of phenol leads to other, less chlorinated naphthalene and furan products, as will be discussed.

Yields of CO from the decomposition and oxidation of chlorophenol were a maximum at 700^{o}C, with peak yields of 63% for 2-CP, 43% for 3-CP, and 60% for 4-CP. At higher temperatures CO oxidation to CO_2 occurs (Sawerysyn et al., 2004).

The total yields of dibenzofuran products peaked between 625^{o}C and 675^{o}C, with maximum yields of 0.21%, 2.2% and 1.3% for 2-CP, 3-CP and 4-CP, respectively. Dibenzo-p-dioxin (DD) was observed only from 2-CP, with a peak yield of 0.05% observed at 650^{o}C. These results confirm that dibenzofuran formation is favored by meta substitution in the parent chlorophenol (Nakahata and Mulholland, 2000), and that ortho chlorine is necessary for dibenzo-p-dioxin formation (Mulholland et al., 2000).

Maximum yields of naphthalene products were observed between 675^{o}C and 725^{o}C, with yields of 0.91%, 0.39% and 0.94% from 2-CP, 3-CP and 4-CP, respectively. Thus, ortho and para substitution on the parent phenol favored naphthalene product formation. Based on the low yield of benzene (not shown) and styrene (not detected), naphthalene formation via phenol decomposition to two- or three-carbon species and subsequent growth by HACA pathways was not significant under our experimental conditions.

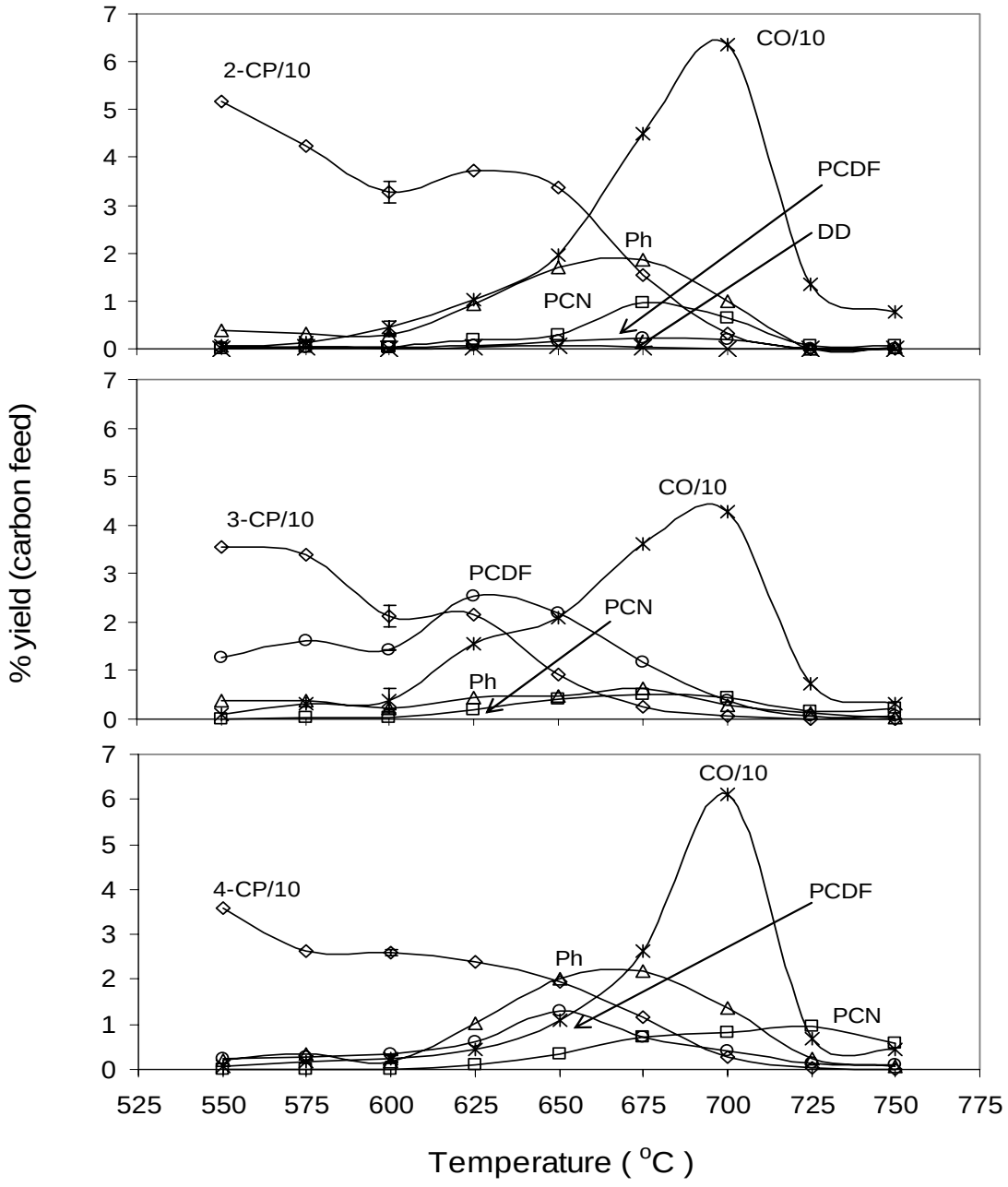

Figure 6.10 CP recovery and product yields from 2-CP (top), 3-CP (middle) and 4-CP (bottom)

The ratio of naphthalene to dibenzofuran products was greatest for 2-CP and least for 3-CP (Figure 6.11). As temperature increased, this ratio increased for each of the CP reactants. These results suggest that CO elimination (step 4 in Figure 6.6) that leads to naphthalene formation becomes increasingly favored relative to tautomerization (step 2 in Figure 6.6) that leads to dibenzofuran formation as temperature increases.

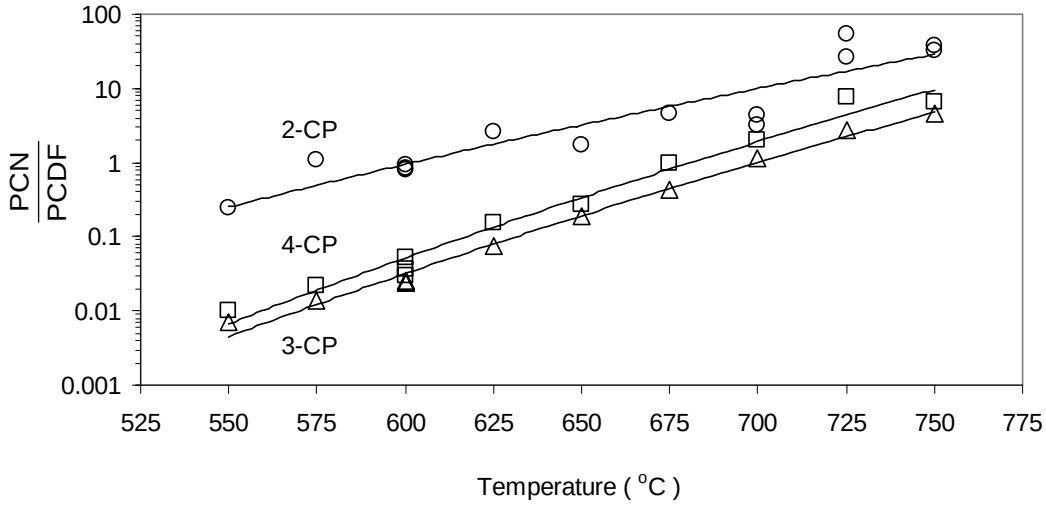

Figure 6.11 Ratio of total naphthalene to total dibenzofuran product yields from CPs

6.6.2 PCDF and PCN Homologue Distributions

Total yields of naphthalene (N), chlorinated naphthalenes (MCN and DCN homologues), dibenzofuran (DF), and chlorinated dibenzofurans (MCDF and DCDF homologues) are shown in Figure 6.12 on a percent of carbon feed basis. At lower temperatures, DCDF products are favored. As temperature increases, the total yields of MCDF and DF become bigger fractions of the total dibenzofuran product yield. At 750°C, DF was the major dibenzofuran product.

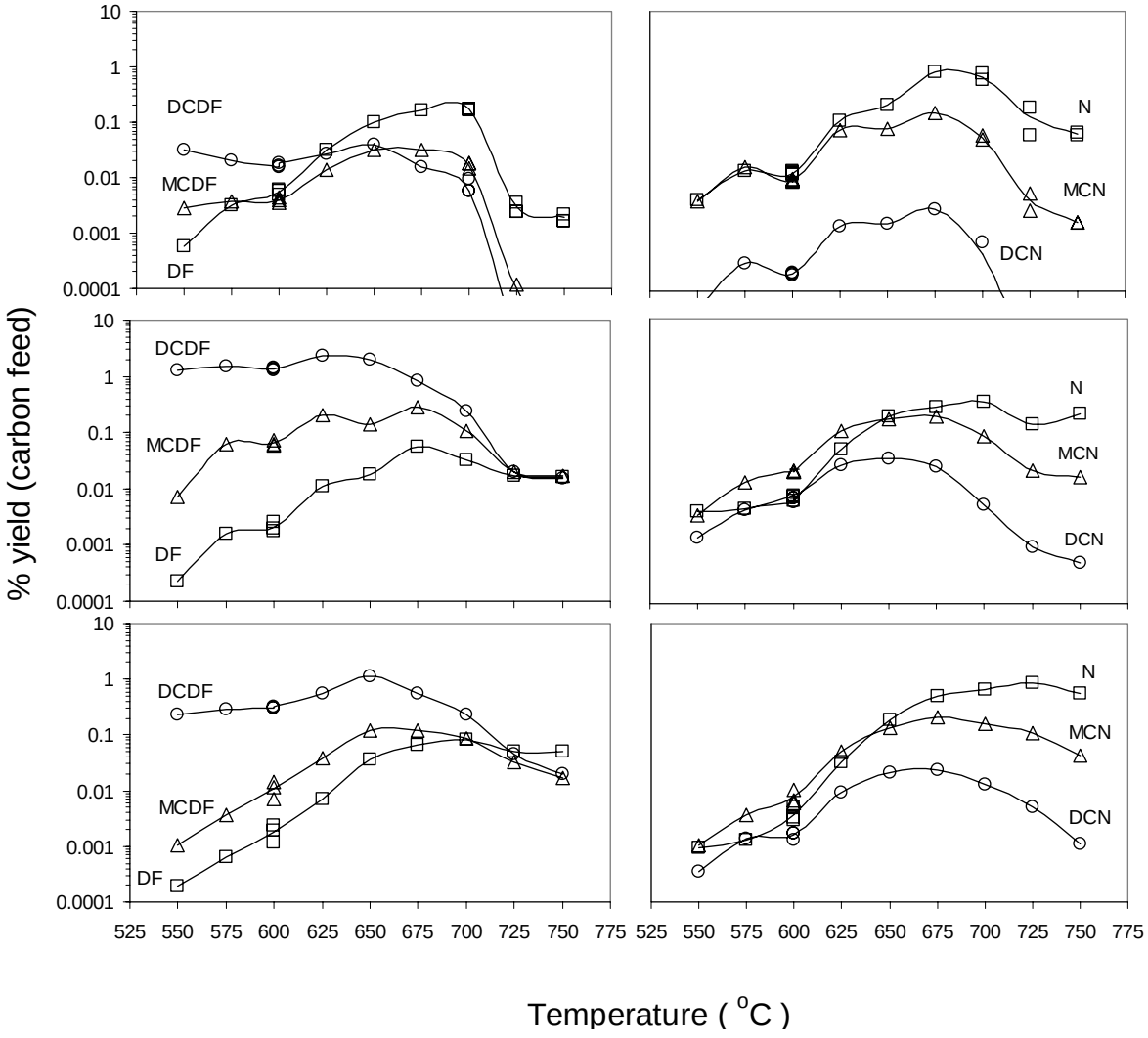

Figure 6.12 PCDF (left) and PCN (right) homologue distributions from 2-CP (top), 3-CP (middle) and 4-CP (bottom)

The PCN homologue distributions show a similar trend with temperature as the PCDF homologue distributions, with the unchlorinated congener becoming increasingly the dominant product at high temperatures. Unlike the dibenzofuran homologue distribution, however, the total yields of monochlorinated and unchlorinated congeners were greatest in the case of naphthalene formation even at the lowest temperature studied (550^{o}C).

For all three CPs, the high yields of DCDF and DCN products at low temperatures, relative to DCDF and DCN yields at high temperatures, are consistent with ortho-ortho carbon coupling of two chlorophenoxy radicals. As temperature increases, organic chlorine decreases. Increases in MCDFs and DF relative to DCDFs and MCNs and N relative to DCNs suggest coupling of chlorophenoxy radical with phenoxy radical. The identification of DCDF and DCN isomers, discussed in the next section, confirms this conclusion.

Another inference can be drawn from examination of the PCN and PCDF homologue distributions. PCN products from all three chlorophenols were less chlorinated than PCDF products. DCDF yields were a couple of orders of magnitude higher than DCN yields, MCDF yields were similar to MCN yields, and dibenzofuran yields were an order of magnitude lower than naphthalene yields. The presence of chlorine may suppress CO elimination in the ring systems by withdrawing electron density, leading to higher DCDF yields than DCN yields.

6.6.3 PCDF and PCN Isomer Distributions

Naphthalene and dibenzofuran product peaks observed in these experiments are listed in Table 6.2, with each set of isomer peaks listed in order of most abundant to least. All expected PCDF and PCN isomers produced by the coupling of two chlorophenoxy radicals (Table 6.1) were observed (Table 6.2), except for 1,8-DCN. Trace amounts of 1,8-DCN were observed from 2-CP, with yields of less than 0.0001%. In addition, several unexpected PCDF and PCN peaks were observed, consistent with the coupling of chlorophenoxy radical with phenoxy radical and the coupling of two phenoxy radicals. For example, 2-CP produced 4-MCDF and DF in addition

to the expected 4,6-DCDF. 4-CP produced 2-MCDF and DF in addition to the expected 2,8-DCDF, as well as 1- and 2-MCNs and N in addition to the expected 1,6-, 1,7-, 2,6- and 2,7-DCN products.

Table 6.2 Observed PCN and PCDF product peaks from chlorophenols

Chlorophenol reactant	Naphthalene products	Dibenzofuran and dibenzo-*p*-dioxin products
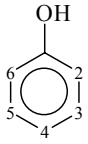	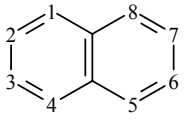	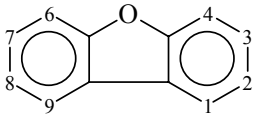
2-CP	1,5-/1,6-/1,7-, 2,6-/2,7-, 1,8-DCNs 1-, 2-MCNs N	4,6-DCDF 4-MCDF DF, DD
3-CP	2,6-/2,7-, 1,5-/1,6-/1,7-DCNs 2-, 1-MCNs N	1,7-, 3,7-, 1,9-DCDFs 1-, 3-MCDF DF
4-CP	2,6-/2,7-, 1,5-/1,6-/1,7-DCNs 2-, 1-MCNs N	2,8-DCDF 2-MCDF DF

PCDF and PCN product yields at each temperature are provided in Table A.8 in Appendix A. In Figure 6.13, ratios of MCDF and DCDF isomers produced from 3-CP are shown as a function of temperature. The results show that the MCDF and DCDF isomer distributions are only weak functions of temperature. In Figure 6.14, ratios of MCN and DCN isomer peaks produced from each of the chlorophenols are shown as a function of temperature. The results show that the MCN and DCN isomer distributions from 2-CP and 4-CP are strong functions of temperature, whereas the MCN and DCN isomer distributions from 3-CP are not. The selectivity

to particular PCN isomers decreased as temperature increased; that is, the ratios tended to go toward one.

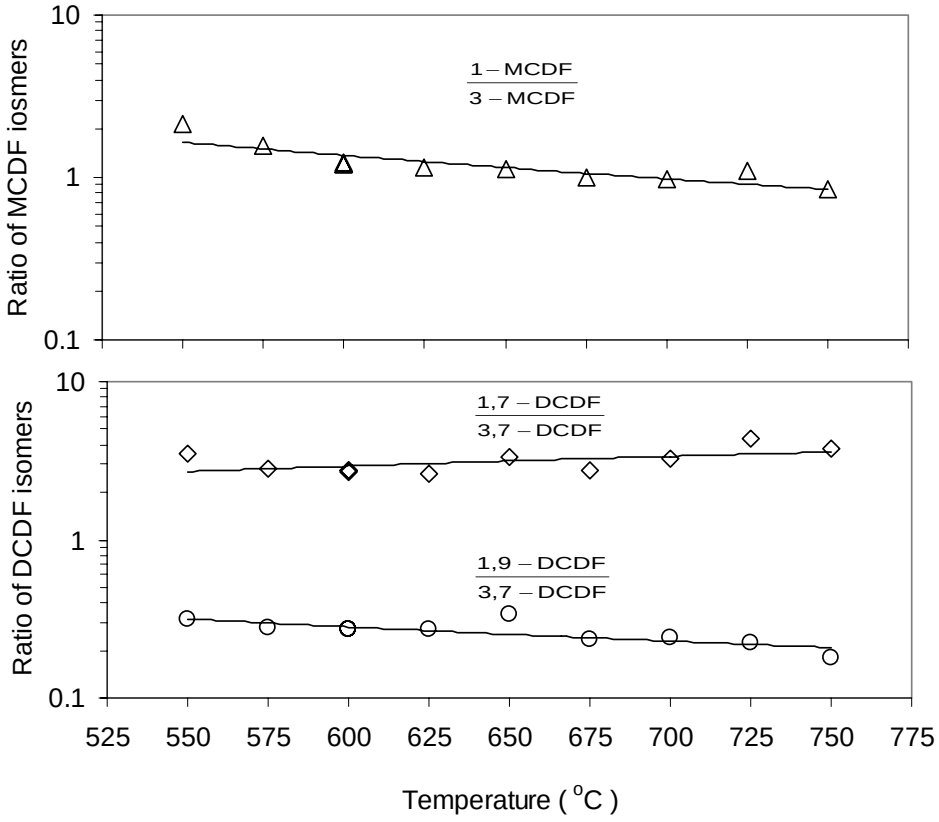

Figure 6.13 Ratios of MCDF and DCDF isomers from 3-CP

Different ortho-ortho phenoxy radical couplings, which are only possible in the case of 3-CP, result in the formation of different PCDF isomers and different sets of PCN isomers. The distributions of these isomers were found to be weakly dependent on temperature, consistent with a low activation energy process for phenoxy radical recombination. The distributions of different PCN isomers formed from 2- and 4-CP, on the other hand, were found to be much more sensitive to temperature, suggesting that the alternative fusion routes from the same dihydrofulvalene

intermediate have different activation energies. These fusion routes involve three-member ring closure by intramolecular radical addition to π-bond.

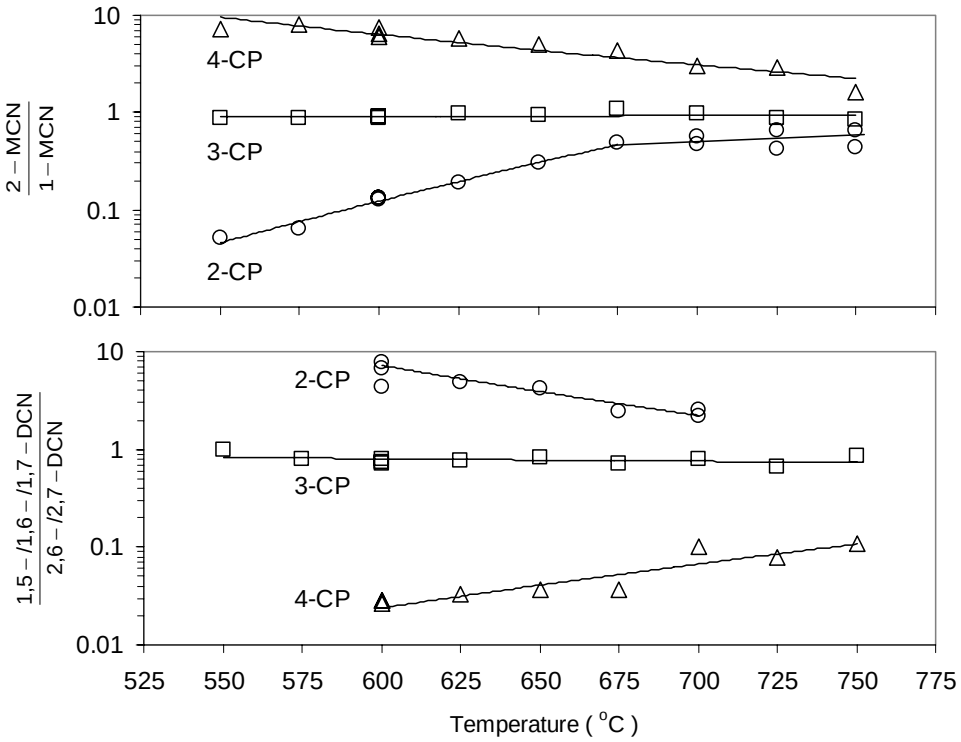

Figure 6.14 Ratios of MCN and DCN isomers from chlorophenols

Alternative routes of PCN formation are possible. A detailed computational study was performed on the keto-enol tautomerization of phenol and 2,4-cyclohexadienone, with CO elimination from the keto tautomer (2,4-cyclohexadienone) to form cyclopentadiene via an acyclic intermediate (Zhu and Bozzelli, 2003). A heat of reaction of 20 kcal/mol for the formation of naphthalene from the 2-chlorophenol radicals via the recombination of cyclopentadiene radicals has been reported (Evans and Dellinger, 2003; Evans and Dellinger, 2005). Another possible reaction sequence that may affect PCN formation from CPs is chlorine migration.

Intramolecular rearrangement of chlorine by 1,5-sigmatropic shift in the cyclopentadiene ring has a similar energy barrier as that of hydrogen (Mikhailov et al., 1994; Okajima and Imafuku, 2002), suggesting that chlorine can move as easily as hydrogen. Such chlorine migration would lead to the formation of additional PCN isomers.

6.7 Conclusions

In summary, this work addresses the formation of PCNs and PCDFs from chlorophenols in post-combustion gas streams. The experimental results presented here support the hypothesis that PCNs and PCDFs are formed from a common intermediate produced by ortho-ortho carbon coupling of phenoxy radicals. The distributions of PCN and PCDF products indicate that phenoxy radical couplings containing fewer chlorine substituents tend to form naphthalenes rather than dibenzofurans. PCN isomer distributions were found to be temperature sensitive, with selectivity to particular isomers decreasing with increasing temperature. These experimental results provide information that can be used to develop and test detailed mechanisms for the formation of PCNs from phenols in combustion exhaust gas.

6.8 References

Abad, E., Caixach, J. and Rivera, J., Dioxin like compounds from municipal waste incinerator emissions: assessment of the presence of polychlorinated naphthalenes. *Chemosphere* 38:109-120 (1999).

Born, J.G.P., Louw, R. and Mulder, P., Formation of dibenzodioxins and dibenzofurans in homogeneous gas-phase reactions of phenols. *Chemosphere* 19:401-406 (1989).

Castaldi, M.J., Marinov, N.M., Melius, C.F., Huang, J., Senken, S.M., Pitz, W.J. and Westbrook, C.K., Experimental and modeling investigation of aromatic and polycyclic aromatic hydrocarbon formation in a premixed ethylene flame. *Proc. Combust. Inst.* 26 :693-702 (1996).

Cieplik, M.K., Epena, O.J. and Louw, R., Thermal Hydrogenolysis of Dibenzo-p-dioxin and Dibenzofuran. *Eur. J. Org. Chem.* 2002:2792-2799 (2002).

Cypres, R. and Bettens, B., La formation de la plupart des composes aromatiques produits lors de la pyrolyse du phenol, ne fait pas intervenir le carbone porteur de la fonction hydroxyle. *Tetrahedron* 39:359-365 (1975).

Eiceman, G.A., Clement, R.E., and Karasek, F.W., Analysis of fly ash from municipal incinerators for trace organic compounds. *Analytic. Chem.* 51:2343-2350 (1979).

Engwall, M., Brundstrom, B. and Jakobsson, E., Ethoxyresorufin O-deethylase (EROD) and aryl hydrocarbon hydroxylase (AHH)-inducing potency and lethality of chlorinated naphthalenes in chicken (Gallus domesticus) and eider duck (Somateria mollissima) embryos. *Archives of Toxicology* 68:37-42 (1994).

Falandysz, J., Polychlorinated naphthalenes: an environmental update. *Environ. Pollut.* 101:77-90 (1998).

Frank, P., Herzler, J., Just, TH. and Wahl, C., High-temperature reactions of phenyl oxidation. *Proc. Combust. Inst.* 25:833-840 (1994).

Friderichsen, A.V., Shin, E.-J., Evans, R.J., Nimlos, M.R., Dayton, D.C. and Ellison, G.B., The pyrolysis of anisole ($C_6H_5OCH_3$) using a hyperthermal nozzle. *Fuel* 80**:**1747-1555 (2001).

Hanberg, A., Wærn, F., Asplund, L., Haglund, E. and Safe, S., Swedish dioxin survey: determination of 2,3,7,8-TCDD toxic equivalent factors for some polychlorinated biphenyls and naphthalenes using biological tests. *Chemosphere* 20:1161-1164 (1999).

Horn, C., Roy, K., Frank, P. and Just, TH., Shock-tube study on the high-temperature pyrolysis of phenol. *Proc. Combust. Inst.* 27:321-328 (1998).

Imagawa, T. and Yamashita, N., Isomer specific analysis of polychlorinated naphthalenes in halowax and fly ash. *Organohalogen Compounds* 19:215-218 (1994).

Järnberg, U., Asplund, C. and Jakobsson, E., Gas chromatographic retention of polychlorinated naphthalenes on non-polar, polarizable, polar and semectic capillary columns. *J. Chromat*. 683A:385-396 (1994).

Liu, R., Morokuma, K., Mebel, A.M. and Lin, M.C., *Ab inito* study of the mechanism for the thernal decomposition of the phenoxy radicals. *J. Phys. Chem.* 100:9314-9322 (1996).

Lovell A.B., Brezinsky, K. and Glassman, I., Benzene oxidation perturbed by NO_2 addition. *Proc. Combust. Inst*. 22:1063-1074 (1988).

McEnally, C.S. and Pfefferle, L.D., The use of carbon-13-labeled fuel dopants for identifying naphthalene formation pathways in non-premixed flames. *Proc. Combust. Inst.*28:2569-2576 (2000).

Manion, J. and Louw, R., Rates, products, and mechanisms in the gas-phase hydrogenolysis of phenol between 922 and 1175 K. *J. Phys. Chem*. 93:3563-3574 (1989).

Marinov, N.M. Castaldi, M.J., Melius, C.F., and Tsang, W., Aromatic and Polycyclic Aromatic Hydrocarbon Formation in a Premixed Propane Flame, *Combust. Sci. Technol.* 128:295-342 (1997).

Melius, C.F., Colvin, M.E., Marinov, N.M., Pitz, W.J. and Senkan, S.M., Reaction mechanisms in aromatic hydrocarbon formation involving the C_5H_5 cyclopentadienyl moiety. *Proc. Combust. Inst.* 26:685-692 (1996).

Mikhailov, I.E., Dushenko, G.A., Kisin, A.V., Mügge, C., Zschunke, A. and Minkin, V.I., 1,5-sigmatropic shifts of chlorine in the cyclopentadiene ring. *Mendeleev Commun* (3):85-88 (1994).

Mulholland, J.A., Lu, M. and Kim D.H., Pyrolytic growth of polycyclic aromatic hydrocarbons by cyclopentadienyl moieties. *Proc. Combust. Inst.* 28:2593-2599 (2000).

Nakahata, D.-T. and Mulholland, J.A., Effects of dichlorophenol substitution pattern on furan and dioxin formation. *Proc. Combust. Inst.* 28:2701-2707 (2000).

Okajima, T. and Imafuku, K., Theoretical study on chlorine and hydrogen shift in cycloheptatriene and cyclopentadiene derivatives. *J. Org. Chem.* 67:625-632 (2002).

Olie, K., Vermeulen, P.L. and Hutzinger, O., Chlorodibenzo-p-dioxins and chlorodibenzofurans are trace components of fly ash and flue gas of some incinerators in the Netherlands. *Chemosphere* 6:455-459 (1977).

Olivella, S., Sole, A. and García-Raso, A., *Ab intio* calculations for the potential surface for the thermal decomposition of the phenoxy radicals. *J. Phys. Chem.* 99:10549-10556 (1995).

Schneider, M., Stieglitz, L., Will, R. and Zwick, G., Formation of polychlorinated naphthalenes on fly ash. *Chemosphere* 37:2055-2070 (1998).

Spielmann, R. and Cramers, C.A., Cyclopentadienic compounds as intermediates in the thermal degradation of phenols: Kinetics of thermal decomposition of cyclopentadiene. *Chromatographia* 5:295-300 (1972).

Weber, R. and Hagenmaier, H., On the mechanism of the formation of polychlorinated dibenzofurans from chlorophenols. *Organohalogen Compounds* 31:480-485 (1997).

Yang, Y., Mulholland, J.A., and Akki, U., Formation of furans by gas-phase reactions of chlorophenols. *Proc. Combust. Inst.* 27:1761-1768 (1998).

Zhu, L. and Bozzelli, J.B., Kinetics and thermochemistry for the gas-phase keto-enol tautomerization of phenol ⟷ 2,4-cyclohexadiene. *J. Phys. Chem. A* 107:3696-3703 (2003).

CHAPTER 7

FORMATION OF CHLORINATED NAPHTHALENES FROM DICHLOROPHENOLS

[Material presented in this chapter is adapted from the manuscript published in *Organohalogen Compounds* 66:1043-1049 (2004) entitled, "Chlorinated Naphthalene Formation from Chlorophenols," and from the manuscript submitted to *Chemosphere* entiled, "Chlorinated Naphthalene Formation from Dichlophenols."]

Abstract

Polychlorinated naphthalenes (PCNs) formed along with dibenzo-p-dioxin and dibenzofuran products in the slow combustion of dichlorophenols (DCPs) at 600^{o}C were identified. Each DCP reactant produced a unique set of PCN products. Major PCN congeners observed in the experiments were consistent with products predicted from a mechanism involving an intermediate formed by ortho-ortho carbon coupling of phenoxy radicals; polychlorinated dibenzofurans (PCDFs) are formed from the same interemediate. Tautomerization of the intermediate and H_2O elimination produces PCDFs; alternatively, CO elimination to form dihydrofulvalene and fusion produces naphthalenes. Only trace amounts of tetrachloronaphthalene congeners were formed, suggesting that the preferred PCN formation pathways from chlorinated phenols involve loss of chlorine. 3,4-DCP produced the largest yields of PCDF and PCN products with two or more chlorine substituents. 2,6-DCP did not produce tri- or tetra-chlorinated PCDF or PCN congeners. It did produce 1,8-DCN, however, which could not be explained.

7.1 Introduction

Formation of polychlorinated naphthalenes (PCNs) along with other halogenated aromatic compounds, such as polychlorinated biphenyls (PCBs), polychlorinated dibenzo-*p*-dioxins (PCDDs) and polychlorinated dibenzofurans (PCDFs), has been observed to occur in combustion exhaust gas (Olie et al., 1977; Eiceman et al., 1979; Imagawa and Takeuchi, 1995). Recent studies showed a strong correlation between several PCN and PCDF congeners in municipal waste incinerator (MWI) fly ash, suggesting that the formation pathways might be similar (Iino et al., 1999; Imagawa et al., 2001; Weber et al., 2001). It has also been reported that the amount of PCNs formed from a pilot-scale solid waste incinerator was the same order of magnitude as PCDD/F yields (Sakai et al., 1996). While the mechanism of PCN formation in incinerators is not well understood, concern about the presence of PCNs in environment has risen.

Formation of naphthalene at high temperatures in flames has largely been attributed to the hydrogen-abstraction/acetylene-addition (HACA) mechanism (Frenklach et al., 1984; Frenklach and Warnatz, 1987; McEnally and Pfefferle, 2000). In post-combustion gas, however, under conditions in which PCDDs and PCDFs are formed from chlorinated phenols, PCNs may be formed directly from coupling of chlorinated phenoxy radicals. In previous studies in this laboratory, formation of PCNs with PCDDs/PCDFs was observed in gas-phase pyrolysis (Akki, 1997) and oxidation (Yang et al., 1998) of chlorinated phenols. No attempt was made to elucidate the detailed mechanism of PCN formation as many of the PCN congeners were unidentified.

Some studies suggest that naphthalene formation from phenol in flames can occur by combination of cyclopentadienyl (CPDyl) radicals, produced from the decomposition of phenoxy radical via loss of CO (Spielmann and Cramers, 1972; Manion and Louw, 1989; Castaldi et al., 1996; Marinov et al., 1997). Melius and coworkers (1996) performed quantum chemical modeling on naphthalene formation from dihydrofulvalene, proposing that the recombination of CPDyl radicals produces dihydrofulvalene which then undergoes intramolecular rearrangements

via resonance-stabilized radicals. Three-member ring closure and opening results in fusion of the bi-cyclic dihydrofulvalene intermediate to form naphthalene.

In a previous work at this laboratory, PCN formation pathways from the slow oxidation of monochlorophenols (MCPs) was proposed based on the published mechanisms of PCDF formation from chlorinated phenols and naphthalene formation from dihydrofulvalene (Kim et al., 2004). Major dibenzo-p-dioxin, dibenzofuran and naphthalene products in each homologue class from each of the three MCPs are listed in Table 7.1. Overall pathways to major products from 2-MCP are depicted in Figure 7.1.

Table 7.1 Major naphthalene, dibenzofuran and dibenzo-p-dioxin products from MCPs

reactant	naphthalenes	dibenzofurans and dibenzo-p-dioxins
2-MCP	1,5-DCN 1-MCN N	4,6-DCDF 4-MCDF DF DD
3-MCP	2,6-, 2,7-, 1,6-, 1,7-DCNs 1-, 2-MCNs N	1,7-, 3,7-, 1,9-DCDFs 1-, 3-MCDFs DF
4-MCP	2,6-, 2,7-DCNs 2-MCN N	2,8-DCDF 2-MCDF DF

In combustion exhaust gas at temperatures between 550 and 750°C, chlorophenols form resonance-stabilized radicals either by loss of the phenolic hydrogen or loss of a chlorine substituent and migration of the phenolic hydrogen to form the stable radical. Chlorophenoxy radical coupling between an oxygen and an ortho carbon with chlorine substituent (pathway I, Figure 7.1) leads to the formation of dibenzo-p-dioxin products via a five-member ring intermediate and loss of two chlorine atoms (Sidhu et al., 1995). Carbon-carbon coupling at

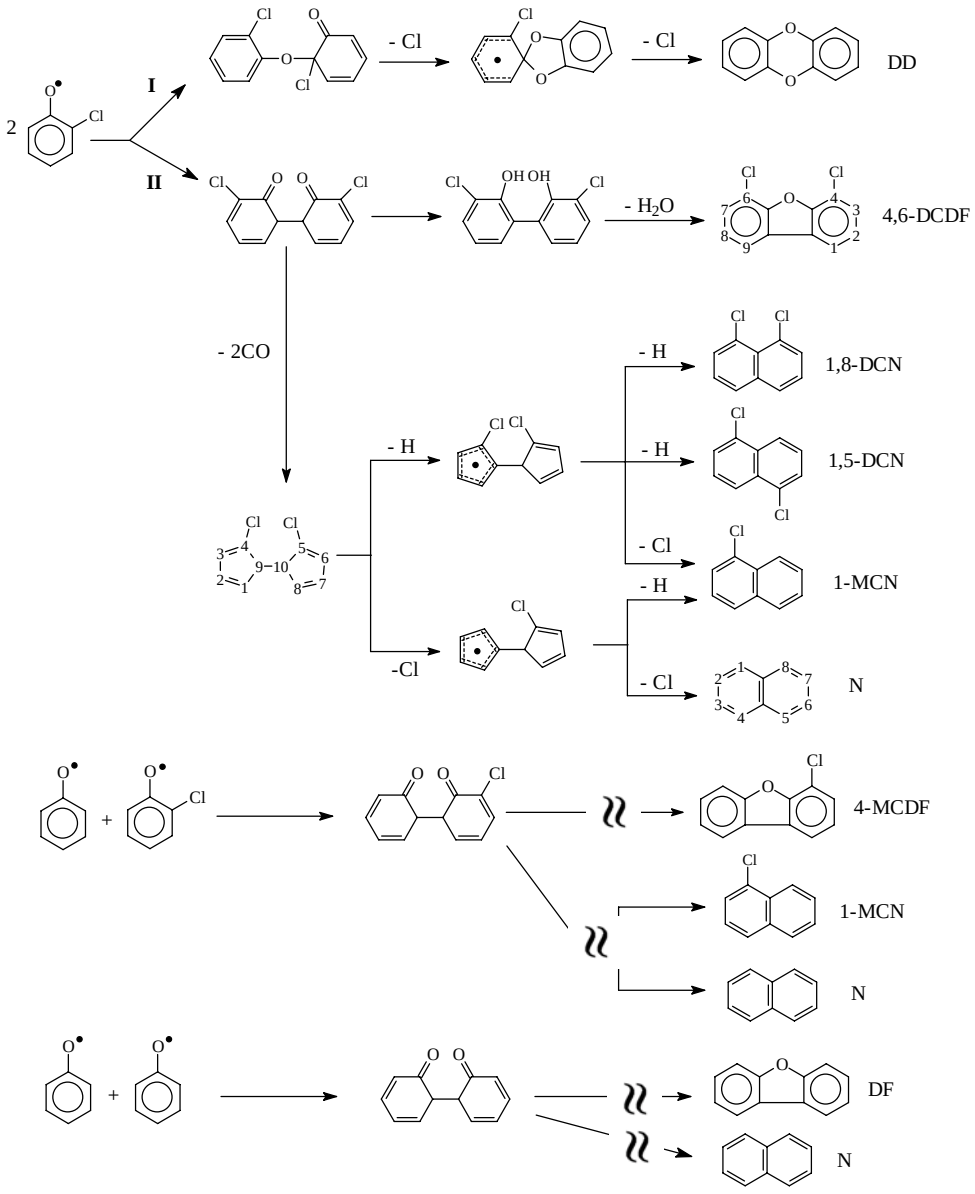

Figure 7.1 Major dibenzo-p-dioxin, dibenzofuran, and naphthalene products from 2-MCP

unchlorinated ortho sites of pairs of chlorophenoxy and/or phenoxy radicals (pathway II, Figure 7.1) results in the formation of both dibenzofuran products without chlorine loss and naphthalene products with loss of zero to two chlorine atoms. In the formation of dibenzofuran products, tautomerization produces the dihydroxybiphenyl (DOHB) intermediate, followed by loss of H_2O to yield dibenzofuran (Born et al., 1989; Weber and Haganmaier, 1999; Evans and Dellinger, 2005). Alternatively, elimination of CO from each ring system yields a dihydrofulvalene intermediate, followed by naphthalene formation via pathways analogous to the mechanism proposed by Melius et al. (1996). The predominant naphthalene products observed in the MCP experiments were isomers formed by fusion across the 9-10 dihydrofulvalene bond. From each of the three MCPs, dichloronaphthalene yields were much lower than monochlorinated and unchlorinated congener yields.

In this chapter, we present dibenzo-p-dioxin, dibenzofuran and naphthalene product yields from the slow combustion of the six dichlorophenols (DCPs). Predicted products, based on reaction pathways developed from the MCP experimental results, are compared with experimental observations. Possible correlations between PCN and PCDF yields are assessed.

7.2 Experimental Methods

A laminar flow, isothermal quartz tube reactor (40 cm in length and 1.7 cm in diameter; 10 second residence time) was used to study PCN formation from each of the six DCPs. DCP reactant was dissolved in benzene (1:2 molar ratio) and fed by syringe pump into a glass vessel, located upstream of reactor inlet. The glass vessel was heated to vaporize the reactant stream. Nitrogen with 8% oxygen and 0.1% DCP vapor was injected into the reactor. Experiments were conducted at 600^{o}C, the temperature at which PCN yields were greatest under our experimental condition (Nakahata and Mulholland, 2000). The entire product stream was immediately quenched at the outlet of the reactor and collected in an ice-cooled dichloromethane double trap system. Gas and rinse solutions were filtered to remove soot.

Benzene was used to get the DCP reactant into solution. Experiments with benzene only (i.e. without DCP reactant) demonstrated that phenol was almost entirely derived from hydroxylation of benzene and not dechlorination of DCP. Otherwise, benzene was not reactive under these conditions.

Analysis of PCDD, PCDF and PCN congeners was accomplished with a Hewlett-Packard 6890 series gas chromatography with HP-5MS column (30m, 0.25 mm i.d., 0.25 μm film thickness) coupled to a Hewlett-Packard 5973 mass spectrometer. The column oven temperature was programmed as follows: 38 to 80°C at a rate of 3°C/min, 180 to 250°C at a rate of 5°C/min, 250 to 280°C at a rate of 6°C/min, and a final hold time of 3 min. For quantification, the mass spectrometer was operated in selective ion mode at the two most intensive and characteristic ion masses.

Procedures for identifying PCDF and PCDD products have been published previously (Yang et al., 1998; Nakahata and Mulholland, 2000). PCN congeners were identified based on the published relative retention time and elution order of PCNs in Halowax 1001, 1014, and 1051 (Abad et al., 1999; Schneider et al., 1998; Järnberg et al., 1994). Unchlorinated dibenzo-p-dioxin, dibenzofuran and naphthalene were used as universal response factors to estimate yields of PCDD, PCDF and PCN products, respectively.

7.3 Predicted Dibenzo-p-dioxin, Dibenzofuran and Naphthalene Products from DCPs

To test our proposed reaction scheme, we developed a priori hypotheses for the major dibenzo-p-dioxin, dibenzofuran and naphthalene products from DCPs; these are listed in Table 7.2. Based on the MCP experimental results, we predicted major isomer products in each homologue by considering the following reaction schemes: coupling of two dichlorophenoxy radicals to yield dichlorodibenzo-p-dioxin (DCDD), tetrachlorodibenzofuran (T_4CDF), tetrachloronaphthalene (T_4CN), trichloronaphthalene (T_3CN) and dichloronaphthalene (DCN)

products; coupling of dichlorophenoxy radical with the monochlorophenoxy radical formed by loss of ortho chlorine to form monochlorodibenzo-p-dioxin (MCDD), trichlorodibenzofuran (T_3CDF), T_3CN, DCN and monochloronaphthalene (MCN) products; coupling of dichlorophenoxy radical with a phenoxy radical formed via hydroxylation of benzene to form

Table 7.2 Predicted major chlorinated naphthalene, dibenzofuran and dibenzo-p-dioxin products from DCPs

reactant	naphthalenes	dibenzofurans and dibenzo-p-dioxins
2,4-DCP	1,3,5,7-, 1,3,6,8-T_4CNs 1,3,6-, 1,3,7-T_3CNs 1,3-, 2,6-, 2,7-DCNs 2-MCN	2,4,6,8-T_4CDF 2,4,8-T_3CDF 2,4-DCDF 2-, 4-MCDFs 2,7-, 2,8-DCDDs
2,5-DCP	1,4,5,8-T_4CN 1,4,5-, 1,4,6-, 1,4,7-, 1,4,8-T_3CNs 1,4-, 1,5-, 1,6-, 1,7-, 1,8-DCNs 1-, 2-MCN	1,4,6,9-T_4CDF 1,4,7-, 1,4,9-T_3CDFs 1,4-DCDF 1-, 3-, 4-MCDFs 2,7-, 2,8-DCDDs
3,5-DCP	1,3,5,7-, 1,3,6,8-T_4CNs 1,3,6-, 1,3,7-T_3CNs 1,3-, 2,6-, 2,7-DCNs 2-MCN	1,3,7,9-T_4CDF 1,3,7-, 1,3,9-T_3CDFs 1,3-DCDF 1-, 3-MCDFs
2,3-DCP	1,2,5,6-, 1,2,7,8-T_4CNs 1,2,5-, 1,2,6-, 1,2,7-, 1,2,8-T_3CNs 1,2-, 1,5-, 1,6-, 1,7-, 1,8-DCNs 1-, 2-MCN	1,3,7,9-T_4CDF 3,4,7-, 3,4,9-T_3CDFs 3,4-DCDF 1-, 3-, 4-MCDFs 1,6-, 1,9-DCDDs
3,4-DCP	1,2,6,7-, 2,3,6,7-, 1,2,7,8-T_4CNs 1,2,5-, 1,2,6-, 1,2,7-, 1,2,8-, 2,3,5-, 2,3,6-T_3CNs 1,2-, 2,3-, 1,5-, 1,6-, 1,7-, 1,8-DCNs 1-, 2-MCN	1,3,7,8-, 1,3,8,9-, 2,3,7,8-T_4CDFs 1,2,7-, 1,2,8-, 1,2,9-, 2,3,7-, 2,3,8-, 2,3,9-T_3CDFs 1,2-, 2,3-DCDFs 1-, 2-, 3-MCDFs
2,6-DCP	1,5-, 1,8-DCNs 1-MCN	4,6-DCDF 4-MCDF 1,6-, 1,9-DCDDs 1-MCDD

dichlorodibenzofuran (DCDF), DCN and MCN products and naphthalene (N); coupling or monochlorophenoxy radical with phenoxy radical to produce MCDF products. As an example, pathways to major isomer products in each dibenzo-p-dioxin, dibenzofuran and naphthalene homologue are depicted for 2,4-DCP in Figure 7.2.

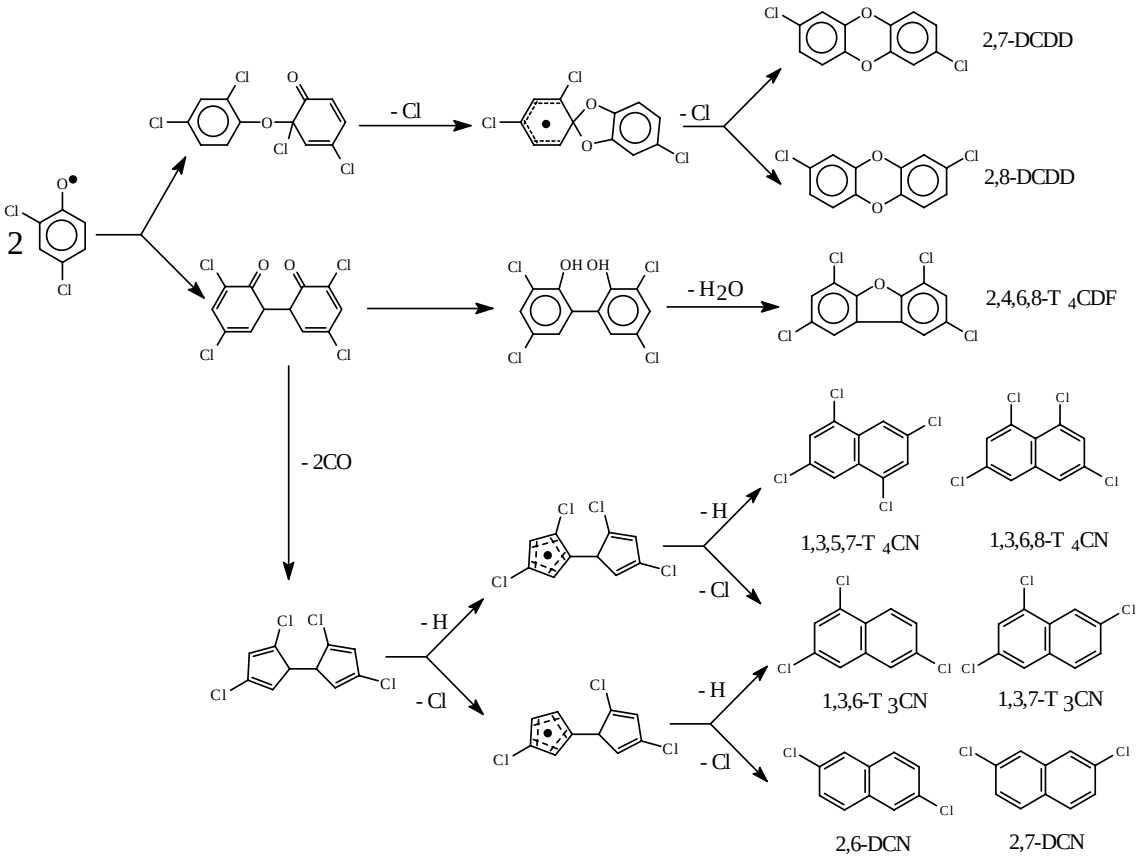

Figure 7.2 Predicted dibenzo-p-dioxin, dibenzofuran, and naphthalene products from 2,4-DCP

Additional dibenzofuran and naphthalene products expected from the following couplings:

2,4-dichlorophenoxy + 4-chlorophenoxy → 2,4,8-T_3CDF

2,4-dichlorophenoxy + phenoxy → 2,4-DCDF, 1,3-DCN, 2-MCN

4-chlorophenoxy + phenoxy → 2-MCDF

2-chlorophenoxy + phenoxy → 4-MCDF

phenoxy + phenoxy → DF, N

7.4 Results and Discussion

7.4.1DCP Recovery and Overall Product Distribution

DCP reactant recovery and yields of phenol, total MCP, total naphthalene, total dibenzofuran, and total dibenzo-*p*-dioxin products for each DCP reactant are shown in Figure 7.3, expressed as a percent DCP conversion (carbon basis). The amount of unreacted DCP recovered ranged from 4% for 3,4-DCP to 13% for 2,4- and 2,6-DCPs. MCP yields from dechlorination of DCP reactants were greatest for 2,4- and 2,6-DCPs, indicating that the ortho and para sites are preferentially dechlorinated. In the case of 2,4-DCP, 4-MCP was the major dechlorination product indicating that dechlorination at the ortho site is greater than dechlorination at the para site. Unchlorinated phenol yields were greater than MCP yields, by more than an order of magnitude for 2,5-, 3,5-, 2,3- and 3,4-DCPs; yields ranged from 0.8% to 2.4% of total DCP feed. Only in the cases of 2,4- and 2,6-DCPs, which had the highest MCP yields, might dechlorination have been a significant source of phenol. Total yields of naphthalene products ranged from 0.004% for 3,5-DCP to 0.009% for 2,3-DCP. Dibenzofuran product yields were higher, ranging from 0.007% for 2,5-DCP to 0.3% for 3,4-DCP. Dibenzo-*p*-dioxin products were observed only from 2,4- and 2,6-DCPs, with yields of 0.001% and 0.003%, respectively. Although not measured in these experiments, it is known from the MCP experiments that CO yields are high under these conditions, with significant decomposition of the DCP to low molecular weight products.

These results do not suggest a correlation between naphthalene and dibenzofuran product yields. For example, 2,3-DCP produced the greatest naphthalene product yield but the second to lowest dibenzofuran product yield. The results show that the presence of ortho chlorine on the DCP reactant inhibits dibenzofuran product formation, promotes dibenzo-p-dioxin product formation, and does not appear to have a significant effect on total naphthalene product formation. It will be shown, however, that ortho chlorine does reduce the formation T_3CN and T_4CN products.

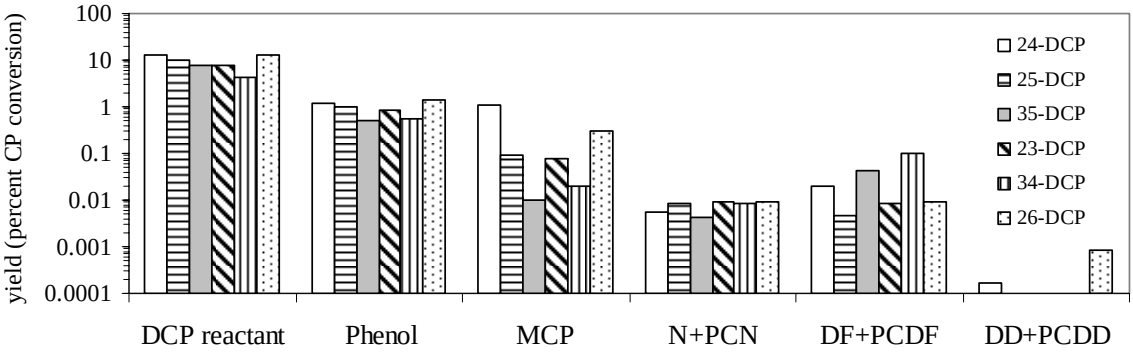

Figure 7.3 DCP recovery and phenol, naphthalene, dibenzofuran and dibenzo-p-dioxin product yields

7.4.2 PCN and PCDF Homologue Distributions

Total naphthalene homologue and dibenzofuran homologue yields are shown in Figure 7.4. T_4CNs were detected only in trace amounts, and only from 3,4-DCP. This suggests that the major route of PCN formation from chlorinated phenols is by loss of at least one chlorine atom. The total T_4CDF yields, on the other hand, were similar in magnitude to the yields of other homologues. In particular, the two DCPs without ortho chlorine (i.e. 3,5- and 3,4-DCPs) had high T_4CDF yields. Yields of N, MCNs and DCNs were of similar order of magnitude. The PCN homologue with greatest yield was unchlorinated naphthalene from 2,3-, 2,4- and 2,5-DCPs, MCN from 3,5- and 2,6-DCPs, and DCN from 3,4-DCP. 3,4-DCP produced the greatest T_3CN yield.

Regarding PCDF formation, 3,4- and 3,5-DCPs produced more T_4CDF products than other homologues. For each of the six DCPs, DCDF product yield exceeded T_3CDF product yield, and DF product yield exceeded MCDF product yield. These results are consistent the major PCDF precursors being DCP reactant and phenol from hydroxylation of benzene. PCDFs are formed without loss of chlorine; therefore, two DCPs produce T_4CDFs, DCP and phenol produce

DCDFs, and two phenols produce DF. MCDF and T_3CDF products are formed from DCP and MCP formed by DCP dechlorination. MCP yields were significantly lower than phenol yields (Figure 7.3).

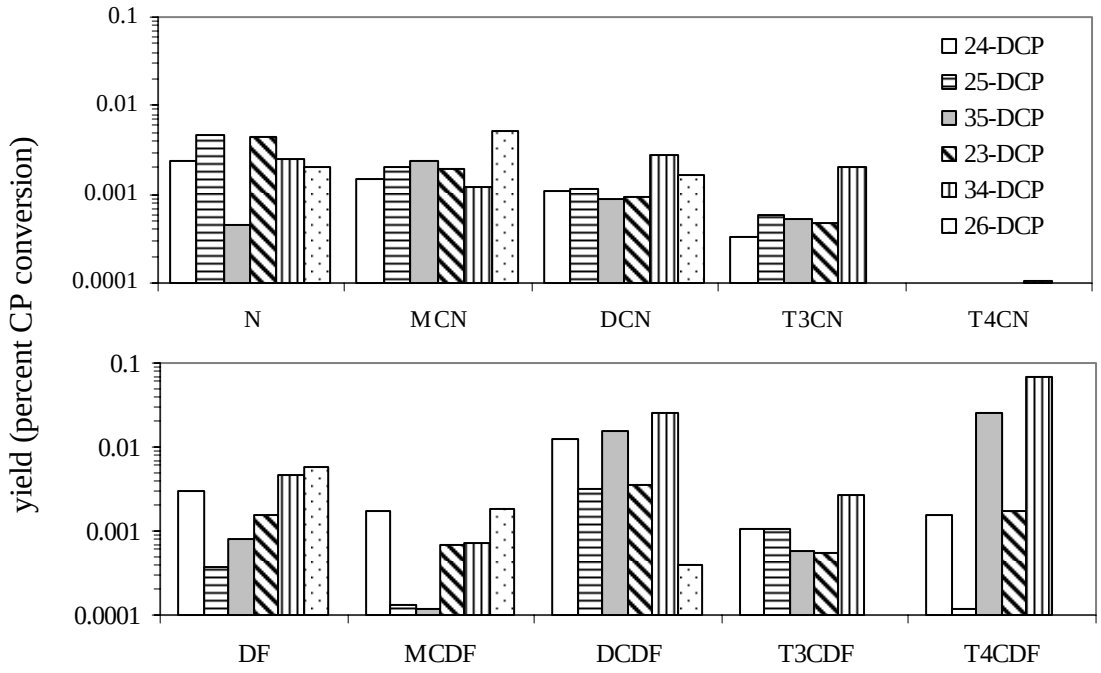

Figure 7.4 PCN (top) and PCDF (bottom) homologue yields from DCPs

2,6-DCP produced no T_3CDF or T_4CDF products and no T_3CN or T_4CN products, consistent with mechanism predictions (Table 7.2). Less chlorinated naphthalene and dibenzofuran products were formed, as expected. 3,4-DCP, on the other hand, produced the greatest DCDF, T_3CDF and T_4CDF product yields, as well as the greatest DCN, T_3CN and T_4CN product yields. Thus, ortho chlorine on phenol appears to inhibit the formation of PCN congeners without chlorine loss, consistent with previous observations on PCN formation from MCPs (Kim et al., 2004).

7.4.3 PCN and PCDF Isomer Distributions

PCN and PCDF isomer fractions are shown in Figures 7.5 and 7.6, respectively. The different patterns of PCN isomers for each DCP supports the finding from the previous MCP study that the primary pathway of PCN formation is not a recombination of chlorinated CPDyl radicals as originally hypothesized (Kim et al., 2004); otherwise, only two different PCN product patterns are expected from the six DCPs because only two types of chlorinated CPDyl radicals are formed via CO elimination from dichlorophenoxy radicals. PCDF isomers also bear the signature of the phenol reactants, as expected. Not only did 3,4-DCP produce the largest yields of di-, tri- and tetra-chlorinated dibenzofurans and naphthalenes (Figure 7.4), but this DCP produced the broadest distribution of PCDF and PCN products (Figures 7.5 and 7.6). This is consistent 3,4-DCP having both ortho sites unchlorinated (unlike 2,3-, 2,4-, 2,5- and 2,6-DCPs) and lacking symmetry(unlike 3,5-DCP).

To more easily compare observed naphthalene, dibenzofuran and dibenzo-p-dioxin products with those predicted (Table 7.2), major product peaks in each homologue are listed in Table 7.3, with predicted products indicated in bold. The observed major peaks agree well with those predicted. All predicted PCDF products were detected, and the less chlorinated congeners (MCDF products and DF) are consistent with those predicted from reactions between MCP and phenol and two phenols. Predicted dibenzo-p-dioxin products were formed in very small amounts relative to dibenzofuran products, except for 2,6-DCP. Observed major PCN peaks agree with those predicted.

Three further observations can be made from the information in Table 7.3. First, the lack of detectable T_4CN products from all DCPs except 3,4-DCP indicates that PCN formation is favored with one chlorine atom loss, particularly when chlorine is at an ortho position. Second, predicted PCN congeners with 1,8 chlorine substituents were not found, except in the case of 2,6-DCP, suggesting that formation of these congeners with greater steric hindrance is not favored. Third, in all cases except 2,6-DCP, the major DCN peak was that produced from DCP and phenol

without chlorine atom loss, not that from two DCPs with loss of two chlorine atoms or that from DCP and MCP with loss of one chlorine atom.

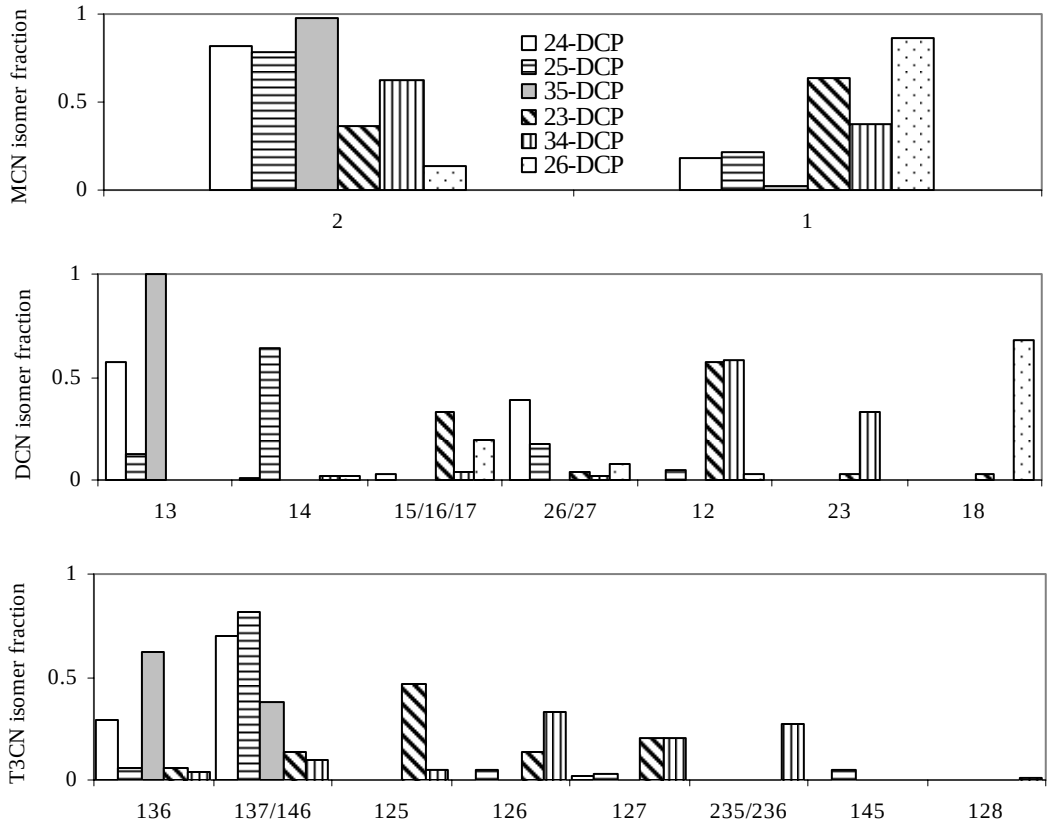

Figure 7.5 PCN isomer fractions from DCPs. Only observed PCN isomers (yield >0.00001%) are listed, in order of elution in our analytic system

The only major PCN peak that is not consistent with our prediction of major products is the formation of 1,8-DCN from 2,6-DCP. While 2,6-DCP dechlorination yields 2-MCP and 2-MCP is expected to produce both 1,5- and 1,8-DCNs, our 2-MCP experimental results indicate that 1,5-DCN, not 1,8-DCN, is the predominant isomer formed from 2-MCP. The 1,8- isomer was the major DCN peak from 2,6-DCP. As stated above, PCN congeners with 1,8 chlorine substitution

are otherwise not observed. One possible explanation is that the 1,8-DCN was formed via the dibenzo-p-dioxin intermediate (oxygen-carbon coupling) rather than the dibenzofuran intermediate (Cieplik et al., 2002).

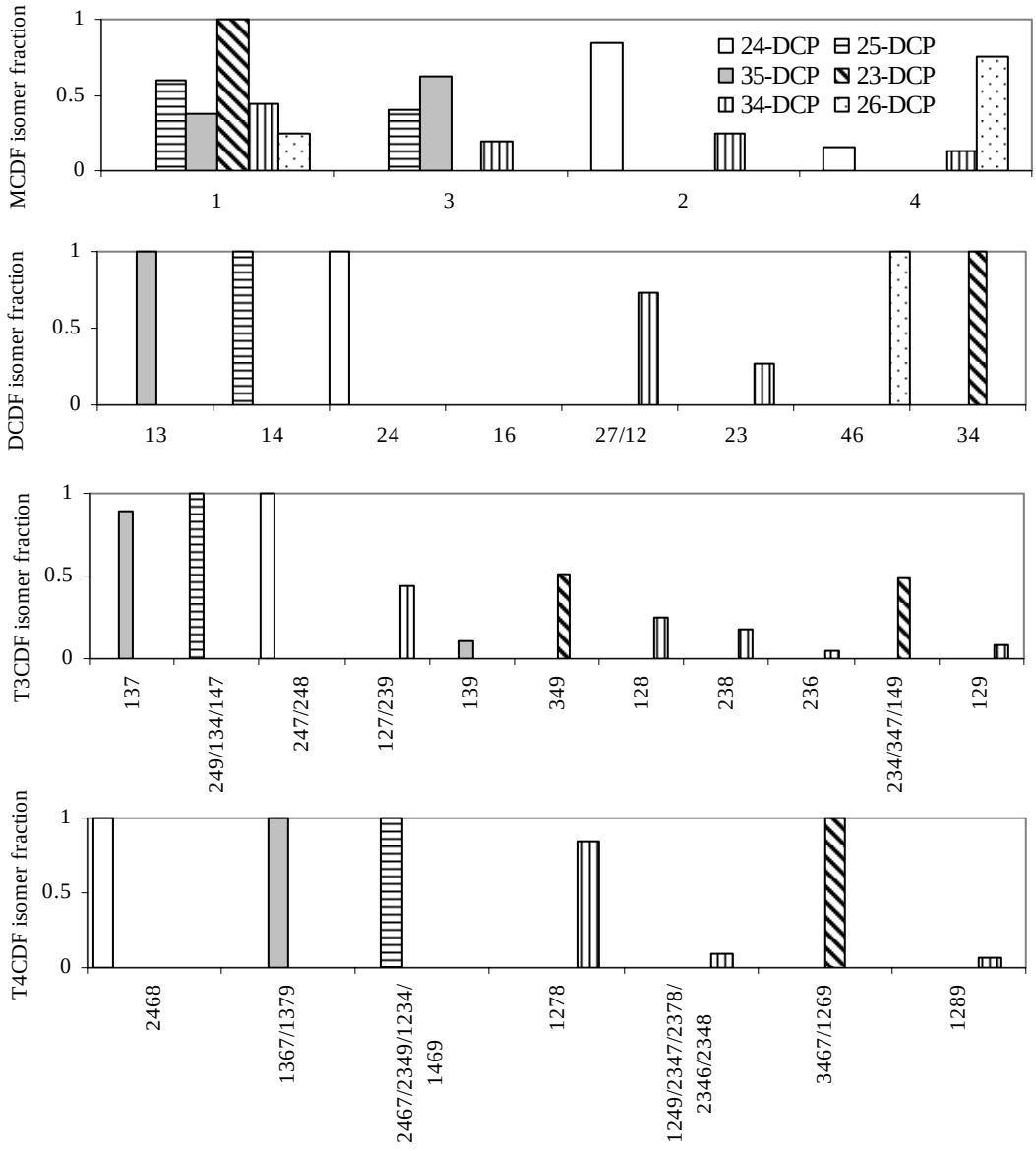

Figure 7.6 PCDF isomer fractions from DCPs. Only observed PCDF isomers (yield >0.00001%) are listed, in order of elution in our analytic system

Table 7.3 Observed major naphthalene, dibenzofuran and dibenzo-p-dioxin products from DCPs*

reactant	observed naphthalene peaks	observed dibenzofuran and dibenzo-p-dioxin peaks
2,4-DCP	**1,3,7**-/1,4,6-, **1,3,6**-T_3CNs **1,3**-, **2,6**-/**2,7**-DCNs **2**-MCN N	**2,4,6,8**-T_4CDF 2,4,7-/**2,4,8**-T_3CDF **2,4**-DCDF **2**-, **4**-MCDF DF **2,7**-, **2,8**-DCDDs
2,5-DCP	1,3,7-/**1,4,6**-T_3CN **1,4**-DCN **2**-MCN N	2,4,6,7-/2,3,4,9-/1,2,3,4-/**1,4,6,9**-T_4CDF 2,4,9-/1,3,4-/**1,4,7**-T_3CDF **1,4**-DCDF **1**-, **3**-MCDF DF
3,5-DCP	**1,3,6**-, **1,3,7**-/1,4,6-T_3CNs **1,3**-DCN **2**-MCN N	1,3,6,7-/**1,3,7,9**-T_4CDF **1,3,7**-T_3CDF **1,3**-DCDF **3**-, **1**-MCDF DF
2,3-DCP	**1,2,5**-, **1,2,7**-, **1,2,6**-T_3CNs **1,2**-, **1,5**-/**1,6**-/**1,7**-DCNs **1**-, **2**-MCN N	**3,4,6,7**-/1,2,6,9-T_4CDF **3,4,9**-, 2,3,4-/**3,4,7**-/1,4,9-T_3CDF **3,4**-DCDF **1**-MCDF DF
3,4-DCP	**1,2,6,7**-T_4CN **1,2,6**-, **2,3,5**-/**2,3,6**-, **1,2,7**-T_3CNs **1,2**-, **2,3**-DCNs **2**-, **1**-MCN N	**1,2,7,8**-, **2,3,7,8**-/…, **1,2,8,9**-T_4CDFs **1,2,7**-/**2,3,9**-, **1,2,8**-, **2,3,8**-, **1,2,9**-T_3CDFs 2,7-/**1,2**-, **2,3**-DCDF **1**-, **2**-, **3**-, 4-MCDF DF
2,6-DCP	**1,8**-DCN **1**-MCN N	**4,6**-DCDF **4**-, 1-MCDF DF **1,6**-, **1,9**-DCDDs **1**-MCDD

* Largest peaks are listed first. Predicted products from Table 2 are bold and underlined.

Since 2,6-DCP does not have an unchlorinated ortho site, only oxygen-carbon coupling occurs without chlorine loss. An alternative pathway of PCN formation from a phenol with both ortho sites chlorinated might lead to other PCN products. Since these phenols are the most

abundant congeners in combustion exhaust (e.g. 2,4,6-trichlorophenol, 2,3,4,6-tetrachlorophenol and pentachlorophenol), more experimental study and computational study are needed to develop a reaction scheme consistent with congener-specific PCN formation from 2,6 chlorinated phenols.

7.5 Comparison between DCP and MCP Results

As mentioned in previous section, unchlorinated phenol from the hydroxylation of benzene contributes significantly to both PCN and PCDF formation from DCP experiments. In order to have better assessment on PCN and PCDF formation from DCPs, the yields of PCN and PCDF homologues formed only from DCPs are calculated based on the isomer composition of each homologue group (Figure 7.7).

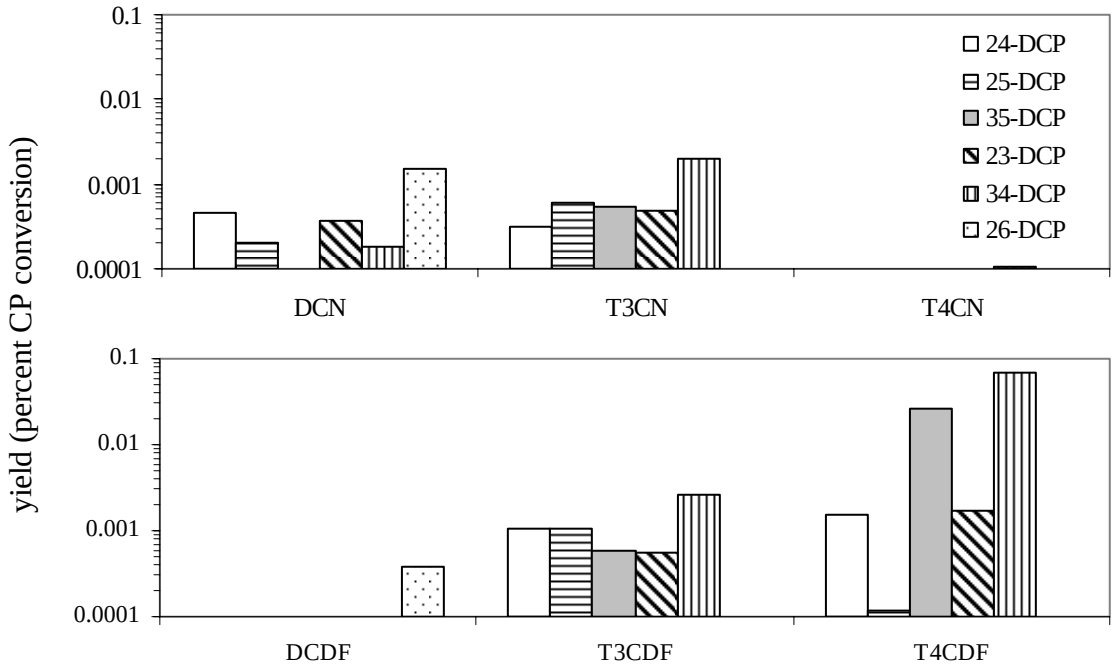

Figure 7.7 The yields of PCN (top) and PCDF (bottom) homologues formed only from DCP reactants

The PCN and PCDF homologue distributions from DCPs in Figure 7.7 show similar trend as those from MCPs (Figure 6.3). Yield order of DCP reactants within each homologue have a similar pattern. 3,4-DCP that had the highest T_3CDF and T_4CDF yields produced the greatest T_3CN and T_4CN yields; 2,6-DCP that had the highest DCDF yield produced the greatest DCN yield.

The PCN and PCDF homologue distributions from DCPs in Figure 7.7 also suggest that highly chlorinated PCN and PCDF products are formed from meta substituted phenols. T_4CDF yields of 3,4- and 3,5-DCPs are an order of magnitude higher than those from other DCPs, T_4CN products were detected only from 3,4-DCP, and 2,6-DCP produced no T_3CDF or T_4CDF products and no T_3CN or T_4CN products. Another inference from Figure 7.7 is that meta substituted phenols favor PCDF formation whereas the ortho/para substituted phenols favor PCN formation. Total PCDF (DCDF, T_3CDF and T_4CDF) yields from 3,4- and 3,5-DCPs were an order of magnitude greater than total PCN (DCN, T_3CN and T_4CN) yields whereas total PCN yield from 2,6-DCP was an order of magnitude greater than total PCDF yield. These results are consistent with the MCP results that the yields of DCN and DCDF from 3-CP are greater than those from 2- and 4-CPs (Figure 6.12) and the ratio of naphthalene to dibenzofuran product yield was least for 3-CP and greatest for 2-CP (Figure 6.11).

7.6 Conclusion

Identification of chlorinated dibenzofuran, dibenzo-p-dioxin and naphthalene congeners from slow combustion of each of the six DCPs supports a proposed mechanism of PCN formation that involves the same phenoxy couple intermediate as that for PCDF formation. This link between PCN and PCDF formation may explain observed correlations of PCN and PCDF yields in combustion systems. These results also provide data that can be used to computationally study congener-specific mechanisms of PCN formation from chlorinated phenols. PCN formation from phenols with 2,6 chlorine substituents requires further study.

7.7 References

Abad, E., Caixach, J. and Rivera, J., Dioxin like compounds from municipal waste incinerator emissions: assessment of the presence of polychlorinated naphthalenes. *Chemosphere* 38:109-120 (1999).

Akki U. and Mulholland J.A., Gas-phase formation of dioxin and other aromatic products from 2,6-dichlorophenol pyrolysis. *Organohalogen Compounds* 31:475-479 (1997).

Born, J.G.P., Louw, R. and Mulder, P., Formation of dibenzodioxins and dibenzofurans in homogeneous gas-phase reactions of phenols. *Chemosphere* 19:401-406 (1989).

Castaldi, M.J., Marinov, N.M., Melius, C.F., Huang, J., Senken, S.M., Pitz, W.J. and Westbrook, C.K., Experimental and modeling investigation of aromatic and polycyclic aromatic hydrocarbon formation in a premixed ethylene flame. *Proc. Combust. Inst.* 26:693-702 (1996).

Cieplik M.K., Epema, O.J. and Louw, R., Thermal hydrogenolysis of dibenzo-p-dioxin and dibenzofuran. *Eur. J. Org. Chem.* 2002:2792-2799 (2002).

Eiceman, G.A., Clement, R.E. and Karasek, F.W., Analysis of fly ash from municipal incinerators for trace organic compounds. *Anal. Chem.* 51:2343-2350 (1979).

Evan, C.S. and Dellinger, B., Mechanisms of dioxin formation from the high-temperature oxidation of 2-chlorophenol. *Environ. Sci. Technol.* 39:122-127 (2005).

Frenklach, M., Clary, D.W., Cardiner, W.C. and Stein, S.E., Detailed kinetic modeling of soot formation in shock-tube pyrolysis of acetylene. *Proc. Combust. Inst.* 20:887-901 (1984).

Frenkalch, M. and Warnatz, J., Detailed modeling of PAH profiles in a sooting low-pressure acetylene flame. *Combust. Sci. Technol.* 51:265-283 (1987).

Iino, F., Imagawa, T., Takeuchi, M. and Sadakata, M. De novo synthesis mechanism of polychlorinated dibenzofurans from polycyclic aromatic hydrocarbons and the characteristic isomer of polychlorinated naphthalenes. *Environ. Sci. Technol.* 33:1038-1043 (1999).

Imagawa, T. and Yamashita, N., Isomer specific analysis of polychlorinated naphthalenes in halowax and fly ash. *Organohalogen Compounds* 19:215-218 (1994).

Imagawa, T. and Takeuchi, M., Relation between isomer compositions of polychlorinated naphthalens and congener compositions of PCDDs/PCDFs from incinerators. *Organohalogen Compounds* 23:487-490 (1995).

Järnberg, U., Asplund, C. and Jakobsson, E., Gas chromatographic retention of polychlorinated naphthalenes on non-polar, polarizable, polar and semectic capillary columns. *J. Chromatogr.* 683A:385-396 (1994).

Kim, D.H., Mulholland, J.A. and Ryu, J.-Y., Formation of polychlorinated naphthalenes from chlorophenols. *Proc. Combust. Inst.* 30:1249-1257 (2004).

Manion, J. and Louw, R., Rates, products, and mechanisms in the gas-phase hydrogenolysis of phenol between 922 and 1175 K. *J. Phys. Chem.* 93:3563-3574 (1989).

Marinov, N.M., Castaldi, M.J., Melius, C.F. and Tsang, W., Aromatic and polycyclic aromatic hydrocarbon formation in a premixed propane flame. *Combust. Sci. Technol.* 128:295-342 (1997).

McEnally, C.S. and Pfefferle, L.D., The use of carbon-13-labeled fuel dopants for identifying naphthalene formation pathways in non-premixed flames. *Proc. Combust. Inst.* 28:2569-2576 (2000).

Melius, C.F., Colvin, M.E., Marinov, N.M., Pitz, W.J. and Senkan, S.M., Reaction mechanisms in aromatic hydrocarbon formation involving the C_5H_5 cyclopentadienyl moiety. *Proc. Combust. Inst.* 26:685-692 (1996).

Mikhailov, I.E., Dushenko, G.A., Kisin, A.V., Mügge, C., Zschunke, A. and Minkin, V.I., 1,5-sigmatropic shifts of chlorine in the cyclopentadiene ring. *Mendeleev Commun.* 3:85-88 (1994).

Nakahata, D.-T. and Mulholland, J.A., Effects of dichlorophenol substitution pattern on furan and dioxin formation. *Proc. Combust. Inst.* 28:2701-2707 (2000).

Olie, K., Vermeulen, P.L. and Hutzinger, O., Chlorodibenzo-p-dioxins and chlorodibenzofurans are trace components of fly ash and flue gas of some incinerators in the Netherlands. *Chemosphere* 6:455-459 (1977).

Schneider, M., Stieglitz, L., Will, R., Zwick, G., Formation of polychlorinated naphthalenes on fly ash. *Chemosphere* 37:2055-2070 (1998).

Sidhu, S.S., Maquad, L., Dellinger, B. and Mascolo, G., The homogeneous, gas-phase formation of chlorinated and brominated dibenzo-p-dioxin from 2,4,6-trichloro- and 2,4,6-tribromophenols. *Combust. Flame* 100:11-20 (1995).

Spielmann, R. and Cramers, C.A., Cyclopentadienic compounds as intermediates in the thermal degradation of phenols: Kinetics of thermal decomposition of cyclopentadiene. *Chromatographia* 5:295-300 (1972).

Weber, R. and Hagenmaier, H., Mechanism of the formation of polychlorinated dibenzo-p-dioxins and dibenzofurans from chlorophenols in gas-phase reactions. *Chemosphere* 38:529-549 (1999).

Yang, Y., Mulholland, J.A., Akki, U., Formation of furans by gas-phase reactions of chlorophenols. *Proc. Combust. Inst.* 27:1761-1768 (1998).

CHAPTER 8

CONCLUSIONS AND RECOMMENDATIONS

8.1 Conclusions

In the pyrolysis of CPD, experimental results showed that major products from CPD pyrolysis were indene and benzene via intramolecular addition routes and naphthalene via β-scission routes. Identification of stable intermediates supports the proposed formation routes. The intramolecular addition products were favored at low temperatures (below 750^{o}C) whereas β-scission routes were favored at high temperatures. Preliminary computational results using the PM3 methods were consistent with these results.

The pyrolysis of CPD-acenaphthylene mixture produced low product yields and less variety of products. The major products were similar to those from the pyrolysis of CPD alone, indicating that the reactivity of CPD to other compounds is much less comparative than that of CPD to compounds with CPD moieties. However, the observation of expected products from the thermal reaction of CPD and acenaphthylene based on proposed reaction pathways further supports that addition of resonance-stabilized cyclopentadienyl radicals may be important in the growth of aromatic hydrocarbons and soot. Given this observation, the yields of products from CPD-acenaphthylene reactions show that CPD preferred to add to the external π-bond. The results add new information to the role of CPD in aromatic combination mechanism and also emphasizes the role of cyclopenta-fused compounds in PAH formation and growth.

Similar results were observed from CPD-styrene mixture and CPD-phenanthrene mixture pyrolysis. The major products from both mixtures resemble those from the pyrolysis of CPD alone. Experimental results suggest that the CPD-styrene and the CPD-phenanthrene reactions are much less favored than the CPD-CPD reaction. Thus, it is concluded that the reactivity of CPD to itself and to compounds having CPDyl moieties are very high and the reaction pathways from

CPD may be important in PAH growth in the region where the ring fragmentation is not significant.

The chlorinated PAH formation in combustion processes involving CPD moieties was also experimentally investigated as well. The slow combustion of MCPs in a laminar flow reactor was studied over the range of 550 to 750^{o}C under oxidative conditions. Maximum PCN and PCDF yields from MCPs were observed between 625 and 725^{o}C. Different distributions of PCN congeners were produced from each MCP. Congener product distributions are consistent with proposed PCN and PCDF formation pathways both involving phenoxy radical coupling at unchlorinated ortho-carbon sites to form a dihydroxybiphenyl keto tautomer intermediate. Tautomerization of this intermediate and subsequent fusion via H_2O loss results in PCDF formation, whereas CO elimination and subsequent fusion with hydrogen and/or chlorine loss leads to PCN formation. The PCN isomer patterns observed are consistent with the major rearrangement path involving translation of the 9,10 carbons of dihydrofulvalene to the 9,10 carbon atoms in naphthalene.

The degree of chlorination of naphthalene and dibenzofuran products decreased as temperature increased, and, on average, the naphthalene congeners were less chlorinated than the dibenzofuran congeners. These results suggest that CO elimination that leads to naphthalene formation becomes increasingly favored relative to tautomerization that leads to dibenzofuran formation as temperature increases and as organic chlorine decreases. PCDF isomer distributions were found to be weakly dependent on temperature, suggesting that phenoxy radical coupling is a low activation energy process. PCN isomers were, on the other hand, found to be more strongly dependent on temperature, with selectivity to particular isomers decreasing with increasing temperature.

The proposed PCN formation scheme was used to predict PCN product distributions from six DCPs dissolved in benzene at 600°C. These experimental results support the proposed

pathways of PCN formation. The lack of detectable tetrachloronapthalene indicates that PCN formation is favored with one chlorine atom loss, particularly when chlorine is at an ortho position. The only observed PCN peak that is not consistent with our prediction of major products is the formation of 1,8-DCN from 2,6-DCP.

Results of this research have provided the information on the role of CPD moiety in both unchlorinated and chlorinated PAH formation in combustion processes, and have contributed to the development of a method that can predict the distribution of PCN congeners from the slow combustion of phenols in the gas phase.

8.2 Recommendations

The following recommendations are proposed to further understanding the formation of aromatic compounds involving cyclopentadienyl moieties in both chlorinated and unchlorinated systems.

While consistent data on the CPD reaction pathways compared to experimental data were obtained with semi-empirical molecular modeling, a higher level of theory should be performed to provide more reliable kinetic information on the proposed pathways. It should be also noted that computational predictions were made under the assumption that the rate-limiting is the first step on the overall reaction though a good agreement between experimental and computational results was achieved. This assumption should be verified with all possible reaction pathways leading to final products. The semi-empirical method may not be able to make reasonable prediction on product yields for CPD and other large aromatic hydrocarbons. Thus, it is further recommended that the using higher-level methods and larger basis sets could be attempted, which has yet to be undertaken.

It would be of interest to conduct experimental study on PAH growth from CPD under the presence of oxygen and water. Oxygen would accelerate the CPD reaction with other hydrocarbons by rapid formation of radical pool in the system. The inclusion of water in the

system would provide more valuable information on PAH growth from CPD by simulating more realistic combustion conditions.

The gas-phase PCN formation pathway from chlorinated phenols is still not fully understood. Computational methods should be used to calculate the kinetic rate for CO elimination and tautomerization from a coupling of phenoxy radicals. The proposed PCN formation pathways was not able to explain the PCN products from ortho chlorinated phenols (i.e. 2,6-DCP, 2,4,6-T_3CP). Thus, it is recommended to perform more experimental study on the PCN formation from mixtures of ortho chlorinated phenols. Recent studies have shown the PCN formation via *de novo* and surface interaction of fly ash. It is further recommended to study naphthalene formation on heterogeneous reactions as well.

In this study, the impact of HACA mechanism on PAH growth was not addressed well because the existing experimental setup is not able to effectively collect low molecular weight hydrocarbons (i.e. methane, ethane and etc.). In addition, the pyrolytic carbon deposited on the quartz tube reactor resulted in low collection efficiency of high molecular weight compounds that tend to be absorbed on the glassy carbon film on the reactor. In future studies, it is recommended that the composition of soot on the reactor be examined. Soot consists of element carbon and organic carbon. To achieve better mass closure, it is recommended that the soot deposited on the reactor wall be oxidized at high temperature after the experiment and that the CO_2 concentration be measured. Along with this better measure of soot yield, the composition of nano organic carbon should be examined using advanced analytical techniques.

APPENDIX A

TABLES OF EXPERIMENTAL PRODUCT YIELDS

GC temperature program

Table A.1, A.4-A.7: initial temperature 32^{o}C (hold 2 min.); 5^{o}C/min to 250^{o}C; 8^{o}C/min to 280^{o}C (hold 3 min)

Table A.2-A.3: initial temperature 37^{o}C (hold 2 min.); 10^{o}C/min to 238^{o}C (hold 1 min); 0.5^{o}C/min to 246^{o}C (hold 3 min); 5^{o}C/min to 280^{o}C (hold 5 min)

Table A.8-A.9: initial temperature 38°C (hold 2 min); 3°C/min to 180°C (hold 2 min); 5°C/min to 250°C (hold 5 min); 6°C/min to 280°C (hold 3 min); 2°C/min to 300°C

Table A.1 Product yields from the pyrolysis of CPD-indene mixture (% of carbon feed; 0.1% (molar) CPD and 0.1% (molar) indene in N_2; 4s)

Name	Formula	Elution Time (minutes)	Temperature (°C) 680	700	720	800	900
benzene	C_6H_6	2.79	1.0616	1.4056	2.1696	3.6061	8.2635
toluene	C_7H_8	4.56	1.4883	1.4995	2.0354	2.3341	1.6609
(p-xylene)	C_8H_{10}	7.22	0.3960	0.3442	0.4493	0.8863	0.1381
phenylethyne	C_8H_8	7.45	0.1003	0.0983	0.1283	0.3066	0.5145
(1,3,5,7-cyclooctatetraene)	C_8H_9	7.85	0.3605	0.2975	0.4948		
(benzene, 1-ethyl-3-methyl)	$C_{11}H_{12}$	10.03	0.0950	0.1166	0.1152		
(benzene, 1,3,5-trimethyl)	$C_{11}H_{12}$	10.24	2.3060	2.2345	2.0619		
(benzene, 1-ethyl-4-methyl)	$C_{11}H_{12}$	10.59	0.0682	0.0778	0.0777		
	$C_{11}H_{12}$	11.01	1.1062	1.1912	1.1201		
(benzene, 1-ethyl-2-methyl)	$C_{11}H_{12}$	11.89	0.0775	0.0680	0.0791		
indane	C_9H_{10}	12.28	0.3470	0.3459	0.1966	0.0505	
indene	C_9H_8	12.56	51.4824	51.6979	46.1341	33.0094	3.9169
(benzene, 4-ethyl-1,2-dimethyl)	$C_{10}H_{14}$	13.05	0.0198	0.0221	0.0130	0.0095	
	$C_{10}H_{12}$	14.17	0.0117	0.0117	0.0115	0.0941	
(methyl indene)	$C_{10}H_{10}$	15.71	0.1371	0.1322	0.1059	0.3815	
(methyl indene)	$C_{10}H_{10}$	15.91	0.4202	0.4556	0.4320	0.0611	
(methyl indene)	$C_{10}H_{10}$	16.12	0.1572	0.1721	0.1206	8.3301	13.2157
naphthalene	$C_{10}H_8$	16.68	1.3934	1.3815	4.7134	17.7479	1.3992
(methyl naphthalene)	$C_{11}H_{10}$	19.80	0.0005		0.0043		
(methyl naphthalene)	$C_{11}H_{10}$	19.81	0.0003	0.0009		0.0213	0.0084
(methyl naphthalene)	$C_{11}H_{10}$	19.83	0.0002			0.0035	0.0046
acenaphthylene	$C_{12}H_8$	23.76	0.0061	0.0057	0.0163	0.1155	0.5202
acenaphthene	$C_{12}H_{10}$	24.60	0.0016	0.0029	0.0022	0.0012	
	$C_{12}H_{10}$	24.91	0.0005	0.0004	0.0005	0.0046	
	$C_{13}H_{12}$	25.41			0.0001	0.0021	
fluorene	$C_{13}H_{10}$	26.96	0.0346	0.0281		0.8088	0.5594
(benzindene)	$C_{13}H_{10}$	27.42	0.0004			0.0074	0.0034
(benzindene)	$C_{13}H_{10}$	27.76	0.0001			0.0057	0.0021
(benzindene)	$C_{13}H_{10}$	27.91	0.0047	0.0044		0.0596	0.0054
(9,10-dihydrophenanthrene)	$C_{14}H_{10}$	29.39	0.0073	0.0068		0.0501	
(methyl fluorene)	$C_{14}H_{12}$	29.56	0.0091	0.0075		0.1245	
(methyl fluorene)	$C_{14}H_{12}$	29.69	0.0229	0.0408	0.0563	0.0526	
(methyl fluorene)	$C_{14}H_{12}$	29.93	0.0605	0.0618	0.1251	0.2628	
	$C_{14}H_{10}$	30.12	0.0049	0.0035	0.0086	0.0344	0.0012
phenanthrene	$C_{14}H_{10}$	31.23	0.2069	0.1606	0.5843	1.6079	3.0169
anthracene	$C_{14}H_{10}$	31.43	0.2168	0.1724	0.4336	1.5978	1.7585
(methyl phenanthrene)	$C_{15}H_{12}$	34.04				0.0047	0.0014
(1H-indene, 2-phenyl)	$C_{15}H_{12}$	34.15				0.0049	0.0012
(naphthalene, 2-phenyl)	$C_{16}H_{12}$	35.09				0.0057	0.0033
fluoranthene	$C_{16}H_{10}$	36.68				0.0183	0.1657
(acephenathrylene)	$C_{16}H_{10}$	37.12				0.0039	0.0236
	$C_{16}H_{10}$	37.44				0.0002	0.0014
(aceanthrylene)	$C_{16}H_{10}$	37.62				0.0016	0.0254
(biindenyl)	$C_{18}H_{14}$	38.93	0.0006	0.0001	0.0013	0.0005	
benzo[a]fluorene	$C_{17}H_{12}$	39.39			0.0004	0.0092	0.0098
benzo[b]fluorene	$C_{17}H_{12}$	39.68	0.0031	0.0022	0.0163	0.0930	0.0521
benzo[c]phenanthrene	$C_{18}H_{12}$	42.53	0.0001	0.0005	0.0020	0.0157	0.0686
benz[a]anthracene	$C_{18}H_{12}$	42.60			0.0004	0.0029	0.0147
chrysene	$C_{18}H_{12}$	43.45	0.0002	0.0001	0.0122	0.1192	0.6401
% soot (assume all carbon)						2.3200	11.0300
% total aromatic compounds			61.6098	62.0510	61.7227	71.8568	35.9960
% carbon recovery			61.6098	62.0510	61.7227	74.1768	47.0260

Table A.2 Product yields from the pyrolysis of indene (% of carbon feed; 0.6% (molar) indene in N_2; 4s)

Name	Formula	Elution Time (minutes)	Temperature (°C) 850	950
(p-xylene)	C_8H_{10}	5.51	0.8399	
(phenylethyne)	C_8H_6	5.64	0.0564	
styrene	C_8H_8	5.89	0.0681	
	C_8H_{10}	5.92	0.0597	
(benzene, 1,3,5-trimethyl-)	C_9H_{12}	7.24	0.3154	
(methyl styrene)	C_9H_{10}	7.72	0.0114	
indene	C_9H_8	8.55	13.0028	0.3949
(4-ethenyl-1,2-dimethyl-benzene)	$C_{10}H_{12}$	9.34	0.0012	
(methyl indene)	$C_{10}H_{10}$	10.18	0.0066	
(methyl indene)	$C_{10}H_{10}$	10.27	0.0050	
	$C_{10}H_8$	10.29	0.0131	
naphthalene	$C_{10}H_8$	10.71	3.4062	3.2424
methyl naphthalene	$C_{11}H_{10}$	12.30	0.0072	
methyl naphthalene	$C_{11}H_{10}$	12.54	0.0087	
acenaphthylene	$C_{12}H_8$	14.42	0.0950	0.0821
acenaphthene	$C_{12}H_{10}$	14.81	0.0000	
fluorene	$C_{13}H_{10}$	16.00	0.0033	
phenanthrene	$C_{14}H_{10}$	18.21	0.0074	0.0062
anthracene	$C_{14}H_{10}$	18.31	0.0048	0.0015
4H-cyclopenta[def]phenanthrene	$C_{15}H_{10}$	19.62	0.0006	0.0007
	$C_{16}H_{12}$	20.13	0.0012	
fluoranthene	$C_{16}H_{10}$	20.99	0.0101	0.1170
pyrene	$C_{16}H_{10}$	21.22	0.0059	0.0046
	$C_{16}H_{12}$	21.39	0.0041	
(1,1'-biindenyl)	$C_{18}H_{14}$	22.05	0.0030	
	$C_{18}H_{12}$	22.11	0.0012	
benzo[a]fluorene	$C_{17}H_{12}$	22.37	0.2971	0.0013
benzo[b]fluorene	$C_{17}H_{12}$	22.53	2.6073	0.0025
(pyrene, 1,3-dimethyl-)	$C_{18}H_{14}$	22.59	0.0313	
benzo[c]phenanthrene	$C_{18}H_{12}$	24.30	0.8413	0.0164
	$C_{18}H_{14}$	24.43	0.1339	0.0056
benz[a]anthracene	$C_{18}H_{12}$	25.06	2.1187	0.1611
chrysene	$C_{18}H_{12}$	25.21	5.3967	0.7385
% soot (assume all carbon)			5.4840	7.7242
% total aromatic compounds			29.3646	4.7748
% carbon recovery			34.8485	12.4990

Table A.3 Product yields from the pyrolysis of indene-acenaphthylene mixture (% of carbon feed; 0.4% (molar) indene and 0.2% (molar) acenaphthylene in N_2; 4s)

Name	Formula	Elution Time (minutes)	Temperature (^oC) 800	850	900	950
(p-xylene)	C_8H_{10}	5.51	0.4825	0.4187	0.0237	
(phenylethyne)	C_8H_6	5.64	0.0165	0.0351	0.0093	
styrene	C_8H_8	5.89	0.0385	0.0328	0.0086	
	C_8H_{10}	5.92	0.0446	0.0253		
(benzene, 1,3,5-trimethyl-)	C_9H_{12}	7.24	0.5324	0.1554		
(methyl styrene)	C_9H_{10}	7.72	0.0550	0.0436		
indane	C_9H_9	8.38	0.0389			
indene	C_9H_8	8.55	20.4647	9.8513	2.5441	0.2227
(4-ethenyl-1,2-dimethyl-benzene)	$C_{10}H_{12}$	9.34	0.0065	0.0000	0.0005	
(methyl indene)	$C_{10}H_{10}$	10.18	0.0236	0.0036	0.0001	
(methyl indene)	$C_{10}H_{10}$	10.27	0.0119	0.0026		
	$C_{10}H_8$	10.29	0.0564	0.0053	0.0002	
naphthalene	$C_{10}H_8$	10.71	1.0640	1.5971	1.7727	1.2755
methyl naphthalene	$C_{11}H_{10}$	12.30	0.0023	0.0041	0.0018	
methyl naphthalene	$C_{11}H_{10}$	12.54	0.0579	0.0188	0.0019	
acenaphthylene	$C_{12}H_8$	14.42	14.1870	9.9166	8.2714	2.6150
acenaphthene	$C_{12}H_{10}$	14.81	0.1239	0.0117	0.0131	
	$C_{13}H_{10}$	15.78	0.0097	0.0038	0.0014	
	$C_{13}H_{10}$	15.90	0.0044	0.0023	0.0007	
fluorene	$C_{13}H_{10}$	16.00	0.0031	0.0055	0.0046	
	$C_{13}H_{10}$	16.03	0.0043	0.0030	0.0014	
	$C_{13}H_{12}$	16.88	0.0014	0.0019	0.0014	
phenanthrene	$C_{14}H_{10}$	18.21	0.0016	0.0053	0.0081	0.0033
anthracene	$C_{14}H_{10}$	18.31	0.0009	0.0023	0.0023	
4H-cyclopenta[def]phenanthrene	$C_{15}H_{10}$	19.62	0.0002	0.0007	0.0018	0.0003
	$C_{16}H_{12}$	20.13	0.0001	0.0005	0.0001	
fluoranthene	$C_{16}H_{10}$	20.99	0.0007	0.0079	0.0400	0.0113
pyrene	$C_{16}H_{10}$	21.22	0.0004	0.0044	0.0071	0.0007
	$C_{16}H_{12}$	21.39	0.0004	0.0019	0.0004	
(1,1'-biindenyl)	$C_{18}H_{14}$	22.05	0.0052	0.0696	0.0325	
	$C_{18}H_{12}$	22.11	0.0009	0.0069	0.0018	
benzo[a]fluorene	$C_{17}H_{12}$	22.37	0.0398	0.1823	0.0559	
benzo[b]fluorene	$C_{17}H_{12}$	22.53	0.5043	1.0937	0.1892	
(pyrene, 1,3-dimethyl-)	$C_{18}H_{14}$	22.59	0.0359	0.0482	0.0000	
benzo[c]phenanthrene	$C_{18}H_{12}$	24.30	0.1129	0.3454	0.1874	0.0018
	$C_{18}H_{14}$	24.43	0.0300	0.0589	0.0258	
benz[a]anthracene	$C_{18}H_{12}$	25.06	0.1322	0.7049	0.3842	0.0057
chrysene	$C_{18}H_{12}$	25.21	0.7121	1.7619	1.1827	0.0270
% soot (assume all carbon)			3.2727	2.9014	5.9141	10.1044
% total aromatic compounds			38.8071	26.4334	14.7762	4.1633
% carbon recovery			42.0806	29.4056	20.6999	14.2677

Table A.4 Product yields from the pyrolysis of CPD (% of carbon feed; 0.7% (molar) CPD in N_2; 4s)

Name	Formula	Elution Time (minutes)	Temperature (°C) 600	700	725	750	775	800
cyclopentadiene	C_5H_6	1.56	90.72	84.88	52.78	45.68	27.51	16.83
methyl-1,3-cyclopentadiene	C_6H_8	2.33	0.9890	0.7924	0.8770	0.0873	0.7361	0.3414
methyl-1,3-cyclopentadiene	C_6H_8	2.38	0.9582	0.6391	0.7039	0.7443	0.5803	0.2449
benzene	C_6H_6	2.55	0.4156	2.1105	2.9967	5.4608	8.6439	15.6989
toluene	C_7H_8	4.42		0.2439	0.6846	1.4784	2.4296	3.5529
(p-xylene)	C_8H_{10}	7.31			0.0729	0.1393	0.2221	0.1385
(phenylethyne)	C_8H_6	7.55			0.0148	0.0711	0.1913	0.2550
styrene	C_8H_8	7.96		0.2688	0.8202	1.7486	2.6614	3.5054
DCPD	$C_{10}H_{12}$	12.24	0.9485	0.6980	0.2266	0.1498	0.0664	
indene	C_9H_8	12.85	0.2053	5.5210	6.5246	11.7942	14.7306	21.6838
(methyl indene)	$C_{10}H_{10}$	16.05	0.0033	0.1680	0.2450	0.3425	0.2694	0.1551
(methyl indene)	$C_{10}H_{10}$	16.24	0.0117	0.9573	0.5632	0.6534	0.4072	1.0663
(methyl indene)	$C_{10}H_{10}$	16.26	0.0043	0.6786	0.3749	0.4643	0.4072	
(dihydro-fulvalene/dihydro naphthalene)	$C_{10}H_{10}$	16.47	0.0323	1.3031	1.1906	1.1419	0.8176	0.4098
naphthalene	$C_{10}H_8$	17.09	0.0376	2.7681	4.7181	9.2532	14.7262	23.7092
methyl naphthalene	$C_{11}H_{10}$	20.15			0.0063	0.0293	0.0660	0.0523
methyl naphthalene	$C_{11}H_{10}$	20.59			0.0063	0.0277	0.0654	0.0747
biphenyl	$C_{12}H_{10}$	22.42					0.0112	0.0074
	$C_{12}H_{10}$	23.22						0.0015
	$C_{12}H_{10}$	23.66						0.0018
acenaphthylene	$C_{12}H_8$	24.19		0.0009	0.0173	0.0749	0.1694	0.3008
acenaphthene	$C_{12}H_{10}$	24.99			0.0006	0.0036	0.0074	
	$C_{13}H_{10}$	26.87						0.0011
	$C_{13}H_{10}$	27.18					0.0063	0.0028
fluorene	$C_{13}H_{10}$	27.30				0.0701	0.3076	0.7710
(benzindene)	$C_{13}H_{10}$	27.76				0.0129	0.0350	0.0148
(benzindene)	$C_{13}H_{10}$	28.11				0.0123	0.0324	0.0110
(benzindene)	$C_{13}H_{10}$	28.25				0.0203	0.0702	0.0402
	$C_{13}H_{12}$	29.03				0.0150	0.0464	
	$C_{14}H_{10}$	29.74						0.0278
methyl fluorene	$C_{14}H_{12}$	29.89			0.0003	0.0184	0.0804	0.0809
methyl fluorene	$C_{14}H_{12}$	30.03			0.0029	0.0478	0.1030	0.0643
	$C_{14}H_{10}$	30.10						
methyl fluorene	$C_{14}H_{12}$	30.27			0.0056	0.0765	0.2192	0.2924
	$C_{14}H_{10}$	30.45					0.0111	0.0155
phenanthrene	$C_{14}H_{10}$	31.56			0.0057	0.0984	0.3774	1.0741
anthracene	$C_{14}H_{10}$	31.76			0.0059	0.1276	0.5155	0.8387
	$C_{16}H_{12}$	33.25						
	$C_{15}H_{12}$	33.90						
	$C_{15}H_{12}$	34.18					0.0091	0.0049
(4H-cyclopenta[def]phenanthrene)	$C_{15}H_{10}$	34.30				0.0036	0.0222	0.0313
(methyl phenanthrene)	$C_{15}H_{12}$	34.39				0.0078	0.0362	0.0282
(methyl anthracene)	$C_{15}H_{12}$	34.47				0.0088	0.0381	0.0346
	$C_{16}H_8$	34.76					0.0066	0.0026
fluoranthene	$C_{16}H_{10}$	37.00						0.0028
(acephenanthrylene)	$C_{16}H_{10}$	37.44						0.0008
pyrene	$C_{16}H_{10}$	37.92						0.0007
	$C_{17}H_{12}$	40.43						
% soot (assume all carbon)								0.01
% total aromatic compounds			2.66	15.45	19.84	34.03	49.06	74.54
% carbon recovery			94.33	101.03	72.84	79.86	76.64	91.38

Table A.4 Product yields from the pyrolysis of CPD (% of carbon feed; 0.7% (molar) CPD in N_2; 4s) (continued)

Name	Formula	Elution Time (minutes)	Temperature (^oC) 825	850	875	900	900	900
cyclopentadiene	C_5H_6	1.56						
methyl-1,3-cyclopentadiene	C_6H_8	2.33	0.0239	0.0251				0.1146
methyl-1,3-cyclopentadiene	C_6H_8	2.38	0.0359				0.0970	0.0640
benzene	C_6H_6	2.55	18.8825	23.7329	24.5405	22.0661	19.1241	19.8799
toluene	C_7H_8	4.42	5.2198	5.7623	3.5746	1.4938	2.4661	2.4138
(p-xylene)	C_8H_{10}	7.31	0.1760	0.1489				
(phenylethyne)	C_8H_6	7.55	0.3097	0.4923	0.5993	0.3556	0.5791	0.6097
styrene	C_8H_8	7.96	3.9865	3.5944	2.1802	0.4872	1.0128	1.0143
DCPD	$C_{10}H_{12}$	12.24						
indene	C_9H_8	12.85	16.4927	8.8136	4.3689	1.4504	2.0477	2.0708
(methyl indene)	$C_{10}H_{10}$	16.05	0.0259	0.0036				
(methyl indene)	$C_{10}H_{10}$	16.24	0.0314					
(methyl indene)	$C_{10}H_{10}$	16.26	0.1999	0.0306	0.0097		0.0053	0.0055
(dihydro-fulvalene/dihydro naphthalene)	$C_{10}H_{10}$	16.47	0.0813	0.0034				
naphthalene	$C_{10}H_8$	17.09	29.1384	30.6145	27.2299	20.9309	19.9975	20.1809
methyl naphthalene	$C_{11}H_{10}$	20.15	0.0687	0.1212	0.0870	0.0201	0.1162	0.1166
methyl naphthalene	$C_{11}H_{10}$	20.59	0.0932	0.1166	0.0633	0.0111	0.0746	0.0763
biphenyl	$C_{12}H_{10}$	22.42	0.0084	0.0199	0.0166	0.0119	0.0644	0.0656
	$C_{12}H_{10}$	23.22	0.0015	0.0015	0.0012	0.0033	0.0000	
	$C_{12}H_{10}$	23.66	0.0031	0.0077	0.0073		0.0181	0.0196
acenaphthylene	$C_{12}H_8$	24.19	0.4584	0.9378	1.2203	1.2803	1.5991	1.6480
acenaphthene	$C_{12}H_{10}$	24.99	0.0024	0.0022	0.0023		0.0062	0.0064
	$C_{13}H_{10}$	26.87		0.0013				
	$C_{13}H_{10}$	27.18		0.0025	0.0010			
fluorene	$C_{13}H_{10}$	27.30	1.3619	1.8591	1.3137	0.5172	0.8680	0.9051
(benzindene)	$C_{13}H_{10}$	27.76	0.0118	0.0120	0.0070		0.0148	0.0161
(benzindene)	$C_{13}H_{10}$	28.11	0.0080	0.0072	0.0043		0.0120	0.0132
(benzindene)	$C_{13}H_{10}$	28.25	0.0038	0.0285	0.0109		0.0234	0.0268
	$C_{13}H_{12}$	29.03						
	$C_{14}H_{10}$	29.74	0.0135	0.0035				
methyl fluorene	$C_{14}H_{12}$	29.89	0.0636	0.0169	0.0006			
methyl fluorene	$C_{14}H_{12}$	30.03	0.0199	0.0029				
	$C_{14}H_{10}$	30.10	0.0042	0.0011				
methyl fluorene	$C_{14}H_{12}$	30.27	0.1629	0.0219	0.0006			
	$C_{14}H_{10}$	30.45	0.0128	0.0042	0.0011			
phenanthrene	$C_{14}H_{10}$	31.56	1.9443	3.6628	3.3171	2.4484	3.0475	3.1997
anthracene	$C_{14}H_{10}$	31.76	1.4941	2.2593	1.6244	0.9302	2.0359	2.1492
	$C_{16}H_{12}$	33.25					0.0982	0.1028
	$C_{15}H_{12}$	33.90						0.0042
	$C_{15}H_{12}$	34.18	0.0037	0.0031	0.0005			
(4H-cyclopenta[def]phenanthrene)	$C_{15}H_{10}$	34.30	0.0533	0.1320	0.0939	0.0307	0.1510	0.1618
(methyl phenanthrene)	$C_{15}H_{12}$	34.39	0.0259	0.0263	0.0076			
(methyl anthracene)	$C_{15}H_{12}$	34.47	0.0442	0.0507	0.0132		0.0143	0.0157
	$C_{16}H_8$	34.76	0.0008					
fluoranthene	$C_{16}H_{10}$	37.00	0.0148	0.1679	0.1986	0.1368	0.3527	0.3763
(acephenanthrylene)	$C_{16}H_{10}$	37.44	0.0030	0.0158	0.0151	0.0087	0.0480	0.0544
pyrene	$C_{16}H_{10}$	37.92	0.0028	0.0228	0.0329	0.0213	0.1404	0.1516
	$C_{17}H_{12}$	40.43	0.0002	0.0021	0.0013			
% soot (assume all carbon)			3.43	4.11	4.63	5.73	2.46	4.00
% total aromatic compounds			80.49	82.74	70.55	52.21	54.09	55.55
% carbon recovery			83.92	86.85	75.18	57.94	56.47	59.46

Table A.4 Product yields from the pyrolysis of CPD (% of carbon feed; 0.7% (molar) CPD in N_2; 4s) (continued)

Name	Formula	Elution Time (minutes)	Temperature (°C) 925	950	975	1000
cyclopentadiene	C_5H_6	1.56	n.m.	n.m.	n.m.	n.m.
methyl-1,3-cyclopentadiene	C_6H_8	2.33				0.1971
methyl-1,3-cyclopentadiene	C_6H_8	2.38				0.0652
benzene	C_6H_6	2.55	24.0482	26.6257	9.2414	18.0459
toluene	C_7H_8	4.42	0.0777	0.1143		0.1479
(p-xylene)	C_8H_{10}	7.31		0.0000		
(phenylethyne)	C_8H_6	7.55	0.0296	0.1880		0.1779
styrene	C_8H_8	7.96	0.0112	0.0221		
DCPD	$C_{10}H_{12}$	12.24		`		
indene	C_9H_8	12.85	0.0216	0.0629		0.0411
(methyl indene)	$C_{10}H_{10}$	16.05				
(methyl indene)	$C_{10}H_{10}$	16.24				
(methyl indene)	$C_{10}H_{10}$	16.26	0.0020	0.0023		
(dihydro-fulvalene/dihydro naphthalene)	$C_{10}H_{10}$	16.47				
naphthalene	$C_{10}H_8$	17.09	16.2506	13.6634	2.0187	5.5211
methyl naphthalene	$C_{11}H_{10}$	20.15	0.0040	0.0021		
methyl naphthalene	$C_{11}H_{10}$	20.59	0.0022	0.0012		
biphenyl	$C_{12}H_{10}$	22.42	0.0048	0.0042		0.0090
	$C_{12}H_{10}$	23.22				
	$C_{12}H_{10}$	23.66	0.0001			
acenaphthylene	$C_{12}H_8$	24.19	1.3387	1.5863	0.0327	1.5218
acenaphthene	$C_{12}H_{10}$	24.99	0.0005			
	$C_{13}H_{10}$	26.87				
	$C_{13}H_{10}$	27.18				
fluorene	$C_{13}H_{10}$	27.30	0.0082	0.0103		0.0042
(benzindene)	$C_{13}H_{10}$	27.76				
(benzindene)	$C_{13}H_{10}$	28.11				
(benzindene)	$C_{13}H_{10}$	28.25				
	$C_{13}H_{12}$	29.03				
	$C_{14}H_{10}$	29.74				
methyl fluorene	$C_{14}H_{12}$	29.89				
methyl fluorene	$C_{14}H_{12}$	30.03				
	$C_{14}H_{10}$	30.10				
methyl fluorene	$C_{14}H_{12}$	30.27				
	$C_{14}H_{10}$	30.45				
phenanthrene	$C_{14}H_{10}$	31.56	1.6199	1.0019	0.0054	0.3635
anthracene	$C_{14}H_{10}$	31.76	0.2509	0.1672	0.0005	0.0474
	$C_{16}H_{12}$	33.25				
	$C_{15}H_{12}$	33.90				
	$C_{15}H_{12}$	34.18				
(4H-cyclopenta[def]phenanthrene)	$C_{15}H_{10}$	34.30	0.0020	0.0029		
(methyl phenanthrene)	$C_{15}H_{12}$	34.39				
(methyl anthracene)	$C_{15}H_{12}$	34.47				
	$C_{16}H_8$	34.76				
fluoranthene	$C_{16}H_{10}$	37.00	0.3356	0.1671	0.0034	0.1893
(acephenanthrylene)	$C_{16}H_{10}$	37.44	0.0058	0.0065		0.0046
pyrene	$C_{16}H_{10}$	37.92	0.0356	0.0234	0.0012	0.0658
	$C_{17}H_{12}$	40.43				
% soot (assume all carbon)			11.67	7.64	11.11	15.07
% total aromatic compounds			44.05	43.65	11.30	26.40
% carbon recovery			55.72	51.29	22.42	41.47

Table A.5 Product yields from the pyrolysis of CPD-acenaphthylene mixture (% of carbon feed; 0.56% (molar) CPD and 0.14% (molar) acenaphthylene in N_2; 4s)

			Temperature (^oC)					
Name	Formula	Elution time (minutes)	600	700	800	800	800	825
cyclopentadiene	C_5H_6	1.56	72.3216	72.3216	31.1010			13.3604
methyl-1,3-cyclopentadiene	C_6H_8	2.33	0.5206	0.3266	0.2134	0.1384	0.0886	0.0453
methyl-1,3-cyclopentadiene	C_6H_8	2.38	0.4989	0.2706	0.1806	0.1047	0.0277	0.0000
benzene	C_6H_6	2.55	0.2227	1.8932	7.6971	8.6241	10.8777	13.5476
toluene	C_7H_8	4.42		0.2700	1.6033	1.7170	2.1289	2.2872
(p-xylene)	C_8H_{10}	7.31			0.0482	0.0371	0.1349	0.0881
(phenylethyne)	C_8H_6	7.55			0.0945	0.0970	0.1780	0.2198
styrene	C_8H_8	7.96		0.1806	1.6499	1.7575	2.1710	2.2032
indene	C_9H_8	12.85	0.0246	2.4439	13.1100	12.9566	12.3245	8.9962
(methyl indene)	$C_{10}H_{10}$	16.05		0.0472	0.0580	0.0454	0.0465	0.0106
(methyl indene)	$C_{10}H_{10}$	16.24	0.0001	0.3741	0.5601	0.1571	0.1232	0.0211
(methyl indene)	$C_{10}H_{10}$	16.26		0.2565		0.2983	0.2462	0.0571
(dihydro-fulvalene/dihydro naphthalene)	$C_{10}H_{10}$	16.47	0.0039	0.5372	0.2455	0.2025	0.1642	0.0294
naphthalene	$C_{10}H_8$	17.09	0.0225	1.8936	18.4200	18.7911	17.1150	19.2232
methyl naphthalene	$C_{11}H_{10}$	20.15			0.0097	0.0094	0.0131	0.0172
methyl naphthalene	$C_{11}H_{10}$	20.59	0.0193	0.0326	0.0758	0.0833	0.1036	0.0790
	$C_{12}H_{10}$	22.42				0.0015	0.0032	0.0034
	$C_{12}H_{10}$	23.22				0.0025	0.0024	0.0013
	$C_{12}H_{10}$	23.66						0.0011
acenaphthylene	$C_{12}H_8$	24.19	26.9256	17.5254	17.7746	18.2898	16.5586	13.9155
acenaphthene	$C_{12}H_{10}$	24.99	3.0105	1.9938	0.1285	0.1218	0.1157	0.0152
	$C_{13}H_{10}$	26.87		0.0066	0.0256	0.0227	0.0170	0.0114
	$C_{13}H_{10}$	27.18			0.0135	0.0128	0.0108	0.0097
fluorene	$C_{13}H_{10}$	27.30			0.4243	0.5105	0.4837	0.7689
(benzindene)	$C_{13}H_{10}$	27.76			0.0073	0.0066	0.0043	0.0054
(benzindene)	$C_{13}H_{10}$	28.11			0.0051	0.0046	0.0029	0.0036
(benzindene)	$C_{13}H_{10}$	28.25			0.0119	0.0132	0.0109	0.0137
	$C_{13}H_{12}$	29.03		0.0038			0.0014	
	$C_{14}H_{10}$	29.74			0.0103	0.0116	0.0072	0.0059
methyl fluorene	$C_{14}H_{12}$	29.89			0.0263	0.0322	0.0220	0.0224
methyl fluorene	$C_{14}H_{12}$	30.03			0.0222	0.0240	0.0170	0.0061
	$C_{14}H_{10}$	30.10				0.0042	0.0015	0.0030
methyl fluorene	$C_{14}H_{12}$	30.27			0.1204	0.1378	0.1068	0.0652
	$C_{14}H_{10}$	30.45			0.0043	0.0039	0.0026	0.0035
phenanthrene	$C_{14}H_{10}$	31.56			0.4311	0.5685	0.5235	1.0155
anthracene	$C_{14}H_{10}$	31.76			0.2472	0.3065	0.2413	0.5168
	$C_{16}H_{12}$	33.25						
(CPD-acenaphthylene dimer)	$C_{17}H_{14}$	33.45		0.0946				
	$C_{15}H_{12}$	33.90						
(CPD-acenaphthylene dimer)	$C_{17}H_{14}$	33.99		0.0190				
	$C_{15}H_{12}$	34.18			0.0015	0.0016	0.0007	0.0012
(4H-cyclopenta[def]phenanthrene)	$C_{15}H_{10}$	34.30			0.0265	0.0419	0.0389	0.0702
(methyl phenanthrene)	$C_{15}H_{12}$	34.39			0.0100	0.0120	0.0095	0.0101
(methyl anthracene)	$C_{15}H_{12}$	34.47			0.0090	0.0130	0.0090	0.0154
	$C_{16}H_8$	34.76			0.0009	0.0010	0.0003	0.0003
fluoranthene	$C_{16}H_{10}$	37.00			0.0038	0.0052	0.0070	0.0181
(acephenanthrylene)	$C_{16}H_{10}$	37.44			0.0019	0.0024	0.0030	0.0087
pyrene	$C_{16}H_{10}$	37.92			0.0009	0.0014	0.0016	0.0031
	$C_{17}H_{12}$	40.43			0.0607	0.0507	0.0439	0.0563
% soot (assume all carbon)					1.56	1.69	1.42	4.21
% total aromatic compounds			103.57	100.49	94.44	65.22	63.99	76.76
% carbon recovery			103.57	100.49	96.00	66.92	65.41	80.96

Table A.5 Product yields from the pyrolysis of CPD-acenaphthylene mixture (% of carbon feed; 0.56% (molar) CPD and 0.14% (molar) acenaphthylene in N_2; 4s) (continued)

			Termperature (°C)					
Name	Formula	Elution time (minutes)	850	875	900	925	950	975
cyclopentadiene	C_5H_6	1.56	3.3006	3.1198	0.4418	0.2636	0.1612	0.0346
methyl-1,3-cyclopentadiene	C_6H_8	2.33	0.0298					
methyl-1,3-cyclopentadiene	C_6H_8	2.38						
benzene	C_6H_6	2.55	14.1476	17.4715	17.7593	16.7051	17.4372	14.9158
toluene	C_7H_8	4.42	2.3866	1.8420	0.8390	0.1274	0.0472	0.0281
(p-xylene)	C_8H_{10}	7.31	0.0448					
(phenylethyne)	C_8H_6	7.55	0.2454	0.3053	0.1923	0.0483	0.0641	0.0410
styrene	C_8H_8	7.96	2.0092	1.0531	0.2109	0.0111		
indene	C9H8	12.85	5.5598	2.7274	1.1818	0.2251	0.0407	0.0113
(methyl indene)	$C_{10}H_{10}$	16.05	0.0004					
(methyl indene)	$C_{10}H_{10}$	16.24	0.0031	0.0038	0.0022			
(methyl indene)	$C_{10}H_{10}$	16.26	0.0031					
(dihydro-fulvalene/dihydro naphthalene)	$C_{10}H_{10}$	16.47	0.0011					
naphthalene	$C_{10}H_8$	17.09	21.3290	19.6385	17.3109	13.8429	10.4577	6.8450
methyl naphthalene	$C_{11}H_{10}$	20.15	0.0246	0.0208	0.0077	0.0015		
methyl naphthalene	$C_{11}H_{10}$	20.59	0.0599	0.0240	0.0056	0.0012		
	$C_{12}H_{10}$	22.42	0.0049	0.0051	0.0034	0.0009	0.0006	
	$C_{12}H_{10}$	23.22	0.0006					
	$C_{12}H_{10}$	23.66	0.0021	0.0019				
acenaphthylene	$C_{12}H_8$	24.19	15.5463	13.0393	10.6423	6.8614	4.1475	2.1688
acenaphthene	$C_{12}H_{10}$	24.99	0.0111	0.0111	0.0100	0.0027	0.0006	
	$C_{13}H_{10}$	26.87	0.0099	0.0041	0.0020			
	$C_{13}H_{10}$	27.18	0.0076	0.0030	0.0011			
fluorene	$C_{13}H_{10}$	27.30	1.0801	0.6894	0.3115	0.0413	0.0055	0.0004
(benzindene)	$C_{13}H_{10}$	27.76	0.0042	0.0025	0.0013			
(benzindene)	$C_{13}H_{10}$	28.11	0.0031	0.0016	0.0007			
(benzindene)	$C_{13}H_{10}$	28.25	0.0124	0.0039	0.0012			
	$C_{13}H_{12}$	29.03		0.0009	0.0026	0.0017	0.0003	
	$C_{14}H_{10}$	29.74	0.0016					
methyl fluorene	$C_{14}H_{12}$	29.89	0.0074					
methyl fluorene	$C_{14}H_{12}$	30.03	0.0010					
	$C_{14}H_{10}$	30.10	0.0016	0.0002				
methyl fluorene	$C_{14}H_{12}$	30.27	0.0091					
	$C_{14}H_{10}$	30.45	0.0017	0.0001	0.0001			
phenanthrene	$C_{14}H_{10}$	31.56	1.8182	1.6683	1.3614	0.8371	0.4478	0.1004
anthracene	$C_{14}H_{10}$	31.76	0.8411	0.6681	0.3742	0.1425	0.0310	0.0045
	$C_{16}H_{12}$	33.25	0.0041	0.0054	0.0050	0.0016	0.0002	
(CPD-acenaphthylene dimer)	$C_{17}H_{14}$	33.45						
	$C_{15}H_{12}$	33.90	0.0016	0.0004				
(CPD-acenaphthylene dimer)	$C_{17}H_{14}$	33.99	0.0014	0.0004				
	$C_{15}H_{12}$	34.18	0.0009					
(4H-cyclopenta[def]phenanthrene)	$C_{15}H_{10}$	34.30	0.1433	0.1043	0.0537	0.0120	0.0032	0.0007
(methyl phenanthrene)	$C_{15}H_{12}$	34.39	0.0091					
(methyl anthracene)	$C_{15}H_{12}$	34.47	0.0177	0.0032				
	$C_{16}H_8$	34.76						
fluoranthene	$C_{16}H_{10}$	37.00	0.1701	0.3240	0.4009	0.2883	0.1291	0.0192
(acephenanthrylene)	$C_{16}H_{10}$	37.44	0.0471	0.0497	0.0352	0.0116	0.0041	0.0008
pyrene	$C_{16}H_{10}$	37.92	0.0298	0.0525	0.0667	0.0354	0.0204	0.0063
	$C_{17}H_{12}$	40.43	0.1283	0.0223	0.0077	0.0001		
% soot (assume all carbon)			5.75	7.80	7.23	12.13	12.27	15.97
% total aromatic compounds			69.06	62.87	51.23	39.46	33.00	24.18
% carbon recovery			74.81	70.67	58.47	51.60	45.27	40.15

Table A.5 Product yields from the pyrolysis of CPD-acenaphthylene mixture (% of carbon feed; 0.56% (molar) CPD and 0.14% (molar) acenaphthylene in N_2; 4s) (continued)

Name	Formula	Elution time (minutes)	1000
cyclopentadiene	C_5H_6	1.56	
methyl-1,3-cyclopentadiene	C_6H_8	2.33	
methyl-1,3-cyclopentadiene	C_6H_8	2.38	
benzene	C_6H_6	2.55	13.7855
toluene	C_7H_8	4.42	0.0210
(p-xylene)	C_8H_{10}	7.31	
(phenylethyne)	C_8H_6	7.55	0.0241
styrene	C_8H_8	7.96	
indene	C_9H_8	12.85	0.0048
(methyl indene)	$C_{10}H_{10}$	16.05	
(methyl indene)	$C_{10}H_{10}$	16.24	
(methyl indene)	$C_{10}H_{10}$	16.26	
(dihydro-fulvalene/dihydro naphthalene)	$C_{10}H_{10}$	16.47	
naphthalene	$C_{10}H_8$	17.09	4.0782
methyl naphthalene	$C_{11}H_{10}$	20.15	
methyl naphthalene	$C_{11}H_{10}$	20.59	
	$C_{12}H_{10}$	22.42	
	$C_{12}H_{10}$	23.22	
	$C_{12}H_{10}$	23.66	
acenaphthylene	$C_{12}H_8$	24.19	0.9956
acenaphthene	$C_{12}H_{10}$	24.99	
	$C_{13}H_{10}$	26.87	
	$C_{13}H_{10}$	27.18	
fluorene	$C_{13}H_{10}$	27.30	
(benzindene)	$C_{13}H_{10}$	27.76	
(benzindene)	$C_{13}H_{10}$	28.11	
(benzindene)	$C_{13}H_{10}$	28.25	
	$C_{13}H_{12}$	29.03	
	$C_{14}H_{10}$	29.74	
methyl fluorene	$C_{14}H_{12}$	29.89	
methyl fluorene	$C_{14}H_{12}$	30.03	
	$C_{14}H_{10}$	30.10	
methyl fluorene	$C_{14}H_{12}$	30.27	
	$C_{14}H_{10}$	30.45	
phenanthrene	$C_{14}H_{10}$	31.56	0.0200
anthracene	$C_{14}H_{10}$	31.76	0.0006
	$C_{16}H_{12}$	33.25	
(CPD-acenaphthylene dimer)	$C_{17}H_{14}$	33.45	
	$C_{15}H_{12}$	33.90	
(CPD-acenaphthylene dimer)	$C_{17}H_{14}$	33.99	
	$C_{15}H_{12}$	34.18	
(4H-cyclopenta[def]phenanthrene)	$C_{15}H_{10}$	34.30	
(methyl phenanthrene)	$C_{15}H_{12}$	34.39	
(methyl anthracene)	$C_{15}H_{12}$	34.47	
	$C_{16}H_8$	34.76	
fluoranthene	$C_{16}H_{10}$	37.00	0.0108
(acephenanthrylene)	$C_{16}H_{10}$	37.44	0.0005
pyrene	$C_{16}H_{10}$	37.92	0.0038
	$C_{17}H_{12}$	40.43	
% soot (assume all carbon)			29.58
% total aromatic compounds			18.94
% carbon recovery			48.52

Table A.6 Product yields from the pyrolysis of CPD-styrene mixture (% of carbon feed; 0.3% (molar) CPD and 0.3% (molar) styrene in N_2; 4s)

Name	Formula	Elution time (minutes)	Temperature (^oC) 600	700	750	800	850	900
methyl-1,3-cyclopentadiene	C_6H_8	2.28	0.1668	0.4006	0.4131	0.2932	0.1195	0.1036
methyl-1,3-cyclopentadiene	C_6H_8	2.31	0.0370		0.2228			
benzene	C_6H_6	2.48	0.1702	2.6794	7.0897	17.3077	31.0919	38.1975
toluene	C_7H_8	4.08	0.0836	1.2372	3.3379	6.7788	6.2886	1.7099
	C_7H_8	4.91	0.0464	0.0989	0.0291	0.0287	0.1089	
(ethyl benzene)	C_8H_{10}	6.38	0.0483	0.1181	0.0864	0.0480		
(ethyl benzene)	C_8H_{10}	6.60		0.0242	0.0326	0.0670	0.0456	
phenyl ethyne	C_8H_6	6.81		0.1434	0.8747	3.3257	6.8320	4.7619
styrene	C_8H_8	7.27	61.6968	66.0371	64.0166	51.0777	29.3988	5.6806
	C_9H_{10}	8.84			0.0258	0.0398		
(1-methyl-2-propenyl-cyclohexane)	C_7H_{14}	8.90	0.0195	0.0204	0.0280	0.0271	0.0208	0.0192
(methyl styrene)	C_9H_{10}	9.69				0.0606		
(methyl styrene)	C_9H_{10}	9.95				0.1198	0.0254	
	C_9H_{10}	10.24		0.0299	0.0325	0.0602		
(ethylmethylbenzene)	C_9H_{10}	10.32		0.0540	0.0286	0.1546	0.0986	
	C_9H_{10}	10.42				0.0550	0.0365	
indane	C_9H_{10}	11.28	0.0334	0.0192	0.0675	0.0908	0.0151	
indene	C_9H_8	11.79	0.0416	0.7475	2.7102	4.7400	3.2247	1.1675
	$C_{10}H_{10}$	13.93			0.0108	0.0442	0.0482	
methyl indene	$C_{10}H_{10}$	14.28				0.0179	0.0171	
methyl indene	$C_{10}H_{10}$	14.92		0.0421	0.1141	0.0612	0.0091	
methyl indene	$C_{10}H_{10}$	15.09		0.1220	0.2262			
	$C_{10}H_8$	15.12		0.0889	0.1925	0.2165	0.0365	0.0064
(dihydrofulvalene/dihydronaphthalene)	$C_{10}H_{10}$	15.33	0.0070	0.3160	0.4521	0.1580	0.0099	0.0328
naphthalene	$C_{10}H_8$	15.92	0.0177	0.8372	3.2535	7.7751	10.1049	8.8727
methyl naphthalene	$C_{11}H_{10}$	18.96		0.0169	0.1730	0.2599	0.2691	0.0595
methyl naphthalene	$C_{11}H_{10}$	19.41		0.0175	0.1024	0.3985	0.3730	0.0447
	$C_{11}H_{10}$	19.97				0.0074		0.0117
biphenyl	$C_{12}H_{10}$	21.23			0.0513	0.5569	1.4364	0.6605
(2-methyl-1,1'-biphenyl)	$C_{13}H_{12}$	21.78				0.0001		0.0001
(ethenyl naphthalene)	$C_{12}H_{10}$	22.04				0.0128	0.0235	0.0111
(ethenyl naphthalene)	$C_{12}H_{10}$	22.46				0.2649	0.1070	0.0695
(methyl biphenyl)	$C_{13}H_{12}$	22.60				0.0420	0.0662	0.0173
acenaphthylene	$C_{12}H_8$	22.91			0.0002	0.0015	0.0049	0.0085
acenaphthene	$C_{12}H_{10}$	23.79				0.0001	0.0001	0.0001
(methyl biphenyl)	$C_{13}H_{12}$	23.88			0.0001	0.0003	0.0003	
	$C_{13}H_{12}$	24.08				0.0002	0.0001	
(1,1'-diphenyl-ethylene)	$C_{14}H_{12}$	24.63			0.0001	0.0004	0.0004	
	$C_{14}H_{12}$	24.81			0.0001	0.0005	0.0003	
(1H-phenalene)	$C_{13}H_{10}$	25.97				0.0059	0.0089	
fluorene	$C_{13}H_{10}$	26.09			0.0406	0.4405	1.1362	0.5224
	$C_{13}H_{10}$	26.56			0.0084	0.0334	0.0585	
(ethenyl biphenyl)	$C_{14}H_{12}$	26.78				0.0185	0.0281	

Table A.6 Product yields from the pyrolysis of CPD-styrene mixture (% of carbon feed; 0.3% (molar) CPD and 0.3% (molar) styrene in N_2; 4s)

Name	Formula	Elution time (minutes)	Temperature (°C) 600	700	750	800	850	900
	$C_{13}H_{10}$	26.89			0.0090	0.0350	0.0592	0.0097
	$C_{13}H_{10}$	27.04				0.0334	0.0527	0.0138
	$C_{14}H_{12}$	27.28				0.0188	0.0401	
	$C_{14}H_{10}$	27.88				0.0050	0.0512	0.0084
(dihydrophenanthrene)	$C_{14}H_{12}$	28.53		0.0133	0.0918	0.2382	0.1258	0.0048
(dihydroanthracene)	$C_{14}H_{12}$	28.69				0.0537	0.0344	
	$C_{14}H_{12}$	28.82			0.0103	0.0315	0.0072	
	$C_{14}H_{12}$	28.95			0.0619	0.2282	0.1674	
	$C_{14}H_{12}$	29.05			0.0289	0.1232	0.0405	
	$C_{14}H_{10}$	29.25				0.0137	0.0515	0.0110
	$C_{15}H_{12}$	29.30				0.0215	0.0330	
	$C_{15}H_{12}$	29.65				0.0151	0.0229	
(1H-indene-phenyl)	$C_{15}H_{12}$	30.21				0.0238	0.0388	
phenanthrene	$C_{14}H_{10}$	30.35			0.0382	0.5554	2.2845	2.5971
anthracene	$C_{14}H_{10}$	30.55			0.0194	0.3028	0.8400	0.5782
(methyl phenanthrene)	$C_{15}H_{12}$	31.05					0.0086	
(methyl anthracene)	$C_{15}H_{12}$	31.14					0.0138	
	$C_{16}H_{12}$	32.03			0.0065	0.1209	0.3788	0.2753
	$C_{15}H_{12}$	32.13				0.0304	0.0523	
	$C_{15}H_{12}$	32.71					0.0108	
	$C_{15}H_{12}$	32.79					0.0100	
	$C_{15}H_{10}$	33.08				0.0160	0.0842	0.0768
4H-cyclopenta[def]phenanthrene	$C_{15}H_{12}$	33.18				0.0173	0.0364	
	$C_{15}H_{12}$	33.26				0.0199	0.0382	
	$C_{16}H_{12}$	34.20				0.0631	0.2585	0.1981
fluoranthene	$C_{16}H_{10}$	35.78					0.1186	0.3331
(acephenanthrylene)	$C_{16}H_{10}$	36.22					0.0233	0.0645
pyrene	$C_{16}H_{10}$	36.70					0.0524	0.1409
% soot							0.41	3.48
% total aromatic compound			0.67	7.03	19.87	45.48	66.58	60.59
% carbon recovery			62.37	73.06	83.89	96.56	96.39	69.75

Table A.7 Product yields from the pyrolysis of CPD-phenanthrene mixture (% of carbon feed; 0.8% (molar) CPD and 0.1% (molar) phenanthrene in N_2; 4s)

			Temperature (°C)				
Name	Formula	Elution time (minutes)	700	800	850	900	950
methyl-1,3-cyclopentadiene	C_6H_8	2.27	0.5628	0.3993	0.1190		0.1369
benzene	C_6H_6	2.46	2.0248	11.1383	14.9956	14.0690	20.1656
toluene	C_7H_8	4.07	0.3310	3.2340	4.2221	1.8266	0.2886
(ethyl benzene)	C_8H_{10}	6.29			0.1377		
p-xylene	C_8H_{10}	6.60		0.1207	0.1179		
phenyl ethyne	C_8H_6	6.81		0.2280	0.4104	0.6084	0.2655
styrene	C_8H_8	7.19	0.2260	1.8274	2.0765	0.9018	0.0579
(ethylmethylbenzene)	C_9H_{10}	10.32	0.0500	0.0795	0.0212		
indene	C_9H_8	11.78	2.2427	10.5393	5.4352	2.1091	0.2443
methyl indene	$C_{10}H_{10}$	14.92	0.2224	0.2466	0.0240	0.0111	
methyl indene	$C_{10}H_{10}$	15.12	0.5669	0.8242	0.1030		
(dihydrofulvalene/dihydronaphthalene)	$C_{10}H_{10}$	15.33	0.8331	0.3832	0.0248	0.0006	0.0413
naphthalene	$C_{10}H_8$	15.97	2.0107	18.4750	22.3485	18.6632	14.9099
methyl naphthalene	$C_{11}H_{10}$	18.96		0.1134	0.1910		0.0279
methyl naphthalene	$C_{11}H_{10}$	19.41		0.1422	0.1858	0.1361	0.0204
biphenyl	$C_{12}H_{10}$	21.22		0.0524	0.1051	0.0317	0.0673
(ethenyl naphthalene)	$C_{12}H_{10}$	22.03		0.0088	0.0076		
(ethenyl naphthalene)	$C_{12}H_{10}$	22.45		0.0118	0.0320		
acenaphthylene	$C_{12}H_8$	22.91	0.0238	0.4713	1.0775	1.7666	2.7535
acenaphthene	$C_{12}H_{10}$	23.78	0.0241	0.0318	0.0176	0.0096	0.0056
(1,1'-diphenyl-ethylene)	$C_{14}H_{12}$	24.67			0.0061		0.0057
	$C_{13}H_{10}$	25.67		0.0078			
(1H-phenalene)	$C_{13}H_{10}$	25.97		0.0215	0.0113	0.0033	
fluorene	$C_{13}H_{10}$	26.10	0.0074	1.0493	1.7567	1.1060	0.1358
	$C_{13}H_{10}$	26.55		0.0774	0.0337	0.0119	
(methyl fluorene)	$C_{14}H_{12}$	26.61			0.0148	0.0016	
	$C_{13}H_{10}$	26.89		0.0695	0.0300	0.0153	
	$C_{13}H_{10}$	27.04		0.1550	0.1019	0.0382	
(dihydrophenanthrene)	$C_{14}H_{12}$	28.53		0.0966	0.0259	0.0010	
(methyl fluorene)	$C_{14}H_{12}$	28.69		0.2268	0.0798	0.0010	
(methyl fluorene)	$C_{14}H_{12}$	28.82			0.0204		
(methyl fluorene)	$C_{14}H_{12}$	29.05		0.4375	0.0879		
	$C_{14}H_{10}$	29.25		0.0746	0.0381	0.0317	0.0055
phenanthrene	$C_{14}H_{10}$	30.43	12.3988	13.3183	13.8628	14.2193	7.8742
anthracene	$C_{14}H_{10}$	30.57	0.1213	1.5110	2.4210	2.4964	0.8315
(9-ethenyl anthracene)	$C_{16}H_{12}$	32.03		0.0135	0.0484	0.1165	0.0506
(methyl phenanthrene)	$C_{15}H_{12}$	32.68		0.0187	0.0266		
(methyl phenanthrene)	$C_{15}H_{12}$	32.79		0.0224	0.0372		
	$C_{15}H_{12}$	32.96		0.0282	0.0134		
(4H-cyclopenta[def]phenanthrene)	$C_{15}H_{10}$	33.08		0.1227	0.1830		0.0626
	$C_{15}H_{12}$	33.16		0.1050	0.0663	0.2347	
	$C_{15}H_{12}$	33.25		0.1117	0.0982		
	$C_{16}H_{12}$	34.20			0.0242		0.0338
fluoranthene	$C_{16}H_{10}$	35.78		0.0196	0.1598	0.8093	1.1262
(acephenanthrylene)	$C_{16}H_{10}$	36.22			0.0417	0.2625	0.1487
pyrene	$C_{16}H_{10}$	36.71			0.0670	0.4017	0.4911
%soot				0.01	4.45	7.64	9.07
%total aromatic compound			9.25	52.50	57.05	45.67	41.88
% total carbon recovery			21.65	65.82	75.36	67.52	58.82

Table A.8 Phenol product yields from monochlorophenols (% of carbon feed; 0.9% (molar) CP in 8% O_2 in N_2; 10s)

			Temperature (^oC)					
Reactant	Product	Elution time (min)	550	575	600	600	600	625
2-CP	2-CP	11.95	51.7745	42.5040	0.2527	0.2863	0.3256	37.3295
	CO		0.6108	1.2217	3.6650	6.1083	3.5632	10.3842
	phenol	11.89	0.3792	0.3356	30.3303	32.8182	34.9054	0.9342
	napthhalene	20.93	0.0041	0.0139	0.0137	0.0118	0.0131	0.1127
	2-MCN	29.37	0.0002	0.0010	0.0011	0.0010	0.0011	0.0121
	1-MCN	29.63	0.0039	0.0154	0.0082	0.0080	0.0089	0.0627
	15-/16-/17-DCN	36.73	0.0001	0.0003	0.0002	0.0002	0.0002	0.0012
	26-/27-DCN	37.07	n.d.[b]	trace[c]	0.0000	0.0000	0.0000	0.0002
	DF	35.03	0.0006	0.0031	0.0061	0.0049	0.0058	0.0316
	4-MCDF	42.80	0.0028	0.0038	0.0035	0.0040	0.0045	0.0138
	46-DCDF	49.47	0.0310	0.0208	0.0156	0.0167	0.0187	0.0274
	DD	37.74	0.0152	0.0191	0.0011	0.0014	0.0016	0.0386
3-CP	3-CP	21.82	35.4738	33.8259	18.6750	22.5143	22.5588	21.4742
	CO		0.9163	3.0542	6.5156	2.8506	1.8325	15.4745
	phenol	11.89	0.3923	0.3949	0.1952	0.2408	0.1866	0.4364
	naphthalene	20.93	0.0041	0.0047	0.0078	0.0075	0.0064	0.0518
	2-MCN	29.37	0.0017	0.0062	0.0106	0.0095	0.0100	0.0528
	1-MCN	29.63	0.0019	0.0072	0.0118	0.0107	0.0111	0.0550
	15/16/17-DCN	36.73	0.0007	0.0020	0.0027	0.0029	0.0031	0.0120
	26/27-DCN	37.07	0.0007	0.0025	0.0035	0.0041	0.0041	0.0156
	DF	35.03	0.0002	0.0016	0.0025	0.0020	0.0018	0.0112
	1-MCDF	41.63	0.0048	0.0384	0.0410	0.0316	0.0337	0.1076
	3-MCDF	42.05	0.0022	0.0245	0.0340	0.0261	0.0273	0.0940
	17-DCDF	47.91	0.9264	1.0626	0.9803	0.8922	0.9116	1.5502
	37-DCDF	48.66	0.2635	0.3773	0.3613	0.3259	0.3330	0.5963
	19-DCDF	50.07	0.0823	0.1041	0.0990	0.0885	0.0909	0.1600
4-CP	4-CP	21.82	35.9636	26.4475	25.7177	26.8998	25.7177	23.9358
	CO		0.6108	1.8325	2.7488	3.0542	1.2217	4.2758
	phenol	11.89	0.2129	0.3507	0.1735	0.1347	0.1735	1.0277
	naphthalene	20.93	0.0009	0.0013	0.0052	0.0032	0.0029	0.0330
	2-MCN	29.37	0.0009	0.0032	0.0087	0.0059	0.0054	0.0420
	1-MCN	29.63	0.0001	0.0004	0.0014	0.0010	0.0007	0.0073
	15/16/17-DCN	36.73	n.d.	n.d.	0.0000	0.0000	0.0000	0.0003
	26/27-DCN	37.07	0.0004	0.0014	0.0017	0.0017	0.0012	0.0090
	DF	35.03	0.0002	0.0006	0.0019	0.0012	0.0023	0.0071
	2-MCDF	42.25	0.0011	0.0038	0.0113	0.0069	0.0141	0.0393
	28-DCDF	48.94	0.2320	0.2816	0.3069	0.3080	0.3267	0.5514

Table A.8 Phenol product yields from monochlorophenols (% of carbon feed; 0.9% (molar) CP in 8% O_2 in N_2; 10s) (continued)

Reactant	Product	Elution time (min)	650	675	700	725	750
2-CP	2-CP	11.95	33.8293	15.4041	3.2119	0.0105	0.0310
	CO		19.5467	44.7945	63.5268	13.4384	7.6354
	phenol	11.89	1.7175	1.8600	0.9875	0.0050	0.0187
	napthhalene	20.93	0.2120	0.8033	0.5840	0.0618	0.0616
	2-MCN	29.37	0.0186	0.0503	0.0214	0.0004	0.0003
	1-MCN	29.63	0.0612	0.1045	0.0377	0.0023	0.0014
	15-/16-/17-DCN	36.73	0.0013	0.0021	0.0005	n.d.	n.d.
	26-/27-DCN	37.07	0.0003	0.0009	0.0002	n.d.	n.d.
	DF	35.03	0.0997	0.1627	0.1754	0.0024	0.0017
	4-MCDF	42.80	0.0309	0.0318	0.0182	0.0001	trace
	46-DCDF	49.47	0.0402	0.0159	0.0059	trace	trace
	DD	37.74	0.0546	0.0266	0.0098	0.0002	0.0002
3-CP	3-CP	21.82	9.0654	2.3811	0.5642	0.0041	0.0072
	CO		20.7684	36.0392	42.7584	7.3300	3.0542
	phenol	11.89	0.4808	0.6293	0.2850	0.1326	0.0316
	naphthalene	20.93	0.1929	0.2828	0.3430	0.1372	0.2125
	2-MCN	29.37	0.0874	0.0986	0.0423	0.0100	0.0077
	1-MCN	29.63	0.0913	0.0916	0.0438	0.0114	0.0091
	15/16/17-DCN	36.73	0.0156	0.0109	0.0024	0.0004	0.0002
	26/27-DCN	37.07	0.0187	0.0152	0.0030	0.0006	0.0003
	DF	35.03	0.0176	0.0561	0.0317	0.0166	0.0165
	1-MCDF	41.63	0.0759	0.1434	0.0522	0.0106	0.0080
	3-MCDF	42.05	0.0674	0.1430	0.0534	0.0096	0.0094
	17-DCDF	47.91	1.4342	0.5707	0.1774	0.0157	0.0119
	37-DCDF	48.66	0.4298	0.2083	0.0547	0.0036	0.0032
	19-DCDF	50.07	0.1459	0.0493	0.0130	0.0008	0.0006
4-CP	4-CP	21.82	19.5361	11.7435	2.6042	0.1873	0.0032
	CO		10.9950	26.2659	61.0834	6.7192	4.2758
	phenol	11.89	2.0037	2.1807	1.3604	0.2246	0.0728
	naphthalene	20.93	0.1880	0.4896	0.6548	0.8569	0.5470
	2-MCN	29.37	0.1130	0.1688	0.1200	0.0807	0.0262
	1-MCN	29.63	0.0229	0.0390	0.0394	0.0277	0.0164
	15/16/17-DCN	36.73	0.0007	0.0008	0.0012	0.0004	0.0001
	26/27-DCN	37.07	0.0205	0.0226	0.0118	0.0047	0.0010
	DF	35.03	0.0353	0.0674	0.0817	0.0512	0.0514
	2-MCDF	42.25	0.1219	0.1181	0.0890	0.0319	0.0172
	28-DCDF	48.94	1.1362	0.5473	0.2331	0.0459	0.0203

Table A.9 Phenol product yields from dichlorophenols in benzene at 600°C (% of carbon feed; 0.4% (molar) DCP and 0.8% (molar) benzene in 8% O_2 in N_2; 10s)

	Elution time (min)	2,4-DCP	2,5-DCP	3,5-DCP	2,3-DCP	3,4-DCP	2,6-DCP
CPs:							
2,4-DCP	20.23	3.560					
2,5-DCP	20.34		2.860				
3,5-DCP	30.42			2.036			
2,3-DCP	20.64				1.971		
3,4-DCP	31.38					1.113	
2,6-DCP	21.85						3.301
phenol	11.89	0.324	0.343	0.139	0.224	0.146	0.272
2-CP	11.95	0.019	0.081		0.009		0.007
3-CP and 4-CP	21.82	0.280		0.001	0.013	0.005	0.016
PCNs:							
N	20.93	6.39E-04	1.25E-03	1.22E-04	1.15E-03	6.66E-04	5.45E-04
2-MCN	29.37	3.12E-04	4.29E-04	6.00E-04	1.83E-04	1.99E-04	1.82E-04
1-MCN	29.63	7.20E-05	1.19E-04	1.44E-05	3.25E-04	1.22E-04	1.21E-03
13-DCN	36.06	1.68E-04	3.86E-05	2.37E-04			
14-DCN	36.57		1.90E-04			1.34E-05	7.42E-06
15-/16-/17-DCN	36.73	8.89E-06			8.19E-05	3.14E-05	8.35E-05
26-/27-DCN	37.07	1.14E-04	5.29E-05		1.02E-05	1.64E-05	3.50E-05
12-DCN	37.42		1.46E-05		1.41E-04	4.33E-04	1.21E-05
23-DCN	38.66				7.97E-06	2.47E-04	
18-DCN	39.68				6.02E-06		2.93E-04
136-T3CN	42.49	2.49E-05	9.41E-06	8.88E-05	7.76E-06	1.79E-05	6.64E-06
137-/146-T3CN	42.94	5.99E-05	1.28E-04		1.72E-05	5.26E-05	4.93E-06
124-T3CN	43.25			5.40E-05			
125-T3CN	43.62				6.02E-05	2.54E-05	5.09E-06
126-T3CN	43.90		7.08E-06		1.70E-05	1.75E-04	1.66E-06
127-T3CN	44.23		5.30E-06		2.57E-05	1.08E-04	4.60E-06
167-/236-T3CN	44.55					1.41E-04	
145-T3CN	45.45		7.61E-06				
128-T3CN	46.87					7.14E-06	3.34E-06
1367-T4CN	49.12					3.95E-06	
1368-/1256-T4CN	49.39					3.31E-06	
1267-T4CN	50.86					1.13E-05	

Table A.9 Phenol product yields from dichlorophenols in benzene at 600°C (% of carbon feed; 0.4% (molar) DCP and 0.8% (molar) benzene in 8% O_2 in N_2; 10s) (continued)

	Elution time (min)	2,4-DCP	2,5-DCP	3,5-DCP	2,3-DCP	3,4-DCP	2,6-DCP
PCDFs:							
DF	35.03	8.14E-04	1.00E-04	2.18E-04	4.20E-04	1.21E-03	1.52E-03
1-MCDF	41.63		2.03E-05	1.20E-05	1.77E-04	8.10E-05	1.15E-04
3-MCDF	42.05		1.39E-05	1.99E-05		3.57E-05	
2-MCDF	42.25	3.40E-04				4.52E-05	
4-MCDF	42.80	6.33E-05				2.37E-05	3.56E-04
13-DCDF	47.06			4.13E-03			
14-DCDF	48.13		8.37E-04				
24-DCDF	48.37	3.35E-03					
27-/12-DCDF	48.78					4.80E-03	
23-DCDF	49.10					1.74E-03	
46-DCDF	49.47						1.03E-04
34-DCDF	49.77				9.52E-04		
137-T3CDF	53.26			1.35E-04			
247-/248-T3CDF	54.61	2.74E-04	2.74E-04				
127-/239-T3CDF	54.90					3.10E-04	
139-T3CDF	55.05			1.62E-05			
349-T3CDF	55.15				7.62E-05		
128-T3CDF	55.32					1.71E-04	
238-T3CDF	55.56					1.22E-04	
236-T3CDF	55.83					3.57E-05	
348-/346-T3CDF	56.06				7.16E-05		
129-T3CDF	56.84					5.55E-05	
2468-T4CDF	58.65	4.13E-04					
1347-/1346-/1378-/1247-T4CDF	58.78						
1367-/1379-T4CDF	58.99			6.80E-03			
2467-/2349-/1234-/1469-T4CDF	59.79		3.13E-05				
1278-T4CDF	60.00					1.55E-02	
1249-/2347-/2378-/2346-/2348-T4CDF	60.39					1.69E-03	
3467-/1269-T4CDF	60.84				4.55E-04		
1289-T4CDF	61.66					1.30E-03	

APPENDIX B

CHROMATOGRAMS AND MASS SPECTRA OF SELECTED PRODUCTS

B.1 Dicyclopentadiene pyrolysis at 600^{o}C (gas sample)

(a) Ion Chromatogram

(b) Mass Spectrum of cyclopentadiene

B.2 Dicyclopentadiene pyrolysis at 775^{o}C

(a) Total Ion Chromatogram

(b) Mass Spectra: indene, methyl indene and $C_{10}H_{10}$

(c) Mass Spectra: dihydronaphthalene, naphthalene and fluorene

(d) Mass Spectra: 9,10-dihydrophenanthrene, methyl fluorene and phenanthrene

B.3 Dicyclopentadiene-acenaphthylene mixture pyrolysis at 900^{o}C

(a) Total Ion Chromatogram

(b) Mass Spectra: acenaphthylene and fluoranthene

B.4 Halowax 1000

(a) Total Ion Chromatogram and Mass Spectrum: MCN

(b) Total Ion Chromatogram and Mass Spectrum: DCN

B.5 Halowax 1001

(a) Total Ion Chromatogram and Mass Spectrum: T_3CN

(b) Total Ion Chromatogram and Mass Spectrum: T_4CN

B.6 Halowax 1014

(a) Total Ion Chromatogram and Mass Spectrum: P_5CN

(b) Total Ion Chromatogram and Mass Spectrum: H_6CN

B.7 Halowax 1051

(a) Total Ion Chromatogram and Mass Spectrum: H_7CN

(b) Total Ion Chromatogram and Mass Spectrum: OCN

B.1 Dicyclopentadiene pyrolysis at 600^{o}C (gas sample)

(a) Ion Chromatogram

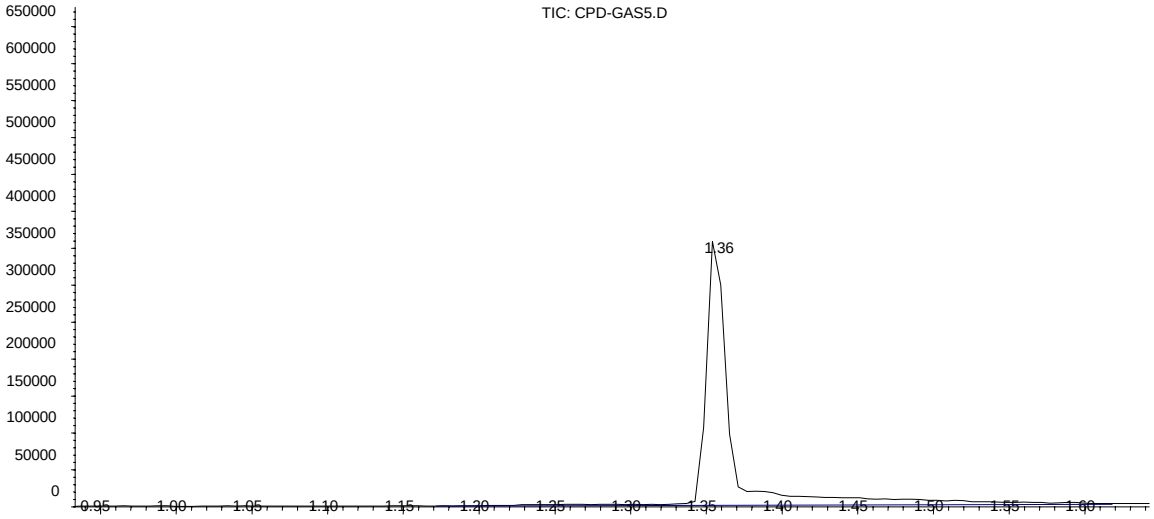

(b) Mass Spectra of cyclopentadiene

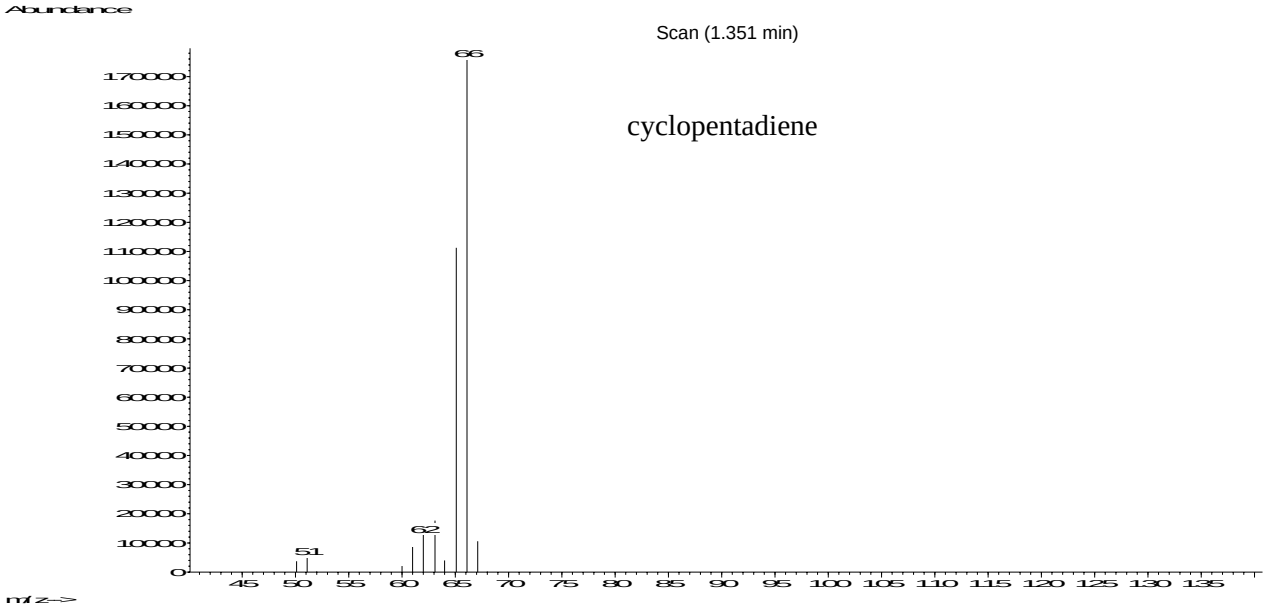

B.2 Dicyclopentadiene pyrolysis at 775°C

(a) Total Ion Chromatogram

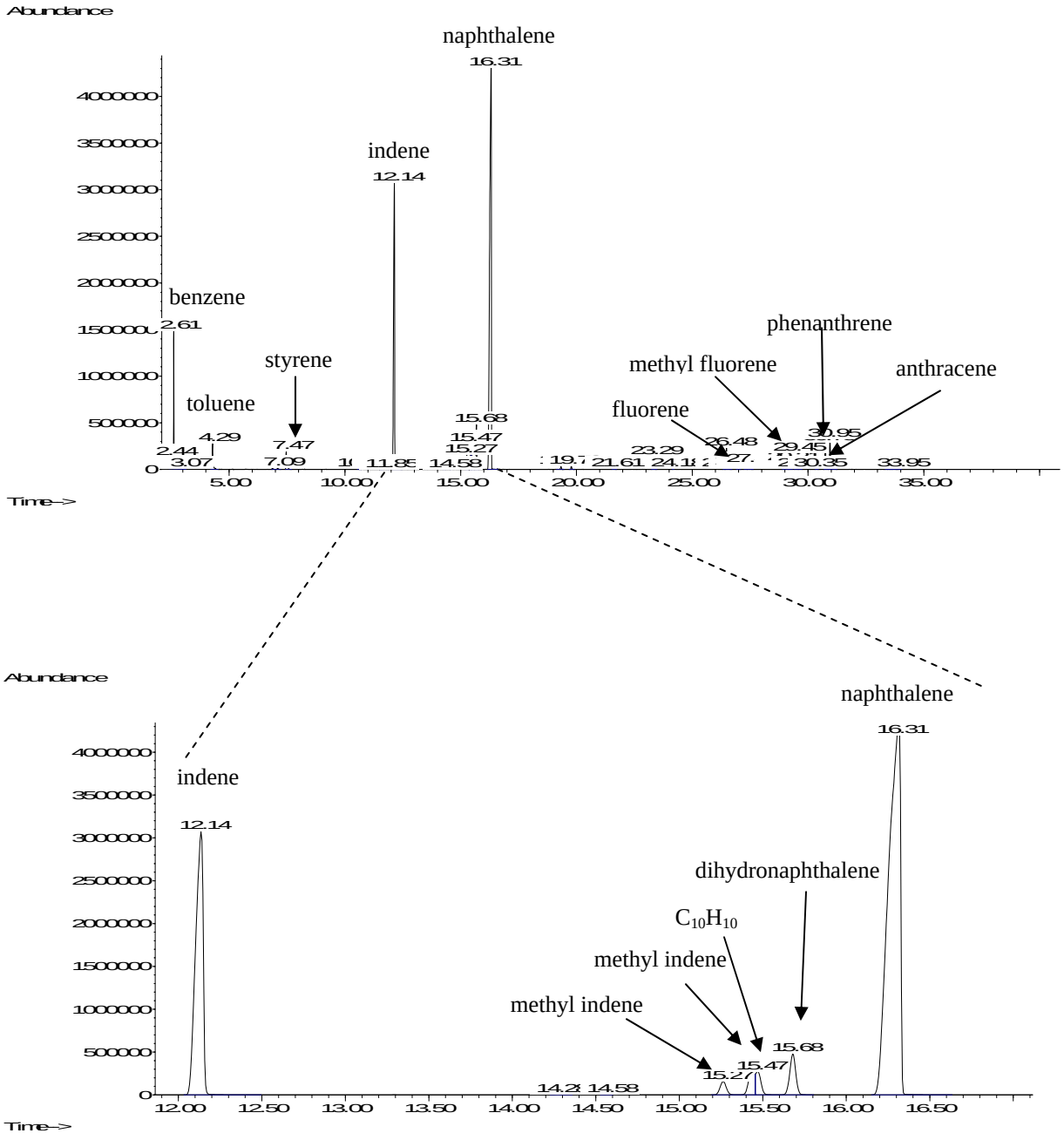

B.2 Dicyclopentadiene pyrolysis at 775°C

(a) Total Ion Chromatogram (continued)

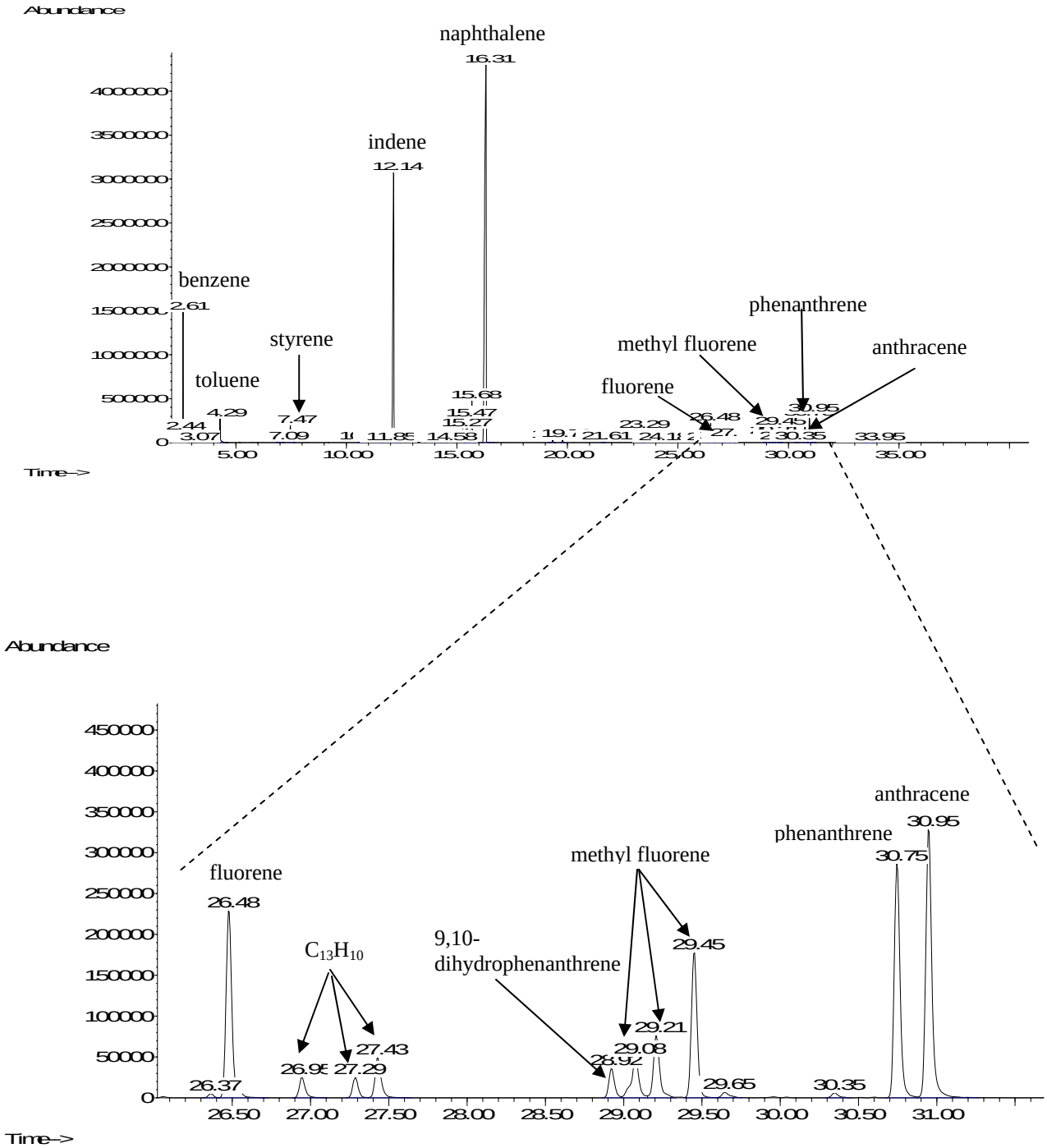

B.2 Dicyclopentadiene pyrolysis at 775^{o}C

(b) Mass Spectra: indene, methyl indene and $C_{10}H_{10}$

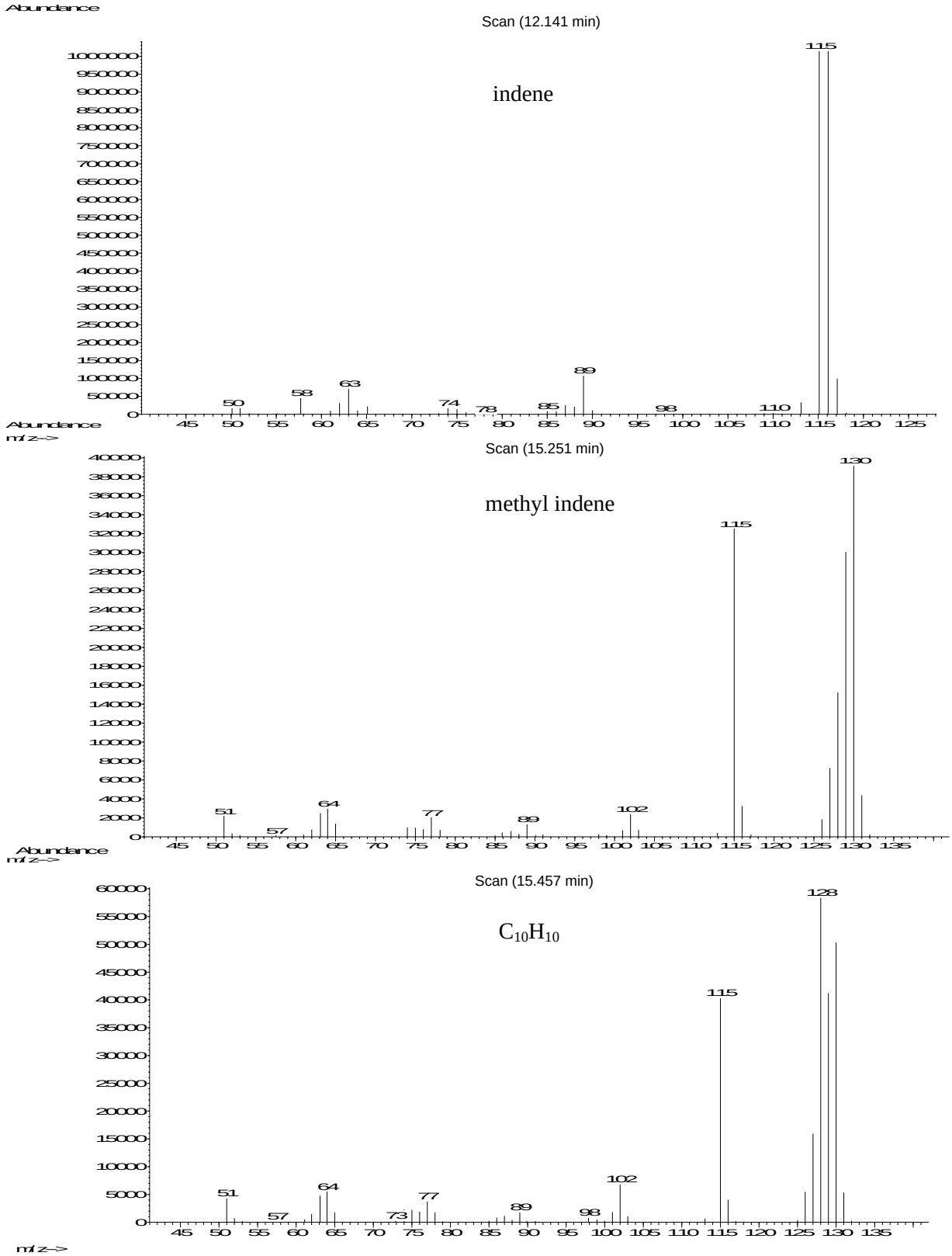

B.2 Dicyclopentadiene pyrolysis at 775^{o}C

(c) Mass Spectra: dihydronaphthalene, naphthalene and fluorene

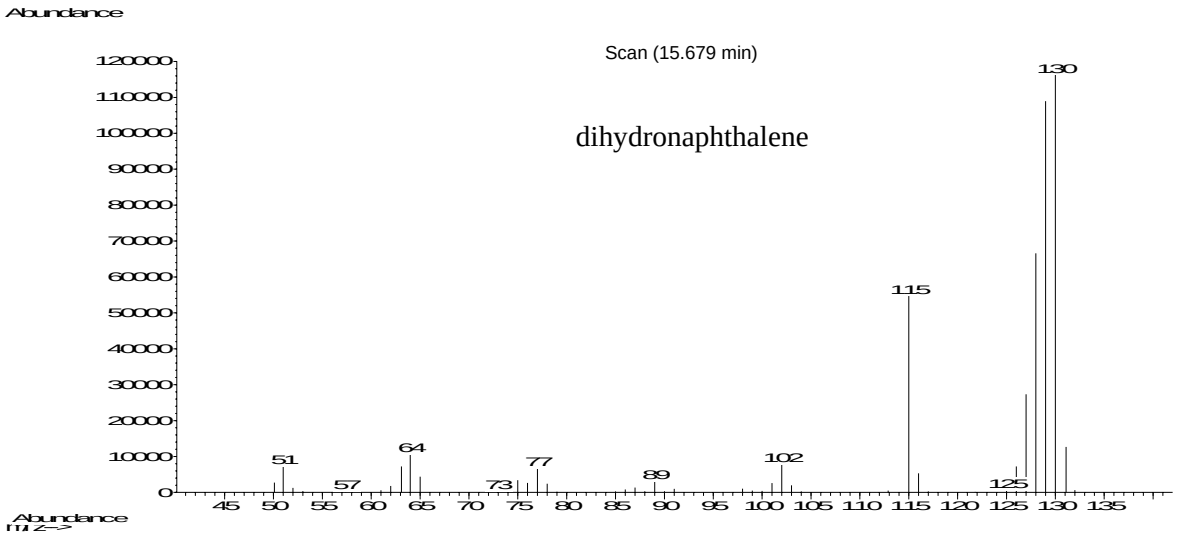

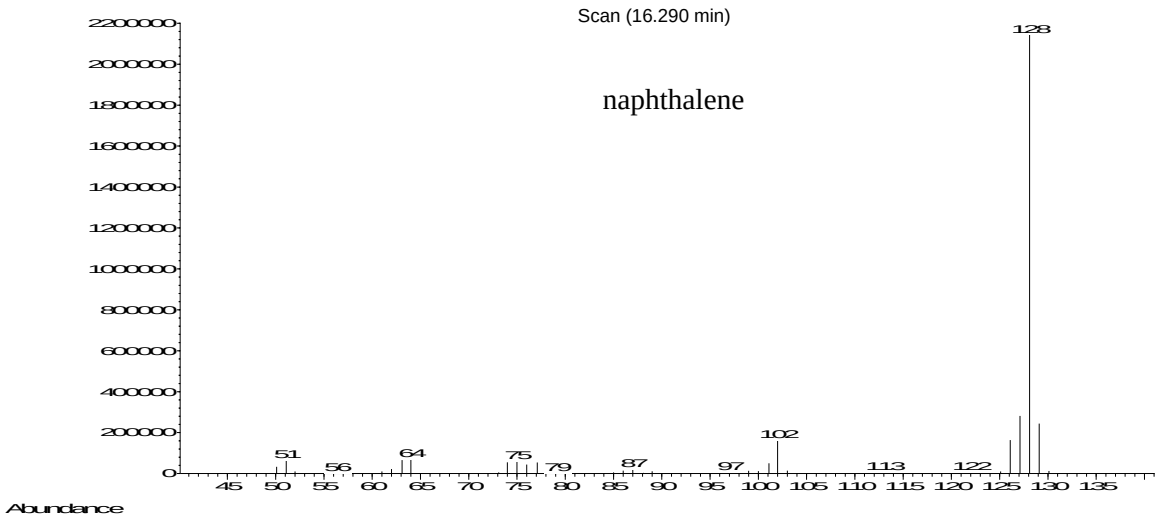

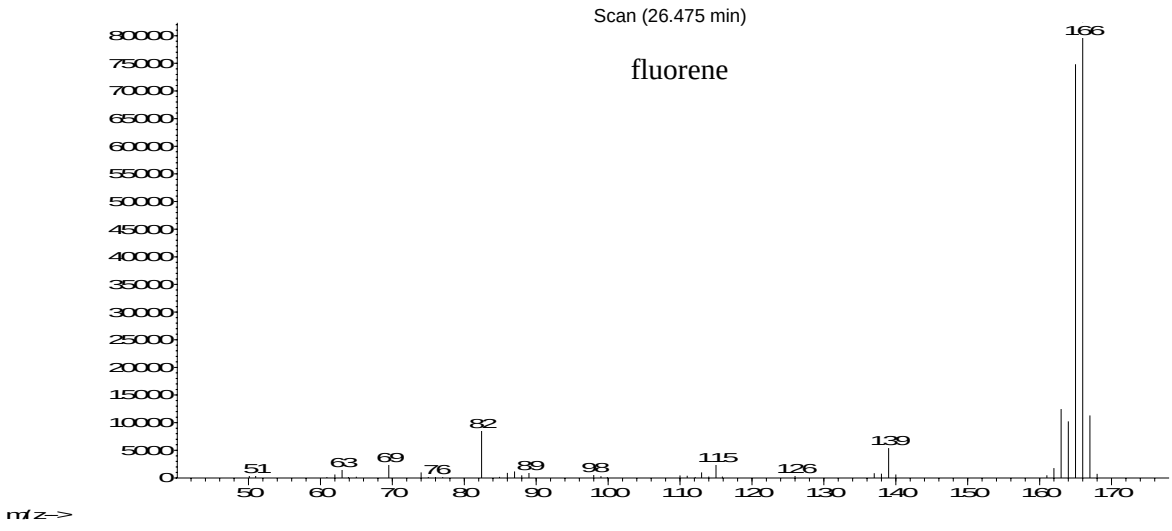

B.2 Dicyclopentadiene pyrolysis at 775^{o}C

(d) Mass Spectra: 9,10-dihydrophenanthrene, methyl fluorene and phenanthrene

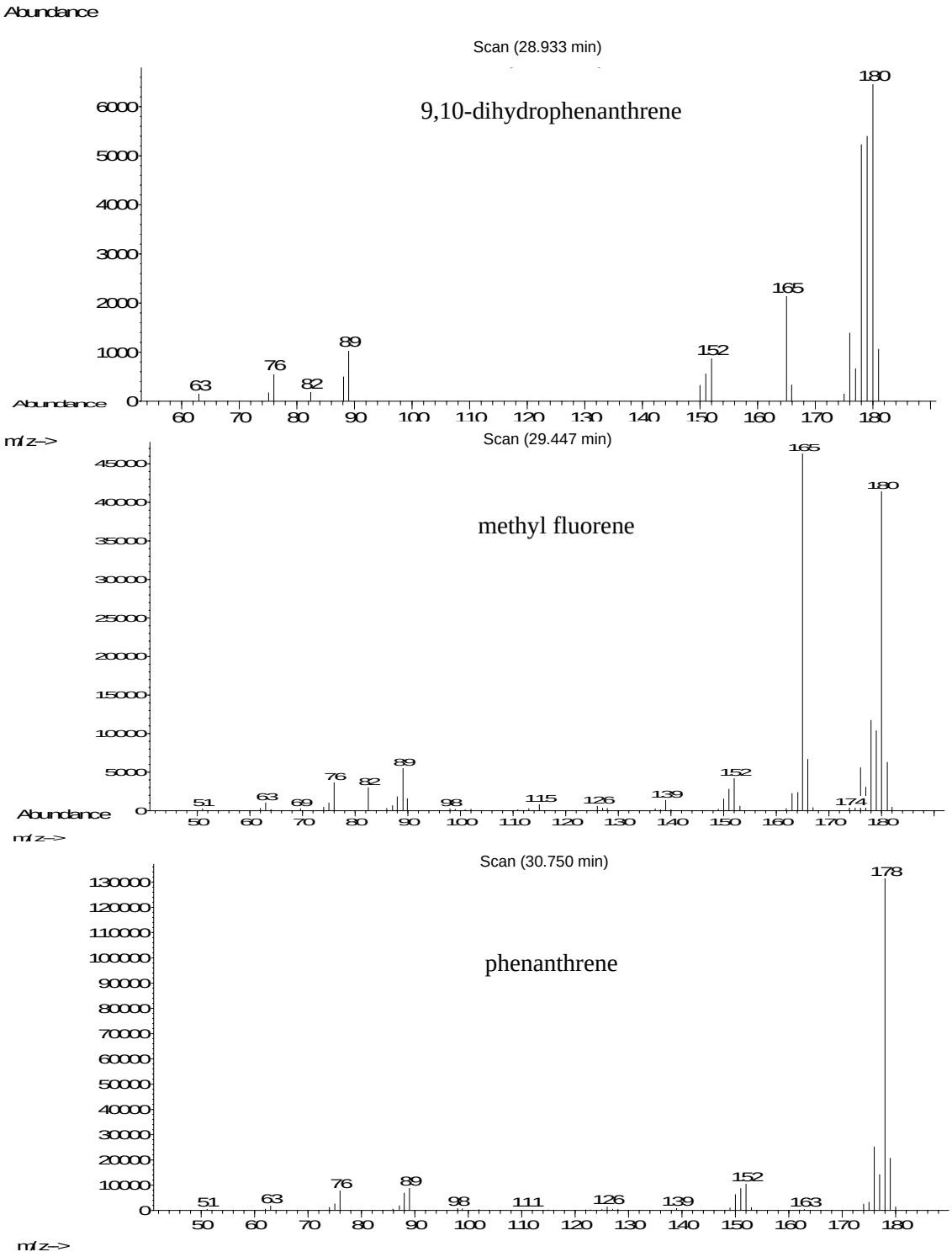

B.3 Dicyclopentadiene-acenaphthylene mixture pyrolysis at 900°C

(a) Total Ion Chromatogram

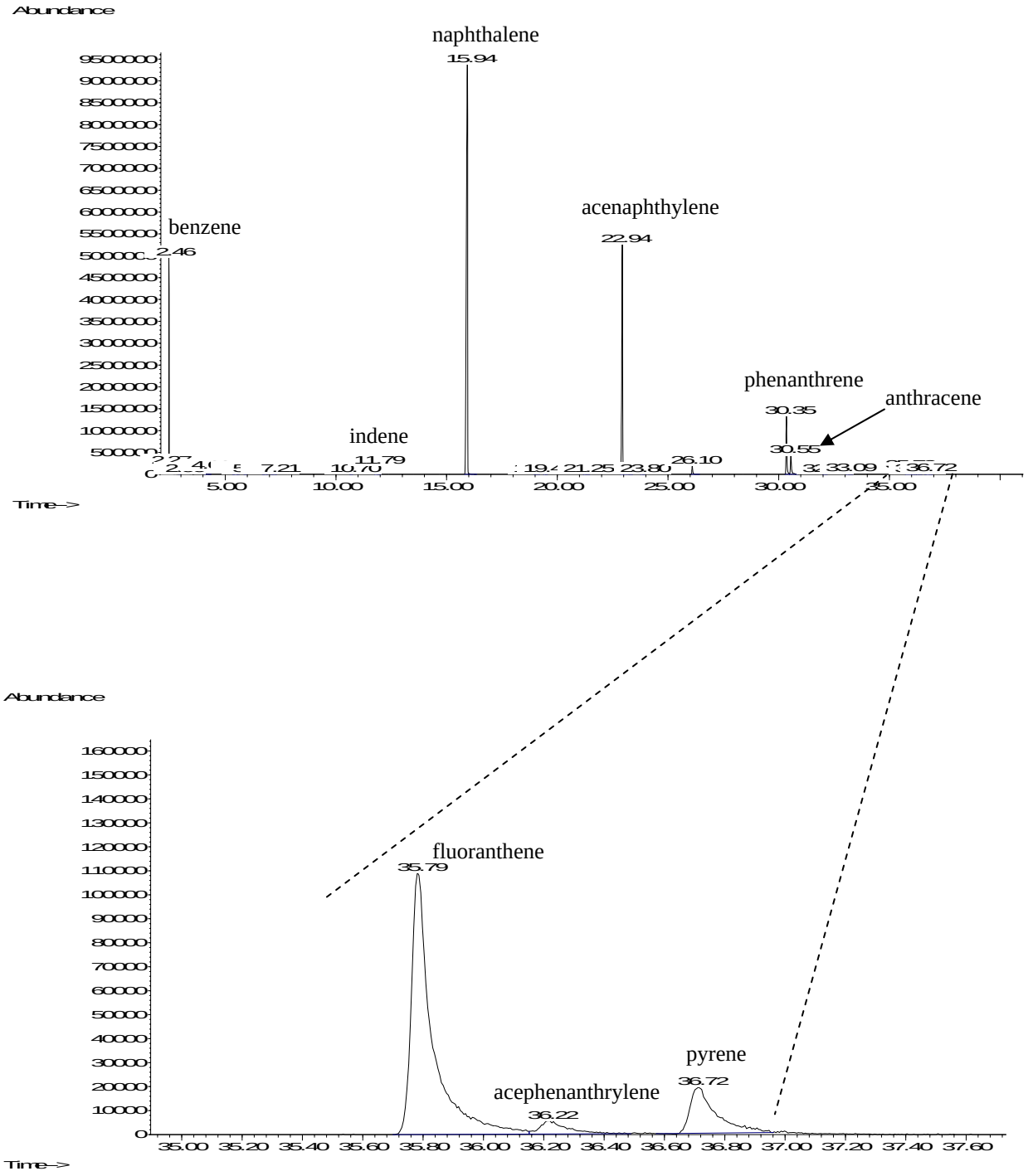

B.3 Dicyclopentadiene-acenaphthylene mixture pyrolysis at 900°C

(b) Mass Spectra: acenaphthylene and fluoranthene

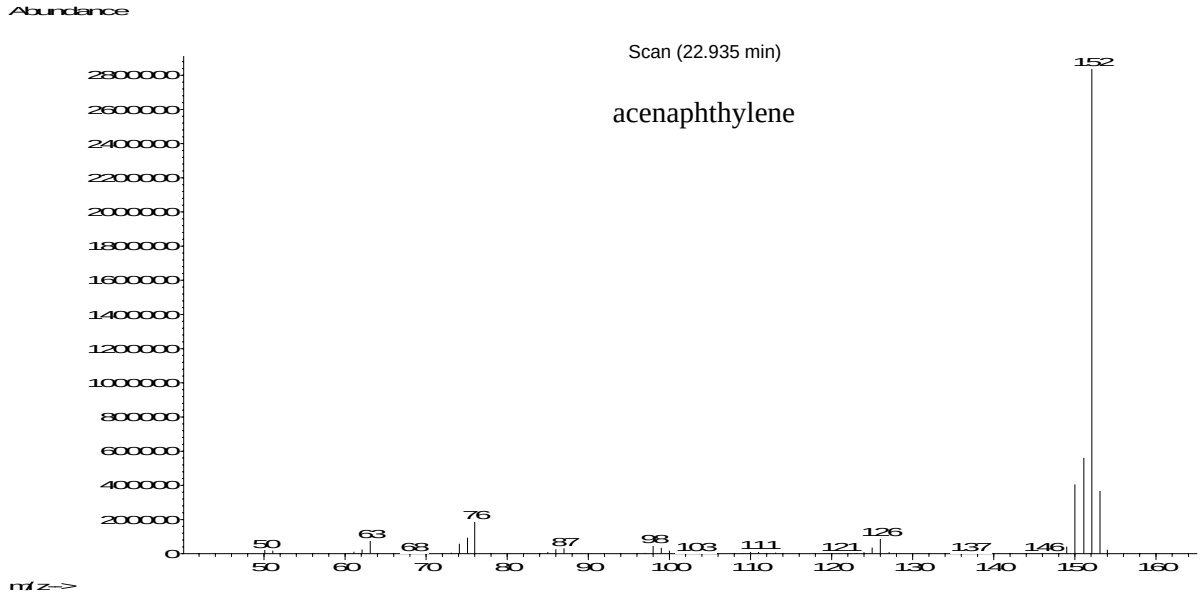

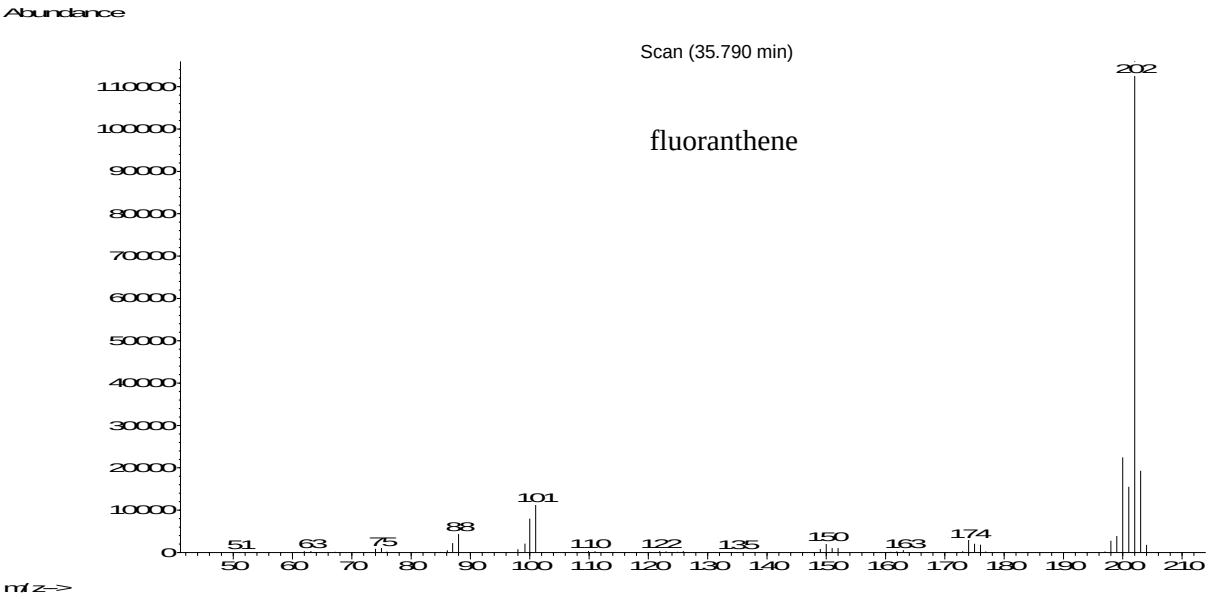

B.4 Halowax 1000

(a) Total Ion Chromatogram and Mass Spectrum: MCN

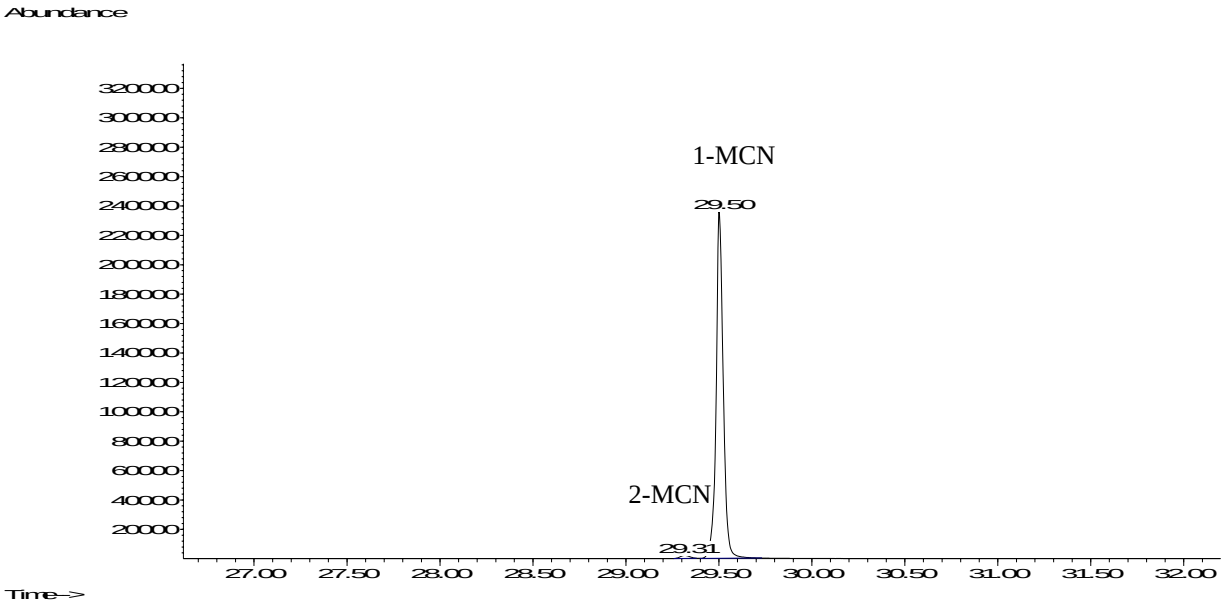

B.4 Halowax 1000

(b) Total Ion Chromatogram and Mass Spectrum: DCN

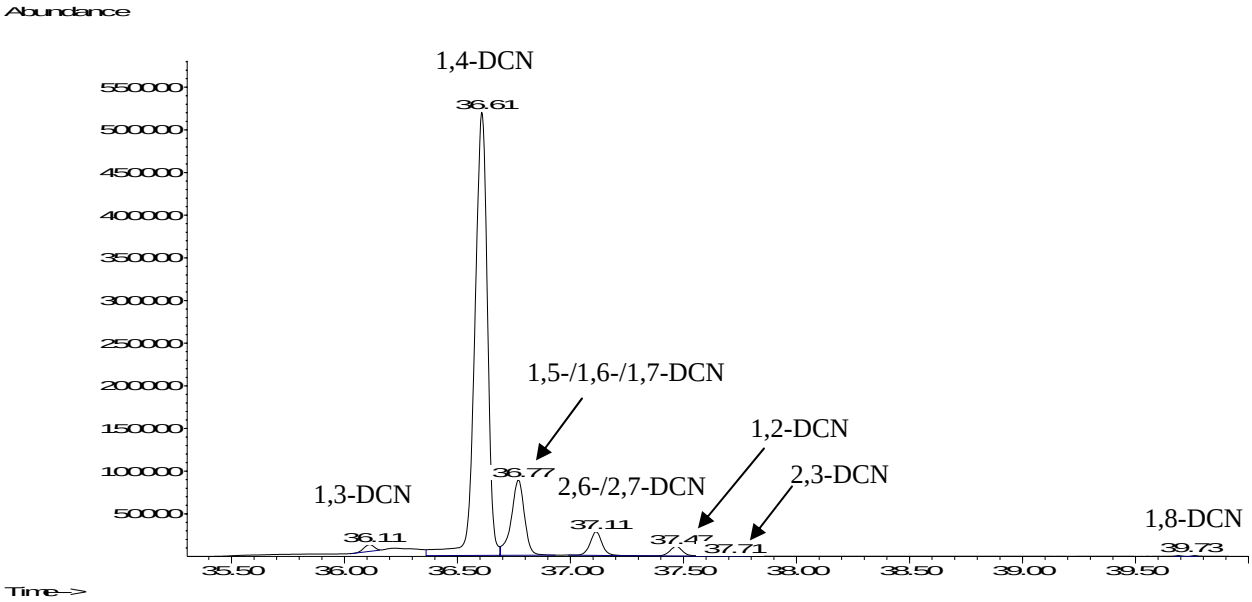

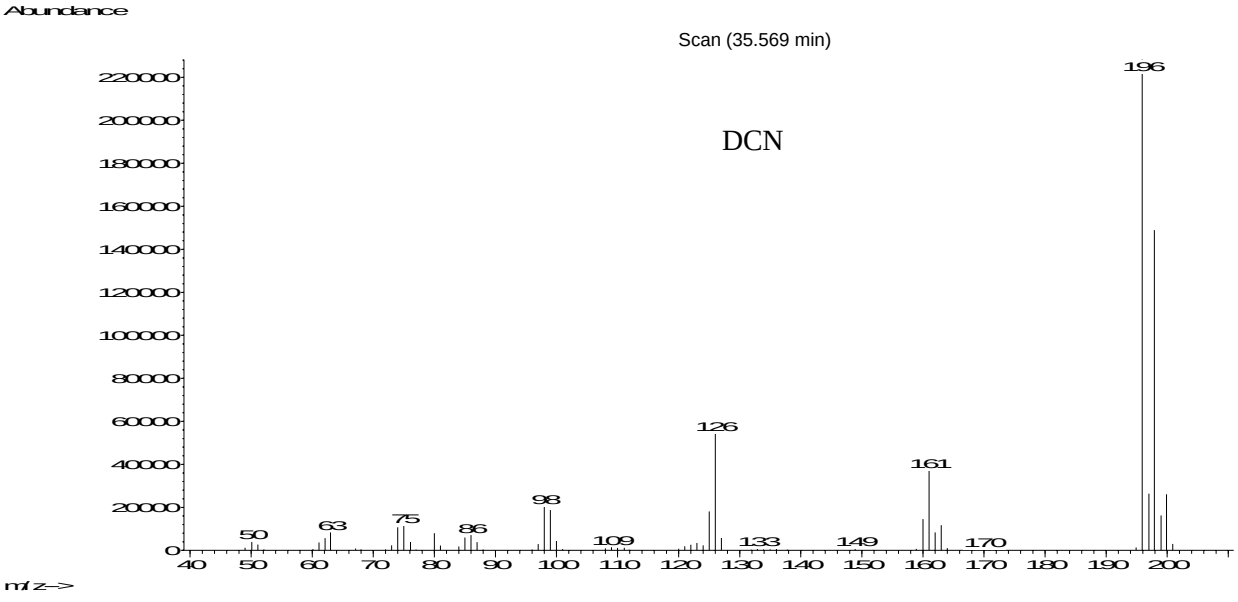

B.5 Halowax 1001

(a) Total Ion Chromatogram and Mass Spectrum: T_3CN

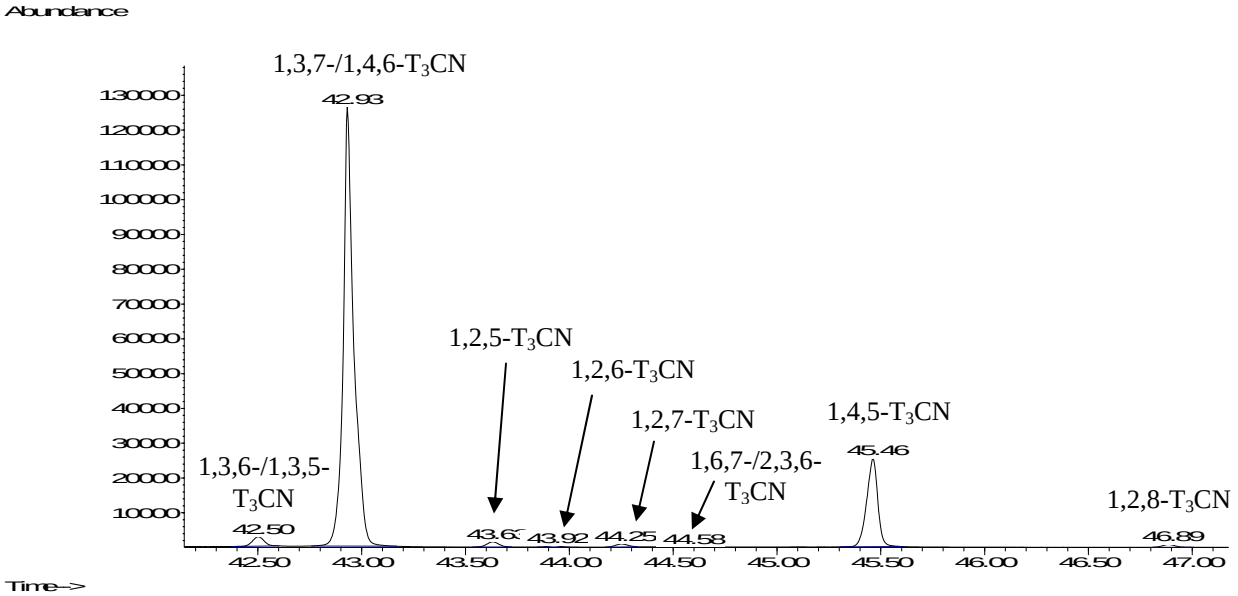

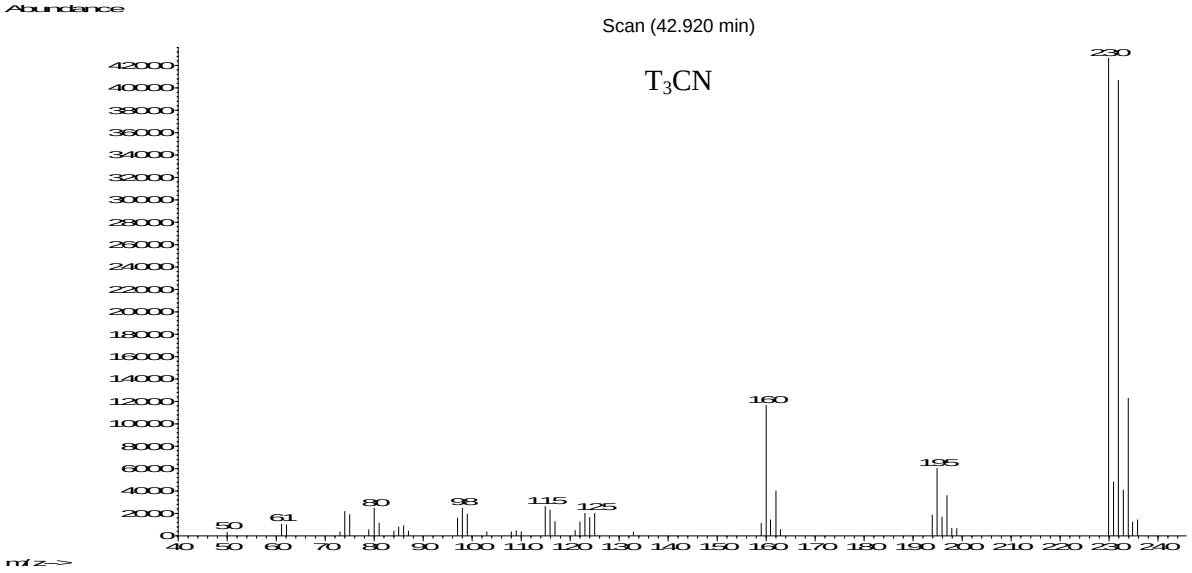

B.5 Halowax 1001

(b) Total Ion Chromatogram and Mass Spectrum:T_4CN

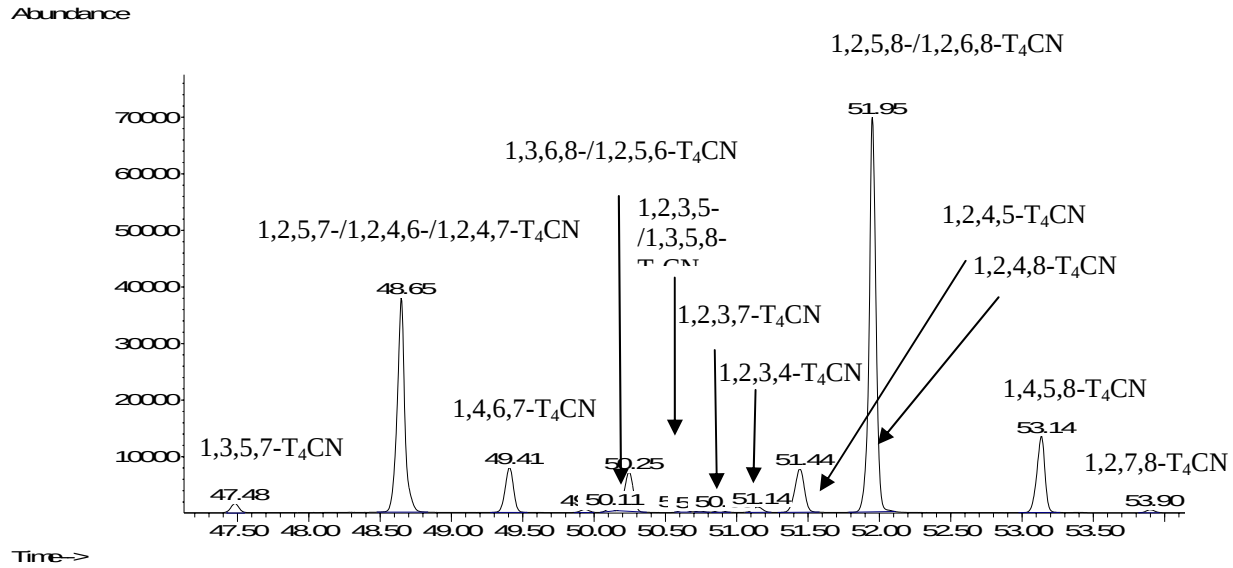

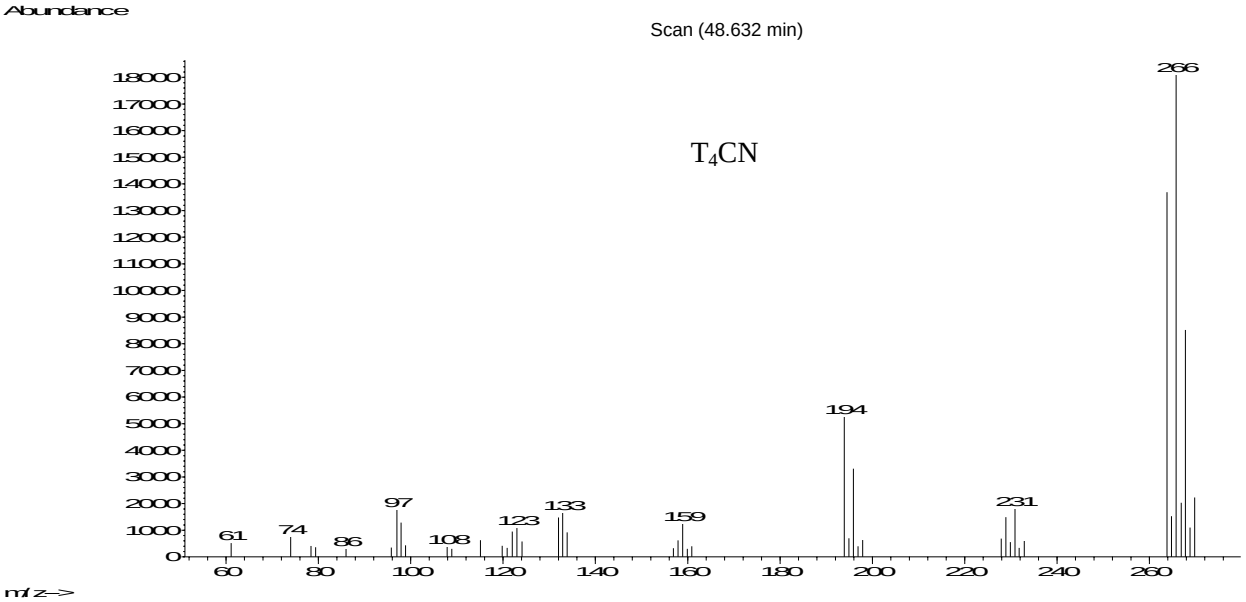

B.6 Halowax 1014

(a) Total Ion Chromatogram and Mass Spectrum: P_5CN

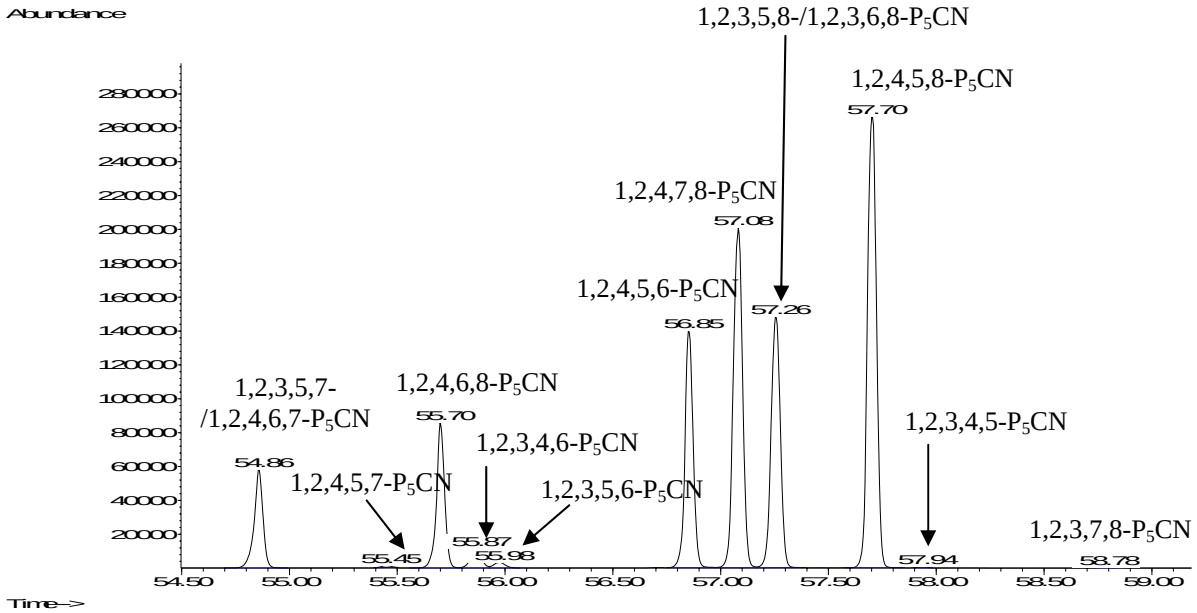

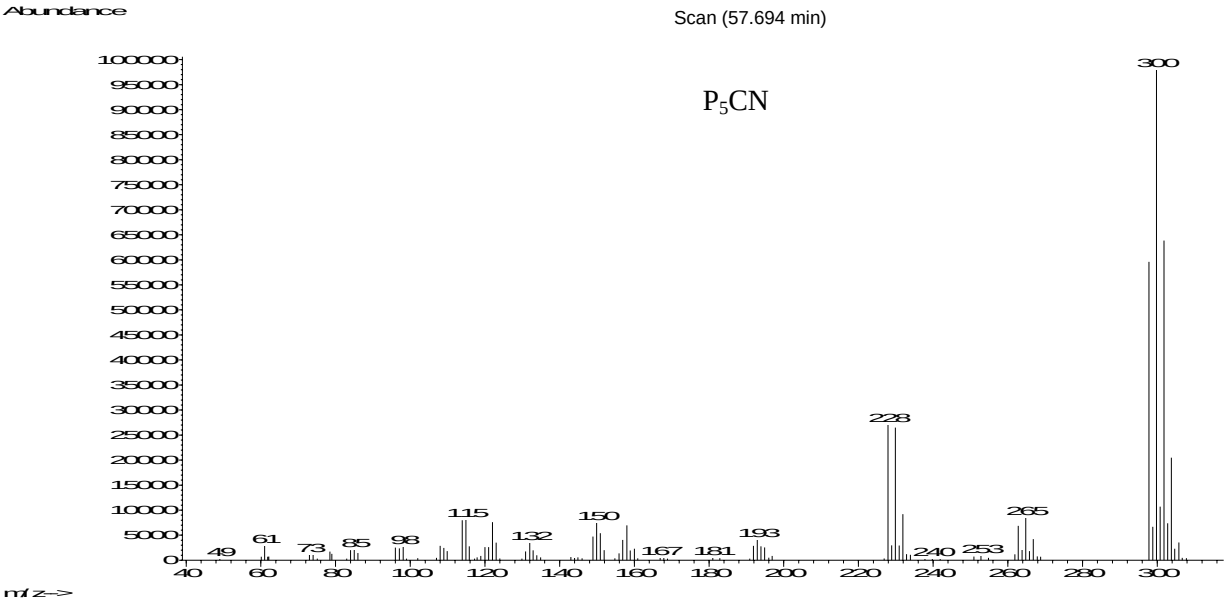

B.6 Halowax 1014

(b) Total Ion Chromatogram and Mass Spectrum: H_6CN

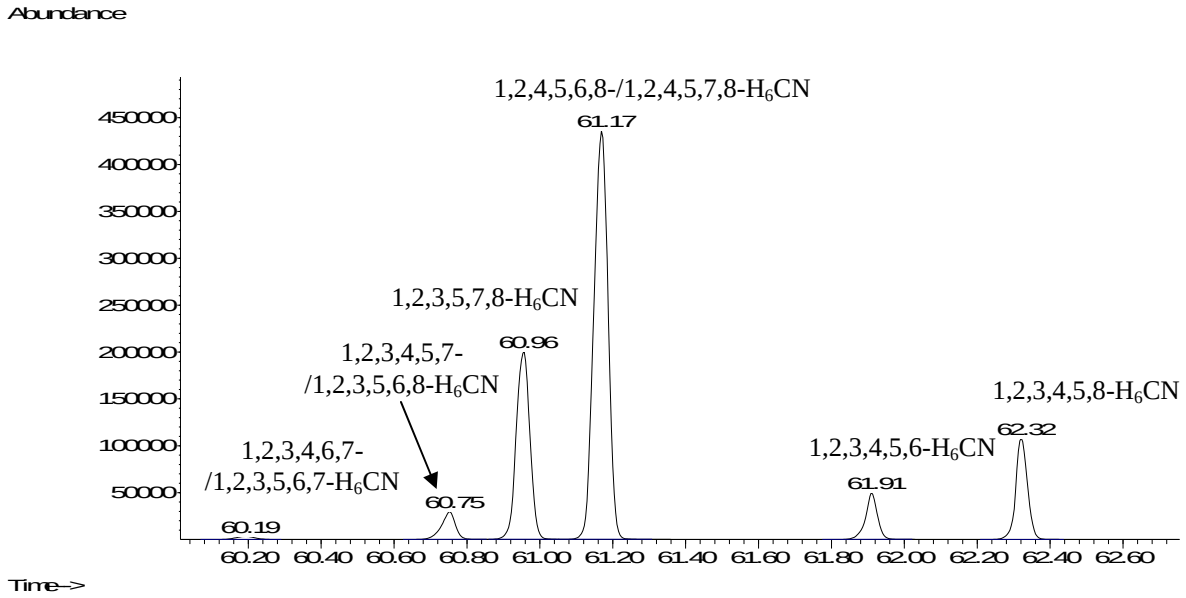

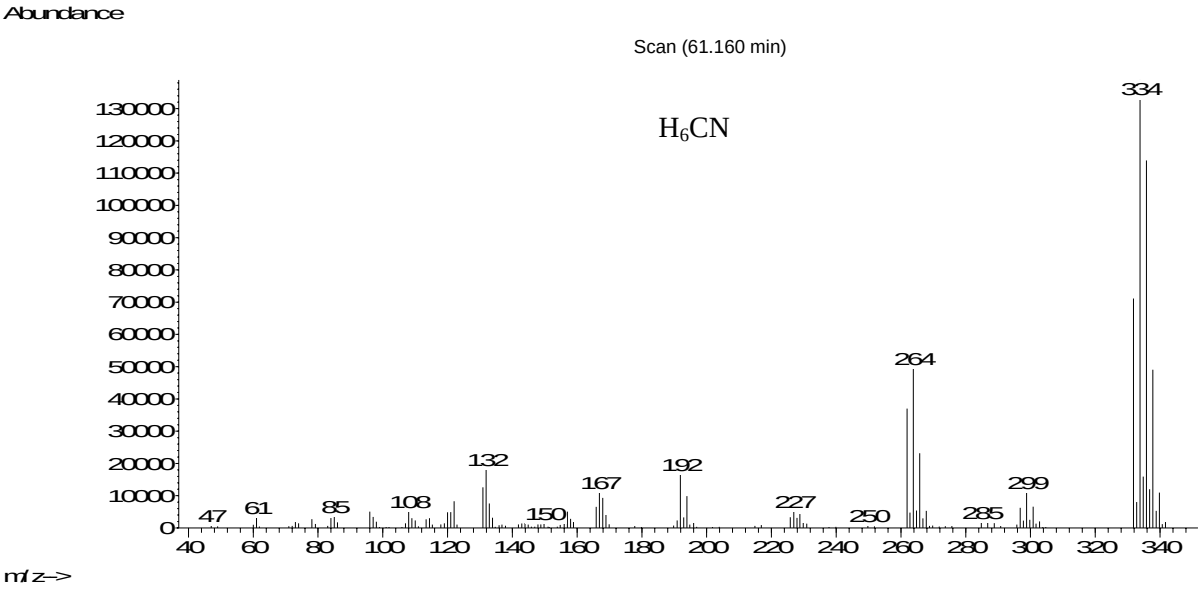

B.7 Halowax 1051

(a) Total Ion Chromatogram and Mass Spectrum: H_7CN

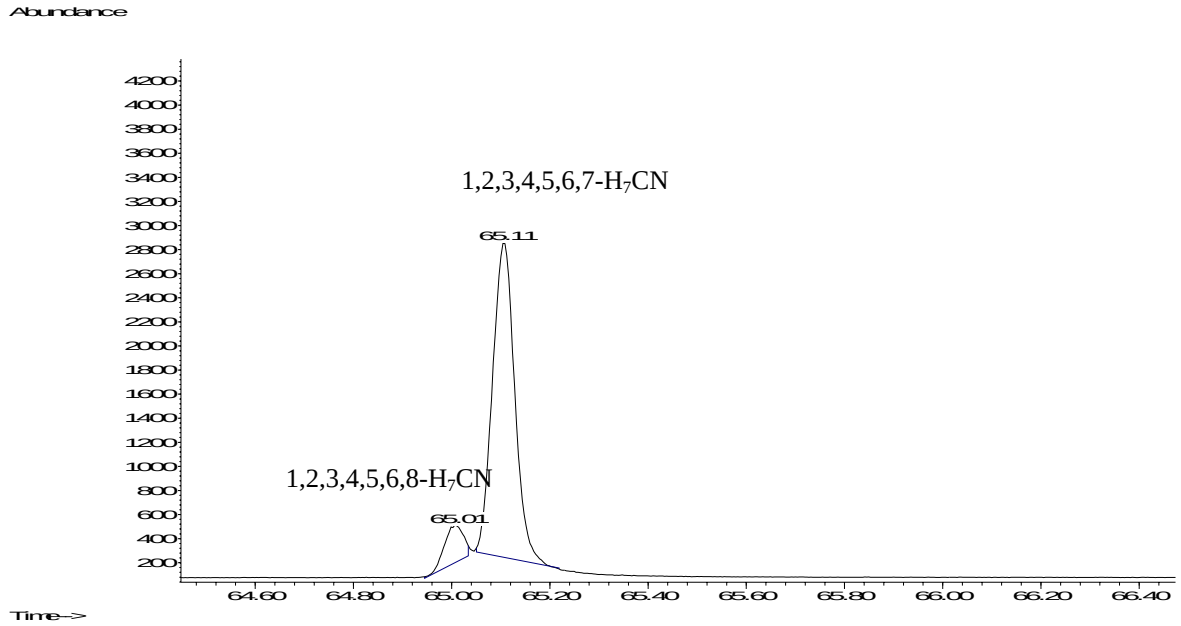

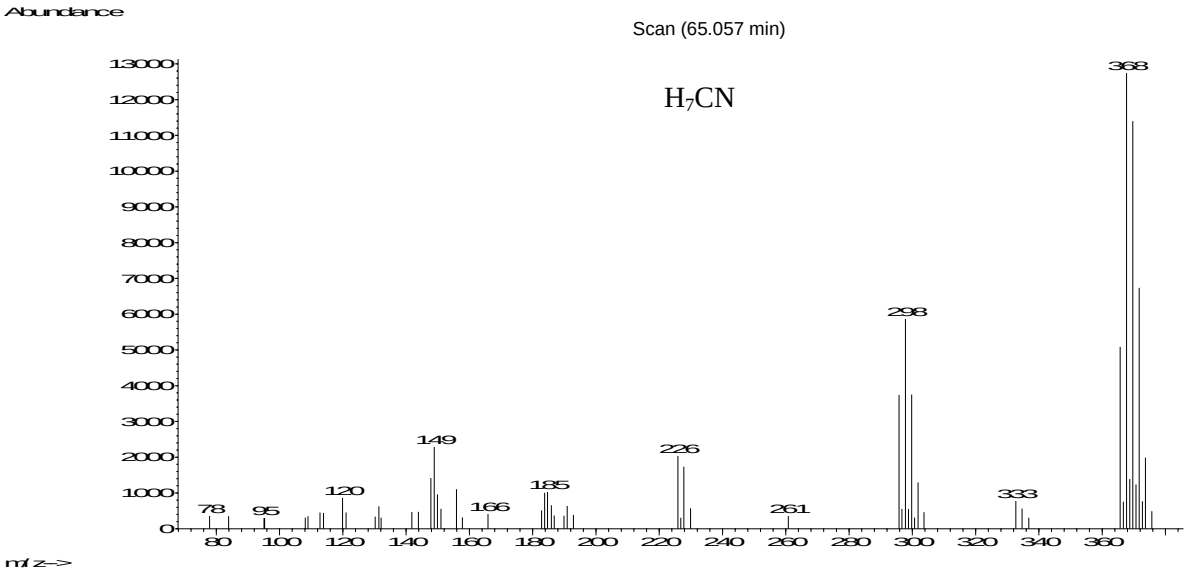

B.7 Halowax 1051

(b) Total Ion Chromatogram and Mass Spectrum: OCN

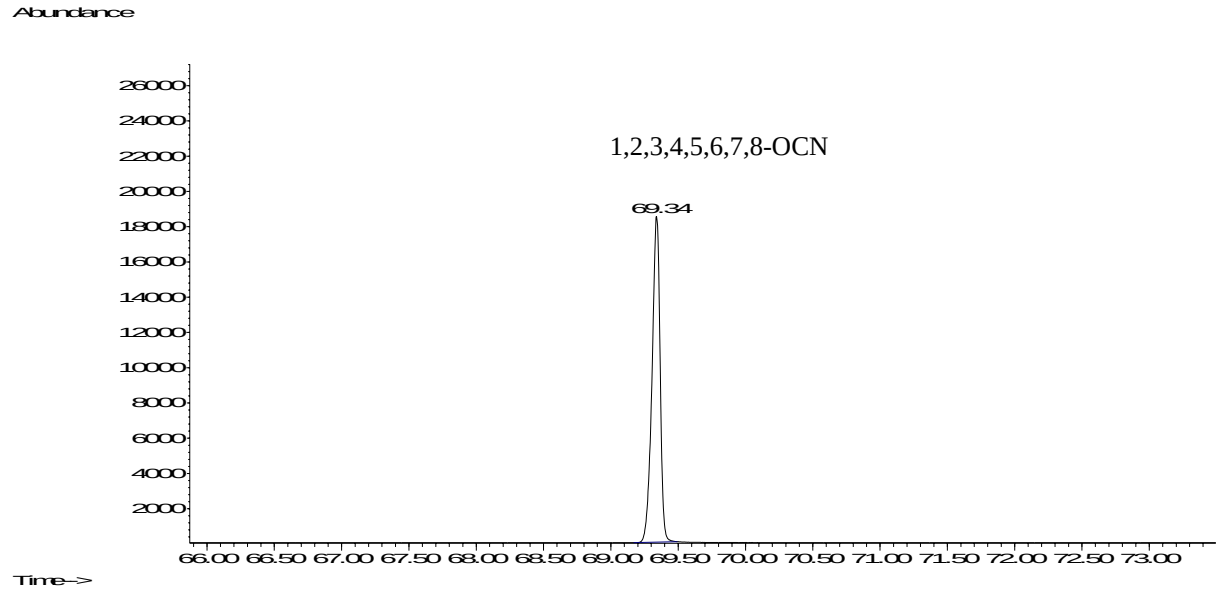

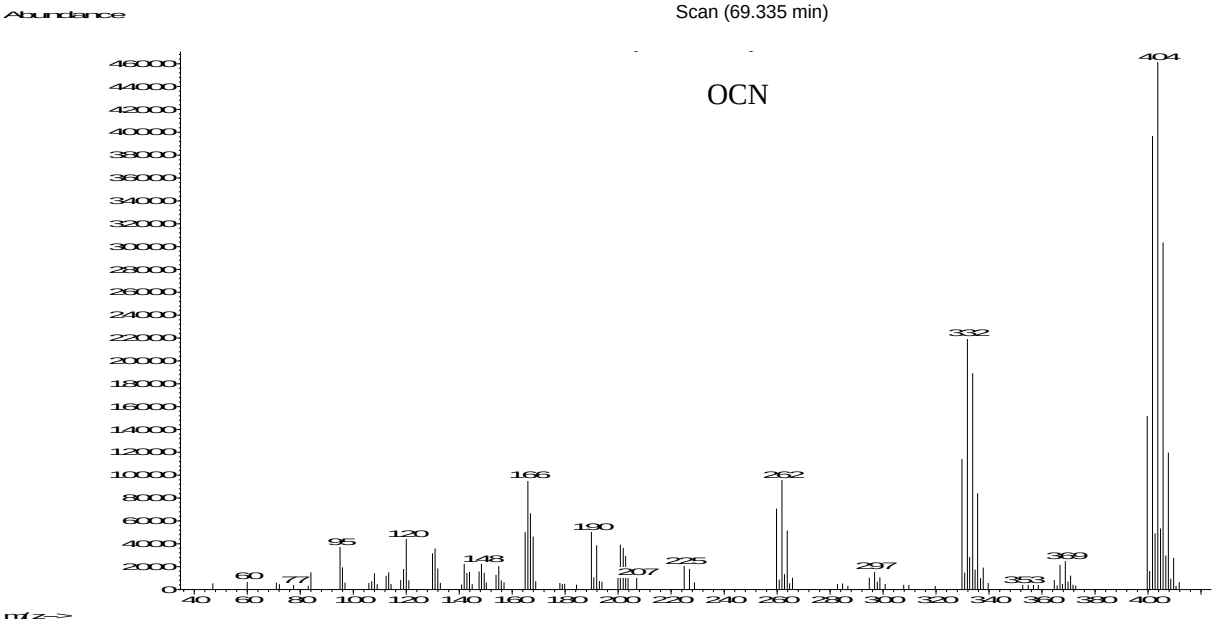

VITA

Do Hyong Kim was born on December 5, 1973 in Daegu, South Korea. In 1990, he immigrated to the United States and graduated from Los Angeles High School with honors in 1993. He entered University of California at Berkeley and received the BS in 1997, majoring in civil and environmental engineering. Beyond his BS he began pursuing higher degree in the School of Civil and Environmental Engineering at Georgia Institute of Technology in 1998 and earned his MS in 2001 with the special research project entitled "Kinetic Modeling of Polycyclic Aromatic Hydrocarbon Formation from Neutral, Ambident Radicals." He continued his research on formation of combustion byproducts and finally earned his Ph.D in 2005. His research topic was titled, "Formation of Aromatic Compounds by Cyclopentadiene Moieties in Combustion Processes."